Department of Molecular and Clinical Pharmacology
Institute of Translational Medicine
University of Liverpool

The Role of Regulator of Calcineurin 1 (RCAN1) Signalling in Endothelial Cells

Thesis submitted in accordance with the requirements of the University of Liverpool
for the degree of Doctor in Philosophy

Ahmad Fahad Alghanem

Supervisor: Dr Michael Cross

August 2014

Abstract

Regulator of calcineurin 1 (RCAN1) has been shown to act as a negative regulator of vascular endothelial growth factor (VEGF)-signalling in endothelial cells. Two isoforms are detectable in cells, RCAN1.1 and RCAN1.4, produced by alternative splicing of the *RCAN1* mRNA. In this study it was demonstrated that only RCAN1.4 is induced in human dermal microvascular endothelial cells (HDMECs) in response to VEGF. Using siRNA-mediated gene silencing this work shows that RCAN1 depletion leads to a reduction in VEGFR-2 internalisation following VEGF-A stimulation. RCAN1 depletion also leads to a reduction in cell polarity and cytoskeletal reorganisation in response to VEGF. siRNA-mediated silencing of RCAN1 led to an inhibition of VEGF-A mediated migration of HDMECs. These effects of RCAN1 knockdown appear to be specific to VEGFR-2, as no apparent effect on hepatocyte growth factor receptor (HGFR) internalisation and cytoskeletal reorganisation and migration in response to HGF was observed in HDMECs. Over-expression of RCAN1.4 isoform using adenoviral mediated gene delivery resulted in increased migration of HDMECs in the absence of ligand. This effect was insensitive to the calcineurin inhibitor cyclosporine, indicating that RCAN1.4 was not operating through the classical calcineurin/NFAT pathway to regulate cell migration. Instead, the RCAN1.4 effect was sensitive to a small molecule VEGFR-2 kinase inhibitor, which blocked cell migration.

This study also examined the role of phospholipase D (PLD) in endothelial cell function. By utilising siRNA for PLD1 and PLD2 it was shown that both PLD1 and PLD2 are required for VEGF-A mediated proliferation, migration and tubular morphogenesis in HDMECs.

Overall, the data presented in this thesis defines a novel role for both RCAN1 and PLD in regulating in endothelial cell function. Both proteins could be potential therapeutic targets to regulate vascular function.

Declaration

I declare that this thesis is my own work and all the sources have been quoted and acknowledged by means of complete references.

Acknowledgements

First of all I want to thank my great supervisor Dr.Micheal Cross. I am glad to be his first PhD student in Liverpool University. He has taught me how to think and plan the experiments with scientific thinking in the field of molecular signalling and angiogenesis. I appreciate all his contributions of time and ideas to my PhD, I owe you so much.

I am very grateful to so many people for the unlimited help they have given me during my PhD study. Firstly, past and present group members that I met and I had the pleasure to work with or alongside in Sherrington building at G28 lab. Thanks to all the postdocs I worked with: Dr. Katherine Holmes and Dr. Maxine Seaton, also all graduate students who have helped me with lab techniques and rotation. I would like to thank Dr. Maxine Seaton and Dr. Parveen Sharma for help with compiling the Materials and Methods section. Also I would like to thank the Saudi Embassy in London for making this study possible by providing the financial funding.

This work would not have been possible without the support of my wife Ashwag Almohaisen. You stand next to me any time I need help and also when I need moral support. Mere words are not enough to thank my mother, father, brothers and sisters for support and encouragement every day. Thank you all.

AHMAD ALGHANEM
Liverpool University
August 2014

List of Abbreviation:

Arp2/3: actin-related proteins 2/3
BSA: Bovine serum albumin
c-Met: Hepatocyte Growth Factor Receptor
Ca^{2+}: ionized calcium
cDNA: complementary DNA
CHO: Chinese hamster ovary cells
Cho: choline
DMEM: Dulbecco's modified Eagle's medium
DMSO: Dimethyl sulphoxide
DNA: Deoxyribonucleic acid
DSCR: Down Syndrome Critical Region
EBM-2: Endothelial Cell Basal Medium-2
ECM: Extracellular Matrix
EDTA: Ethylenediaminetetraacetic acid
EEA1: Early Endosome Antigen 1
EGFR: Epidermal growth factor receptor
FAK: focal adhesion kinase
FBS: Foetal bovine serum
FGF: Fibroblast Growth Factor
GEF: guanidine exchange factor
GFP: Green Fluorescence Protein
GTP: guanosine triphosphate (GTP)
HDMEC: Human Dermal Microvascular Endothelial Cells
HEK293: Human embryonic kidney 293
HIF-1: Hypoxia-inducible factor-1
HGF: Hepatocyte Growth Factor
HRP: Horseradish peroxidase
HUVEC: Human Umbilical Vein Endothelial Cell
IF: Immunofluorescence
IgG: Immunoglobulin G
kDa: Kilo Dalton
LPA: lyso-phosphatidic acid

LB: Lysogeny broth

MAE: Mouse Aortic Endothelial Cell

MMP1: matrix metalloproteinase

NHDF: Normal Human Dermal Fibroblast

Nrp: Neuropilin

PBS: Phosphate-Buffered Saline

PCR: Polymerase Chain Reaction

PFA: Paraformaldehyde

PLCγ: Phospholipase C gamma

PIGF: placental growth factor

PI3-K: phosphoinositide 3-kinase

PIP$_2$: phosphatidylinositol (4,5)-bisphosphate

PIP$_3$: phosphatidylinositol (3,4,5)-trisphosphate

PtdCho: phosphatidyl choline

PtdOH: phosphatidic acid

PA: phosphatidic acid

PLD1: Phospholipase D1

PLD2: Phospholipase D2

q-RT-PCR: quantitative Real Time-Polymerase chain reaction

RCAN1: Regulator of Calcineurin

Rho-A: Ras homolog gene family member A

ROCK: Rho-associated serine/threonine kinase

RNA: Ribonucleic acid

RTK: Receptor Tyrosine Kinase

SDS-PAGE: Sodium dodecyl sulphate polyacrylamide gel

siRNA: small interfering Ribonucleic Acid

TBS: Tris-Buffered Saline

TLC: thin layer chromatography

TBST: Tris-Buffered Saline and Tween

VEGF-A: Vascular endothelial growth factor A

VEGF-B: Vascular endothelial growth factor B

VEGF-C: Vascular endothelial growth factor C

VEGFR-1: Vascular endothelial growth factor receptor 1/Flt-1

VEGFR-2: Vascular endothelial growth factor receptor 2/Flk-1/KDR

VEGFR-3: Vascular endothelial growth factor receptor 3/Flt-4

WB: Western Blot

List of figures

List of Tables

Table of content

Chapter 1

Introduction

1.1 The vascular system and endothelial cells

The structure of the large macrovascular vessels, such as arteries and veins, consists of an inner layer (tunica intima) comprising a monolayer of endothelial cells surrounded by a sheet-like basement membrane home to the extracellular matrix proteins (ECM). This basement membrane is surrounded by the tunica media layer, which consists of vascular smooth muscle cells, whose function is to allow vessel contraction. The outermost tunica adventia layer provides the supporting connective tissue. By contrast, the structure of the microvascular vessels, for example capillaries and arterioles, comprises a monolayer of endothelial cells surrounded by a basement membrane and stabilised by a layer of specialised smooth muscle cells, known as pericytes (Aird, 2007).

The continuous endothelial monolayer lining the blood vessels forms a size-selective and semipermeable barrier between the blood plasma and interstitium. The passage of proteins, solutes and gases is controlled by transcellular and paracellular processes. Transcellular transport involves transcytosis, an energy-dependent trafficking of vesicles across the endothelium, which results in the transport of macromolecules such as albumin (Komarova and Malik, 2010). Paracellular transport is regulated by interendothelial junctions. Two types of interendothelial junctions are present in the endothelium, tight junctions and adherens junctions, which regulate the movement of solutes larger than 3nm in size (Komarova and Malik, 2010).

The endothelium regulates haemostasis by promoting anti-coagulant properties and counteracting platelet activation and aggregation. Binding of antithrombin III and thrombomodulin (TM) expression inhibit blood coagulation (van Hinsbergh, 2012). Platelet adhesion and activation are regulated by von Willebrand factor (vWF) released from endothelial cells. vWF is stored in Weibel-Palade bodies within the endothelial cells and released by vasoactive agents such as histamine, bradkinin and thrombin (van Hinsbergh, 2012). Nitric oxide released to the vascular lumen is an inhibitor of adhesion and platelet aggregation. Furthermore, endothelial expressed cyclooxygenease-2 (COX-2) generates the eicosanoid prostacyclin (PGI_2), which inhibits platelet activation (Weksler et al., 1977).

Inflammatory cytokines such as tumour necrosis factor α (TNFα) and interleukin-1β (IL-1β) cause endothelial dysfunction and induce expression of adhesion molecules such as vascular cell adhesion molecule-1 (VCAM-1) and E-Selectin leading to leukocyte adhesion and infiltration into surrounding tissues (Hayden and Ghosh, 2004) One of the central mediators of most inflammatory stimuli is the transcription factor nuclear factor κB (NF-κB) (Hayden and Ghosh, 2004). The net effect of NF-κB activation is the disruption of the non-inflammatory, non-thrombogenic endothelial surface. Conversely, laminar shear stress (LSS) induces the expression of various factors including endothelial NOS (eNOS) and thrombomodulin (TM) (Topper et al., 1996) that are essential for regulation of vascular tone and maintenance of a quiescent endothelium.

Endothelial surface enzymes modify vasoactive peptides in the bloodstream. Angiotensin-converting enzyme is expressed on the luminal surface of endothelial cells which converts angiotensin I to angiotensin II resulting in vasoconstriction.. Endothelial nitric oxide synthase (eNOS) generates the vasoprotective molecule nitric oxide (NO) (Förstermann et al., 1994). Furthermore, vascular nitric oxide dilates blood vessels by stimulating soluble guanylyl cyclase (sGC) and increasing cGMP in smooth muscle cells (Förstermann et al., 1994).

1.2 Angiogenesis

Angiogenesis is the process involved in the growth of new blood vessels from pre-existing vessels (Dulak, 2005). It is one of the fundamental biological processes in higher vertebrates and involves a number of steps. First of all, the basement membrane of the existing blood vessels is degraded, and then endothelial cells migrate into the interstitial space in the direction of the angiogenic stimulus. The endothelial cells then proliferate while other endothelial cells generate the stalk of the sprout. Then the sprout develops a lumen and becomes a mature capillary. The maturation process is completed when pericytes and smooth muscle cells develop to stabilise the new blood vessels. Subsequently, these vessels differentiate into venules and arterioles. The degradation step is mediated by proteolytic enzymes and cell adhesion molecules. Angiogenic factors support proliferation and differentiation of the new vessels (Douglas et al., 2005).

Angiogenesis is a process that occurs both in the physiological and pathological state. The physiological states dependent on angiogenesis include: wound healing, repair, ovulation, placenta formation and chronic inflammation (Hoeben et al., 2004). Pathological angiogenesis is induced in diseases such as cancer, atherosclerosis, stroke, and diabetic retinopathies. Experiments have shown that angiogenesis-dependent diseases are caused by unchecked production of normal and abnormal forms of pro-angiogenic mediators and insufficient inhibitory molecules (Felmeden et al., 2003). In chronic cardiac conditions such as myocardial infraction and stroke, dysfunction of angiogenesis leads to loss of tissue and eventually increased morbidity and mortality (Nishida et al., 2004, Leon et al., 2005). Angiogenesis is driven by a number of growth factors (Senger et al., 1997) and pro-angiogenic cytokines acting on their cognate receptor (Fiedler and Augustin, 2006) and moderated by a number of endogenous inhibitors resulting in tightly regulated process; imbalance results in malignant, immune disorders, ischaemic, inflammatory and infectious disorders (Douglas et al., 2005, Lamalice et al., 2007).

1.3 Molecular regulation of angiogenesis

Regulators of angiogenesis can be broadly categorised into stimulators and inhibitors. Most regulators are proteins, primarily growth factors that stimulate endothelial cells to divide and migrate towards the stimuli. There exist numerous factors that can trigger angiogenesis and the most prominent of these is hypoxia (Minchenko et al., 1993). Hypoxia-inducible factor-1 (HIF)-1 is composed of two subunits, an oxygen-sensitive HIF-1α subunit and a constitutively expressed HIF-1β subunit (Wang and Semenza, 1995). Both HIF-1α and HIF-1β are members of the basic helix-loop-helix Per/Sim/Arnt (HLH-PAS) family of transcription factors (Salceda and Caro, 1997). In contrast to the constitutively expressed HIF-1β subunit, HIF-1α is an oxygen labile protein that becomes stabilized in response to hypoxia, iron chelators, and divalent cations (Lok and Ponka, 1999). Under normal oxygen levels (normoxia) in the body, HIF-1α is hydroxylated on proline residues by a family of prolyl hydroxylase (PHD) enzymes which ultimately leads to degradation by promoting interaction with the von Hippel-Lindau tumor-suppressor protein (pVHL) and subsequent proteosomal degradation (Masson et al., 2001). In low oxygen environments (hypoxia) HIF-1α hydroxylation is prevented, leading to a substantial increase in the half-life of the protein which facilitates dimerisation with

HIF-1β and translocation to the nucleus where the HIF-1 complex binds to the hypoxia responsive elements in the promoter region of a number of genes which regulate glucose homeostasis, vascular physiology and adaption to a low oxygen environment. The VEGF-A gene contains a hypoxia response element (HRE) element in its promoter and hypoxia leads to an upregulation in *VEGF-A* mRNA and subsequent translation of the VEGF-A protein (Pugh and Ratcliffe, 2003, Laughner et al., 2001).

The vascular endothelial growth factor (VEGF) family comprises five members VEGF-A, -B, -C, -D and placental growth factor (PIGF). These ligands bind to three different receptor tyrosine kinases (RTK) known as VEGF-receptor 1, 2 and 3 (VEGFR) (Figure 1). VEGFR-1 is involved in haematopoietic cell development; VEGFR-2 is involved in vascular endothelial development and VEGFR-3 is involved in lymphatic endothelial cell development (Holmes et al., 2007).

VEGF-A binds and activates VEGFR2 expressed on endothelial cells. This binding leads to receptor dimerization and phosphorylation of specific tyrosine residues in the intracellular domain of the receptor (Clauss and Breier, 2005). As a result, docking sites for several adaptor molecules are created. A number of key signalling molecules such as mitogen activated protein kinases are activated in order to regulate endothelial proliferation, vascular permeability and migration. In addition, VEGF-A binds to VEGFR1, expressed on haematopoietic progenitor cells, macrophages and monocytes. VEGFR1 activation results in chemotactic signals in hematopoietic progenitor cells. In mammals, VEGF-A exists in a number of different isoforms following alternative splicing of a single precursor mRNA (Robinson and Stringer, 2001). In humans, six VEGF-A splice variants have been detected: VEGF-A_{121}, VEGF-A_{145}, VEGF-A_{165}, VEGF-A_{183}, VEGF-A_{189} and VEGF-A_{206}. Although VEGF-A_{121}, VEGF-A_{183} andVEGF-A_{189} are expressed in various tissues, VEGF-A_{165} is the most abundantly expressed form, whereas VEGF-A_{145} and VEGF-A_{206} are relatively rare (Robinson and Stringer, 2001, Zacharoulis et al., 2005). All isoforms except VEGF-A_{121} bind to heparan sulphate proteoglycans found on the plasma membrane of most cells and in the extracellular matrix. They create a concentration gradient that guides the endothelial cells to efficiently migrate to the region of hypoxia. VEGF-B also binds to VEGFR1. Recently, it has been shown that VEGF-B acting on

VEGFR-1 is required for the uptake of fatty acids from the heart and skeletal muscle endothelium (Hagberg et al., 2010). PIGF also binds to VEGFR1 where it works in synergy with other VEGF in the regulatory process. VEGF-C and VEGF-D bind to VEGFR3, however, their role in the development of blood vessels is not so prominent (Felmeden et al., 2003).
VEGF-E which is expressed in the parapox Orf virus-encoded VEGF (Takahashi and Shibuya, 2005) and VEGF-F which is expressed in snake venom (Suto et al., 2005, Holmes et al., 2007) bind to VEGFR-2.

Another factor that regulates angiogenesis is the angiopoietin system (Felmeden et al., 2003). In humans, the system consist of three ligands: angiopoietin (ANGPT)1, 2 and 4 and their cognate receptor, TIE-2 (Augustin et al., 2009), The function of a closely related orphan receptor, TIE-1, is less well understood, but it has been shown to dynamically interact with TIE-2 and to modulate its function upon binding of different angiopoietins (Seegar et al., 2010). The role of ANGPTs in angiogenesis are complex and context dependent. Depending on the level of expression and the presence of other factors such as VEGF, ANGPT1 and ANGPT2 have either pro- or anti-angiogenic effects and are believed to oppose each others function by competing for binding to TIE-2 (Maisonpierre et al., 1997). The general model is that ANGPT1, which is expressed by mural cells, pericytes and fibroblasts, activates TIE-2 on endothelial cells which results in stabilization of endothelial junctions and recruitment of pericytes, ultimately leading to vascular quiescence (Saharinen et al., 2008). ANGPT2 is predominantly expressed by endothelial cells and stored in specialized granules (Weibel-Palade bodies), from where it is released upon angiogenic or inflammatory activation. ANGPT2 normally does not induce TIE-2 phosphorylation. Instead, it inhibits activation of TIE-2 by ANGPT1, leading to vessel destabilization and pericyte detachment and thereby sensitizes endothelial cells to angiogenic and pro-inflammatory signals (Fiedler et al., 2006).

Inflammatory cells associated with the inflammatory stage of wound healing promote angiogenesis. Chronic inflammation is characterised by an increase in oxygen utilisation by the neutrophil cells leading to localised hypoxia. This condition induces stabilisation of HIF-1α that stimulates pro-angiogenic growth factors (Bonnet and Walsh, 2005). Pro-inflammatory cytokines activate endothelial cells thereby inducing development of several angiogenesis stimulating factors such as matrix-degrading proteases. Inflammatory cells produce chemokines that are involved in control of angiogenesis. Leukocytes that are recruited from the blood stream to the inflammation site secrete a number of pro-angiogenic factors such as VEGF (Boghozian et al., 2013).

Angiogenesis is down-regulated by anti-angiogenic factors such as as angiostatin, endostatin and thrombospondin (TSP-1) (Lawler and Lawler, 2012). These factors inhibit angiogenesis through antagonising the effects of VEGF. Angiostatin is a 38 kDa proteolytic fragment of a larger protein, plasminogen (O'Reilly et al., 1994). Endostatin is a naturally-occurring, 20-kDa C-terminal fragment derived from type XVIII collagen, a component of the extracellular matrix (ECM) (O'Reilly et al., 1997). Both angiostatin and endostatin have been shown to inhibit endothelial cell migration in response to FGF and VEGF stimulation (Eriksson et al., 2003). However, the agents have been shown to have many pleiotropic effects in endothelial cells. Thrombospondin-1 (TSP-1), a multifunctional extracellular protein, was the first naturally occurring angiostatic agent to be discovered (Good et al., 1990). Unlike many angiostatic agents such as endostatin and angiostatin, TSP-1 is not a cleavage product and is effective as native, full-length protein (Tabruyn and Griffioen, 2007). The antiangiogenic effects of thrombospondin (TSP-1) have been most extensively characterized in the tumour microenvironment. TSP-1 antagonizes VEGF in several important ways, via inhibition of VEGF release from the extracellular matrix, direct interaction, and inhibition of VEGF signal transduction (Good et al., 1990). Thrombospondin binds to CD3, CD47 and integrin receptors. CD36 and beta-1 integrins work together in transmitting signals initiated by the anti-angiogenic factors (Lawler and Lawler, 2012).

1.3.1 VEGF-A

VEGF-A is the most potent stimulator of angiogenesis. It is produced by a wide variety of cells, organs and tissues including tumour cells, the corpus luteum, the heart, liver, stomach mucosa, adrenal cortex cardiac myocytes, renal glomeruli, epithelial cells of lung and macrophages (Berse et al., 1992).

The importance of VEGF-A in vascular function was highlighted by the fact that *VEGF-A* knock out in mice results in such severe defects that mice die due to a lack of vascular development at E9.5-10.5 (Carmeliet et al., 1996). Another study demonstrated that the lack of just one VEGF-A allele results in death and vascular abnormalities at E11-12 (Ferrara et al., 1996).

In humans the VEGF-A gene is located on chromosome 6p21.3 (Vincenti et al., 1996). Six VEGF-A splice variants are expressed in humans, differing in the number of amino acids they contain and are named accordingly; VEGF-A_{121}, VEGF-A_{145}, VEGF-A_{165}, VEGF-A_{183}, VEGF-A_{189} and VEGF-A_{206}. (Figure 1.1) (Robinson and Stringer, 2001). The most commonly expressed isoform is VEGF-A_{165}, which like all other isoforms is expressed as a covalently linked homodimeric protein of two 23KDa subunits.

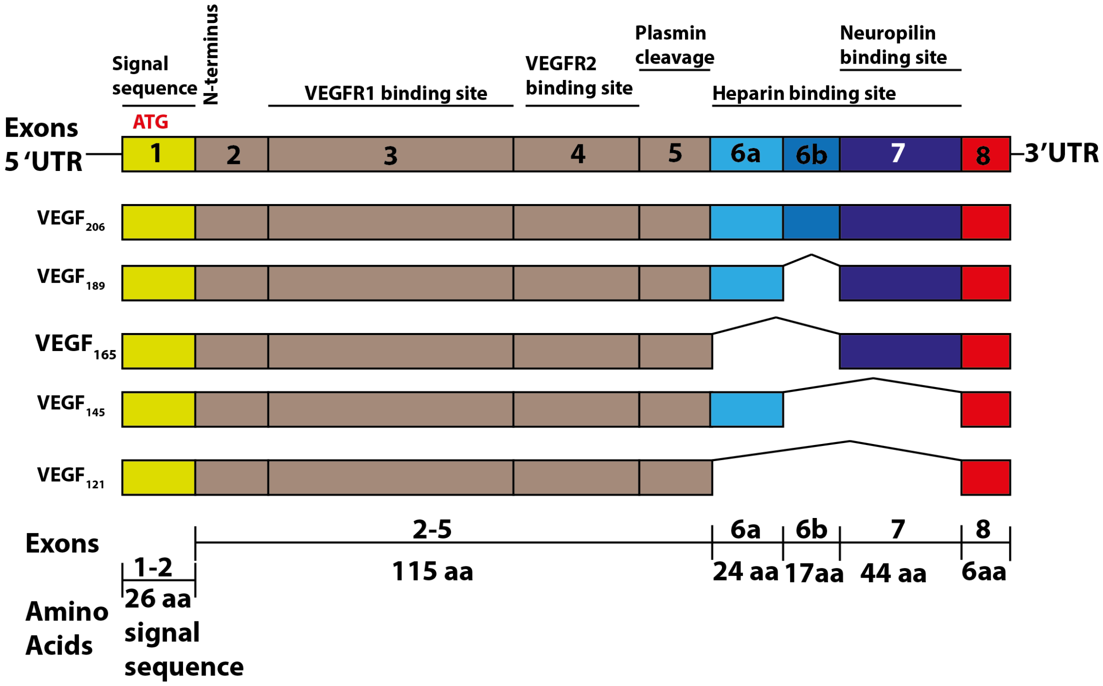

Figure 1.1:Exon structure of human VEGF-A mRNA splice variants

This diagram illustrates the gene encoding VEGF-A comparing the 8 exons which code for the different motifs. In humans the most predominant form is VEGF-A_{165}. Different mRNA splicing can generate the formation of many isoforms that vary in amino acid number. Adapted from Holmes et al., 2007.

VEGF-A_{121} lacks any heparin binding domains from exons 6 and 7 whereas the other variants have varying numbers of these domains. These heparin binding domains allow VEGF isoforms to bind to heparan sulfate proteoglycan (HSPG) and the co-receptor neuropilins in the extracellular matrix (ECM), which help enhance activation and migration in endothelial cells. VEGF isoforms also contain a plasmin cleavage domain which has been shown to play a key role in cleaving ECM-bound VEGF thereby releasing soluble and bioactive proteolytic fragments (Park et al., 1993). In 2005 it was demonstrated that extracellular VEGF can be regulated by matrix metalloproteinases (MMPs) and that they may cleave matrix bound VEGF-A_{165} to generate non-heparin binding fragments indicating that the regulation of extracellular VEGF may also play a critical role in vascular development (Lee et al., 2005).

As discussed previously, one of the key regulators of VEGF-A expression is oxygen tension. Alterations in the amount of oxygen tension during hypoxia results in a significant increase in the expression of *VEGF-A* mRNA through the hypoxia responsive element in the 5′ and 3′ flanking regions of human *VEGF-A* gene (Minchenko et al., 1993, Shweiki et al., 1992). In addition to the classical VEGF-A isoforms, a novel VEGF-A_{165}b isoform was discovered and reported as a key regulator of angiogenesis in health and disease (Bates et al., 2002, Perrin et al., 2005). VEGFA-A_{165}b is generated by exon 8 distal splice site (DSS) selection. It has been reported that alternative *VEGF-A* mRNA splicing potentially generates two families of proteins that differ by their c-terminal six amino acids. The difference between VEGF-A_{165} and VEGF-A_{165}b is a change of the 6 c-terminal the amino acids from CDKPRR to SLTRKD (Harper and Bates, 2008). It has been shown that VEGF-$_{165}$b behaves as a partial VEGFR-2 agonist (Kawamura et al., 2008) as it is no longer able to bind to neuropilin. More recent data has shown that *in vivo,* overexpression of VEGF165b, leads to insufficient angiogenesis in patients with systemic sclerosis (Manetti et al., 2011).

1.3.2 The VEGF Receptors

It has been shown that VEGF receptors function similarly to other receptor tyrosine kinases such as epidermal growth factor receptor (EGFR), hepatocyte growth factor receptor (HGFR) and platelet derived growth factor receptor (PDGFR). Ligand interaction with the cognate receptor induces receptor dimerization, which creates a docking site for signalling and the activation of the tyrosine kinase. In addition, VEGFRs induce cellular functions that are common to wide variety of growth factor receptors which include cell survival, proliferation and cell migration (Olsson et al., 2006). VEGF-A can also bind to neuropilin, which acts as a co-receptor for VEGF-A, augmenting its signalling (Soker et al., 1998).

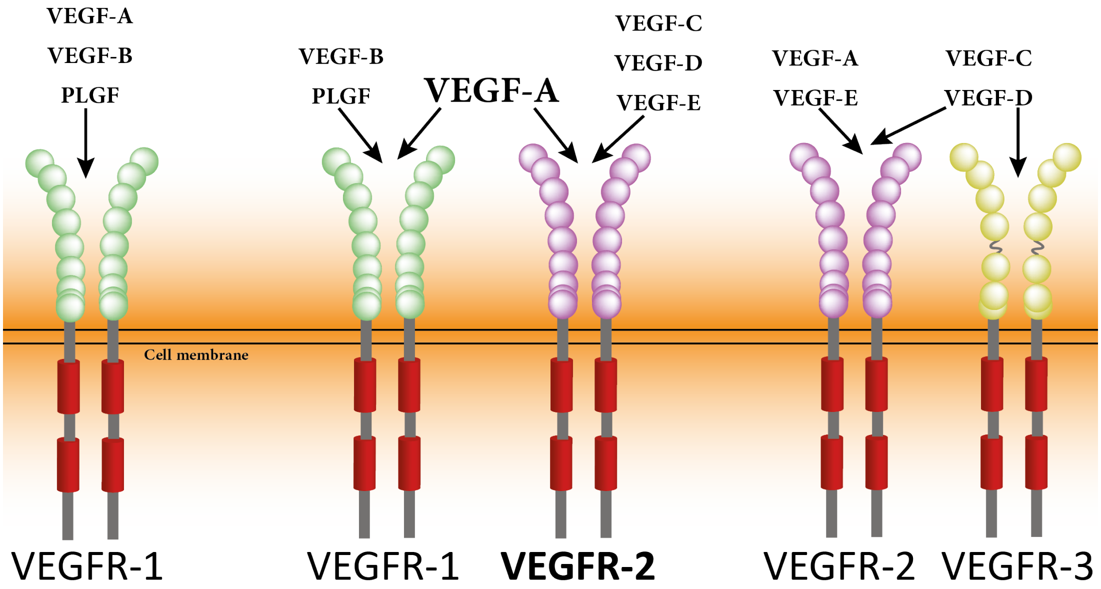

Figure 1.2: VEGF receptor binding properties

This diagram shows the different VEGF ligands and which VEGF receptors they are able to bind to. Adapted from Holmes et al., 2007.

The VEGFR receptors are key regulators of angiogenesis; vasculogenesis and lymphangiogenesis (Lohela et al., 2009). VEGF receptors are expressed on a range of different cell types. VEGFR1 (Flt1) plays a role in hematopoietic stem cell migration of macrophages and monocytes (Olsson et al., 2006). VEGFR1 and VEGFR2 (Flk1/KDR) are both expressed on the vascular endothelial cells (Olsson et al., 2006). VEGFR2 activates a range of responses such as cells migration and proliferation ultimately leading to angiogenesis (Zeng et al., 2002, Holmes et al., 2007). VEGFR3 (Flt4) is expressed predominantly on lymphatic endothelial cells (see Figure 1.1 and Figure 1.2) (Olsson et al., 2006). VEGF-A has been shown to bind and activate VEGFR1 and 2 on endothelial cells (Figure 1.2). The co-receptor neuropilins (NRP-1&2) are transmembrane non-protein tyrosine kinases which have been shown to interact with VEGFR2 in the presence of VEGF-A_{165} at endogenous and exogenous levels in endothelial cells (Whitaker et al., 2001). When VEGF-A binds to neuropilin it promotes complex formation with VEGFR2 and enhances VEGFR-2 function (Whitaker et al., 2001, Soker et al., 2002, Terman et al., 1991, Simons, 2012).

VEGF-B binds only to VEGFR1; this interaction however can be blocked by excess VEGFR1 suggesting that binding sites on the receptor are somewhat overlapping (Olofsson et al., 1998). Although VEGF-C and D have been shown to play a role in the development of primary capillary vasculatures of mid-gestation embryos, they later promote the growth and maintenance of the lymphatic vasculature (Mäkinen et al., 2001). Both VEGF- C and D are initially secreted as pro-peptides, which then undergo proteolytic processing. Partially processed VEGF-C and VEGF-D can bind to and activate VEGFR-3, whereas the fully processed forms of VEGF-C and VEGF-D can bind to and activate both VEGFR-2 and VEGFR-3 (Joukov et al., 1996).

Studies have identified a novel member of the VEGF family termed VEGF-E, which is encoded in the sequence of parapox Orf virus. VEGF-E binds with high affinity only to VEGFR2, which leads to receptor autophosphorylation and increases calcium (Ca^{2+}) concentration. This suggests the activation of VEGFR2 can stimulate angiogenesis (Meyer et al., 1999, Simons, 2012).

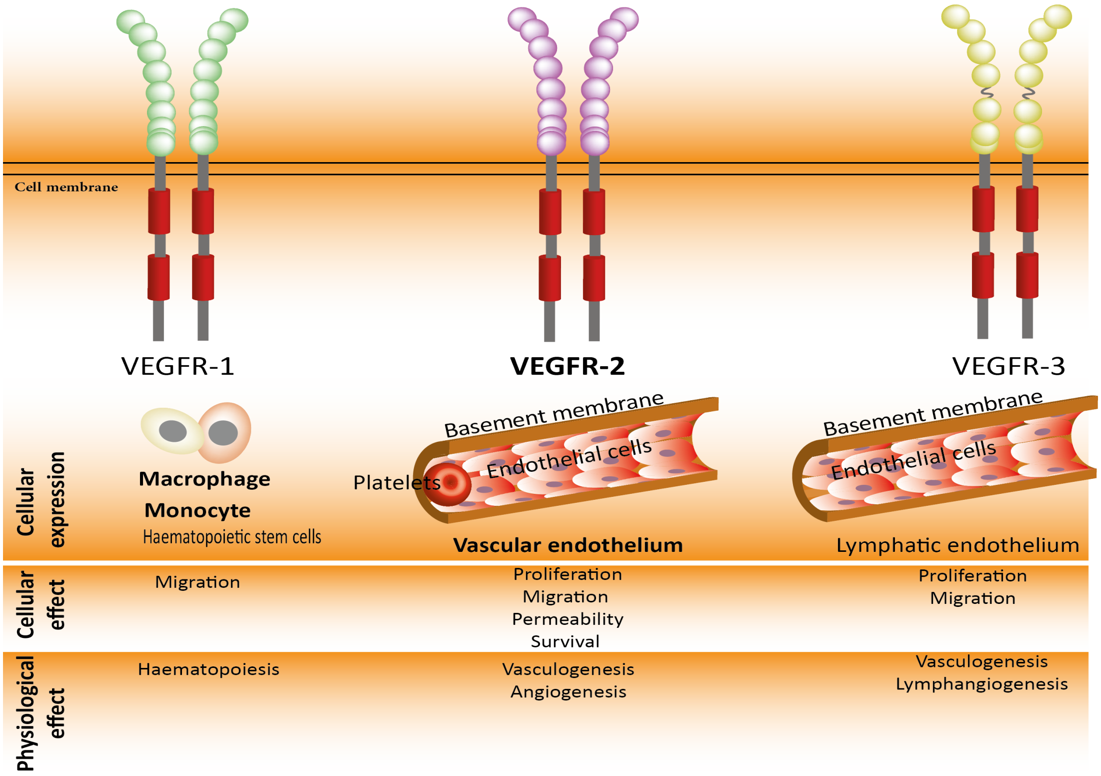

Figure 1.3: Receptor tyrosine kinase expression patterns and downstream functioning

VEGFR1 is expressed on haematopoietic stem cells, monocytes, vascular endothelium and macrophages. VEGFR2 is expressed on lymphatic and vascular endothelium. VEGFR3 is predominantly expressed on the lymphatic endothelium. The cellular effect on these receptors in the vascular endothelium includes cell migration, proliferation, survival and subsequent angiogenesis. Adapted from Holmes et al., 2007.

1.3.3 VEGFR2

In early mouse development, VEGFR2 was initially identified at E7.0 in mesodermal blood island progenitors. Later in development, expression is located in the blood vessels and developing endothelial cells suggesting that it could be an early marker of endothelial cell precursors (Yamaguchi et al., 1993). The most significant function of VEGFR2 has been revealed through a study of knockout mice which demonstrated that VEGFR-2 $^{-/-}$ mutant embryos die *in utero* between E8.5 and 9.5 because of damage in development in endothelial cells, haematopoietic and blood islands, which suggests that VEGFR2 is critical for vasculogenesis in the developing mouse embryo (Shalaby et al., 1995).

1.3.4 VEGFR2 Intracellular Signalling

VEGFR2 (also known as kinase-insert domain receptor (KDR) and foetal liver kinase (Flk)-1) plays a critical role in cellular physiology, pathological and vascular development upon stimulation by VEGF-A in endothelial cells. In 1991 Terman and colleagues identified VEGFR2 from a human endothelial cell cDNA library. The human VEGFR2 gene is 7.0 kb and is located on chromosome 4 (Terman et al., 1991). In-depth analysis using *in situ* hybridization has localized the human VEGFR2 gene to chromosome 4q11q12 which is in close proximity to the locus of two other RTKs namely PDGFR-α and c-KIT (Shibuya, 2002). Full-length VEGFR2 is 1365 amino acids (Sait et al., 1995) and structurally comprises an extracellular region containing 7 immunoglobulin-like (Ig-like) domains and an intracellular (cytoplasmic) region which contains the tyrosine kinase domain (Shibuya, 2002). The immature form of VEGFR2 is translated as a 150-kDa protein without glycosylation. It then undergoes post-translational modification in the form of glycosylation after which it is expressed on the cell surface as a mature 230 kDa protein (Takahashi and Shibuya, 1997).

The first mapping of VEGFR2 to determine the location of residues implicated in autophosphorylation in a bacterial model identified tyrosines Y951, Y996, Y1054, Y1059 as potential phosphorylation sites. These were later determined to be the identical phosphorylated sites of VEGF2 in human cells (Doughervermazen et al., 1994). VEGFR2 binds to phospholipase Cγ through the autophosphorylation sites Y801 and Y1175 (Cunningham et al., 1997). The main phosphorylation sites of VEGFR2 are Y951 in the kinase insert domain and Y1175 and Y1214 located in the C-terminal tail of the receptor (Matsumoto et al., 2005).

After phosphorylation of tyrosine Y951, VEGFR-associated protein (VRAP also known as T-cell adaptor TSAd) is able to bind VEGFR2. VRAP is a highly expressed adaptor protein that has been identified in human umbilical vein endothelial cells (HUVECs), spleen, peripheral leukocytes, thymus, heart and lung. In endothelial cells VRAP acts to recruit downstream effector protein such as PLCγ and PI3 kinase to induce physiological responses (Wu et al., 2000).

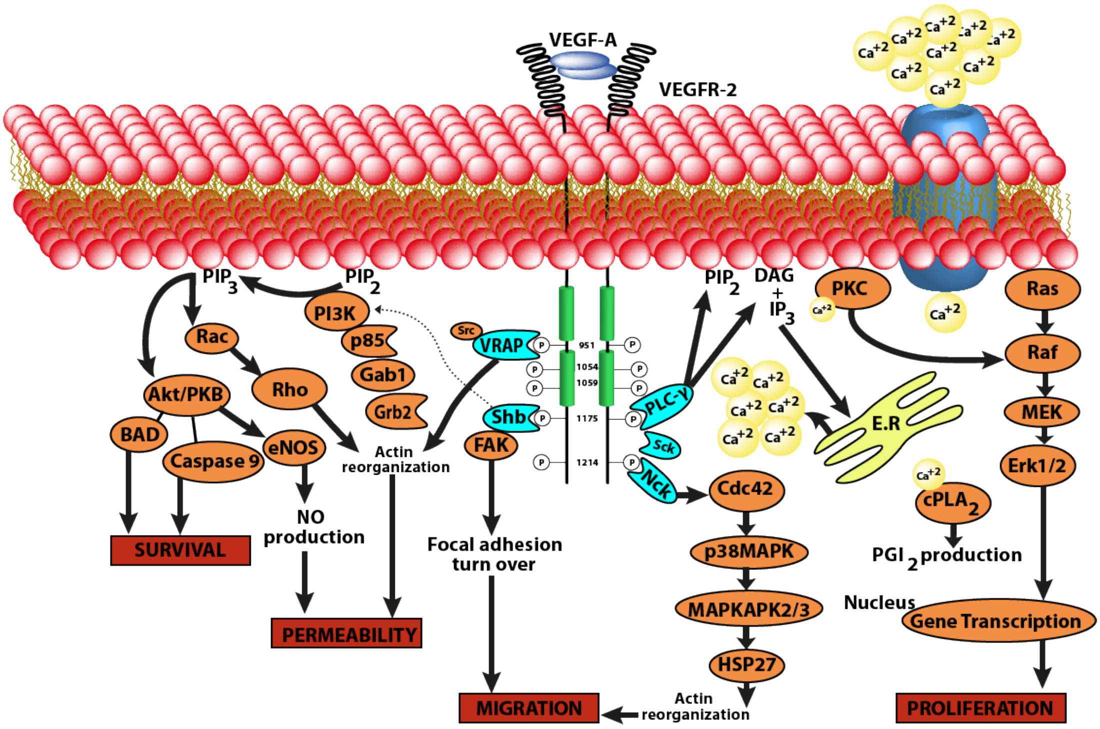

Figure 1.4: VEGFR-2 intracellular signalling

VEGF-A binding to VEGFR2 leads to dimerisation and autophosphorylation at specific tyrosine residues. The resulting downstream signalling cascade stimulates cell survival, permeability, migration and proliferation. Adapted from Holmes et al., 2007.

1.3.5 VEGFR2 and Cell Survival

In a study of HUVECs, VEGF activation of VEGFR2 was able to prevent apoptosis occurring through the activation of the PI3K/AKT signal transduction pathway (Gerber et al., 1998a).

Phosphoinositide 3-kinase (PI3K) is activated in response to VEGFR2 stimulation to catalyse the production of membrane bound phosphatidylinositol (3,4,5)-trisphosphate (PIP_3) from phosphatidylinositol (4,5)-bisphosphate (PIP_2). PIP_3 then engages the AKT PH domain, resulting in the translocation of AKT from the cytoplasm to the plasma membrane and enhances conformational changes that reveal the catalytic kinase core. This prepares AKT for phosphorylation at two regulatory sites. Firstly, phosphorylation of Thr308 within the catalytic domain, which is mediated by phosphoinositide-dependent kinases 1 (PDK 1) (Lawlor and Alessi, 2001). Secondly, the Ser473 in the hydrophobic motif, which has been proposed to occur through phosphoinositide-dependent kinases 2 (PDK 2) (Toker and Marmiroli, 2014, Cantley, 2002). This activated AKT then inhibits two pro-apoptotic proteins, Bcl-2 associated death promoter (BAD) and caspase 9 by phosphorylating them and suppressing apoptosis therefore supporting cell survival (Cardone et al., 1998) (Song et al., 2005). VEGF-A also induces the expression of anti-apoptotic proteins Bcl-2 and A1, which have been shown to play a critical role in mediating the survival of endothelial cells (Gerber et al., 1998a). More recent data has shown that VEGF-mediated activation of the ERK5 kinase is able to regulate AKT phosphorylation and tubular morphogenesis in human endothelial cells (Roberts et al., 2010).

Survival of endothelial cells can also be affected by the surrounding microenvironment of the extracellular matrix. VEGFR2 can interact with integrin $\alpha_v\beta_3$ which results in enhanced VEGFR2 activation and AKT activity (Soldi et al., 1999). Furthermore, VEGF mediated angiogenesis has been shown to induce expression of $\alpha_1\beta_1$ and $\alpha_2\beta_2$ integrins in endothelial cells, which appears to increase angiogenic potential and vessel formation on collagen (Senger et al., 1997).

1.3.6 Cell motility

Cell motility is defined as the ability to move actively while consuming energy resources at the same time. Cell migration is a complex, dynamic process that involves continuous remodeling of the cellular architecture, which is needed in order for the cell to move and adapt to changes in the surrounding environment. Cell migration in a 3D extracellular matrix (ECM) is a multistep process involving changes in the cytoskeleton, cell-substrate adhesions and the extracellular matrix components. Cell migration is generally initiated in response to extracellular stimuli, which can be diffusible factors, signals on neighboring cells, and/or signals from the extracellular matrix. Cell migration is regulated by the coordinated activation of Rho family GTPases (Hall, 1998), which regulate various aspects of cytoskeletal reorganisation. In 1992, Hall and co-workers identified Rho-A as a regulator of lyso-phosphatidic acid (LPA)-mediated actin-stress fibre formation (Ridley and Hall, 1992) and Rac as a regulator of growth factor stimulated lamellipodia (membrane ruffle) formation (Ridley et al., 1992). Later work revealed that, upon activation, Cdc42 induced peripheral actin-rich microspikes (filopodia) and also activated Rac (producing lamellipodia), demonstrating cross-talk within the Rho family (Nobes and Hall, 1995, Kozma et al., 1995). Over the last two decades research has revealed the molecular regulation of Rho family GTPases and cytoskeletal reorganisation leading to cell migration, which can be divided into five separate steps (Lauffenburger and Horwitz, 1996):

1) **Lamellipodia extension at the leading edge**: Lamellipodia consist of branched or unbranched filament networks formed through the actin nucleating activity of the actin-related proteins 2/3 (Arp2/3) protein complex (Pollard et al., 2000). Rac-1 regulates lamellipodia formation in response to growth factors (Hall, 1998). Rac-1 activation is dependent on phosphoinositide 3-kinase (PI3K) activity generating phosphatidylinositol (3,4,5)P_3 (PIP_3) which activates Vav, the Rac guanidine exchange factor (GEF) (Buchsbaum, 2007).
2) **Formation of new focal adhesions complexes:** Extending lammelipodia and filpodia make contact with the ECM via integrin attachment leading to activation of focal adhesion kinase (FAK). FAK is known to regulate Rho-mediated actin stress fibre formation FAK by phosphorylation and activation of p190RhoGEF (Zhai et al., 2003).
3) **Secretion of surface protease to ECM contacts and focalized proteolysis:** In order for cells to migrate it is important to degrade the ECM (Murphy and Gavrilovic, 1999). Activated Rac-1 can induce expression of matrix metalloproteinase (MMP1) in fibroblasts (Kheradmand et al., 1998) and MMP2 in tumour cells (Zhuge and Xu, 2001) facilitating cell migration.
4) **Cell body contraction by actomyosin complexes:** Stress-fibre assembly and contraction are controlled by myosin II and induced by Rho and its important downstream effector, the Rho-associated serine/threonine kinase (ROCK). Rho acts via ROCKs to affect myosin light chain phosphorylation. This generates tension forces which enable retraction of the rear of cell body during migration (Vicente-Manzanares et al., 2008).
5) **Tail detachment:** Cell-substrate linkages are preferentially disrupted at the trailing edge of the cell whereas the leading edge remains attached to the ECM and further elongates (Palecek et al., 1998).

1.3.7 VEGFR2 and Cell Migration

Migration of endothelial cells is one of the key factors in angiogenesis. (Holmes et al., 2007). Angiogenesis only occurs when endothelial cells migrate towards their target. This is controlled by haptotactic, chemotactic and mechanotactic stimuli, which in turn promote cell migration (Lamalice et al., 2007). Chemotaxis is the process by which cells migrate in a directional manner along a gradient of chemoattractant, usually in a fluid phase. One mechanism of chemotaxis is called haptotaxis, which occurs when attractant molecules are attached to a support such as the extracellular matrix (Seppä et al., 1982). In addition, necrotaxis is a special type of chemotaxis, which takes place when chemoattractant molecules are released from apoptotic or necrotic cells. These attractant molecules can influence both cell migration, direction, and speed (Lauber et al., 2003, Zachary, 2003).

Cell migration is a critical component of the angiogenic response as endothelial cells migrate towards growth factors such as VEGF and FGF. The extracellular matrix is critical for stabilising blood vessels through interaction with smooth muscle cells (SMCs), endothelial cells and the basement membrane. These must all be remodelled so that cells can migrate and form new blood vessels during disease and development (Zachary, 2003). This blood vessel interaction can occur by triggered induction of matrix metalloproteinases (MMPs). There are two MMPs, MMP2 and MMP9, that have been shown to play a critical role in enhancing tumour angiogenesis and have been seen to be upregulated along with VEGFR2 in angiogenic lesions (Lee et al., 2005). VEGF receptor-associated protein (VRAP) binds to phosphorylated Y951 of VEGFR2. Its importance has been highlighted as gene ablation of VRAP in mice has been shown to block VEGF-A mediated reorganization of the cytoskeleton and cell migration (Matsumoto et al., 2005). VEGFR-2 also utilises the adaptor protein Shb to regulate cell migration. The Shb protein has been shown to bind to phosphorylated Y1175 in the VEGFR-2 and to regulate activation of PI 3-Kinase and FAK-mediated focal adhesion formation (Holmqvist et al., 2004).

Rho GTPases play a critical role in cell migration and endothelial cell permeability (Wojciak-Stothard and Ridley, 2002). Proteins like Rac1 and RhoA are activated by VEGFR2 phosphorylation at Tyr 951 in response to VEGF-A, which is required for

VEGFR2 mediated endothelial cell migration (Zeng et al., 2002). In addition, a recent study analysing RhoJ, which is known to be expressed in endothelial cells and to regulate endothelial cell chemotaxis (Kaur et al., 2011), reported that RhoJ $^{-/-}$ mice show a reduction in human xenograft tumour growth and diminished tumour vessel density (Wilson et al., 2014).

Phosphorylation of Y1214 on VEGFR2 activation recruits Nck, which leads to the sequential activation of Fyn, and then Cdc42, which in turn activates enhanced stress activated protein kinase, which is also known as p38 mitogen-activated protein kinase (SAPK2/p38 MAPK) leading to actin polymerization and cytoskeleton reorganization in endothelial cells (Lamalice et al., 2004). This leads to phosphorylation of Heat Shock Protein 27 (HSP27) which is an actin capping protein, that once removed allows for actin polymerisation (Lamalice et al., 2007).

Studies in fibroblasts have shown that phosphoinositide 3-kinase (PI3-kinase) plays a critical role in cell migration; through the generation of phosphatidylinositol (3,4,5)-trisphosphate (PIP$_3$)it is able to activate guanosine triphosphate (GTP) binding protein Rac, which results in membrane ruffles and cell motility (Ridley et al., 1992). The Grb2 bound adaptor protein Gab1 has been shown to couple VEGFR2 activation with PI3K/AKT and enhance cellular migration. Gab1 has been demonstrated to bind to the p85 subunit of PI3 Kinase and activate it, although the precise site of interaction with VEGFR2 is unclear (Dance et al., 2006).

Angiogenesis is a complex process that involves the co-ordinated response of endothelial cells to form branched structures. There are two cell types that have been identified to be involved in this process. Firstly, specialised tip cells at the leading front of an angiogenic sprout, form long filopodia in response to VEGF-A. These filopodia are guided by VEGF-A gradients leading to directed migration. Secondly, stalk cells, which sit behind this leading cell, respond to VEGF-A by proliferating rather than migrating. This response is regulated by VEGF-A concentration to enhance stalk cell elongation (Gerhardt et al., 2003). Recent studies in endothelial cells have linked tip cells to increased expression of Delta-like 4 (DLL4). DLL4 is known to be upregulated in response to VEGF signalling in endothelial cells and is induced preferentially in tip cells as they are in contact with the highest levels of VEGF. This membrane bound DLL4 in the tip cell then activates the Notch Receptor, which is expressed by adjacent stalk cells. This Notch signalling then down-regulates the expression of VEGFR2 whilst increasing the expression of VEGFR1, further increasing the VEGF response gap between the stalk and tip cells (Affolter et al., 2009, Tung et al., 2012).

The complex formation of a vessel network is therefore carefully regulated by the specific expression and distribution of VEGF, which is secreted by a wide variety of cells in response to hypoxia and the signalling interactions between DLL4 and Notch that result in endothelial cell migration and tube formation towards hypoxic areas (Fraisl et al., 2009, Affolter et al., 2009).

1.3.8 VEGFR2 Cell Proliferation

VEGFR2 activates cell proliferation via the typical extracellular signal-regulated kinase (Erk) pathway. VEGFR2 signalling occurs through activation of the Raf-1-MEK-MAP kinase cascade, however this seems to be independent of Ras. Studies have shown that dominant negative Ras in primary sinusoidal endothelial cells, did not block VEGF activation of MAP kinase phosphorylation to the same extent as blockade of PKC (Xia et al., 1996). This suggests that VEGF induced activation of Erk is through a PKC-dependent pathway which also includes the activation of PLCγ (Takahashi et al., 1999, Takahashi et al., 2001). Further studies have determined that Ras is linked to proliferation in HUVEC cells via a PKC-dependent pathway. (Meadows et al., 2001, Shu et al., 2002).

Autophosphorylation of Y1175 in the C-terminal tail of VEGF2 results in the binding of PLCγ. Once PLCγ is bound, it is phosphorylated resulting in enhanced catalytic activity. Mutations of Y1175 which block PLCγ binding, significantly reduced MAP kinase phosphorylation and DNA synthesis, suggesting that this interaction is crucial for endothelial cell proliferation (Takahashi et al., 2001).

PLCγ hydrolyses membrane bound PIP_2 to generate diacylglycerol (DAG) and inositol 1,4,5-trisphosphate (IP_3). DAG is a physiological activator of PKC whilst IP_3 production enhances the intracellular calcium concentration by binding to the IP_3 receptor on the endoplasmic reticulum (ER) stimulating release of Ca^{2+} stores. Proliferation in endothelial cells has been linked to several PKC isoforms including α, β and ζ (Xia et al., 1996, Wellner et al., 1999).

1.3.9 VEGFR2 Trafficking and Internalization

Membrane trafficking is important for receptors to detect and respond to external signals (Murphy et al., 2009). Ligand induced activation of receptor tyrosine kinases enhances internalization and trafficking that promotes signalling from plasma membrane and endosomal compartments and ends through lysosomal degradation of the receptor (Horowitz and Seerapu, 2012). Trafficking of VEGFR2 is regulated by different mechanisms to other well-characterised growth factor receptors, e.g. EGFR. VEGFR2 activation occurs by binding VEGF to VEGFR2 which then induces internalization of VEGFR2 by endocytosis. The VEGFR-2 can then be either recycled back to the cell surface, or is delivered to the lysosome for subsequent degradation. Unlike other growth factor receptors, VEGFR2 is constantly cycling between a membrane pool and a cytosolic pool. Receptor tyrosine kinase internalization occurs through the canonical clathrin-dependent endocytic pathway that implicates the small GTP binding protein Rab5 (Goh and Sorkin 2013). VEGFR2 internalisation requires ancilliary proteins such as neuropilin 1 (Soker et al., 1998), synectin (Lanahan et al., 2010), and ephrin-B2 (Sawamiphak et al., 2010). Dephosphorylation of VEGFR2 is regulated by a variety of recently identified phosphatases such as DEP1 (Lampugnani et al., 2003) and VE-PTP, which cause delayed VEGFR2 internalisation (Mellberg et al., 2009).

In vitro studies have revealed that in the absence of VE-cadherin, VEGFR2 undergoes rapid internalisation and is retained in endosomes for longer periods of time (Lampugnani et al., 2006). Further studies suggest that VEGFR2 internalisation may be controlled by another receptor tyrosine kinase, ephrin-B2. Ephrin-B2 located at the tip cell filopodia may regulate activation of VEGFR2 signalling endocytosis to filopodial extension (Sawamiphak et al., 2010).

Stimulation of cells with the NRP-1–binding VEGF-A165 led to sequential NRP-1–mediated VEGFR-2 recycling through Rab5, Rab4, and Rab11 vesicles. Recycling was accompanied by dephosphorylation of VEGFR-2 between Rab4 and Rab11 vesicles. Interestingly, in cells stimulated with VEGF-A165b, an isoform unable to bind NRP-1, VEGFR-2 bypassed Rab11 vesicles and was routed to the degradative pathway specified by Rab7 vesicles (Ballmer-Hofer et al., 2011). Co-localisation of internalised VEGFR-2 with GTPase and Rab7 required for late endosome fusion with lysosomes, indicating that VEGFR-2 was targeted to that compartment rather than to the proteasome (Stenmark, 2009).

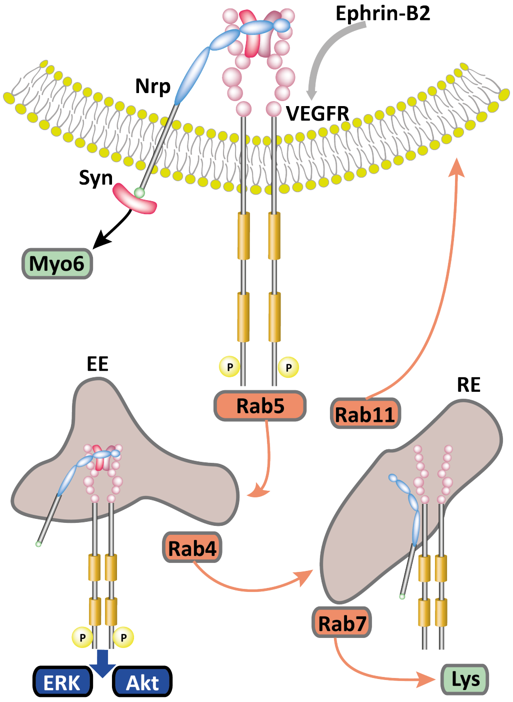

Figure 1.5: VEGFR-2 internalisation

This figure illustrates VEGFR-2 internalisation after VEGF-A by endocytosis. VEGFR2 is mobilised by myosin and cross-linked to neuropilin (Nrp) via synectin and internalises together with Nrp to Early Endosomes (EE) through Rab5. Then early endosomes bring Nrp and VEGF complex to recycling endosomes (RE) through Rab4. Recycling to the cell surface occurs via Rab11 or to lysosomes for degradation through Rab7. This mechanism shows how VGFR signalling from the cell surface via early endosomes results in down-stream activation in Akt and Erk pathways. Adapted from Horowitz and Seerapu, 2012.

1.4 Phospholipases

Phospholipids consist of a fatty acid backbone, phosphate groups, glycerol unit and polar head group molecules. Phospholipase enzymes hydrolyse the membrane phospholipids phosphatidylcholine, phosphatidylserine, phosphatidylglycerol and phosphatidylethanolamine. Phospholipids are hydrolysed by lipolytic enzyme that include: phospholipase A, phospholipase C and phospholipase D, resulting in the conversion of phospholipids into lipid mediators or second messengers that regulate many physiological and pathological cell functions. Dysfunction of phospholipase activity is implicated in diseases such as inflammation and cancer progression (Brown et al., 1993, Flower and Blackwell, 1979).

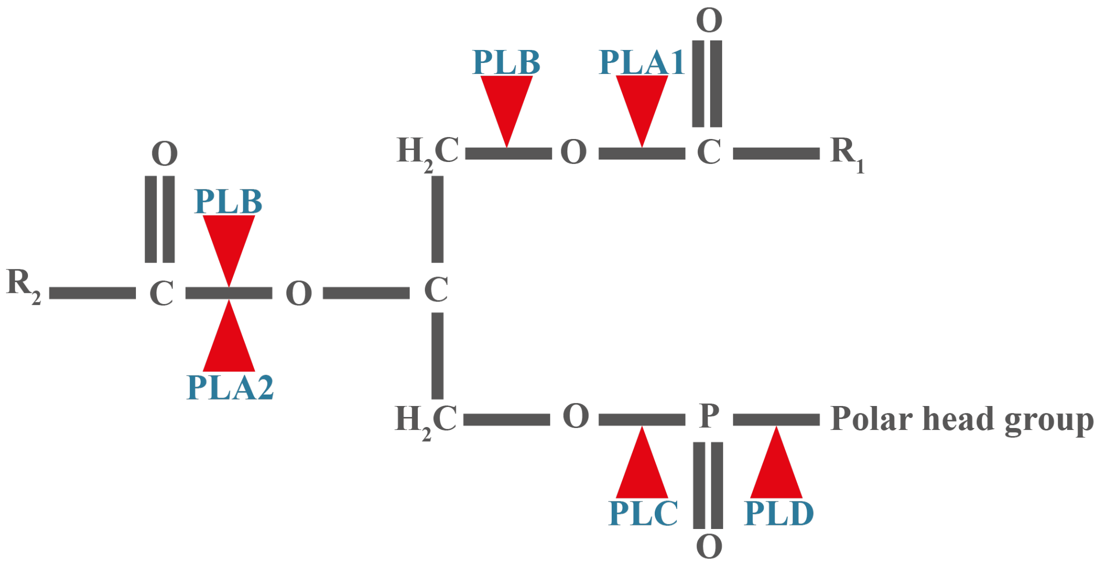

Figure 1.6: Phospholipases

This diagram illustrates the site of action of different phospholipase enzymes in hydrolysing phospholipids. Adapted from Vasudevan et al., 2010.

1.4.1 Phospholipase D

Phospholipase D (PLD) is an enzyme whose key function is to hydrolyse phosphatidyl choline (PtdCho) to produce the signalling molecule phosphatidic acid (PtdOH) and choline (Cho) (Figure 1.7). The PLD reaction activity relies on PIP_2 as a co-factor through conversion of phosphatidylcholine to phosphatidic acid. In the plasma membrane, PIP_2 co-localises with Arf- and Rho-regulated PLD as a result of possible docking of PLD (Hammond et al., 1997). Two mammalian isoforms of PLD have been cloned; PLD1 localized on the long arm (q) of chromosome 3 (3q26)

(Park et al., 1998a) and PLD2 localized on the short arm (p) of chromosome 17 (17p13) (Park et al., 1998b).

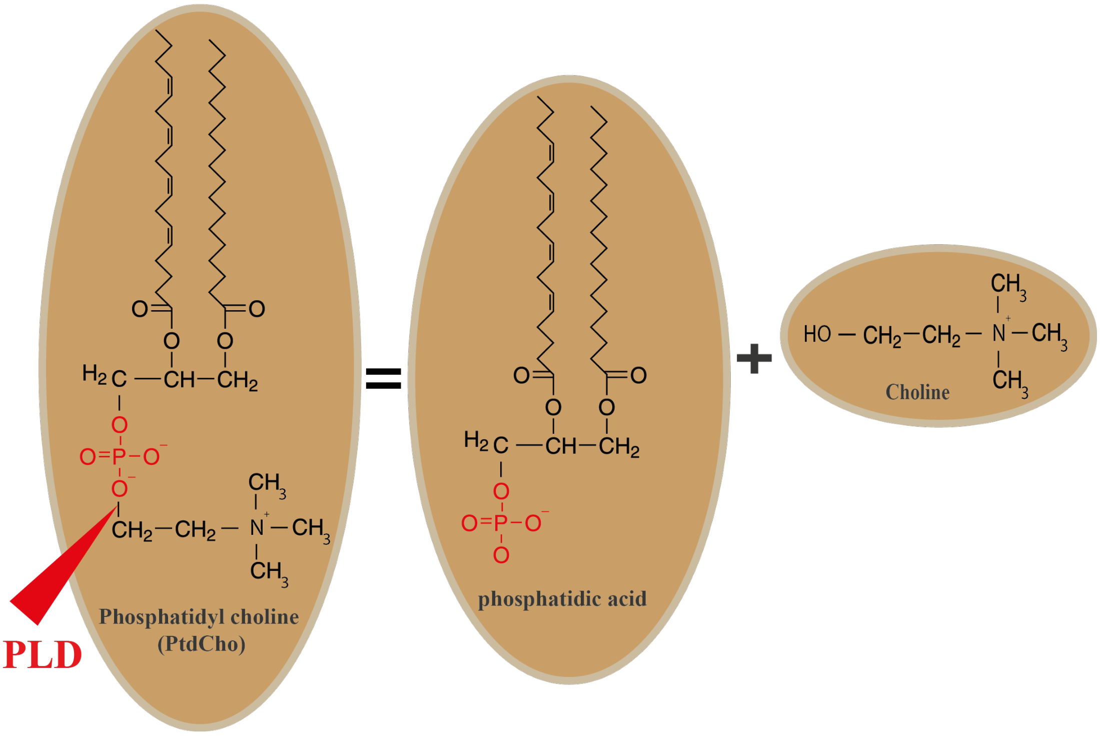

Figure 1.7: Phospholipase D hydrolysis

Phospholipase D hydrolysis of phosphatidylcholine generates phosphatidic acid and choline. Adapted from Formhman and Morris, 1999.

1.4.2 Structure of Mammalian Phospholipase D Isoforms

The first structure for PLD was determined from *Streptomyces* and bacterial endonucleases. The overall structure of PLD is four highly conserved functional and structural domains as illustrated in Figure 1.8 and discussed below.

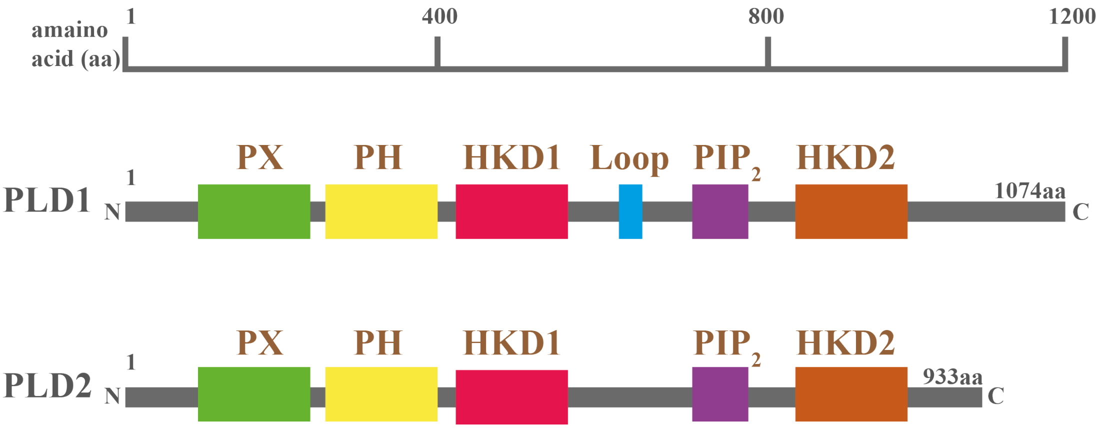

Figure 1.8: Structure and domains of PLD family members

A schematic of mammalian phospholipase D. Top line illustrates amino acid (aa) position. PX, Phox homology domain and PH, Pleackstrin homology domain mediate protein and lipid binding; HKD domain consists of HxKxxxxD/E mediating the catalytic reactions; PIP2, a second phosphatidylinositol 4,5-bisphosphate; Loop domain located in PLD1. Adapted from Peng and Forhman, 2012.

1.4.3 HKD Domain

The PLD superfamily structure possesses two HKD catalytic domains, which are defined by the peptide sequence HxK(x)4D(x)6GSxN. The HKD domains confer strong PLD enzymatic activity and are located in the N-terminal and C-terminal regions (Xie et al., 1998). PLD plays a role in membrane vesicular trafficking and cell signalling. By using site-directed mutagenesis, point mutations in PLD1 suggest the HKD domain and specific serines/threonines in all members of the PLD superfamily are critical for PLD activity and catalytic mechanisms (Sung et al., 1997).

1.4.4 Pleckstrin Homology (PH) Domain

The PH domain is highly conserved between PLD1 and PLD2 and has been shown to be involved in the binding of PIP as well as a number of other proteins. The PH domains of PLD1 and PLD2 have been shown to modulate membrane-recycling machinery. There are two PLD isoforms, *PLD1* and *PLD2*, which share similar domain structures. Both PLD isoform activities rely on PtdIns(4,5)P_2. In addition, high affinity to lipid surfaces containing PtdIns(4,5)P_2 bound to PLD1 indicates a critical role for the PH domain in PLD function.. In summary, the PH domain regulates PLD enzyme activity by mediating interaction with polyphosphoinositide, inducing conformational change, thus regulating catalytic activity (Hodgkin et al., 2000).

PLD generates a lipid-signalling pathway that coordinates membrane trafficking with cellular signalling. Both human and yeast PLD contain N-terminal PH domains that specify both regulation of PLD activity and subcellular localisation through interaction with PtdIns(4,5)P_2. Mutation of PLD PH domains in human and yeast generates active PtdIns(4,5)P_2-regulated enzymes with impaired biological function. Rearrangement of the PH domain of PLD2 causes re-localisation of the protein from PtdIns(4,5)P_2 containing plasma membrane to the endosome (Sciorra et al., 2002). Disruption of the PH domain can be caused by mutations within the PH *in vivo.* As a result, phosphoinositides have a dual role in PLD regulation: stimulation of catalysis mediated by a polybasic motif and membrane targeting mediated by the PH domain (Sciorra et al., 2002).

1.4.5 Phox Homology (PX) Domain

Phosphoinositides are regulators of diverse cellular processes. PX domains are located in a wide range of signalling molecules and bind simultaneously to PtdIns(3)P, PtdIns(3,)P_2, PtdIns(4,5)P_2, PtdIns(3,5)P_2 (XU et al., 2001). PLD facilitates membrane trafficking, and PLD subcellular localisation is regulated by PX, PH domains and PtdIns(4,5)P_2-binding sites critical for PLD activation. In COS-7 cells, PLD co-localises to perinuclear endosomes and the Golgi apparatus. Under stimulation, PLD1 translocates to the plasma membrane and then returns to the endosomes. The PtdIns(4,5)P_2 is known to mediate outward translocation and interaction with the plasma membrane. In the absence of a PX domain, PLD was unable to translocate to the endosomes. The PX and PH domains play a role in internalization; however, the PH domain drives PLD1 to enter into the lipid raft. In comparison, the PX domain mediated binding to PI5P, which is a known lipid recognized to accumulate in endocytosing vesicular trafficking. This study concluded that the PX domain is required for PLD1-regulated exocytosis in PC12 cells (Du et al., 2003).

1.4.6 PLD Expression

Phospholipase D activity was first identified in 1947 in carrots (Hanahan and Chaikoff, 1947) and cabbage leaves (Hanahan and Chaikoff, 1948). The investigation of PLD over the past 60 years has demonstrated many physiological functions such as cardiac and neuronal roles as well as implications in the development of disease. PLD has been shown to be expressed and extracted from rat liver, heart, lung, testis and brain (Bocckino et al., 1991). Currently, specific monoclonal antibodies are commercially available for PLD1, though, due to the lack of a good commercial antibody for PLD2, studies rely on mRNA analysis (Scott et al., 2009).

1.4.7 Animal Knockouts of PLD1 and PLD2

PLD1 knockout mouse models have increased platelet aggregation leading to stroke or myocardial infarction, indicating that PLD1 is an essential regulator of platelet activity in cardiovascular or cerebrovascular diseases (Elvers et al., 2010). In addition, recent studies using PLD1 knockout mice have shown a decrease in starvation-induced autophagosome expansion, which indicates that the PLD1 pathway modulates macroautophagy (Dall'Armi et al., 2010). PLD2 knockout mice identified a critical role for PLD2 in Alzheimer’s disease, suggesting that drugs targeting PLD2 could be a viable therapy target for neurodegenerative disease (Oliveira et al., 2010). Other reports on PLD2 knockout mice have reported normal development with the use of specific PLD inhibitors allowing the identification of PLD1 as a regulator of phorbol-ester-, chemoattractant, adhesion-dependent and Fcγ-receptor-stimulated production of reactive oxygen species (ROS) in neutrophils (Norton et al., 2011).

1.4.8 Physiological Role of PLD1 and PLD2

The physiological role of PLD1 and PLD2 in cell function is based on siRNA knockdown, which established different functions for PLD1 and PLD2. The mammalian target of rapamycin (mTOR) regulates cell proliferation via ribosomal S6 kinase 1 (S6K1) (Fang et al., 2003). This study identified phosphatidic acid (PA) as a mediator of the mTOR pathway and proposed PLD1 as an upstream regulator of mTOR. Overexpression of PLD1 increased S6K1 activity in serum-stimulated cells and, in contrast, knockdown of PLD1 in both HEK293 and COS-7 cells showed reduced cell size suggesting a critical role in cell growth. This study revealed that PLD1 was involved in the mTOR pathway and cell size control, suggesting a molecular mechanism for Cdc42 activation of S6K1, thus proposing a new signalling cascade to connect mitogenic signalling to the mTOR pathway through PLD1and Cdc42 (Fang et al., 2003).

Generally, PLD is involved in multiple types of membrane vesicle trafficking signalling. Studies utilising overexpression of human PLD1 have reported localisation in the Golgi apparatus and perinuclear vesicles (Colley et al., 1997, Toda et al., 1999, Lucocq et al., 2001). In overexpression mouse studies, PLD2 was localized to the plasma membrane. Under serum stimulation conditions, internalisation of membrane vesicles occurs. In addition, overexpression and siRNA of PLD2 revealed that PLD2 blocks angiotensin II receptor internalization at the plasma membrane (Du et al., 2004).

PLD activity generates phosphatidic acid and choline, which is implicated in the regulation of cytoskeleton reorganization. Mast cells stimulated with antigen also illustrate cytoskeleton rearrangement. By using butan-1-ol, which diverts the production of PA generated by PLD to the corresponding phosphatidylalcohol, butan-1-ol inhibited antigen-stimulated membrane ruffling (O'Luanaigh et al., 2002). Blocking by butan-1-ol was reversible, and the activation of PLD by antigen was required for PA production through membrane ruffling. Activation of PLD2 is essential for PIP_2 generation, which regulates actin cytoskeleton rearrangement (O'Luanaigh et al., 2002). This is further supported by the work of Cross et al., who have shown a role for PLD in actin stress fibre formation and cytoskeletal rearrangement in endothelial cells (Cross et al., 1996). Both PLD1 and PLD2 are implicated in the control of the small GTPases, ARF and Rho. A recent review proposed that PLD2 plays a critical role in Rho function, where PLD1 activity is downstream of this activation (Rudge and Wakelam, 2009). A recent report by Powner et al., has concluded that PLD-derived PA regulates integrin activation and the propensity of the cell to adhere to the substratum (Powner et al., 2007).

1.4.9 Mammalian PLD Activities

PLD catalyses the transphosphatidylation reaction, utilizing primary alcohols as a nucleophilic acceptor with a greater affinity than water in the production of phosphatidylalcohols, indicating that PLD plays multiple roles in controlling secretion and membrane trafficking (Frohman and Morris, 1999). To understand PLD activity, many studies have identified phosphatidylalcohol formation as a biological marker for the function of PLD and phosphatidic acid (PA).

Additional studies have investigated stimuli such as phorbol esters, growth factors, GPTγS, FMLP, serum and ATP epinephrine to show activation of PLD activity, whereas PLD facilitates the degradation of phosphatidic acid and PtdCho in diacylglycerol pathways. In addition, a clear link demonstrated PLD hydrolysis of phosphatidylcholine and an increase in phosphatidic acid, which clarified that PLD was not involved in the phospholipase C pathway (Frohman and Morris, 1999).

1.4.9.1 Receptor Tyrosine Kinases and PLD

In many cell types, PLD has been activated by a wide variety of cytokines and growth factors, hormones and neurotransmitters. These growth factors act through cognate membrane receptors coupled to G-proteins whose final concentration stimulates downstream signalling cascades. Specifically, the receptor tyrosine kinase has been implicated to regulate PLD phosphorylation. In HUVEC, VEGFR2 co-localized in the endothelial caveolae with PLD2 and Ras, which, in turn, suggests that PKC and PLD responded to VEGF stimulation and activate MEK and ERK pathways involved in the regulation of cellular function (Cho et al., 2004).

1.4.9.2 Signalling Proteins such as PKC

Phorbol esters stimulate activation of PKC in a range of cell types (Castagna et al., 1982). Down-regulation of PKC isoforms by chronic exposure to phorbol esters leads to reduced PLD activity in most mammalian cells (Exton, 1997). In addition, there are three isoforms of PKCα: β or γ stimulated by DAG, Ca^{+2} and PtdSer.

1.4.9.3 Phosphorylation of PLD

Selective inhibitors for tyrosine kinase have also implicated these kinases in the activation of PLD by agonists acting via these receptors that couple to G-protein. Vanadate, an inhibitor of tyrosine phosphatases (Weiser and Shenolikar, 2003), inhibited the activation of PLD by ATP in the human promonocytic leucocyte line (U937) (Dubyak et al., 1993). In addition, in Swiss 3T3 fibroblast cells, the effect of PKC down-regulation indicated that protein-tyrosine kinase and PKC participate to induce PLD activation in these cells (Kim and Exton, 1998).

PLD phosphorylation has been identified to work indirectly and directly in regulating PLD (McDermott et al., 2004). Many studies have reported that PLD activation used a wide variety of growth factors, such as FGF, IGF-I and FGF-2, in *vitro* and in *vivo*. Using a selective inhibitor for protein kinase C, this study reports that the activation of EGF, IGF-I and bFGF stimulates PLD activity (Rydzewska and Morisset, 1995). Interestingly, EGF stimulates both PLD isoforms 1 and 2, whereas EGFR has been reported to induce phosphorylation only with PLD2 at the Tyr11 residue of PLD2 following EGF stimulation (Slaaby et al., 1998).

1.4.10 Intracellular localisation of PLD

Phospholipase D1 and 2 have been expressed in many cells and tissues (Meier et al., 1999). In MDCK-D1 cells, PLD activity has been characterised in the nuclei (Balboa and Insel, 1995), and has also been shown to be located in the Golgi complex, indicating a possible link between transport events and the lipid bilayer (Ktistakis et al., 1995). Furthermore, analysis of rat tissue samples has revealed that PLD is present in all tissue fractions with the highest activity in the spleen, lung and kidney. In subcellular fractions of rat liver, PLD activity was increased in all tissue compartments using GTP except microsomes and mitochondria, which showed low activity (Provost et al., 1996).

Additional studies have shown the regulation of PLD by small GTP-binding proteins in a HL60 membrane study, which was activated by GPTγS and confirmed the critical role of phosphatidylinositol(4,5)P_2. This molecule is stimulated by small GTP-binding protein, which indicates that PLD activity plays a critical role in the action of the ADP-ribosylation factor (Arf) (Brown et al., 1993). In another study, PLD expression was purified from pig brain, where it was localised in membranes, and showed an increase in activity by Rho, ARF, and PtdIns(4,5)P_2, indicating localisation in the cell membrane and suggesting a link for the physiological regulation of PLD (Brown et al., 1995). Phosphorylation of cofilin by LIM-Kinase1 caused relocalisation of PLD1 from the intracellular compartment to the plasma membrane (Han et al., 2007). Furthermore, in a study on human parotid duct cells, PLD was determined to be involved in the formation of Golgi-associated clathrin-coated vesicles and in the structure of the Golgi apparatus (de Souza et al., 2014). A recent review showed that PLD1 is mostly localised in the endosome, Golgi apparatus, secretory granules and lysosome compared to PLD2, which is localised at the plasma membrane, indicating different physiological roles for phospholipase D isoforms (Peng and Frohman, 2012).

1.4.11 Phospholipase D Inhibitors

Due to the lack of commercial inhibitors, most studies of PLD inhibition depend on primary alcohols, for instance butan-1-ol, which prevents phosphatidic acid generation. The chemical reaction of PLD with primary alcohols causes transphosphatidylation, generating a phosphatidylalcohol alternative instead of phospatidic acid owing to the fact that primary alcohols are stronger nucleophilic acceptors in the transphosphatidylation reaction than water. The discovery of specific small molecule PLD inhibitors is essential for the PLD research field. A selective inhibitor called 5-fluoro-2-Indolyl des-chlorohalopemide (FIPI) has demonstrated the effective inhibition of PLD and prevents cell spreading, chemotaxis and cytoskeletal reorganization (Su et al., 2009, Monovich et al., 2007). Another PLD1 and PLD2 is halopemide, which is used therapeutically in psychiatric disorders and can inhibit dopamine receptors. Both inhibitors have been proposed as part of a novel approach for the treatment of cancer (Scott et al., 2009).

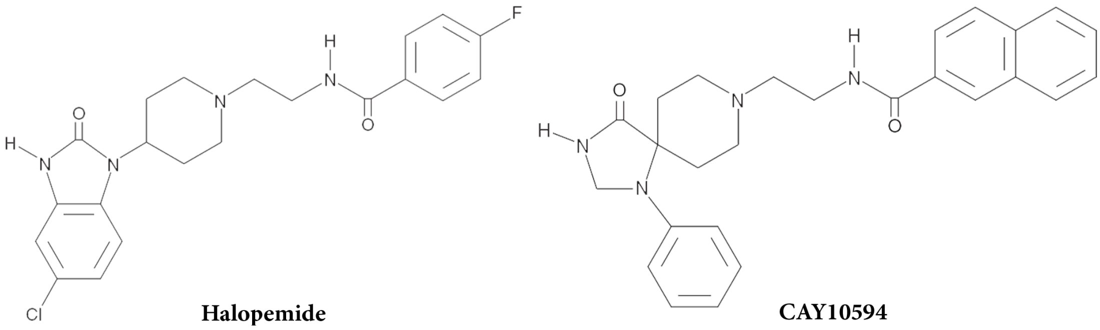

Halopemide **CAY10594**

Figure 1.9: Phospholipase D inhibitors structure

This figure illustrates PLD structure. Halopemide is a potent inhibitor of PLD1and PLD2 inhibiting both human PLD1 and PLD2 *in vitro*. CAY10594 is a potent inhibitor of PLD2, inhibiting human PLD2 *in vitro*. Adapted from Scott et al., 2009.

1.4.12 Phospholipase D in Cancer and Tumour Angiogenesis

Recently, research on phospholipase D and cancer has increased significantly. Breast cancer research has shown that PLD2 activity is involved in cell migration and in the growth and development of breast lung metastases *in vivo*. In the breast cancer model (MDA-MB-231), lentiviral-mediated PLD2 knockdown of cell followed by xenografts in mice indicates a reduction by about 65% of tumour compared to controls (Henkels et al., 2013). In support of a role for PLD2 in cancer, overexpression of PLD2 in breast cancer cells (MCF-7) using a retroviral vector followed by tumour xenografts in mice resulted in overgrowth and development of lung tumours (Hsu et al., 2010). Taken together this data implicates PLD2 in the development of metastasis and development of breast cancer, thus highlighting its potential as a selective therapeutic target (Hsu et al., 2010).

1.4.13 Phospholipase D and Endothelial Function

PLD has been demonstrated in many studies to play a critical role in endothelial cell function. A study carried out on bovine pulmonary artery endothelial cells (BPAEC) showed a breakdown of phosphatidylcholine (PC) following stimulation with purinergic agonist (Martin and Michaelis, 1989). A study using HUVECs showed for the first time that PLD could be involved in mediating endothelial cell responses to tumour-secreted VEGF, especially cytoskeletal reorganisation and endothelial cell migration (Seymour et al., 1996). Analysis of FGFR-1 signalling in PAE cells revealed that FGFR-1 mutation of Y766F, which prevents PLC-gamma binding and subsequent activation of PLC, resulted in a loss of both PLD and PLA_2 activity (Cross et al., 2000). A study of bovine pulmonary artery endothelial cells (BPAECs) suggests that PLD could play a critical role in vascular endothelial cell lipid signalling function and cardiovascular diseases (Sherwani et al., 2013). In human pulmonary artery endothelial cells (HPAECs), it has been shown that a signal cascade initiated by sphingosine 1-phospahate (S1P) leads to the activation of the PLD2 pathway, suggesting PLD2 plays a critical role in stimulating the migration of lung endothelial cells (Gorshkova et al., 2008). Another study showed that PLD signalling in mercury-induced endothelial dysfunction was an indicator for many heart diseases (Hagele et al., 2007). Endothelial cells function as a regulator of thrombosis, inflammatory disease and haemostasis by secreting various factors such as von Willebrand Factor (vWF). A study has shown that PLD1 regulates vWF secretion by translocating PLD1 to the plasma membrane upon stimulation of the endothelium (Disse et al., 2009).

1.5 The Regulator of Calcineurin (RCAN1)

1.5.1 The Discovery of RCAN1

The three members of the regulator of calcineurin (RCAN) family were first identified by the group of Estivil in 2007 (DSCR1/RCAN1) RCAN1, RCAN 2 and RCAN3. RCAN1 was originally named Down Syndrome Critical Region 1 (DSCR1) due to its location on chromosome 21 from region 21q22.1-q22.2; trisomy of chromosome 21 results in Down Syndrome (Fuentes et al., 1997, Davies et al., 2007). RCAN1 is a protein containing an acidic domain with serine-proline motif, a putative DNA binding domain and a proline-rich region that may bind to SH3 domains. This could suggest that RCAN1 is involved in signal transduction and activation of transcription factors. RCAN1 is extensively expressed in the heart and brain. Furthermore, overexpression of RCAN1 suggests a role in mental retardation and cardiac defects in patients with Down syndrome (Fuentes et al., 1995).

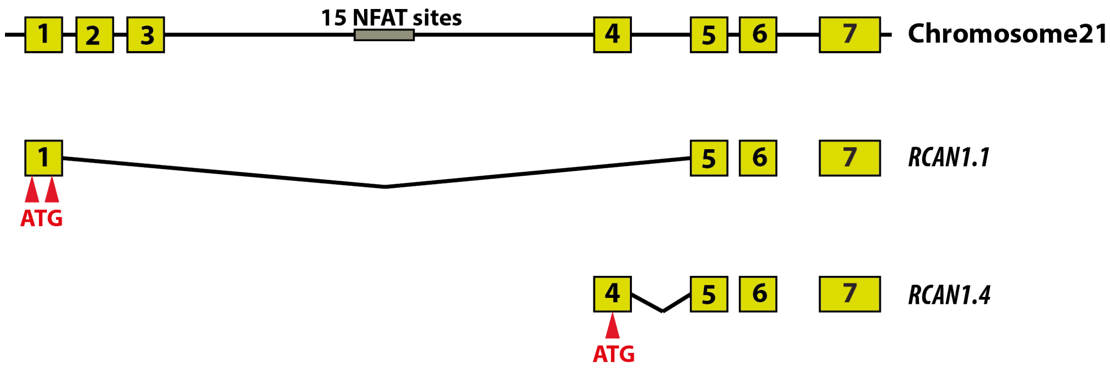

Figure 1.10: The exon structure of the human *RCAN1* isoform

Exon structure of RCAN1, illustrating the alternative first exons used by RCAN1.1 and RCAN1.4 isoform. Adapted from Holmes et al., 2010.

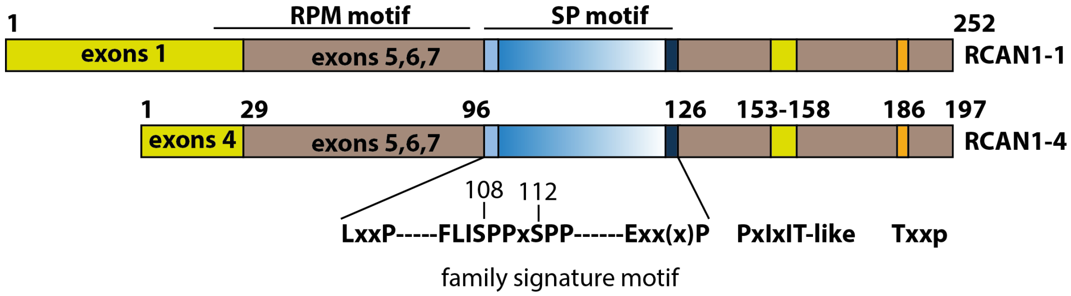

Figure 1.11: Structure of RCAN1

This figure illustrates the major RCAN1 family protein isoforms and protein motifs.. RPM=(RNA recognition motif); SP=(serine/proline) motif incorporating the LxxP. Family signature and ExxP domains = PxIxIT-like domain and TxxP motif. Adapted from Pritch and Martin, 2013.

RCAN1 has also been termed Adapt 78 (Crawford et al., 1997) myocyte-enriched calcinurin interacting protein 1 (MCIP1) (see Table 1.1). Muscle differentiation results in expression of RCAN1 and inhibition of the calcineurin pathway, which can regulate hypertrophic growth in striated muscles (Rothermel et al., 2000).

Down syndrome results from trisomy of chromosome 21 resulting in an extra copy of this chromosome. Patients with Down syndrome display congenital heart malformation and mental retardation (Baird and Sadovnick, 1987). Down syndrome also involves other clinical features such as immune system defects, gastrointestinal anomalies and Alzheimers disease. Overexpression of RCAN1 in the brain in Down syndrome leads to interaction with calcineurin A, a protein phosphatase. This study revealed that overexpression of RCAN1 inhibited calcineurin activity and subsequent nuclear translocation of NFAT affecting numerous cell functions (Fuentes et al., 2000). The physiological role of RCAN1 is to protect cells against numerous cell stress, such as reactive oxygen species and increased calcium signalling (Porta et al., 2007).

Table 1.1 Overview of historical RCAN1 Gene Names

Name	Source
The *RCAN1* gene	
DSCR1	*Homo sapiens*
	Saccharomyces cerevisia
	Caenorhabitis elegans
Dscr1	*Mus musculus*
Adapt78	*Criceltulus griseus*
	Homo sapiens
MCIP1	*Mus musculus*
	Homo sapiens
Calcipressin 1 (Csp1, CALP1)	*Homosapiens*
RCAN1, Rcan1p	*Saccharomyces cerevisia*
CBP1	*Cryptococcus neoformans*
RCN-1	*Caenorhabitis elegans*
Nebula (nla)	*Drosophila melanogaster*
Sarah (sra)	*Drosophila melanogaster*
RCAN1	*Homo sapiens*
The *RCAN2* gene	
ZAKI-4	*Homo sapiens*
Dscr111	*Mus musculus*
MCIP2	*Mus musculus*
Calcipressin 2	*Mus musculus*
The *RCAN3* gene	
DSCR1L2	*Homo sapiens*
Dscr112	*Mus musculus*
RCAN3	*Homo sapiens*

This table is adapted from Davies et al., 2007.

1.5.2 Regulation of RCAN1 expression

Alternative first exons, allowing the generation of different isoforms, which show different patterns of expression and regulation (Fuentes et al., 1997). Exon one gives rise to the isoform RCAN1.1 (Genescà et al., 2003). Exon two lacks a methionine start site required for translation, and exon three encodes only three amino acids. Exon four gives rise to the isoform RCAN1.4 and is under the control of calcineurin responsive promoter, comprising multiple consensus binding sites for the transcription factor of activated T-cells (NFAT) (Yang et al., 2000) GATA-2/3 sites (Minami et al., 2004). Five consensus binding sites for activator protein 1 (AP-1) transcription factors have been identified in the region flanking exon four (Zhao et al., 2008). Recent data has shown that the CCAAT/enhancer binding protein beta (C/EBPbeta) cooperates with NFAT to control expression of the calcineurin regulatory protein RCAN1-4 (Oh et al., 2010).

1.5.3 Role of RCAN1 in Regulating Intracellular Signalling

Endothelial cells are involved in vascular disorders involving inflammation, atherosclerosis and tumour growth (Hesser et al., 2004). Microarray analysis revealed that upregulation of RCAN1.4 was stimulated by VEGF and thrombin providing a negative feedback regulator of the Ca^{+2} /calcineurin/ NFAT signalling pathway. *In vivo* experiments have shown overexpression of RCAN1.4 reduced vascular density and melanoma growth in an animal human tumour xenograft model, suggesting a negative feed-back loop of RCAN1.4 induction and inhibition of NFAT pathway signalling (Minami et al., 2004).

A recent study has investigated the role of c-Jun in the regulation of ER stress using Thapsigargin (an inhibitor of sarco/endoplasmic reticulum Ca^{+2} ATPase). This study revealed that c-Jun, a down stream target of the JNK signalling pathway upregulates RCAN1 expression in response to thapsigargin-induced endoplasmic reticulum (ER) stress and contributes to protection against thapsigargin-induced cell death (Zhao et al., 2008).

Furthermore, the role of RCAN1 *in vivo* has been identified in $RCAN^{-}/^{-}$ mice where gene knockout of RCAN1.4 and RCAN1.1 resulted in no anatomical abnormalities (Hoeffer et al., 2007). In addition, a recent study with $RCAN^{-}/^{-}$ mice focussing on tumour angiogenesis identified hyperactivation of the calcineurin/NFAT pathway in endothelial cells from these mice resulting in endothelial cell apoptosis. This finding lead to decreased tumour angiogenesis in a murine tumour xenograft (Ryeom et al., 2008). Recently, a study reported overexpression of RCAN1 in mice protects against post-ischaemic neuronal injury (Brait et al., 2012). Several studies have been reported that RCAN1 is also regulated via phosphorylation at multiple sites, which modulate its calcineurin binding activity leading to subcellular localisation and a decrease in RCAN1 half-life (Genescà et al., 2003).

1.5.4 Calcineurin

Calcineurin (CN), also called protein phosphatase 2B, is a heterodimeric Ca2+/calmodulin-dependent serine/threonine protein phosphatase composed of CNB regulatory and CNA catalytic subunits (Rusnak and Mertz, 2000). Originally identified in the brain, CN was later found to play a critical role in T cell function, through activation of nuclear factor of activated T cell-mediated transcription of cytokine genes, including the IL-2 gene (Snyder et al., 1998). Calcineurin is a target for the immunosuppressants, cyclosporin A and FK506, which associate with immunophilins and bind to and inactivate calcineurin. More recently, calcineurin has been shown to play an important role in CNS functions, including neurite extension, synaptic plasticity and learning and memory (Winder and Sweatt, 2001, Zeng et al., 2001).

Calcineurin has been implicated in the development of cardiac hypertrophy (Wilkins et al., 2004). RCAN1.4 binds the catalytic domain of calcineurin and inhibits its activity. RCAN1.4 is phosphorylated by MAPK and glycogen synthase kinase 3 (GSK-3) and allows phosphorylated RCAN1.4 to act as a substrate for calcineurin (Vega et al., 2002). Overexpression of RCAN1 protein inhibits calcineurin in the nanomolar range, acting similar to the pharmacological agents FK506 and Cyclosporin A (Chan et al., 2005).

1.6 VEGFR2 and RCAN1 Signalling

The first study showing VEGF-stimulated regulation of RCAN1 looked at genome analysis and identified RCAN1.4 to be significantly induced by VEGF (Hesser et al., 2004). RCAN1 acts on calcineurin signalling by blocking dephosphorylation of nuclear factor of activated T-cell (NAFT) preventing nuclear translocation (Hesser et al., 2004). Studies in HDMECs have shown that cyclosporin prevented VEGF-mediated induction of RCAN1.4 and that siRNA mediated silencing of RCAN1.4 increased the expression of NFAT-regulated genes such as *COX-2* and *IL-8* (Holmes et al., 2010). However, this study also reported that PMA-stimulated RCAN1.4 expression was not blocked by pre-incubation with cyclosporine but was blocked by pre-incubation with the PKC inhibitor GF 109203X (Holmes et al., 2010). To confirm this finding, siRNA-mediated silencing of multiple PKC isoforms revealed that silencing of PKC-delta expression blocked VEGF-stimulated RCAN1.4 expression. This data suggests that in addition to the classical PLC-gamma mediated hydrolysis of PIP_2, generating an intracellular increase in Ca^{2+} and subsequent activation of calcineurin/NFAT resulting in RCAN1.4 expression, an additional pathway from DAG-mediated PKC-delta activation also regulated RCAN1.4 expression suggesting the existence of an NFAT-independent pathway leading to RCAN1.4 expression. Interestingly, it has been shown that the CCAAT/enhancer binding protein beta (C/EBPbeta) cooperates with NFAT to control expression of RCAN1.4 (Oh et al., 2010).

Analysis of endothelial cell function has revealed that siRNA mediated silencing of RCAN1 results in disrupted VEGF-mediated tubular morphogenesis and cell migration (Holmes et al., 2010). Endothelial cells isolated from RCAN1 -/- mice show increased apoptosis (Ryeom et al., 2008), suggesting that RCAN1.1 and RCAN1.4 function to negatively regulate the calcineurin/NFAT pathway in endothelial cells.

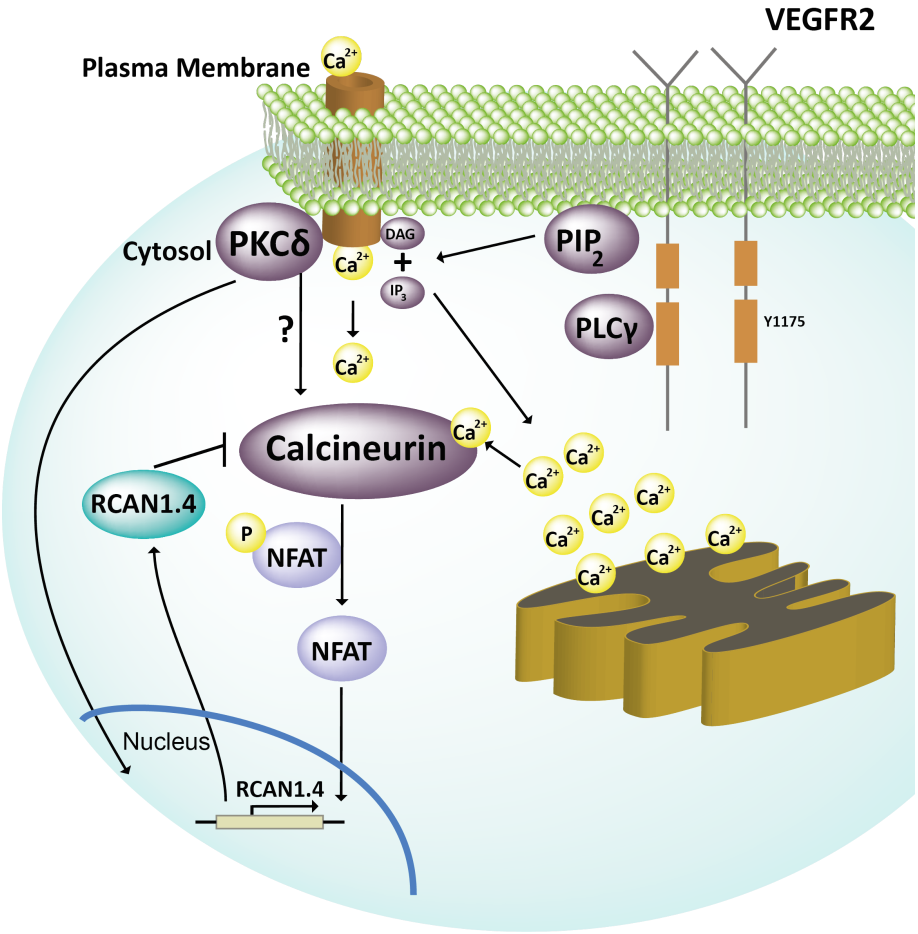

Figure 1.12: Overview of RCAN1.4 regulation pathway

VEGFR2 activation leads to PLC-γ activation and an increase in intracellular Ca^{2+} that causes activation of calcineurin and NFAT that enhance RCAN1.4 expression to increase. VEGFR2 activation results in phosphorylation of PKCδ, which contributes to the up-regulation of RCAN1.4 through an unknown pathway. RCAN1.4 acts to regulate VEGFR2 mediated tubular morphogenesis and migration. Adapted from Holmes et. al 2010.

1.7 Human Dermal Microvascular Endothelial cells (HDMECs) as a Model Cell Line

In vitro culture of endothelial cells from human dermal microvascular endothelial cells (HDMECs) has provided a suitable model for investigation of microvascular behaviour and functions having a broad range of applications such as tumour metastasis, cell differentiation, cytokine expression, haemorrhagic disorder, thrombosis, and hypersensitivity (Florey, 1966, Simionescu and Simionescu, 1992, Miyasaka and Tanaka, 2004, Förstermann and Münzel, 2006). In this current study

HDMECs were utilised as a model for *in vivo* vascular physiology. HDMECs keep their cobblestone morphology and endothelial characteristics from passage one until passage twelve. Studies in microvascular endothelial cells and pulmonary artery endothelial cells show cellular junction formation and permeability is preserved in multiple passaged cells (Kelly et al., 1998). The characteristic morphology of HDMECs is normally assessed by immunofluorescence using specific markers for endothelial cells such as CD-31, VEGFR2 and von-Willebrand factor. Furthermore, HDMECs form capillary–like tubes within 4-6 hours when overlaid with a collagen matrix and stimulated with VEGF-A (Roberts et al., 2010). Overall, these cells provide a suitable model in which to study vascular physiology and angiogenesis.

1.8 Aims of the thesis

Previous work within the group has identified a role for RCAN1 in regulating VEGF-mediated gene expression and ultimately cell migration (Holmes et al., 2010). Cell migration is a critical component of the angiogenic response and deregulation of RCAN1 signalling could have profound implications for both physiological and pathological angiogenesis. The initial aim of this thesis was to identify the mechanism by which RCAN1 regulated VEGF-mediated migration by studying effects on VEGFR-2 activation and downstream signalling. This would utilise both siRNA to target RCAN1.1 and RCAN1.4 and adenoviral mediated overexpression of the RCAN1.4 isoform. By analysing effects of other growth factors, the specificity of RCAN1 for regulating VEGF signalling will also be analysed. The second aim was to determine the role of RCAN1 in affecting the ability of endothelial cells to undergo tubular morphogenesis and vascular sprout formation using 3D spheroid assays. The final aim of the thesis was based around analysing the role of PLD activity in endothelial cells as this phospholipase has not been studied in any detail with respect to endothelial cell function.

Chapter 2

Materials and Methods

2.1 Materials

All materials listed in every experimental protocol

2.2 Reagents

All reagents were obtained from Invitrogen (Paisley, U.K), Peprotech EC (Rocky Hill, NJ, U.S.A), R&D System Inc. (Minneapolis, MN, U.S.A), Sigma Aldrich (Dorset, UK), GE Healthcare (Amersham, U.K), Greiner Bio one (Stonehouse, U.K) Fisher Scientific (Loughborough, U.K) unless stated otherwise.

2.3 Equipment

Table 2.2: Equipment

Equipment	Manufacture and Model
Cell culture hoods (1)	TriMAT^2 Class I, BS5726, CAS, Manchester,UK
Cell culture hoods (2)	ESCO Class II, BSC
Cells culture incubators	SANYO MCO-18 AIC, Loughborough, U.K
Cold Centrifuge	Sigma, 3k30C, Philip Harris
Centrifuge	Spectrafuge 24D, JENCONS-PLS
Sonicator	MSE Soniprep 150
Heating mixer	Thermomixer comfort, Eppendorf
Heating block	PCH-1, Grant, Bio, Scientific Laboratory Supplier
Nano Drop	NanoDrop®, Spectrophotometer ND-1000
q-RT-PCR	ABI Prism®, 700 Sequence Detection System
PCR machine	GeneAmp® PCR system 9700, Applied Biosystems
Gel system	Invitrogen
Gel power pack	Invitrogen
-80˚ Freezer	SANYO, VIP Series
Balance	Acculab, Sartorius group
Vortex	Stuart, BioCote
Centrifuge rotors	MSE, Mistral 2000
Waterbath	Clifton, Nickel-Electro, LTD
Cell Microscope	Nikon, Eclipse-TS100
Imaging unit	Nikon, Digital Sight
Fluorescence microscope	Axio Observer Zesis microscope
Aspirator	VASCUSAFE Comfort, IBS Integra, Biosciences
Autoclave	Priorclave EV150
Liquid Nitrogen	State Bourne, Biorack 3000

2.4 Solutions

The solutions used are described in Table 2.3. Water was ultra deionized 18.2 megohm H_2O as the standard solution applied unless otherwise stated.

Table 2.3: Solutions

Buffer	Composition
LB	20g LB Broth, 1 litre ddH_2O
MOPS buffer Running buffer (WB)	(209.2g MOPS, 121.2g Tris, 800ml ddH_2O), 6g EDTA, 20ml (20%SDS) ≈ 100 dH_2O
SDS-Page Tank Running Buffer for(WB)	30g/l Tris, 144 g/l Glycine, 50 ml SDS (20%)
Transfer buffer for (WB)	18.2 g Tris, 90 g Glycine, 100ml Methanol and dH_2O 380ml
X10 Tris Buffer Saline (TBS)	24.2g/l Tris, 80g/l NaCl, 950ml dH_2O, pH7.6
TBST	1L 1X TBS+ 10ml (10%Tween)
5% BSA Blocking buffer for (WB)	25g BSA+ 500ml 1X TBST
2% BSA Blocking buffer for (WB)	10g BSA+ 500ml 1X TBST

2.5 Cell Culture

2.5.1 Cell Lines and Primary Cells

Table 2.4: Cell Lines used in this Study

Name	Cell type	Source
HDMEC	Human Dermal Microvascular Endothelial Cells Juvenile cells established from a 3 year old male Caucasian (Lot Number 6060707.1).	PromoCell (C-12210) (Heidelberg, Germany)
NHDF	Normal Human Dermal Fibroblast Cells Juvenile cells established from a 5 year old male Caucasian (Lot Number 0083002.2)	PromoCell (C-12300) (Heidelberg, Germany)
A375	Malignant Melanoma Cells	ATCC (CRL-1619)
MAE wt	Mouse Aortic Endothelial Cells	Angio-proteomie (cAP-m0001)
HEK293a	Human Embryonic Kidney Cells	Life Technology
HeLa	Cervical Cancer Cells	Sigma -12B006

2.5.2 Cell Culture Technique

All work was carried out in a sterile cell culture hood. Media was warmed in the water bath at 37˚C before use. All cells were cultured in a 37˚C incubator, with an atmosphere of 5% CO_2 and a humidified environment.

2.5.3 Culture of HDMECs

Human Dermal Microvascular Endothelial Cells (HDMECs) were cultured on gelatin coated 10cm dishes (Greiner, #664160). Gelatin (Sigma #G1890) was made up as a 1% (w/v) solution, in dH_2O and autoclaved prior to use. Dishes were coated for approximately 15 minutes in a 37˚C incubator and gelatin aspirated off immediately prior to addition of cells. Endothelial cells were grown in EBM MV2 kit (PromoCell #C-22121), consisting of Endothelial Basal Media (EMB) MV2 containing 5% (v/v) FCS, VEGF (0.5ng/ml), EGF (5ng/ml), R_3IGF-1 (20ng/ml), FGF-2 (10ng/ml), ascorbic acid (1µg/ml) and hydrocortisone (0.2µg/ml).

2.5.4 Culture of NHDFs

Normal Human Dermal Fibroblasts (NHDF) were cultured on gelatin coated 10cm dishes (as above) in Fibroblast Growth Medium Kit (PromoCell #C-23110) which consists of Fibroblast Basal Media containing basic human Fibroblast Growth Factor (1ng/ml) and insulin (5µg/ml).

2.5.5 Culture of HEK293T, Hela, A375 and MAE cells

These cells were cultured in vented T75 flasks (Fisher Scientific, #1036-4131) in Dulbecco's Modified Eagle's Medium (DMEM, Sigma #D6429) supplemented with 10% Foetal Calf Serum (FCS, Invitrogen #10270-098).

2.5.6 Defrosting Frozen Cell Vials

Cells were stored in liquid nitrogen and thawed in a 37˚C water bath for 3 minutes. The vial was disinfected with 100% isopropanol before pipetting the contents of the tube into 9ml of growth media in a 15ml tube. This was then centrifuged at 92 x g for 5 minutes before aspirating off the supernatant containing any remaining freeze media. The cells were then re-suspended in 8ml fresh media and seeded in a gelatin coated 10 cm dish. Plates were incubated for 24 hours before changing the media.

2.5.7 Routine Cell Culture and Passaging

All cells were split at approximately 80-90% confluence, and seeded at an appropriate ratio (see Table 2.5). Cells were washed twice with 4ml of Versene (Dulbeccos Ca^{+2}/Mg^{+2}-free PBS, Lonza #BE17-512F supplemented with 0.5mM EDTA, Sigma #E7889). Plates were then incubated with 1ml of 0.05% Trypsin EDTA (Invitrogen, #25300-054) for 3 minutes at 37˚C to detach the cells from the flask. Cells were collected and re-suspended in the appropriate media and split onto new dishes, see Table 2.5.

Table 2.5: Routine Cell Culture and Passaging

Cell Type	Media	Ratio	Passage (from-to)
HDMEC	EBM MV2 plus growth factors	1:4 every 2 days	p4-p12
NHDF	Fibroblast growth medium	1:5 every 2 days	p4-p25
HEK293	DMEM containing 10% FCS	1:8 every 2 days	p1-p25
A375	DMEM containing 10% FCS	1:10 every 2 days	p1-p25
MAE	DMEM containing 10% FCS	1:6 every 2 days	p1-p25

2.5.8 Serum Starvation

To create a low serum environment prior to agonist stimulation, cells were first washed twice in PBS with calcium and magnesium (Lonza # 3MB057) and then placed in the media described in Table 2.6 overnight in a 37˚C incubator, with an atmosphere of 5% CO_2 and a humidified environment.

Table 2.6: Serum Starvation Medias

Cell Type	Media
HDMEC	EBM MV2 plus 1% FCS (Promocell, #proC-22221)
NHDF	Fibroblast growth medium plus 1% FCS (Promocell, #C-23320)
HEK293	DMEM plus 1% FCS (Invitrogen, #10270-098)
A375	DMEM 1% FCS (Invitrogen, #10270-098)
MAE	DMEM 1% FCS (Invitrogen, #10270-098)

2.5.9 Cell Counting

Before any experiment, cells were counted. This involved washing with PBS and trypsinising in 1ml of trypsin for 3 minutes followed by re-suspending in media.

Cells were then counted on a Neubauer Improved haemocytometer (Heacht Assistant, Sondheim Germany) and resuspended in growth media at relevant density.

2.5.10 Cell Transfection

2.5.11 Transient Transfection of Mammalian Cells with Plasmid DNA

Cells were transiently transfected with plasmid DNA constructs (see Table 2.10) using the transfection reagent Lipofectamine™ 2000 (Invitrogen #11668-027). Cells were seeded at 1×10^5 per well of a 6-well plate 24 hours before the transfection. Two tubes were filled with 250µl of OPTIMEM (+GlutaMAX I) media (Invitrogen #51985-026). To one tube 5µl of Lipofecatmine™ 2000 was added and to the second tube, 1µg of plasmid was added. Both tubes were left for five minutes at room temperature. The lipofectamine mixture was added slowly to the plasmid mix and incubated for a further 20-30 minutes at room temperature. Prior to the end of the incubation, media was aspirated from the cells and replaced with 2 ml of OPTIMEM. After gentle mixing the mixture was added drop-wise to the cells. The plate was returned to the incubator for 6 hours and then the transfection mixture was removed and the cells washed twice with PBS containing Mg^{+2}/Ca^{+2}. Fresh growth media was added to the cells and returned to the incubator for 24 hours, after which the cells were used experimentally such as growth factor stimulation (section 2.6.1) or a wound healing assay (section 2.17.1).

2.5.12 RNA Interference of Mammalian Cells (siRNA)

To selectively knockdown the expression of a particular protein, small interfering RNAs (siRNA) were transfected into cells. Pre-designed siRNAs (see Table 2.7) were used. On day zero cells were seeded at 1×10^5 cells per well of a 6-well plate in growth media for approximately 24 hours before transfection. On the day of transfection, two tubes were prepared containing 250µl of OPTIMEM (+GlutaMAX I) media (Invitrogen #51985-026). To one tube 2.5µl of Lipofectamine™ RNAi MAX (Invitrogen #51985-026) was added, to the second tube the required amount of siRNA duplex was added to give a final concentration of 20nM in a 2.5 ml final volume and left for 5 minutes at room temperature. The lipofectamine mixture was added slowly to the siRNA mix and incubated for a further 20-30 minutes at room temperature. Once again, media was aspirated from cells and replaced with 2ml OPTIMEM. The transfection mix was added dropwise to each well giving a final volume of 2.5ml. The plates were returned to the incubator for 6 hours. After 6 hours the transfection mix was removed, and cells were washed with PBS containing Mg^{+2}/Ca^{+2}. After washing, 2ml of growth media was added, and the cells returned to the incubator for 24 hours. On the third day, the cells were serum starved overnight prior to stimulation.

2.5.13 siRNA Oligonucleotides

A list of all small interfering ribonucleic acids used in this work.

Table 2.7: siRNA Oligonucleotides

Target Gene	Target sequence	Company
AllStar Neg. control	CAGGGTATCGACGATTACAAA	Qiagen
Negative Control siRNA	AATTCTCCGAACGTGTCACGT	Qiagen
PLD1_7	TACCGGGTATATGTCGTGATA	Qiagen
PLD1_8	ACCGGCGGAGGAAATGCTCTA	Qiagen
PLD1_3	ATGGGATATTTGATTACGTAA	Qiagen
PLD1_6	CAGGCCTGACGCATTCTCGTA	Qiagen
PLD2_5	TGGGCGGACGGTTCTGAACAA	Qiagen
PLD2_6	CAGCAAGGTGCTCATCGCAGA	Qiagen
PLD2_2	CCGGCCTTTCGAAGATTTCAT	Qiagen
PLD2_3	CAGCCTGCTGACAGACACTAA	Qiagen
PLD1-(1)	CAACAGAGUUUCUUGAUAU	Dharmacon
PLD1-(2)	GGUAAUCAGUGGAUAAAUU	Dharmacon
PLD1-(3)	CCAUGGAGGUUUGGACUUA	Dharmacon
PLD1-(4)	CCGGGUAUAUGUCGUGAUA	Dharmacon
RCAN1	Hs_DSCR1_5 HP, SI03224900*	Qiagen
RCAN1	Hs_DSCR1_6 HP, SI03246208*	Qiagen

* Sequence not provided by the supplier and product code provided instead.

2.5.14 Amaxa Nucleofector Transfection

Amaxa Nucleofector and HMVEC-L Nucleofector® Kit (Lonza; Cat#VPB-1003) was used according to the manufacturer's instructions. Briefly, 5 × 10^5 cells per sample were first counted and then re-suspended in 100µl Nucleofector Solution at room temperature. This was then combined with 2µg DNA (pmaxGFP) and the suspension transferred into a certified cuvette. The amount of DNA used was optimised according the to manufacture's protocol. The bottom of the cuvette was covered by sample without any air bubbles and the cap closed. The Nucleofector Programe S-005 was selected and the cuvette inserted into the Nucleofector cuvette holder and the selected program run. The cuvette was taken out of the holder when the program was finished and 500µl of growth media added to the cuvette. The resulting suspension was then carefully transferred into a well of a 12 well plate. Finally cells were incubated over night before being analysed.

2.5.15 Transfection with NEB Transpass

Cells were plated at 4 × 10^4 cells per well in a 12-well plate in 1ml of growth media overnight for 24 hours at 37˚C. On the day of transfection, the media on the cells was changed to fresh growth media whilst the transfection mix was prepared according to the manufacturer's instructions in the Transpass HUVEC Transfection Reagent kit (NEB# M2558S). Firstly, 100µl of OPTIMEM (+GlutaMAX I) (Invitrogen/Gibco #51985-026) media was placed in a tube along with 1 µg of plasmid DNA, 2µl of HUVEC Reagent Component and 2µl of the Transpass V Component. This was mixed gently and incubated for 30 minutes. This transfection mixture was then added drop-wise to the cells and the plate gently swirled five times to ensure the reagent reached all the cells before incubating for six hours at 37˚C. After 6 hours the transfection mix was removed from the plates and the cells washed with PBS containing Mg^{+2}/Ca^{+2} before adding 1ml of normal growth media and returning to the incubator for 24 hours.

2.5.16 Infection of HDMEC with Adenovirus

HDMECs were plated at 7 × 104^4 cells/well in 12 well plates. Cells were grown for 24 hours in the plates and cells were infected with an empty control virus and adenovirus expressing RCAN1.4 from see Table 2.10 at a multiplicity of infection

(MOI) of 50. Previous work in the group had shown that a MOI of 50 gave optimal over-expression of RCAN1.4 (K.Holmes, unpublisded data). After 24 hours of transfection the virus was removed and media changed on the cells.

2.6 Cell Stimulation and Signalling Inhibition

2.6.1 Cell Stimulation

Before stimulating the cells with growth factors, they were serum starved for at least 16 hours at 37˚C (see Section 2.5.8). Growth factors (see Table 2.8) were then diluted in the relevant low serum media (see Table 2.6). The final concentration and the respective incubation times for each condition used in this study are given in the text.

Table 2.8: Growth Factors

Growth Factors	Company	Code
VEGF-A_{165}	R and D system	#293-VE-050
VEGF-A_{121}	Peprotech	#100-20A
HGF	Peprotech	#100-39
FGF-2	Peprotech	#100-18B
EGF	Peprotech	#AF-100-15

2.6.2 Signal Transduction Inhibition

All inhibitors in this study were dissolved in sterile (1-30µM) DMSO and aliquoted and stored at -80˚C. Before use, they were warmed to room temperature and then diluted to the relevant concentration. Where a vehicle control is included, an equivalent volume of DMSO was used instead of the inhibitor. Exact concentrations used and incubation times are listed where relevant in the results section.

Table 2.9: Inhibitors Used in the Study

Name	Target	Company
ZM323881	VEGFR2	Tocris (#2475)

SGX-523	HGFR2 (c-Met)	Selleck Chemicals (#S1112)
Cyclosporin A	Cacineurin	Calbiochem (#239835)
Halopemide	PLD1	Cayman (#13205)
CAY10594	PLD2	Cayman(#13207)

2.7 Plasmid Constructs and Preparation

Table 2.10: Plasmids and viruses Used in this Study

Plasmid or viruses	Description	Source
pcDNA3.1-PLD1	pcDNA mammalian expression vector containing human *PLD1 cDNA* (Brown et al., 1998)	Prof.Michael Wakelam, Babraham Institute
pcDNA3.1-PD2	pcDNA mammalin expression vector containing human *PLD2 cDNA* (Divecha et al., 2000)	Prof.Michael Wakelam, Babraham Institute
pcDNA3.1-RCAN1.4	pcDNA mammalian expression vector containing mouse *RCAN1.4 cDNA*	Dr.Beverly Rothermel, UT Southwestern
Adenoviruses RCAN1.4	Adenoviruses encoding human *RCAN1.4*	Dr.Beverly Rothermel, UT Southwestern

2.7.1 Chemical Transformation of Bacterial Cells (Heat Shock Method)

Prior to commencing, sterile LB media was prepared by adding 20g LB Broth (Sigma, #L3022) to 1L of distilled water and autoclaving. Also, LB plates were poured containing 1L LB media with 15g agar (Sigma, 9012-36-6), 5 g yeast extract, 5 g NaCl, 10 g of tryptan, 1ml of 1M NaOH to 1L distilled water and 50μg/ml ampicillin (Sigma).

One Shot Top10 Chemically Competent *E. coli* cells (Life Technologies, #C4040) were thawed on ice and 50ng of plasmid to be transformed added into the vial and placed on ice for 30 minutes. The tube was then placed in the water bath at 42˚C for

90 seconds and chilled on ice for three minutes. 900µl of warm LB media was added to the cells and incubated at 37˚C for one hour while shaking at 250 rpm. 200µl of this cell suspension was then plated onto LB agar plates and incubated overnight at 37˚C.

2.7.2 Maxi Preparation of Plasmid DNA

Plasmid DNA was prepared using the EndoFree plasmid kit (Qiagen, #12362) according to the manufacture's instructions. Briefly, a single bacterial colony was picked using an autoclaved 200µl tip from LB agar plate containing ampicillin (50µg/ml) and grown for 8 hours at 37°C with shaking at 250 rpm. Then the starter culture was diluted 1:500 in 250ml of LB media and grown at 37°C for 17 hours with shaking at 250rpm. The following day bacterial cells were harvested by centrifuging at 6000 x g for 15 minutes at 4°C. The pellet was re-suspended in 10 ml of buffer P1 until the pellet dissolved and 10 ml of buffer P2 added. The samples were mixed well until a homogenous blue coloured mixture was achieved and incubated for 5 minutes at room temperature. 10 ml of chilled buffer P3 was then added and mixed vigorously. The whole lysate mixture was transferred to QIAfilter cartridges and incubated at room temperature for 10 minutes to allow precipitation to occur. The plunger was inserted into the QIAfilter maxi cartridge and the lysate filtered into a new 50ml tube. 2.5 ml of buffer ER was then added and incubated on ice for 30 minutes. A Qiagen-tip 500 was equilibrated by first adding 10 ml of buffer QBT. The lysate was then added to Qiagen-tip 500 and allowed to enter the resin using gravity flow. The Qiagen-tip was washed twice with 30 ml of buffer QC and plasmid DNA was eluted by the addition of 15 ml of buffer QN. Genomic DNA was precipitated by adding 10.5ml of isopropanol, mixing and then centrifuging at 15,000 xg for 30 minutes at 4°C. The supernatant was removed and the pellet washed with 5 ml of 70% ethanol and centrifuged again. The pellet was then air dried for 10 minutes before being re-suspended with double distilled water. The NanoDrop spectrophotometer was then used to determine the quantity of plasmid DNA by taking measurements of absorbance at 260 nm and 280 nm.

2.8 Preparation of Cell Lysates

Cell lysates were prepared following cell stimulation. Media was first aspirated and cells were then washed twice on ice with ice-cold PBS (without $Ca^{2+/}Mg^{2+}$). The cells were then lysed in the required volume of lysis buffer (20mM Tris pH7.5, 150mM NaCl, 2.5mm EDTA, 10% (w/v) glycerol and 1% (w/v) Triton X-100, 1mM Na_3VO_4 (Sigma S-6508), 10µg/ml Aprotinin (Sigma A-4529), 10µg/ml Leupeptin (Sigma L-8511), 1mM PMSF) and kept on ice with gentle agitation for 15 minutes to allow complete lysis. The cells were scraped into 1.5 ml tubes and cleared of cell debris by centrifugation at 17968 x g for 20 minutes at 4˚C and the supernatant transferred to fresh tubes. For SDS-PAGE an appropriate volume of 1x LDS (Life Technology #NP0008) sample loading buffer was added to the sample which was then heated at 90˚C for 5 minutes before loading.

2.9 Western Blotting

2.9.1 Gel Types

Two types of SDS-PAGE gels have been used throughout this study:

2.9.2 Precast Gels

Pre-cast gels purchased from Invitrogen - NuPAGE® 4-12% Bis Tris Gel 1.5mm, 15 well (Invitrogen, SKU#NP0336BOX) or NuPAGE® 4-12% Bis Tris Gel 1.0mm, 12 well (Invitrogen, SKU#NP0322BOX). Gels were run in 1X MOPS SDS (Invitrogen) for 2 hours, at 200V and 50mA.

2.9.3 Self-Cast Gels

Self-cast gels were made in XCell SurLock™ Mini-Cell, XCell II ™ Blot Module, Cassette 1.5mm (Invitrogen, SKU#NC2015). The desired percentage of acrylamide gel was poured according to the recipe described in the below table. APS and TEMED were added last to catalyze the polymerization. 1ml of water saturated butanol was added to level the running gel and prevent any bubbles and then the gel allowed to set for 30-60 minutes at room temperature. The butanol was then washed and the stacker gel added, (made according to the table below) and a comb placed into the top cassette.

Gels were run in 1X SDS-PAGAE Tris Glycine at 125V and 35mA for the appropriate period of time depending on the percentage of the gel.

Table 2.11: Composition of SDS-PAGE gels

Mini Gel	Units	Stacker	Running Gel						
			5%	6%	7%	8%	10%	12%	15%
30%Acrylamide/0.8%Bis	ml	0.7	1.7	2.0	2.3	2.7	3.3	4.0	5.0
2.0M Tris/HCl pH8.8	ml	-	2.0	2.0	2.0	2.0	2.0	2.0	2.0
0.5M Tris/HCl pH6.8	ml	0.7							
87% Glycerol	ml	-	0.7	0.7	0.7	0.7	0.7	0.7	0.7
dH_2O	ml	3.6	5.6	5.3	5.0	4.6	4.0	3.3	2.3
Total Volume	µl	5	10	10	10	10	10	10	10
10%APS	µl	2.5	22.9	22.9	22.9	22.9	22.9	22.9	22.9
TEMED	µl	5	5	5	5	5	5	5	5

2.9.4 Gel Transfer

Gels were transferred onto Hybond-ECL Nitrocellulose membrane (Amersham Bioscience, RPN3032D) in transfer buffer (Table 2.3: Solutions) for 2 hours at 50 V, 125 mA). The membrane was first blocked in 5% (w/v) BSA in TBST + 0.02% (w/v) azide (Sigma # S-6508) for 1 hour at room temperature and then incubated in primary antibody diluted in 2% BSA in TBST + 0.02% (w/v) azide overnight at 4°C under continuous shaking. The blots were then washed six times in TBST for 10 mins each time with gentle rocking. Blots were then incubated with the appropriate HRP conjugated secondary antibody made up in 2% (w/v) BSA/TBST for two hours at 4°C under gentle agitation. Membranes were again washed six times in TBST for 10 mins each time and the final wash was carried out in TBS only.

2.9.5 Western Blot Development

Membranes were incubated for 5 minutes in ECL reagent (Amersham, RPN2106) to detect signals from HRP conjugated secondary antibodies. The blot was then arranged in a plastic wallet and placed in a cassette for exposure for the desired amount of time on Fuji Medical X-Ray Film, Super RX, 100NF (Jet X-Ray, London). The film was then developed by hand in developer (Sigma #1900984) and fixer (Sigma#1902485) solutions and was then rinsed in water and left to dry.

2.9.6 Antibodies

All antibodies used in this study are listed in tables 2.12 and 2.13 with dilutions used for western blotting (W.B). All species are indicated by the following abbreviations: R=Rabbit, G=Goat, M=Mouse, Rt=Rat.

Table 2.12: Primary antibodies used for W.B

Antibody name	**Antigen**	**W.B**	**Company**	**Catalogue number**
R α Actin	Human Actin	1:1000	Santa Cruz	#sc-1615-R
R αVECadherin	Human VE-Cadherin	1:1000	Cell Signaling Technology	#D87F2
R α RCAN1	Human RCAN1	1:1000	Sigma	#D6694
M αDSCR1	Human DSCR1	1:500	Santa Cruz	#sc-377507
R α PLD1	Human PLD1	1:1000	Santa Cruz	#sc-25512
R α PLD2	Human PLD2	1:1000	Santa Cruz	#sc-25513
R α PLD2	Human PLD2	1:1000	Abcam	#ab86163
R α MAC444	Rat PLD2	1:1000	Babraham Institute, Cambridge Wakelam Lab	NA
R α VEGFR2	Human VEGFR2	1:1000	Cell Signaling Technology	#2479
R α pVEGFR2	Human phosVEGFR2 (Y1175)	1:1000	Cell Signaling Technology	#3770
R α pPLCγ	Human PLCγ	1:1000	Cell Signaling Technology	#2822
G α KDR	Human KDR	1:1000	R&D System	#AF357
R α VEGFR1	Human VEFDR1	1:1000	Cell Signaling Technology	#2893
R α Akt	Human Akt	1:1000	Cell Signaling Technology	#9272
R α pAkt	Human phosAkt	1:1000	Cell Signaling Technology	#4060
R α Erk1/2	Human Erk1/2	1:2000	Cell Signaling Technology	#9102
R α pErk1/2	Human phosErk1/2	1:1000	Cell Signaling Technology	#9101
R α GFP	Human GFP	1:1000	Cell Signaling Technology	#2956
R α Caspase3	Human Caspase3	1:1000	Cell Signaling Technology	#9665
R α GAPDH	Human GAPDH	1:1000	Cell Signaling Technology	#5174
G α c-Met	Human c-Met	1:1000	R&D System	#AF276
R α c-Met	Human c-Met	1:1000	Cell Signaling Technology	#8198
R α p-cMet	Human c-Met	1:1000	Cell Signaling Technology	#3133

Table 2.13: Secondary antibodies used for W.B

Antibody	Species	Antigen	W.B	Company	Catalogue number
HRP-α-R	Mouse	Rabbit IgG	1:5000	Jackson Labs	#211-032-171
HRP-α-M	Sheep	Mouse IgG	1:5000	GE Healthcare	#NA931V
HRP-α-G	Rabbit	Goat IgG	1:10000	Sigma	#A0545
HRP-α-Rt	Goat	Rat IgG	1:5000	GE Healthcare	#45001200
HRP-α-R	Donkey	Rabbit IgG	1:5000	Jackson Labs	#111-035-046
HRP-α-M	Donkey	Mouse IgG	1:5000	Jackson Labs	#515-035-062
HRP-α-G	Donkey	Goat IgG	1:5000	Jackson Labs	#705-006-147

2.9.7 Stripping and Re-probing Blots

To re-probe membranes with an alternative antibody, the first set of antibodies were removed using stripping buffer (62.5m Tris-HC1, pH 6.8, 20 (9w/v)% SDS, 100mM of β-Mercaptoethanol) and incubated at 50˚C for 20 minutes with occasional agitation. The membrane was then washed three times in TBST at room temperature using a large volume of TBST buffer and blocked again in 5% BSA in TBST. The membrane was then treated with primary and secondary antibodies as described above.

2.9.8 Densitometric Quantification of Protein Expression

The immune reactive bands detected on X-ray film were quantified to identify the relative amount of specific proteins. The X-ray film was first scanned (Bio Rad #GS-800, Photoshope CS6) and the densitometric analysis was achieved using ImageJ (National Institute of Health (NIH), Version 1.47n). Actin or GAPDH were quantified to correct for protein loading.

2.10 Immunoprecipitation Protocol

Cells were first lysed in lysis buffer ((20mM Tris pH7.5, 150mM NaCl, 2.5mM EDTA, 10% (w/v) glycerol and 1% (w/v) Triton X-100, 1mM Na_3VO_4 (Sigma S-6508), 10µg/ml Aprotinin (Sigma A-4529), 10µg/ml Leupeptin (Sigma L-8511), 1mM PMSF) and 200µl of cell lysate was then taken and mixed with 1µl of primary antibody and incubated with gentle rocking overnight at 4˚C. Twenty-five microliter of protein G of agarose beads (Sigma#027K2030) slurry was then added, mixed and incubated with gentle rocking for 3 hours at 4˚C. Tubes were spun in a benchtop centrifuge to pellet beads and the supernatant taken for an immunodepleted sample. The pellet was then washed three times in 500µl of lysis buffer and finally resuspended in 20µl 3X LDS. The samples were then heated at 90˚C for ten minutes and centrifuged for 1 minute at 17968 x g. The supernatant was then analyzed by western blotting.

2.11 RNA extraction

RNA was extracted using the RNeasy mini kit (Qiagen Cat#74106) according to manufacturer's instructions. Briefly, following treatment, cells were washed with PBS and 600 µl of RLT buffer was added to each well. The cells were scraped with a cell scraper and transferred into a Qiashredder (Qiagen Cat #79656) and centrifuged for two minutes at 8000g. After centrifugation, 420µl of 100% ethanol was added, and 700µl of the sample added onto an RNeasy mini column, spun at 8000 xg for 30 seconds. After centrifugation, 350µl of RW1 buffer was pipetted onto the silica-gel membrane and the flow through discarded. To digest DNA, 80µl of DNase 1 solution was added directly onto the RNeasy silica-gel membrane and incubated for 15 minute at room temperature. The membrane was then washed with 350µl RW1 buffer at 8000g, with the flow disregarded, and 500 µl RPE buffer added. After centrifugation, a final wash 500µl of RPE buffer was added to the RNeasy column and centrifuged for two minutes at 8000g. The RNeasy column was transferred to a new tube and 30µl of RNase free water pipetted onto the membrane to elute the RNA. The quality of RNA was assessed using a Nano Drop ND-1000 spectrophotometer (Labtech International, Lewes, U.K).

2.12 Reverse Transcription of mRNA (cDNA Synthesis)

Prior to cDNA synthesis, each RNA sample was checked using a Nano drop to ensure an accurate concentration measurement. A PCH-1 heating unit was used for all incubation steps. In a sterile 0.5ml eppendorf, 1µl oligo dT (500µg/ml, Oligo d(T)$_{18}$) was mixed with 1µg RNA, and 1µl dNTP mix (10mM, Invitrogen Cat # 18427-013) and dH$_2$O to give a final volume of 12µl. This was then heated to 65°C for five minutes, and then briefly chilled on ice. A master mix was then prepared to add to each tube containing 4µl 5x first strand buffer, 2µl 0.1 MDTT, 1µl RNaseOUT and 1µl of M-MLV Reverse Transcriptase (Invitrogen Cat#28025-013, supplied with 0.1M DTT and 5x First Strand Buffer). 8µl of the master mix was added to each tube and incubated at 25°C for five minutes, and a further 60 minutes at 37°C. The reaction was then inactivated by heating at 70°C for 15 minutes and the sample was diluted with 130µl sterile dH$_2$O to gain a final concentration of 6.7ng/µl.

2.13 Primer Design and PCR Based Primer Testing

Primers were purchased from Invitrogen. Upon arrival primers were spun briefly to collect material in the tube. The primers were reconstituted to 100µM using Tris-EDTA (TE) buffer, pH 8.0, incubated at room temperature for two minutes to rehydrate and vortexed for 20 seconds. A working concentration of 2.5µM prepared in dH$_2$O, was then used in qRT-PCR reactions.

Table 2.14: Primer sequence table

Primer name	Forward Sequence (5 to 3)	Reverse Sequence (5 to3)
RCAN1.1	TCATTGACTGCGAGATGGAG	TGATGTCCTTGTCATACGTCCT
RCAN1.4	CTCACTAGGGGCTTGACTGC	CAGGCAATCAGGGAGCTAAA
PLD1 (2)	AGCGGTGCCATTGCCTTCGT	TCCCCACCACCGAGCATGTCTA
PLD2 (1)	TGCACCCCTTGGTGTTCGCA	AAAGTCGCCGTGAGTCAAGCGG
Actin	GATGAGATTGGCATGGCTTT	CACCTTCACCGTTCCAGTTT
GAPDH	GGCCTCCAAGGAGTAAGACC	AGGGGTCTACATGGCAACTG

To test these primers, a master mix was prepared (1.1x number of samples) with 4µl 5x Buffer, 2.4µl MgCl$_2$, 2µl dNTP mix (2mM of each dNTP, Promega #U1330), 5.8µl dH$_2$O Sigma #W4502), and 0.2µl GoTaq Flexi DNA polymerase (Promega Ca#M8031, supplied with MgCl$_2$ and 5x Buffer). Secondly, the PCR reactions were set up as following, 2µl Forward primer, 2µl Reverse primer, 1.6µl cDNA and 14.4µl

Master mix with the PCR cycles run at 10 minutes at 95°C, and then 15 seconds at 95°C followed by 1 minute at 60°C for 30 cycles.

All PCR products were run on a 4.5% agarose gel, made by adding 4.5g agarose (Melford cat#MB1200) to 150ml TBE buffer (89mM Tris base, 89mM Boric Acid, 2mM EDTA), dissolved by heating and then mixed with Ethidium Bromide (VWR #443922U) to a final concentration of 0.5µg/ml (1:10,000) with gentle swirling. PCR products were loaded in the gel along with 10µl of 100bp DNA Ladder (BioLab Cat#N0467S) and the gel was run at 100V for 1 hour. The DNA bands were visualized using a UV transilluminator and imaged with a camera system (Bio-Rad #170-8265).

2.14 Real-Time PCR

All pipette tips used were RNase, DNase free, sterile filter tips and work was carried out on a clean bench. PCR reactions were set up by mixing 1.5µl (10ng) cDNA template and 2.5µl of nuclease- free ddH_2O (Sigma Cat #W4502), 10µl 2x Power SYBR Green Mastermix Applied Biosystems Cat #4368702), 2µl forward primer final concentration 0.25µM and 2µl reverse primers in a final volume of 20µl for each reaction. qRT-PCR reactions were mixed by vortexing before loading in a 96-well PCR plate (Greiner Cat #652290) and sealed with Optically clear sealing film (Bioline Cat#UC-500). The plate was then run on an ABI 7000 PCR System (Applied Biosystems, Foster City, CA, U.S.A). The following cycling parameters in ABI 7000 software were applied: 50˚C for two minutes and 95˚C for 10 minutes, followed by 40 cycles of 95˚C for 15 second and 60˚C for one minute.

2.15 Interpreting RT-PCR Results

The gene expression of the gene of interest was demonstrated by using the comparative C_t method for relative quantification of gene expression. For the first stage, the mean and standard deviation of the replicate sample results was calculated and for the second stage, the ΔCt value for the basal was calculated by subtracting the Ct value of the target gene from the Ct value for the reference gene as exhibited in this equation below:

$$\Delta Ct = Ct \text{ target gene} - Ct \text{ reference gene}$$

For the third stage, the standard deviation of ΔCt value was calculated from the standard deviation for the target and reference gene Ct values, as shown below:

(s=standard deviation)

s_1= standard deviation of reference gene Ct values

s_2= standard deviation of target gene Ct values

$$s(\Delta Ct)=(s_1^2+s_2^2)^{1/2}$$

For the fourth stage, the ΔΔCt value was calculated by subtracting ΔCt of the stimulated samples from the ΔCt of the basal samples as shown below:

$$\Delta\Delta Ct=\Delta Ct \text{ stimulated samples} - \Delta Ct \text{ basal samples}$$

Finally the range in fold increase was calculated as follows this equation:

$$2^{-(\Delta\Delta Ct+2)} \text{ to } 2^{-(\Delta\Delta Ct-s)}$$

House keeping genes used in this study were either GAPDH or β-Actin.

2.16 Immunofluorescent Staining of Cells

Cells were first washed twice in PBS to remove any media and then fixed with 2% (w/v) paraformaldehyde (PFA, Sigma, #P6148) for 15 minutes at room temperature. This was then aspirated and the cells washed in quench solution (PBS with 50mM ammonium chloride, Sigma #A0171), this was then aspirated and replaced with fresh quench solution for 10 minutes, prior to being washed three times with PBS. To stain intracellular components, cells were permeabilized with PBS containing 0.2% (w/v) Triton X-100 (Sigma, #T9284) for 10 minutes at room temperature and washed twice with TBS. Cells were then blocked for one hour at room temperature with TBS containing 0.1% Tween-20 and 1% BSA (Sigma #A3059) and 5% serum (from the same animal species in which the secondary antibody was raised). The primary antibody was diluted accordingly (Table 2.15) in TBST and incubated for one hour at room temperature, then washed three times for 10 mins in TBST. The alexa fluorophore coupled secondary antibody (Table 2.16) was diluted in TBST and incubated for one hour at room temperature. From this step forward, the dish was covered with foil to protect the plate from light, as the fluorescent dyes are light sensitive. At this step, phalloidin was also included in the incubation if required. The cells were then washed twice in TBST and the nuclei were stained with Hoechst stain

(2µg/ml, Invitrogen, H-21492) for 10 minutes then finally washed three times in TBST. Coverslips were then mounted by adding 10µl of Prolong Gold onto a glass slide and placing the coverslip face down on this, then sealing with clear nail varnish. This was then left to set overnight before imaging and stored at 4°C. All images were visualised and acquired using an inverted Zeiss Axio Observer microscope and analysed with Zen Pro software.

Table 2.15: Primary Antibodies Used for IF

All antibodies used in this study are listed in tables 17 and 18 with dilutions used for Immunofluoresence (IF). All species are indicated by the following abbreviations: R=Rabbit, G=Goat, M=Mouse, Rt=Rat.

Antibody name	Antigen	Dilution	Company	Catalogue number
Mα EEA1	Human EEA1	1:50	BD Bioscience	#610457
R α EEA1	Human EEA1	1:250	Cell Signaling Technology	#3288
M α GM130	Human GM130	1:1000	BD Bioscience	#610823
R α Pericentrin	Human Pericentrin	1:5000	Abcam	#ab4448
R α RCAN1	Human RCAN1	1:200	Sigma	# D6694
M αDSCR1	Human DSCR1	1:100	Santa Cruz	# sc-377507
R α PLD1	Human PLD1	1:100	Santa Cruz	# sc-25512
R α PLD2	Human PLD2	1:100	Santa Cruz	# sc-25513
R α PLD2	Human PLD2	1:100	Abcam	# ab86163
R α VEGFR2	Human VEGFR2	1:100	Cell Signaling Technology	#2479
R α pVEGFR2 (Y1175)	Human phoVEGFR2	1:100	Cell Signaling Technology	#3770
R α pPLCγ	Human PLCγ	1:100	Cell Signaling Technology	#2822
G α KDR	Human KDR	1:100	R&D System	#AF357
G α c-Met	Human c-Met	1:200	R&D System	# AF276
R α c-Met	Human c-Met	1:200	Cell Signaling Technology	#8198
R α p-cMet	Human c-Met	1:200	Cell Signaling Technology	#3133

Table 2.16: Secondary antibodies used for IF

Flurophore	Species	Antigen	Dilution	Company	Catalogue number
Alexa-488	Goat	Rabbit IgG	1:1000	Invitrogen	#A-1103
Alexa-488	Goat	Mouse IgG	1:1000	Invitrogen	#A-11029
Alexa-488	Donkey	Goat IgG	1:1000	Invitrogen	#A-11055
Alexa-488	Donkey	Mouse IgG	1:1000	Invitrogen	#A-21202
Alexa-568	Donkey	Mouse IgG	1:1000	Invitrogen	#A-10037
Alexa-568	Donkey	Rabbit IgG	1:1000	Invitrogen	#A-10042
Alexa-568	Donkey	Goat IgG	1:1000	Invitrogen	#A-11057
Alexa-568	Goat	Rabbit	1:1000	Invitrogen	#A-11035
Alexa-680	Donkey	Rabbit IgG	1:1000	Invitrogen	#A-10043
Alexa-680	Donkey	Mouse IgG	1:1000	Invitrogen	#A-10038
Alexa-568	n/a	Phalloidin	1:300	Invitrogen	#A-12380
UV 350	n/a	Hoechst33342	1:5000	Invitrogen	#H-21492

2.17 Cell Physiology Assays

2.17.1 Wound Healing Migration Assay

HUVECs or HDMECs were seeded in a 12 well plate in 1ml of growth media for 24 hours before being serum starved overnight with 1%FCS media by which time they have formed a confluent monolayer. Using a sterile 200µl pipette tip a scratch wound was introduced in the cells across the centre of the well, using the straight edge of a sterile ruler as a guide. Floating cell debris was removed by washing with PBS and fresh 1% FCS media added with any required growth factors. Cells were left to migrate overnight at 37°C in an incubator or monitored by live cell imaging. After approximately 16 hours cells were washed with PBS and fixed with 2% PFA for 15 minutes at room temperature. Cells were stained by adding 100µl of crystal violet (Sigma #HT90132) to each well and then left at room temperature with gentle swirling for 15 minutes. The cells were then washed in PBS and kept in PBS at 4°C ready for imaging. The scratch was visualized using a Nikon Eclipse TS100 inverted light microscope (10x objective) fitted with LCD colour imaging system.

To calculate wound healing migration, a time zero image was taken immediately after wounding the cells (Figure 2.1). After 16 hours, a further three images were taken of each scratch and migration measured in each image to give an average value for each condition compared to the time zero point (Figure 2.1).

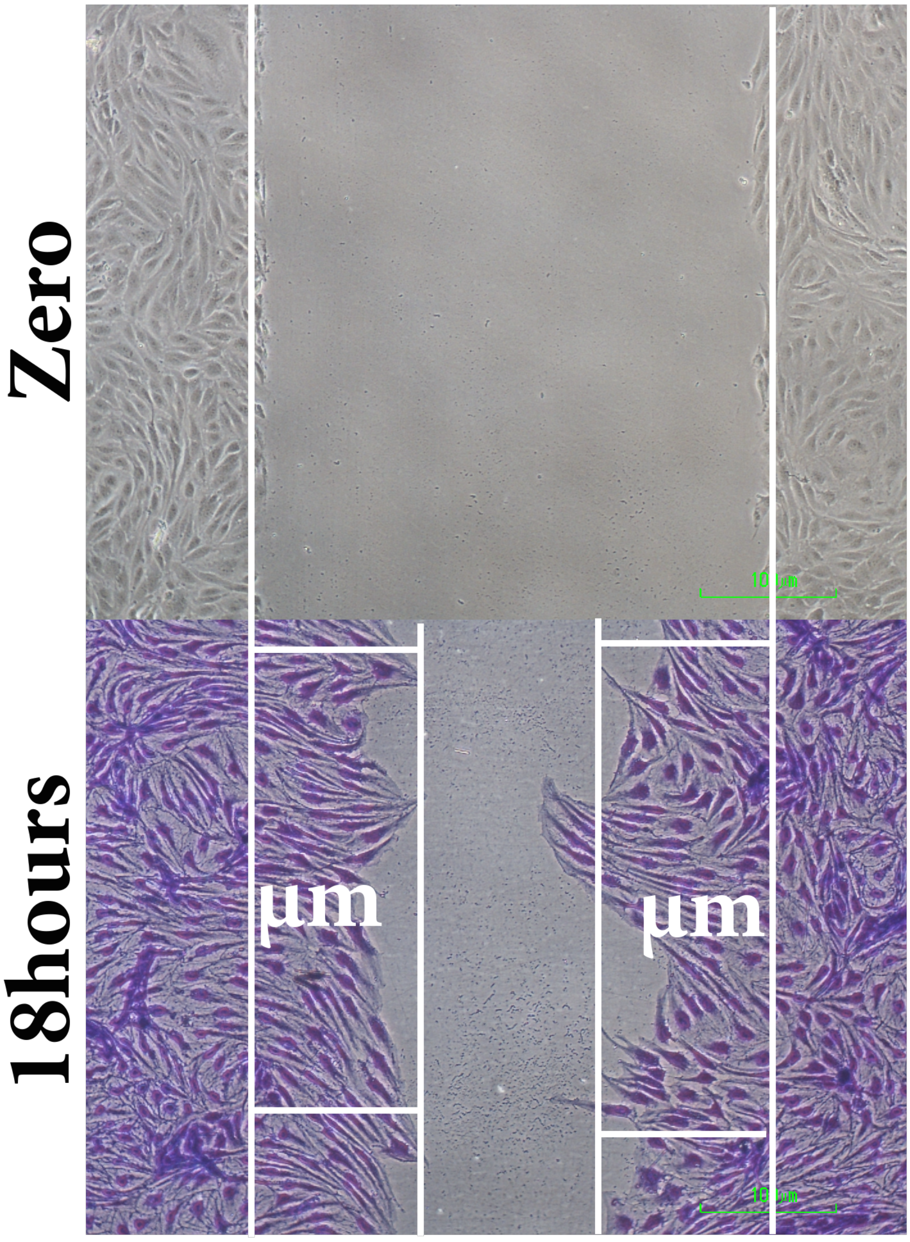

Figure 2.1: Wound healing analysis

This figure shows how wound healing was measured. At time zero an image was taken and then after the cells were fixed, three more images were taken. A line was drawn between zero time and 16 hours stimulation to calculate cell migration and an average of that represented as a bar chart in the results section.

2.17.2 Polarisation Study and Quantification

Cells were set up for a migration assay, as described above, but seeded onto glass coverslips and the scratch wound assay carried out before being fixed with 2%PFA. The cells were then stained (see section 2.16) with the Golgi specific marker GM130 and the centriolar specific marker pericentrin (Table 2.15). To quantify polarisation 10 separate images were taken along the wound edge and then the number of polarised cells counted. Polarisation was determined by drawing a circle in the centre of the nucleus with a 120° segment facing the scratch wound. If the GM130 and pericentrin markers were located within this segment, the cell was counted as polarised (Figure 2.2). This analysis was based on a similar analysis used by Linford et al., (Linford et al., 2012).

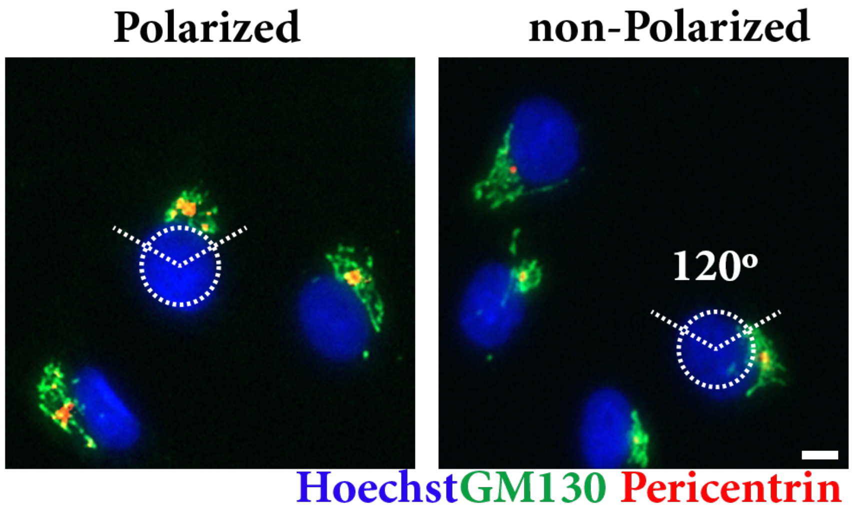

Figure 2.2: Polarisation study

The figure shows how polarity was assessed. Firstly images were taken along the wound edge (top of the image) and polarity was determined by drawing a circle centred on the nucleus of each cell (on Hoechst) with a 120° segment facing the leading edge. If the GM130 (green) and pericentrin (red) staining was within this 120° segment, the cell was determined to be polarised (left panel), whereas if it was outside of this angle, the cell was determined to be non-polarised (right panel). The scale bar is 20 µm.

2.17.3 *In Vitro* 3D-collagen Matrix Tube Formation Assay

This technique consists of sandwiching endothelial cells between two layers of collagen gel, which induces a process of tubular morphogenesis over a period of 16 hours if the cells are exposed to the relevant growth factors (Roberts et al., 2010).

Firstly, the lower layer collagen gel was prepared, making up the necessary volume of collagen mix to plate 300µl of collagen into each well of a 24 well plate. The collagen was made such that it contains ((8 parts Bovine Collagen type-1 solution (PureCol™, #5005), 1 part 0.1 M NaOH (sterile filtered), 1 part x10 Ham's F-12 (PromoCell #C-72190)). To reach the final volume the following was added, diluted as shown (1:50 1M HEPS (Gibco #15630-056). final concentration =20mM), (1:64 7.5% Bicarbonate Solution (Gibco #25080-060). final concentration =0.117%),1:100 Glutamax-1 (Gibco #35050-038) final concentration =1% (2mM)).

The collagen was prepared on ice and then the plate incubated overnight at 37°C to allow the collagen to set. Prior to adding cells, 1ml per well of serum free EBM MV2 endothelial media was added to facilitate cellular adherence and wash the collagen gel.

HDMEC cells, which had been previously been serum starved overnight in EBM MV2 media containing 1% FCS, were washed twice in 4ml of Versene and 1ml of Accutase (PromoCell, #C-41310) added per 10cm dish. Cells were returned to the incubator for approximately 3 minutes and the dissociated cells re-suspended in 3ml of EBM MV2 media with 1% FCS. The cells were then counted using a haemocytometer before being spun at 92 x g for 5min and re-suspended to the required cells density in fresh EBM MV2 media with 1% FCS. Before adding the re-suspended cells to the collagen, the serum free media was aspirated. The required numbers of cells, 90,000 cells per well, were then added gently, swirled and incubated at 37°C for 2 hours to allow cellular attachment. After cell seeding the cellular attachment was judged by examination with an inverted light microscope. Once the cells were fully adhered, the upper layer was made as described previously, making up enough collagen to add 200µl to each well. Before adding the second layer the media was carefully aspirated. The second collagen layer was then allowed to set for between 1.5 to 2 hours. Cells were normally plated out in the absence of growth factors, which were then added following gelification of the upper layer of collagen. A total of 0.5ml of EBM MV2 media with 1% FCS was added to each well, containing X2 concentration of the required growth factor, to correct for the volume of collagen. This was added very gently over the top layer of collagen and cells returned to the incubator at 37°C for 16-24 hours. Cells were normally fixed following tube formation assay by adding 0.5ml of 4% paraformaldehyde and stored at 4°C.

2.17.4 Image Analysis and Quantification of 3D Collagen Tube Formation

The tube formation assay was quantified by imaging three randomly chosen fields of view. In every condition triplicate wells and areas were selected at high magnification (× 10 objective) using an inverted light microscope connected to a Nikon DS-Fi1-L2 digital camera (Nikon, Ltd, U.K). Images were saved as TIF files and the total number of cell junctions, branches, total length of branches and meshes area calculated. Meshes are area enclosed by segments or master segments. Images were quantified using ImageJ and the plugin "Carpentier G., Angiogenesis Analyser for ImageJ (2012)" (Figure 2.3).
(imagej.nih.gov/ij/macros/toolsets/Angiogenesis%20Analyzer.txt)

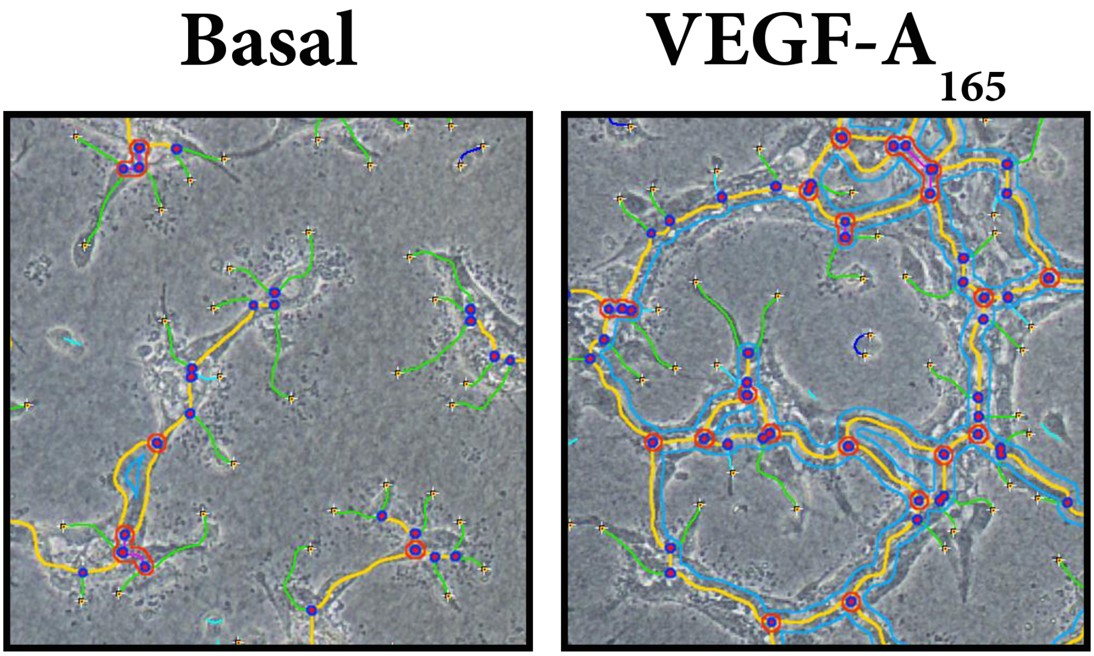

Figure 2.3: Angiogenesis analysis

This figure illustrates how the angiogenesis analyzer allows analysis of cellular networks. Yellow line shows entire junction formed after stimulation, Green line shows branch and Red line shows master junctions.

2.17.5 Proliferation Assays

2.17.6 Crystal Violet

Cells were plated at 15,000 cells per well in a 24 well plate in 0.5ml growth media. Prior to undertaking the proliferation assay, cells were first siRNA transfected (see 2.5.12), after which they were starved in 1% media and the following day stimulated with agonists (see Table 2.8) at 50ng/ml and then incubated for 72 hours. The cells were then washed twice in PBS and 100µl of crystal violet (Sigma #HT90132) stain was added to each well and then incubated for 10 minutes at room temperature. Plates were carefully immersed in a container containing dH_2O to rinse out the crystal violet. The plates were drained on the bench and then 600µl 1% SDS (Sigma, #S1020) added to solubilize the stain. 100µl of this solution was then transferred to a clear flat-bottomed 96-well plate and absorbance read at 570 nm determined on the Varioskan plate reader. On the last day of the experiment, a standard curve was set up by plating cells at the 0, 10,000, 20,000, 40,000, 60,000, 80,000, and 100,000 cells per well in a 24 well plate for 4 hours. These cells were then stained and lysed at the same time as the experimental conditions, allowing cell numbers to be estimated.

2.17.7 CellTiter-Glo Assay

Cell proliferation was also assessed using the CellTiter-Glo® luminescent cell viability kit (Promega, #product code), which quantifies the number of viable cells in every condition based on the quantification of ATP. According to the manufacturer's instructions, both the CellTiter-Glo Buffer and Substrate was thawed and equilibrated to room temperature before being mixed together and vortexed. HDMEC cells were plated out in 24 well plates at a cell density of 15,000 cells per well. The following day, the cells were serum starved with 1% FCS media for 24 hours before being stimulated with agonists (see Table 2.8) for a further 72 hours. Every condition was tested in triplicate. After stimulation media was aspirated from each well and washed in PBS containing Ca^{+2}/Mg^{+2} and a final 200µl of PBS added to each well before lysing in 200µl of the CellTiter-Glow mix. Plates were shaken for two minutes to ensure complete lysis. 100 µl of this lysate was then transferred to a new opaque walled 96 well plate and luminescence was recorded at 570 nm using a Varioskan plate reader (Thermo, Varioskan Flash). On the day of lysis, a standard curve was prepared by plating HDMECs in triplicate at densities of 0, 10,000, 20,000, 40,000, 60,000, 80,000 and 100,000 cells per well. These cells were then incubated for four hours before being also lysed in the same way. Readings collected from these samples were then used to generate a standard curve of cell numbers which would be compared to the final assay results.

2.17.8 Cell Tracker Staining

Pre-warmed EBM MV2 serum free media containing 5µM of Cell Tracker™ Green, Orange, Red or Blue (Invitrogen, C7025, C2927) was incubated with the cells for 30-45 minutes at 37˚C. The Cell Tracker dye is able to cross the membrane and enter live cells where it is then processed into membrane impermeant products by intracellular esterase and fluorescently labels the cells. The dye working solution was then replaced with fresh serum free media for 30 minutes before being washed in PBS and incubated with 1%FCS media.

2.17.9 Statistical analysis

For statistical analysis an unpaired Student's t-test was chosen. This test allows comparison between two different population means which are normally distributed. Data were analysed using an un-paired Student's t-test in Excel. Statistical significance was set at a P-value less than 0.05 (*), or 0.01 (**) or 0.001(***).

Pearson's correlation was performed to analyse co-localisation using ImageJ software. Three regions of interest were analysed for each experimental condition. Background signal was determined from region with no obvious cells structure. Expression of VEGFR-2 was compared with EEA1 and HGFR with EEA1.

Chapter 3

The role of RCAN1 in regulating VEGF-2 signalling and function in endothelial cells

3.1 Introduction

VEGF signalling in endothelial cells is primarily mediated by VEGF receptor 2. The binding of VEGF to VEGFR2 results in receptor activation characterised by receptor autophosphorylation and initiation of series of signalling cascades within the cell (Holmes et al., 2007). RCAN1 is expressed in brain, heart, muscle, adrenal gland and pancreas (Fuentes et al., 1995, Ermak et al., 2001, Peiris et al., 2012). RCAN1 protein commonly exists as two isoforms: RCAN1.4 and RCAN1.1. Targeted gene ablation of RCAN1.1 and RCAN1.4 in mice resulted in mice with no anatomical differences (Hoeffer et al., 2007). Studies aimed at investigating the role of RCAN1 in endothelial cells have utilised endothelial cells of non-human origin including mice (Ryeom et al., 2008, Brait et al., 2012). Data documenting the role of RCAN1 in human endothelial cells has been confined to the use of HDMECs (Holmes et al., 2010). A previous study from the group reported that RCAN1 is highly up-regulated in endothelial cells in response to VEGF, but not to any other growth factors (Holmes et al., 2010).

This chapter describes experiments performed to characterise RCAN1 signalling in HDMECs, with the aim of understanding the signalling pathways potentially perturbed by RCAN1 in response to different growth factors in HDMECs. This project will use a range of specific studies for cell migration such as cell polarity, cytoskeleton reorganisation, and a scratch wound assay to determine which parameters are regulated by RCAN1.

3.2 VEGF-A stimulate an increase in RCAN1.4 expression in HDMECs

The RCAN1 gene consists of seven exons, of which exons one to four can be alternatively transcribed or spliced to produce different mRNA isoforms. This results in a protein of 252 amino acids (RCAN1.1) and 197 amino acids (RCAN1.4) (Figure 1.11). At the start of the project a specific antibody for RCAN1 needed to be validated to determine the specificity and optimum concentration. Different commercial antibodies were used to study the expression of RCAN1 in various cells and tissue profiles. The antibody in this study was validated through three methods: western blot, mRNA level and immunofluorescence.

In order to check the specificity of antibodies short-interfering ribonucleic acid (siRNA) gene silencing was used. This study shows that RCAN1.4 and 1.1 are highly expressed in HEK293, A375 melanoma, human liver, human cardiac myocyte and fibroblast cells (Figure 3.1A). Two individual siRNA duplexes targeting both RCAN1.1 & 1.4 mRNA were utilised to analyse the expression of both RCAN1.1 and RCAN1.4. HDMECs stimulated with VEGF-A for 1 hour showed up-regulation of only the RCAN1.4 isoform, with no up-regulation in RCAN1.1 observed. RCAN1.4 migrated at a molecular weight of 29 kDa whereas RCAN1.1 migrated at around 39 kDa. RCAN1 was assessed using the western blot protocol in combination with siRNA. Lysates from rat cardiac endothelial cells were also included to see if the antibody recognised the rat protein (Figure 3.1A).

To optimize knock down, a pool of two individual siRNA duplexes targeting RCAN1 was used to transfect HDMECs (Figure 3.1B). Non-silence was used in parallel as control for siRNA. Post transfection, cells were serum starved for 24 hours and stimulated for 60 minutes with VEGF-A and harvested for analysis by western blotting. The difference between the specific siRNA and non-silence can be seen in figure 3.1B. The RCAN1 siRNA transfected cells illustrated a complete knock down of both isoform RCAN1.1 and RCAN1.4 in the basal condition compared to untreated or non-silence samples. In addition, one-hour stimulation with VEGF-A showed an increase of RCAN1.4 expression in untransfected and non-silence siRNA conditions compared to the RCAN1 siRNA sample.

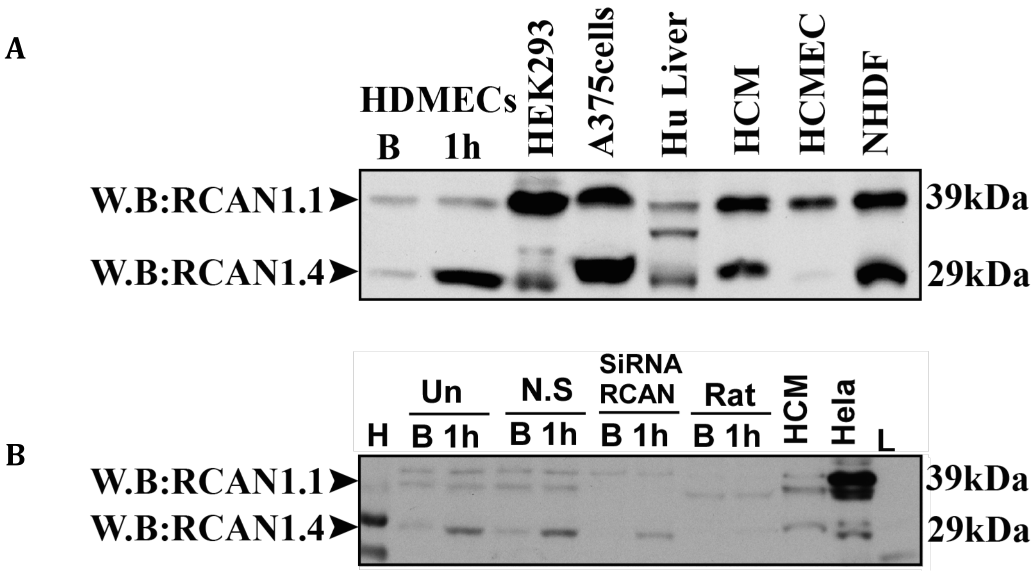

Figure 3.1: Antibody validation for RCAN1

A. HDMECs plated at 7 × 104 and transfected with siRNA. 48 hours post transfection cells were stimulation with VEGF-A for 1 hour then lysed proteins to separate by SDS-PAGE. Levels of RCAN1 (Sigma). Rat (RCEC rat cardiac endothelial cells from VecTechnologies), HCM (Human Cardio Myocytes), Hela cell H=High rainbow marker and L= low rainbow marker. **B.** Western blotted analysis with antibody against RCAN1 protein. All bands showed an expected molecular weight. HDMECs= Human Dermal Microvascular Endothelial Cells, HEK293= Human Endothelial Kidney Cells, A375= Melanoma cells line, Hu Liver= Human Liver, HCM= Human Cardiac Myocytes, HCMEC= Human Cardio Microvascular Endothelial Cells, NHDF= Normal Human Dermal Fibroblast. These experiments have been performed once.

RT-PCR was used to analyse the expression of *RCAN*1.1 and *RCAN1.4* mRNA. In a time course experiment *RCAN1.1* mRNA only increased 2-fold above basal following VEGF-A stimulation for 180 minutes. This is in contrast to expression of RCAN 1.4 mRNA, which showed an increase after 30 minutes VEGF-A stimulation and increased to nearly 20-fold above basal at 60 minutes, remaining at 10-fold above basal after 3 hours (Figure 3.2). This data confirmed that VEGF-A was a potent inducer of *RCAN1.4* mRNA expression.

Analysis of VEGFR-2 signalling in HDMECs revealed that VEGFR2 is down-regulated in response to stimulation with VEGF-A with this being evident at 5 minutes and continuing up to 180 minutes (Figure 3.2). Furthermore, phosphorylation of the VEGFR-2 following agonist stimulation was evident at 5 minutes, with this transient response significantly reduced after 20 minutes. Analysis of downstream signalling pathways revealed that phosphorylation of Akt, required for cell survival (Gerber et al., 1998b), was increased after 10 minutes in response to VEGF-A stimulation. In addition, phosphorylation of Erk1/2, required for cell proliferation (Brunet et al., 1999), increased in response to VEGF-A and was evident at 5 minutes and maximal at 10 minutes. Analysis of RCAN1.1 and 1.4 levels revealed that VEGF-A only induced expression of RCAN1.4, with increased levels evident after 60 minutes stimulation.

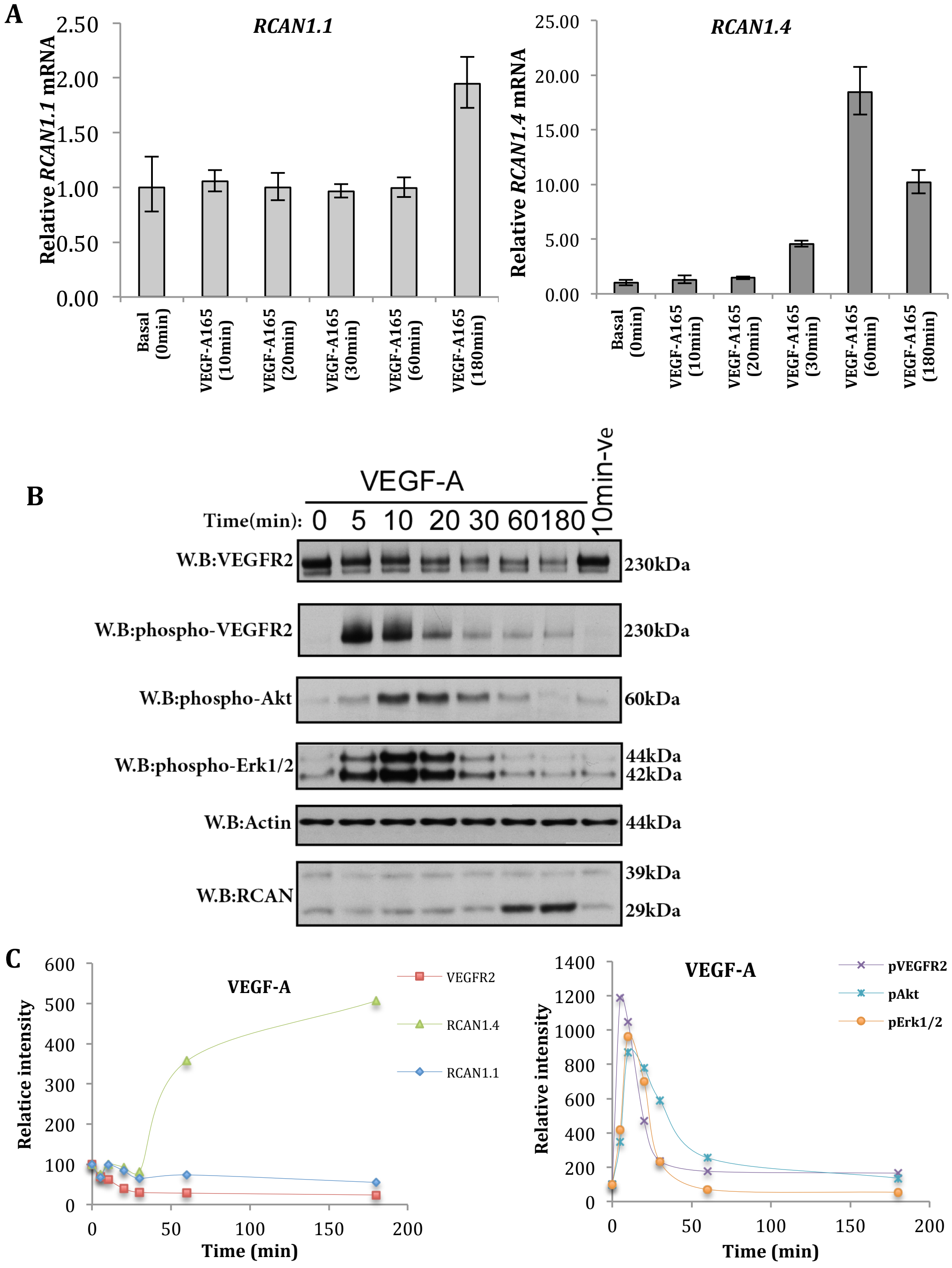

Figure 3.2: Time course of VEGFR-2 stimulation and RCAN1 induction in HDMECs

A. The bar chart shows qRT-PCR analysis for RCAN1.1 and 1.4 mRNA level. HDMECs RNA were extracted and cDNA prepared. Data were analyzed by the ΔΔCt value method and expression was normalized to β-actin expression and illustrated as fold change. HDMECs cells were stimulated with VEGF-A 50ng/ml for 5, 10, 20, 30, 60 and 180 minutes. **B.** Cells were harvested by Triton X-100 lysis. 10µg of loading total protein isolated from HDMECs and subjected to 4-12% NuPAGE gel then analyzed by western blot with anti-Total VEGFR2, pVEGFR2, pAKT, pErk1/2, and RCAN1 antibodies. Actin was used as a loading control. **C.** Graphs illustrate the expression of each protein in response to VEGF-A as determined from relative intensity of the band compared to the basal condition. Data shows mean ± SD. The data is representative of three experiments.

3.2.1 RCAN1 regulates VEGFR2 level in endothelial cells

The human RCAN1 gene consists of seven exons that are spliced into two major isoforms giving rise to RCAN1.4 (197 amino acids) and RCAN1.1 (252 amino acids). The regulation of RCAN1 is activated by the calcineurin NFAT pathway in response to different growth factors such as VEGF (Hesser et al., 2004, Minami et al., 2004). In endothelial cells, VEGF-A_{165} stimulates expression of RCAN1.4 (Holmes et al., 2010), an effect not observed with other growth factors such as HGF and FGF-2. This previous study also reported that RCAN1 was required for VEGFR2-mediated migration of HDMECs. The current study focussed on exploring the mechanism utilised by RCAN1.4 to regulate VEGFR2 physiological functions and endothelial cell migration. Two independent duplexes of siRNA were used to target RCAN1.1 and RCAN1.4 as it has not been possible to design isoform-specific siRNAs.

In endothelial cells, VEGF-A induced increased phosphorylation of the VEGFR-2 and an apparent decrease in total receptor level (see Figure 3.3). In contrast, levels of VEGFR-1 did not appear to change following siRNA mediated gene silencing of RCAN1. Analysis of downstream pathways in the RCAN1 siRNA transfected cells revealed that VEGF-A mediated AKT phosphorylation appeared to be increased at 5 and 10 minutes with a slight increase in ERK1/2 phosphorylation compared with the non-silencing control and untransfected conditions. Downstream targets of VEGFR-2 were analysed: Erk1/2 phosphorylation, which is required for cell proliferation (Brunet et al., 1999) and AKT phosphorylation which is required for cell survival (Gerber et al., 1998b). To analyse the role of RCAN1 in VEGFR2 signalling siRNA mediated gene silencing is used here. Two independent duplexes of siRNA were used to target RCAN1.1 and RCAN1.4 as it has not been possible to design isoform-specific siRNAs. siRNA mediated silencing of RCAN1 caused a decrease in VEGF-A mediated VEGFR2 down-regulation (evident at 10 mins) compared with untransfected and non-silencing conditions (Figure 3.3).

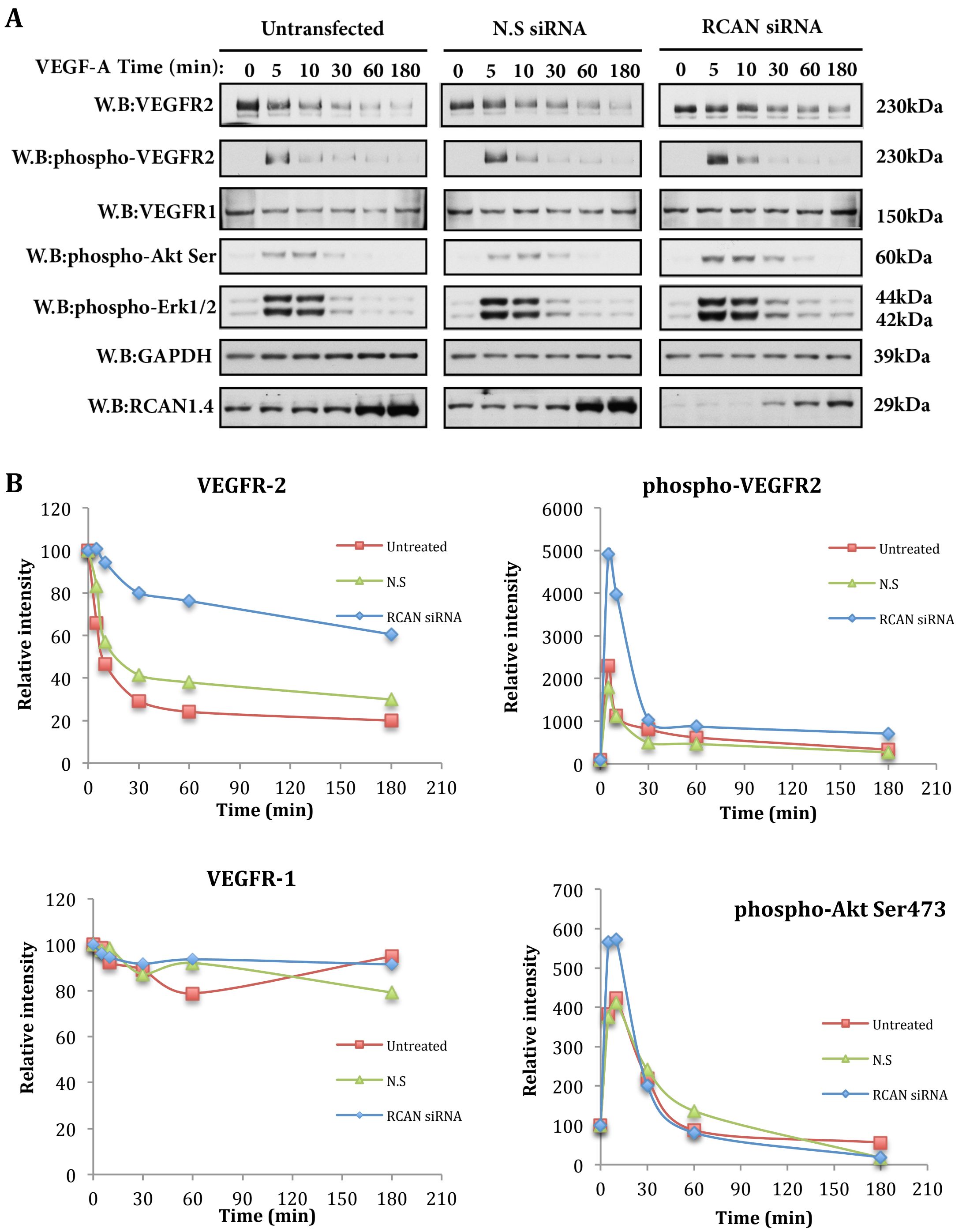

Figure 3.3: RCAN1 regulates VEGFR-2 level in HDMECs

A. HDMEC were transfected with siRNA. 48 hours post transfection cells were stimulated with VEGF-A then lysed proteins to separate by SDS-PAGE. Levels of VEGFR2 phosphorylation (tyrosine 1175), total VEGFR-2, VEGFR-1, phospho-Akt Ser 473, phospho-Erk1/2 and RCAN1.4 expression were determined by western blotting. GAPDH was used as a loading control. **B.** Graphs illustrate the expression of each protein in response to VEGF-A as determined from relative intensity of the band compared to the basal condition. Data shows mean ± SD. The data is representative of three experiments.

In addition, to determine if this effect of RCAN1 on receptor internalisation and downstream targets was apparent with another receptor kinase (RTK) expressed on

HDMECs, we examined the hepatocyte growth factor receptor (HGFR/c-Met). Analysis of HGF stimulation of HDMECs showed that the mature 155 kDa HGFR level decreased, with reduction apparent after 60 minutes of stimulation. siRNA mediated silencing of RCAN1 caused no change in the down-regulation of the HGFR or the downstream intracellular signalling cascade from HGFR, as indicated by Akt and ERK1/2 phosphorylation (Figure 3.4). This result was in contrast to the previous effect of siRNA mediated silencing of RCAN1 on VEGFR-2 downregulation.

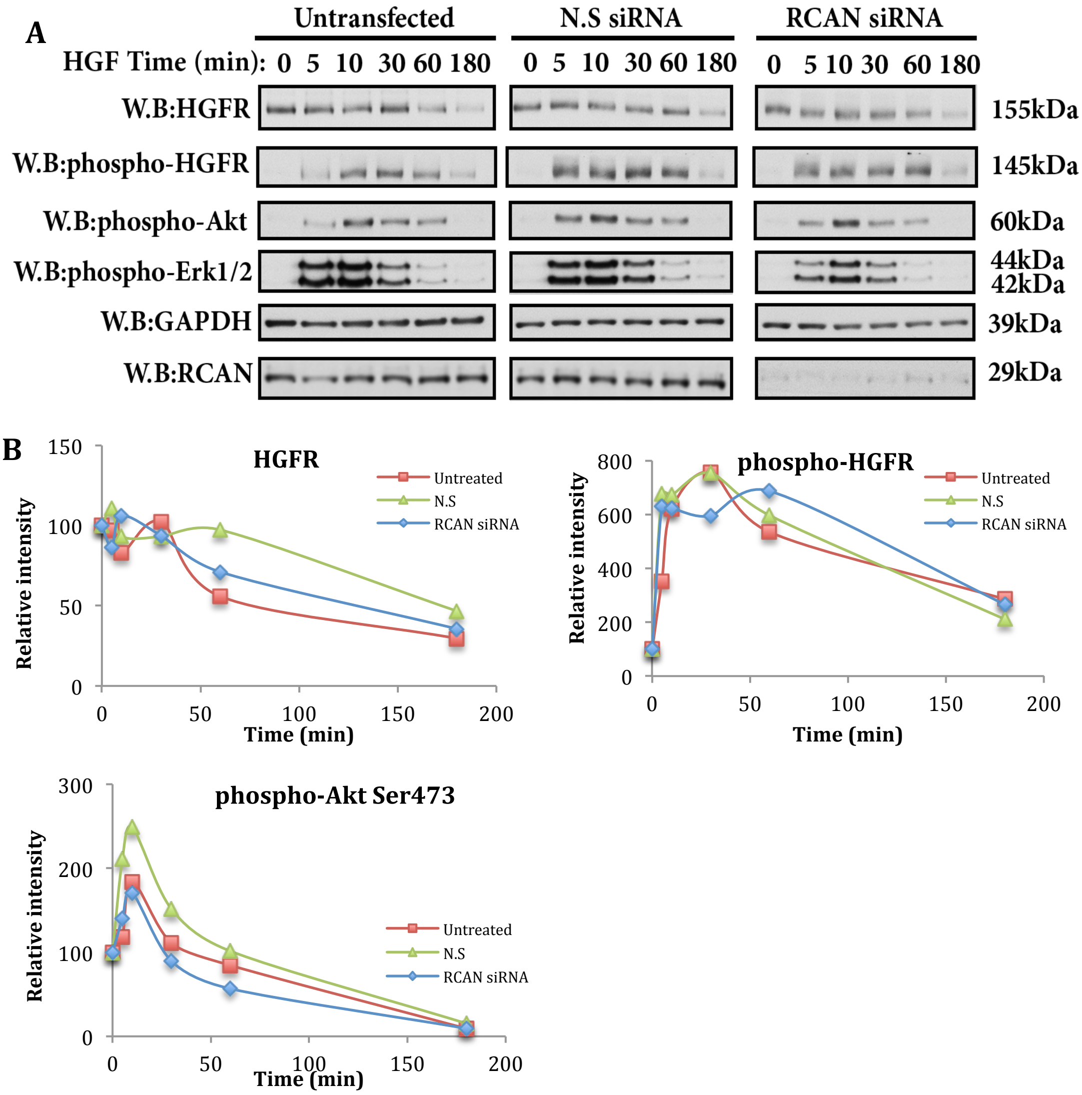

Figure 3.4: HGFR regulation

A. HDMEC were transfected with siRNA as indicated. 48 hours post transfection cells were stimulated with HGF then lysed proteins to separate by SDS-PAGE. Levels of total HGFR, phospho-HGFR, phospho-Akt Ser 473, phospho-Erk1/2 and RCAN1.4 expression were determined by western blotting. GAPDH was used as a loading control. **B.** Graphs illustrate the expression of each protein in response to VEGF-A as determined from relative intensity of the band compared to the basal condition. Data shows mean ± SD. The data is representative of three experiments.

3.3 RCAN1 regulates VEGFR-2 internalisation

Previous data had shown that RCAN1 plays an apparent role in regulating the level of VEGFR-2 following VEGF-A stimulation. However, the western blotting does not reveal the intracellular localisation of the VEGFR-2. VEGF-mediated activation of VEGFR-2 is known to cause receptor internalisation and degradation with intracellular trafficking (Horowitz and Seerapu, 2012). In order to analyse the cell surface expressed VEGFR-2, an antibody to the N-terminal extracellular domain of the VEGFR-2 was used and immunofluorescence analysis performed in the absence of cell permeabilisation, meaning that only receptors present on the cell surface, available for ligand interaction, would be visualised.

To examine whether RCAN1 is directly required for cell surface internalisation of VEGFR2, siRNA was employed to knockdown RCAN1. VEGF stimulation led to a time-dependent decrease in surface VEGFR-2 levels with internalisation evident after 10 min agonist stimulation (Figure 3.5). siRNA-mediated silencing of RCAN1 expression caused a reduction in the degree of VEGFR-2 internalisation as evidenced by increased fluorescence following VEGF stimulation relative to the untreated and non-silencing siRNA samples. Previous data has identified a role for RCAN1 in HDMEC migration using a scratch wound assay (Holmes et al., 2010). Therefore in order to see if VEGFR-2 internalisation was affected in migrating cells, a scratch wound was introduced prior to addition of VEGF-A (Figure 3.5). However, RCAN1 silencing appeared to delay VEGFR-2 internalisation at the leading edge of the scratch wound.

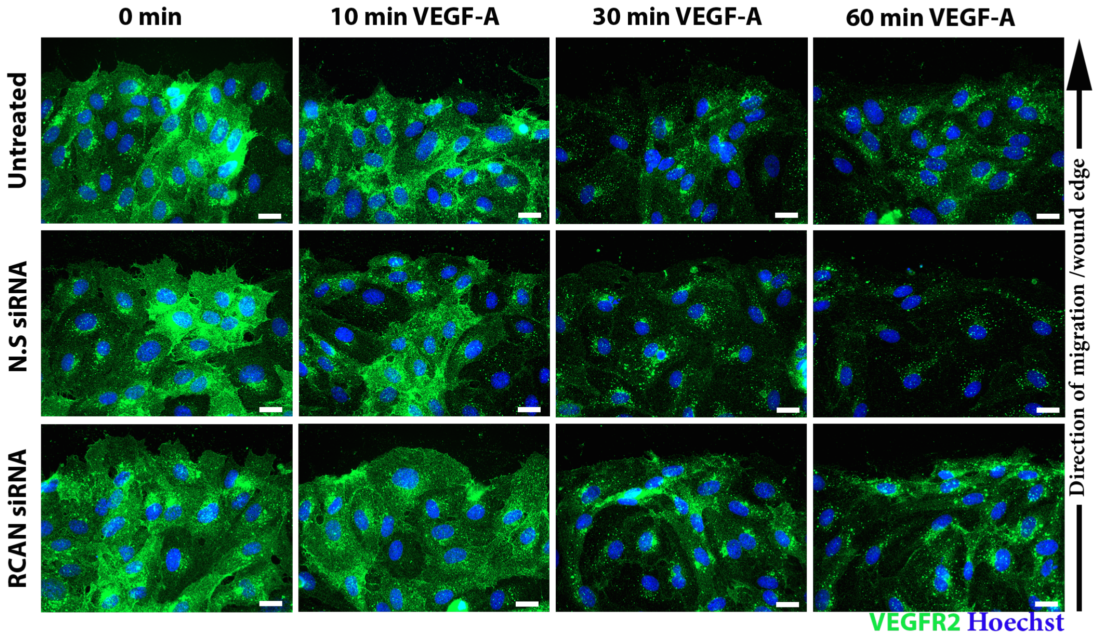

Figure 3.5: RCAN1 and VEGFR2 internalisation

HDMECs were seeded at 7 × 10^4 cells/wells onto pre-coated gelatin for 24 hour using FGM. Cells were transfected with siRNA of RCAN1 and non-silencing (N.S). Cells were serum starved in 1%FCS media overnight. A scratch was introduced to each well using a sterile 200µl Gilson pipette and stimulated with VEGF-A 50ng/ml for 10, 30 and 60 minutes. The cells were fixed with 2% PFA for 10 minutes. Cells were blocked for 1 hour in 5%BSA then incubated for one hour with anti-Goat KDR (R&D system) (1:200) following that secondary for 1 hour. Final staining with Hoechst for nuclei using Hoechst for 10 minutes. Images were taken pairwise with same exposure time for VEGF-A samples for each assay analyzed at 40x object using Zen software. Scale bar: 20µm**.** The data is representative of three experiments.

To analyse the specificity of the effect of RCAN1 siRNA silencing on VEGFR-2 internalisation a similar approach for the HGFR was utilised, with immunofluorescence analysis using an antibody to the extracellular N-terminal domain of the HGFR. Stimulation with HGF caused a time-dependent reduction in surface HGFR levels (Figure 3.6). However, in contrast to the effect on VEGFR-2, siRNA mediated silencing of RCAN1 expression did not affect HGFR internalisation, suggesting that the effect of RCAN1 on receptor internalisation was not a general effect on RTKs.

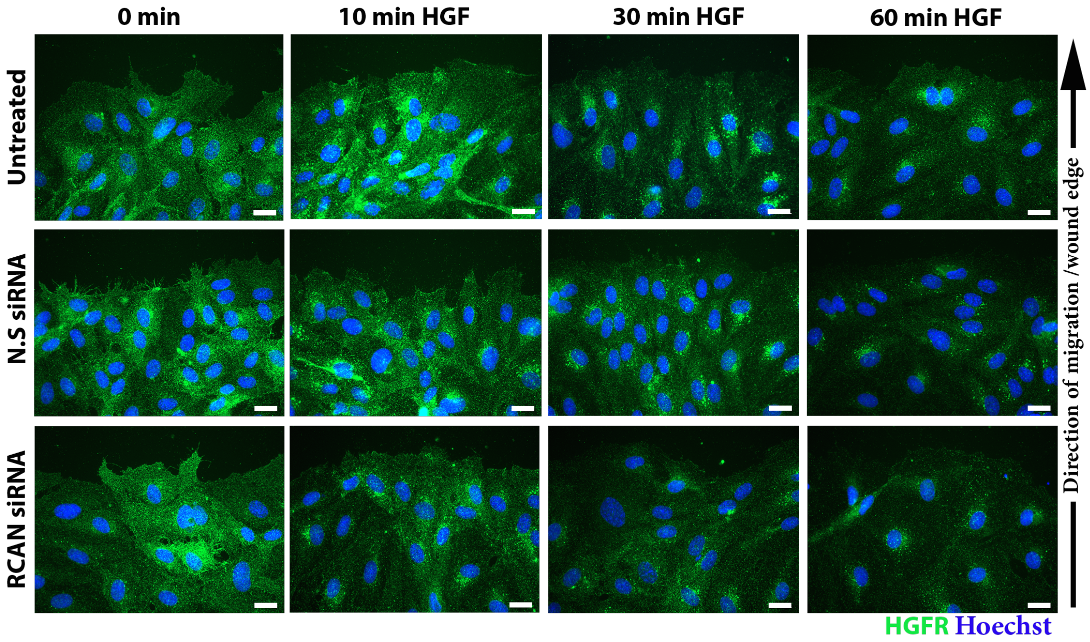

Figure 3.6: RCAN1 siRNA and HGFR internalisation

HDMECs were seeded at 7 × 10^4 cells/well onto gelatin pre-coated glass slides for 24 hour using FGM. The following day, cells were transfected with siRNA of RCAN1 and non-silencing (N.S). Cells were serum starved in 1%FCS media overnight. A scratch was introduced to each well using a sterile 200µl Gilson pipette and stimulated with HGF 50ng/ml for 10, 30 and 60 minutes. The cells were fixed with 2% PFA for 10 minutes. Cells were blocked for 1 hour in 5%BSA then incubated for one hour with anti-HGFR (R&D system) (1:200) following that secondary for 1 hour. Final staining with Hoechst for nuclei using Hoechst for 10 minutes. Images were taken pairwise with same exposure time for HGF samples for each assay analyzed at 40x object using Zen software. Scale bar: 20µm**.** The data is representative of three experiments.

3.3.1 Early endosome co-localization with kinase receptors

The activation of receptor tyrosine kinases by growth factor can lead to downregulation of these receptors and internalisation into early endosomal compartments before trafficking to recycling endosomal compartments or lysosomal degradation of the receptor (Horowitz and Seerapu, 2012). To analyse the trafficking of VEGFR-2, an antibody to the early endosomal marker EEA1 was used. Immunofluorescence staining identified co-localization of VEGFR2 and EEA1 (Figure 3.7). In untreated conditions, co-localization of VEGFR2 and EEA1 in basal, 30 and 60 minutes were clearly visible in peri-nuclear areas. siRNA-mediated silencing of RCAN1 appeared to affect co-localisation between VEGFR-2 and EEA1 at 10 minute time points, suggesting that VEGFR-2 entry into early endosomes was reduced. Pearson's correlation analysis revealed a medium correlation of around 0.46 in all conditions except for RCAN1 siRNA silencing at 10 mins when the correlation reduces to 0.25. Analysis of HGFR co-localisation with EEA1 in HDMECs revealed that similar to VEGFR-2, the HGFR showed a medium degree of co-localisation as evidenced by Pearson's correlation of approximately 0.4; siRNA silencing of RCAN1 did not affect the co-localisation (Figure 3.8).

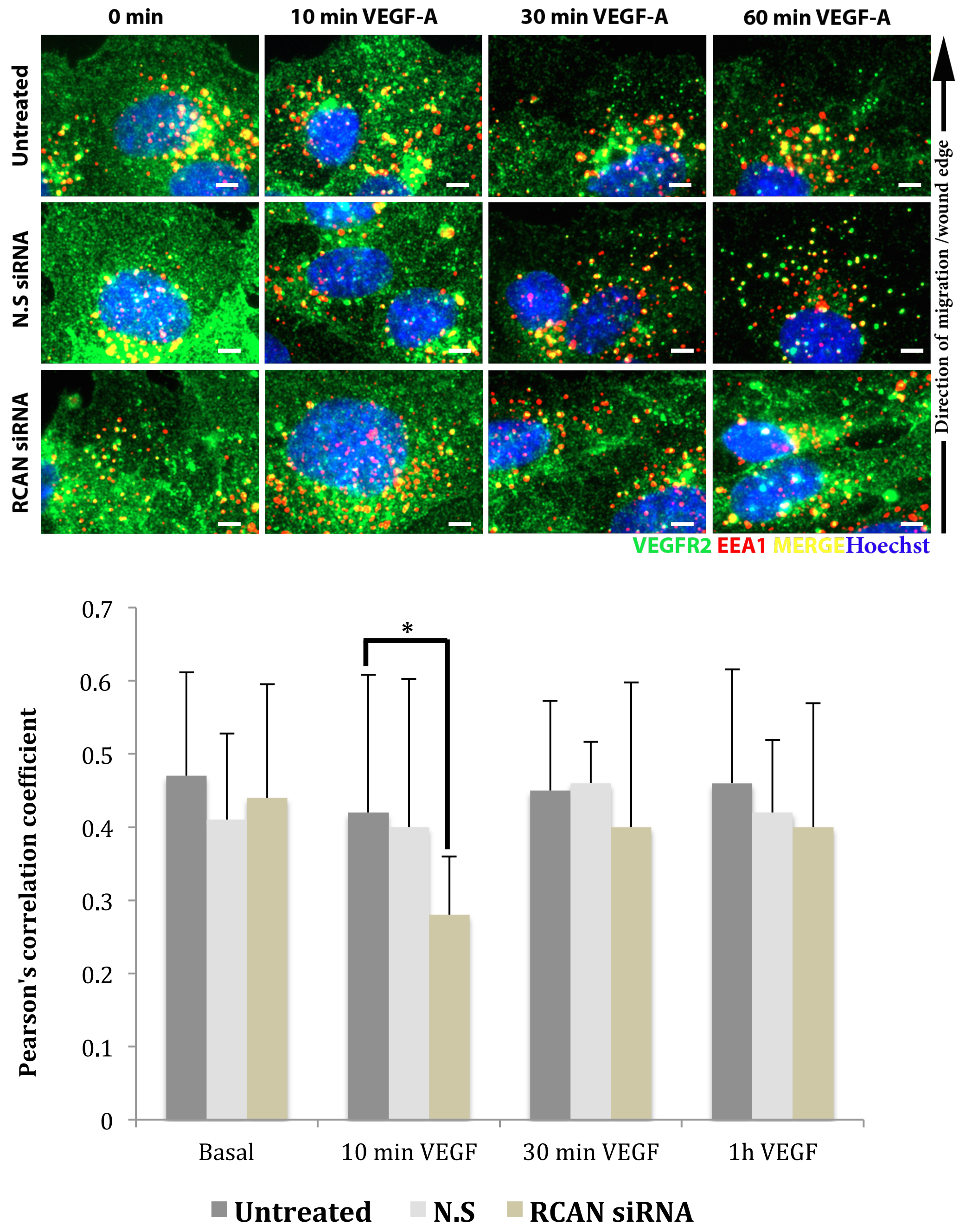

Figure 3.7: Co-localisation of VEGFR-2 and EEA1

HDMECs were seeded at 7 × 104 cells/wells onto pre-coated gelatin for 24 hour using FGM. Cells were serum starved in 1%FCS media overnight. A scratch was introduced to each well using a sterile 200µl Gilson pipette tip and stimulated with VEGF-A165 50ng/ml for 10, 30 or 60 minutes. The cells were fixed with 2% PFA for 10 minutes and permeabilised with Triton X-100 for 10 minutes. Cells were blocked for 1 hour in 5%BSA then incubated for one hour with anti-KDR (R&D system) (1:200) and anti-EEA1 (Cell signal) (1:200), following that secondary for 1 hour. Final staining with HOECHST for nuclei using Hoechst for 10 minutes. Images were taken pairwise with same exposure time for VEGF-A samples for each assay analyzed at 40x object using Zen software. Scale bar: 20µm. Bar chart shows quantitative colocalisation analysis of HDMECs by Pearson's correlation coefficient for VEGFR-2 and EEA1. Data shows mean ± SD (n=3). *P<0.05 siRNA versus Basal unpaired student's t-test. Three images were used for each condition.

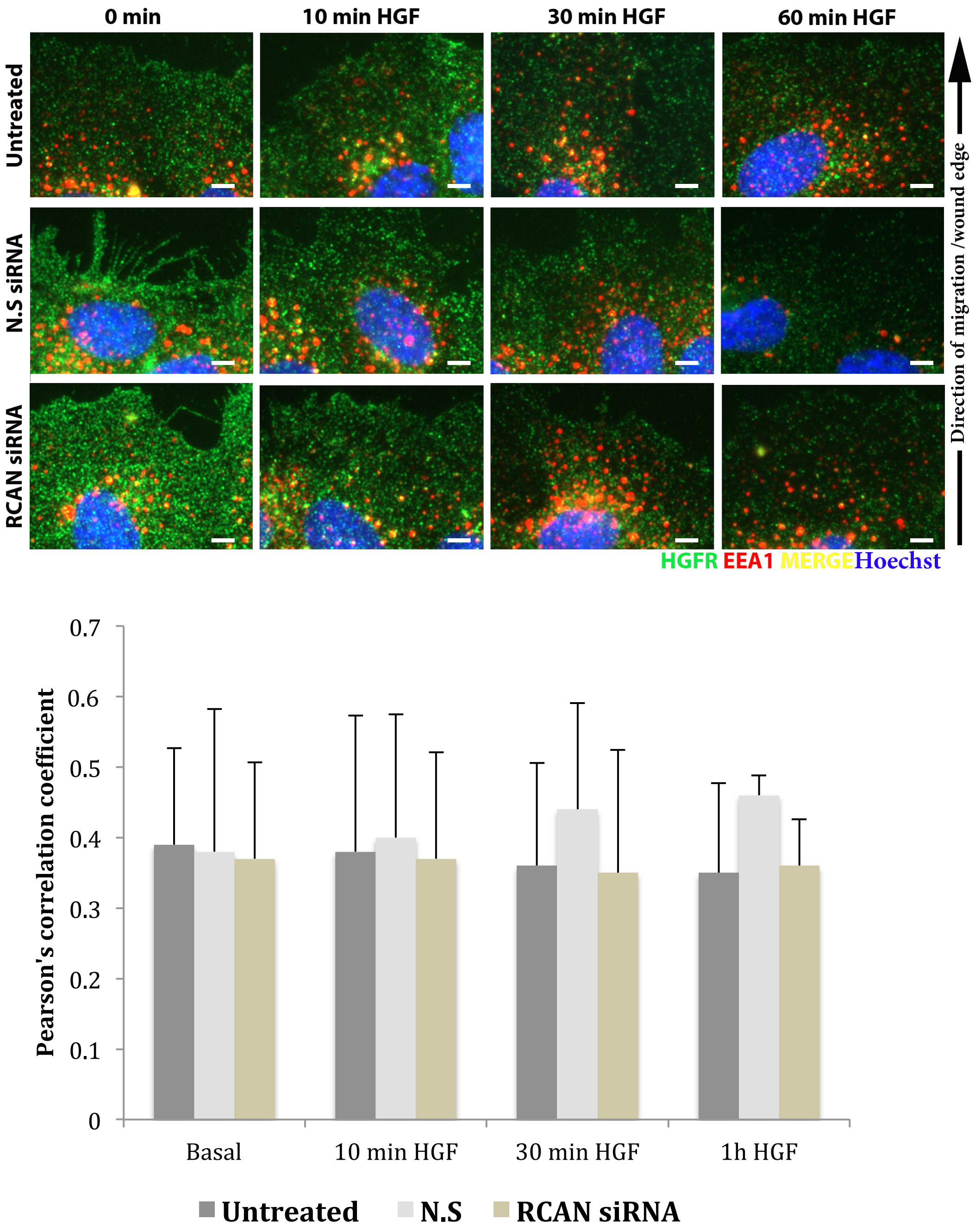

Figure 3.8: Co-localization of HGFR and EEA1

HDMECs were seeded at 7 × 10^4 cells/wells onto pre-coated gelatin for 24 hour using FGM. Cells were serum starved in 1%FCS media overnight. A scratch was introduced to each well using a sterile 200µl Gilson pipette and cells were stimulated with HGF (50ng/ml) for 10, 30 or 60minutes. The cells were fixed with 2% PFA for 10 minutes and permeabilised with Triton X-100 for 10 minutes. Cells were blocked for 1 hour in 5%BSA then incubated for one hour with anti-HGFR (R&D system) (1:200) and anti-EEA1 (Cell signal) (1:200), following that secondary for 1 hour. Final staining with Hoechst for nuclei using Hoechst for 10 minutes. Images were taken pairwise with same exposure time for untreated samples for each assay analyzed at 40x object using Zen software. Scale bar: 20µm. Bar chart shows quantitative colocalisation analysis of HDMECs by Pearson’s correlation coefficient for HGFR and EEA1. Data shows mean ± SD. The data is representative of three experiments. Three images were used for each condition.

3.3.2 Time course of VEGFR-2 and RCAN1 co-localization

The ability of RCAN1 silencing to affect VEGFR-2 internalisation suggested that there could be a possible co-localisation and interaction between VEGFR-2 and RCAN1 in HDMECs following VEGF-A stimulation. In order to analyse this possibility immunofluorescence analysis was performed using antibodies to VEGFR-1 and RCAN1 (Figure 3.9). Co-localisation was apparent at 0, 1, 2 minutes throughout the cell, whereas at later time points of 5, 10 and 60, co-localisation was evident in more peri-nuclear areas.

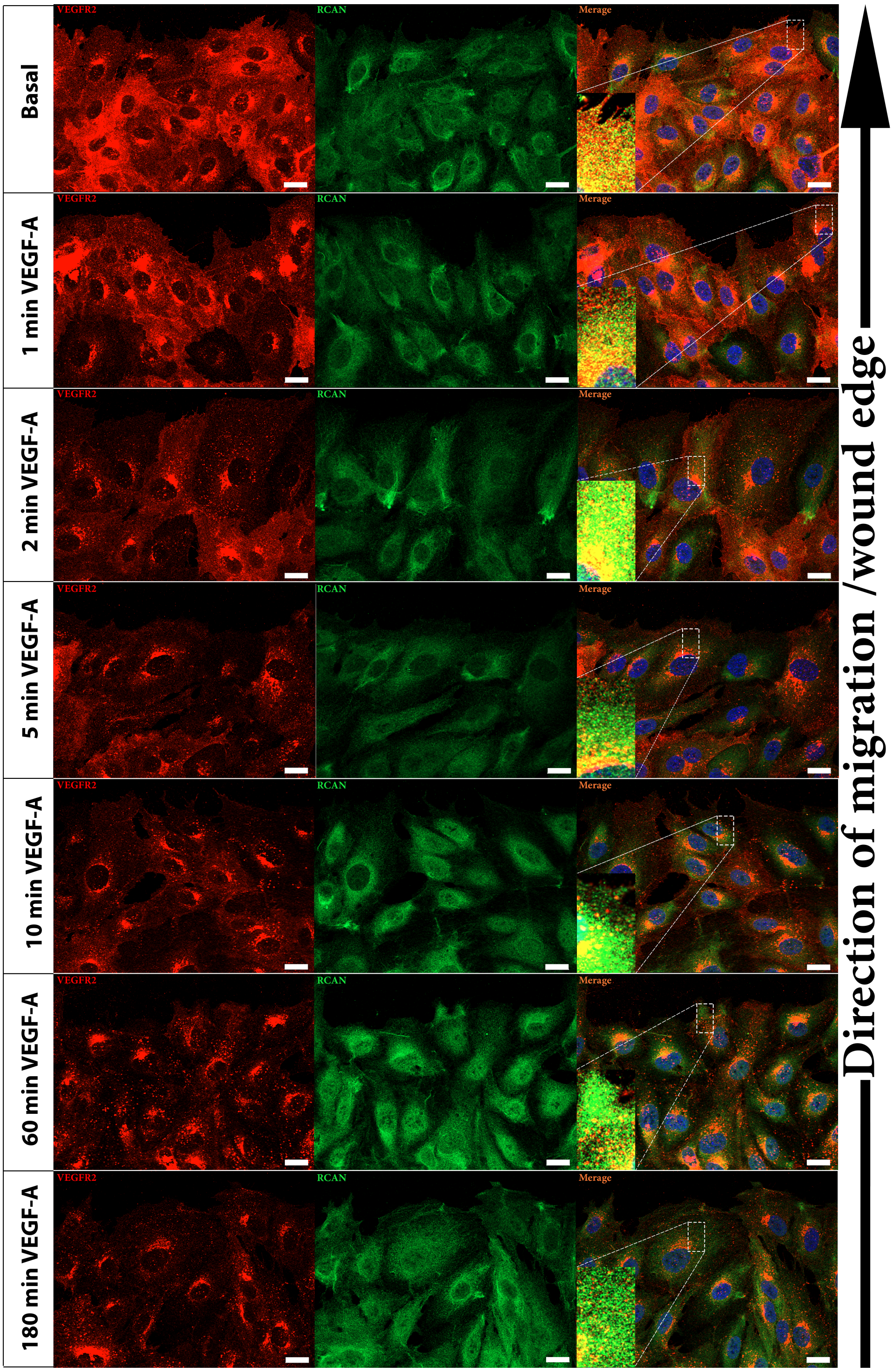

Figure 3.9: Co-localisation of VEGFR-2 and RCAN1

HDMECs were seeded at 7 × 10^4 cells/wells onto pre-coated glass with gelatin for 24 hour using full growth media. Following day cells were serum starved in 1%FCS media overnight. Cells were stimulated with VEGF-A 50 ng/ml for 1, 2, 5,10, 30, 60 and 180 minutes. The cells were fixed with 2% PFA for 10 minutes. Cells were permeabilized with Triton X-100 for 10 minutes and blocked with 5% BSA and incubated for one hour for anti-RCAN1 (Sigma) (1:200) or anti-KDR (R&D system) (1:200) following that secondary for 1 hour. Final staining with Hoechst for nuclei using Hoechst for 10 minutes. Images were taken pairwise with same exposure time for VEGF-A samples for each assay analyzed at 40x object using Zen software. Scale bar: 20μm**.** The data is representative of three experiments.

3.3.3 RCAN1 association with VEGFR-2

The previous immunofluorescence analysis had suggested an association between RCAN1 and VEGFR-2. This was investigated further using co-immunoprecipitation. Analysis of the interaction between RCAN1 and VEGFR-2 was technically challenging in HDMECs due to the low endogenous levels of these proteins. HEK293 cells transiently co-transfected with plasmids encoding VEGFR-2 and GFP-RCAN1.4 were utilised. Cells were stimulated with VEGF for 0, 10 and 60 minutes and lysates prepared in Triton X-100 lysis buffer. Cells were also transfected with empty control plasmids encoding GFP. GFP pull down using anti-GFP agarose beads appeared to show an association on basal between RCAN1.4 and VEGFR-2, which was reduced on VEGF stimulation (Figure 3.10).

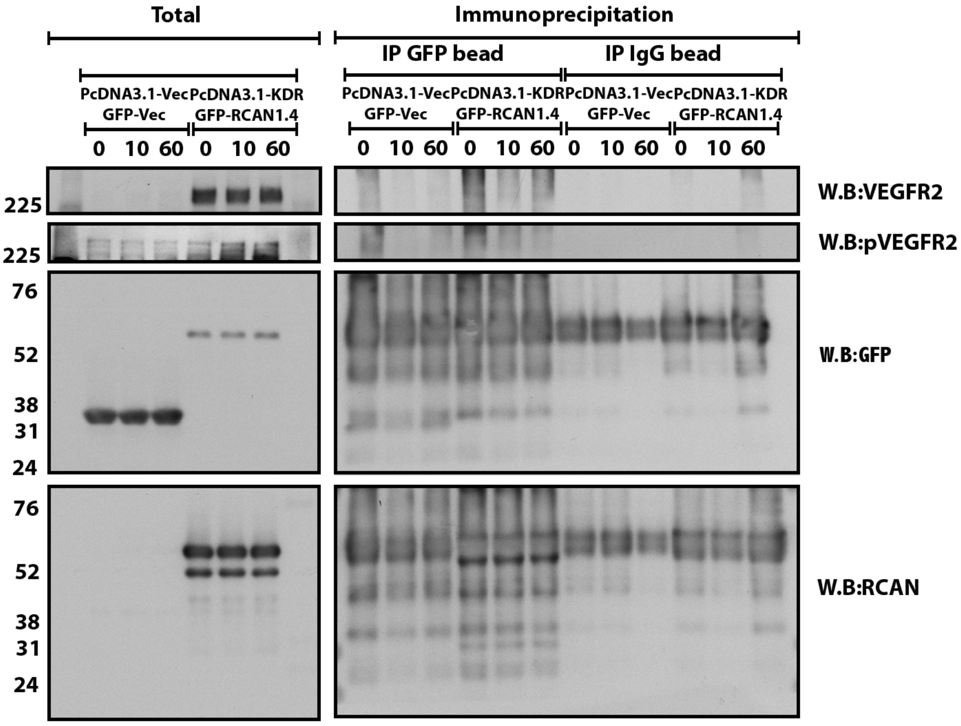

Figure 3.10: RCAN1 and VEGFR2 association by immunoprecipitation

HEK293a were transfected with pcDNA3.1 vector and GFP vector as control or pcDNA3.1-VEGFR2 wild type and GFP-RCAN1.4. Following transfection cells were serum starved for 24 hours then stimulated for 10 and 60 minutes. Cells were lysed with X-100 Triton. Lysates incubated with beads anti-GFP or anti-IgG antibody overnight. The samples were boiled in 2× LDS buffer and subjected to SDS-PAGE gel. The membranes were probed with antibodies to VEGFR-2, phospho VEGFR-2, GFP and RCAN1. The data is representative of three experiments.

The profound effect of RCAN depletion on delaying internalization of ligand-activated VEGFR-2 suggested that RCAN may interact directly with VEGFR-2. The immunoprecipitation experiment was not conclusive in determining an association between RCAN1 and VEGFR-2. Therefore a proximity ligation assay (PLA) was utilised to analyse any potential spatial and temporal interaction between VEGFR-2 and RCAN. This technique generates a fluorescence signal at the precise site of interaction of the proximity ligation probes and consequently the primary antibodies targeting RCAN1 and VEGFR-2 (Söderberg et al., 2006). The PLA revealed a rapid and transient increased co-localisation between VEGFR-2 and RCAN1 in the HDMECs at the leading edge following stimulation with VEGF (Figure 3.11).

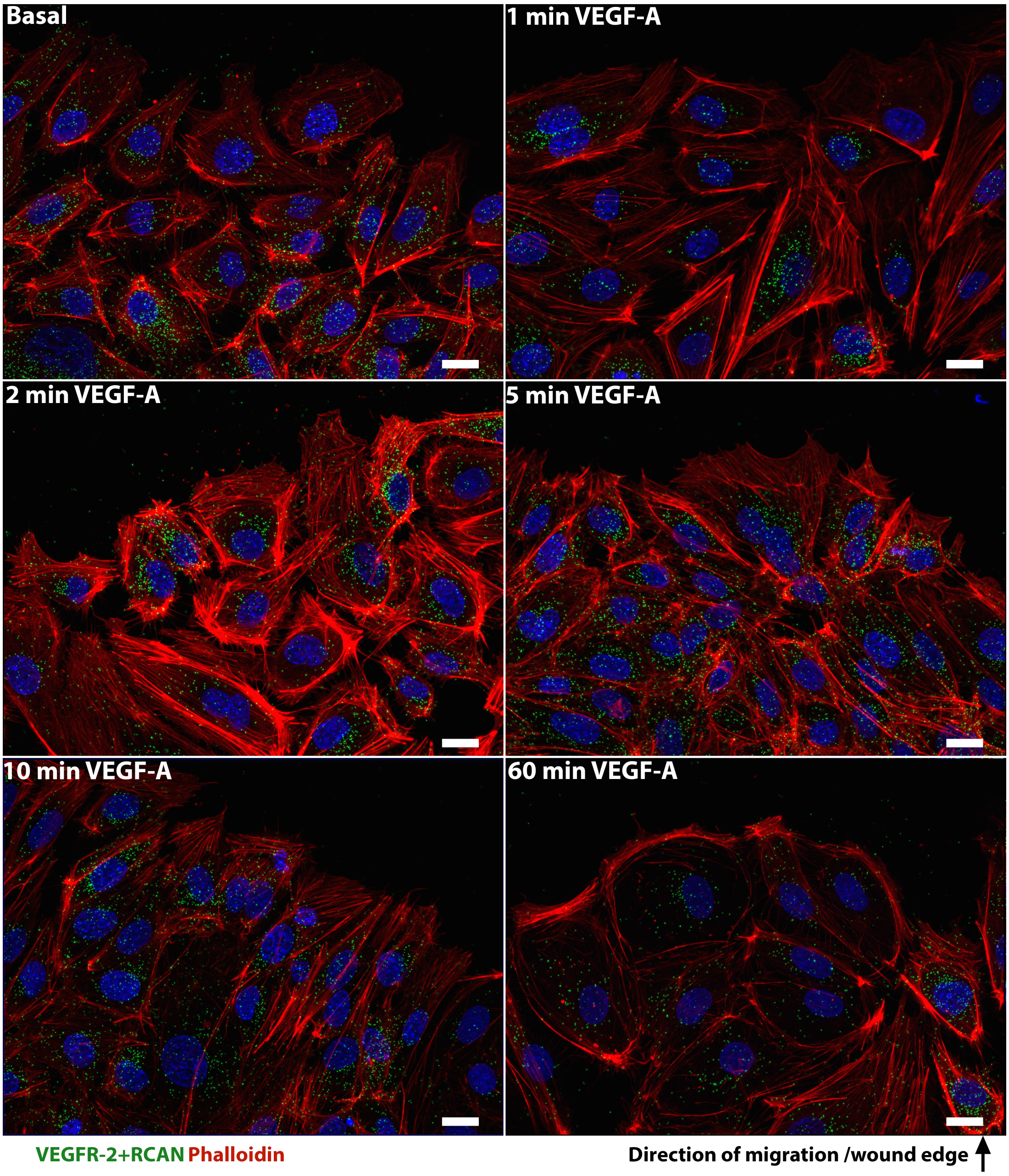

Figure 3.11: RCAN1 and VEGFR2 association by PLA

Detection of RCAN1 and VEGFR2 association in HDMECs using a proximity ligation assay (PLA). HDMECs were seeded at 7 × 10^4 cells/wells onto pre-coated glass with gelatin for 24 hour using full growth media. Following day cells were serum starved in 1%FCS media overnight. Cells were stimulated with VEGF-A 50 ng/ml for 1, 2, 5,10, 30 and 60 minutes. The cells were fixed with 2% PFA for 10 minutes. Cells were worked using PLA commercial protocol. Images were taken pairwise with same exposure time for VEGF-A samples for each assay analyzed at 40x object using Zen software. Scale bar: 20µm**.** This experiment has been performed twice.

3.4 RCAN1 regulates VEGFR2 mediated cytoskeleton reorganisation and cells polarity

Cell migration is important in many biological functions such as angiogenesis, embryonic morphogenesis and tissue repair (Lamalice et al., 2007, Affolter et al., 2009). The mechanism of cell migration involves many multistep processes started by the protrusion of the cell membrane. Cell migration is activated by many growth factors acting on RTKs. These ligands can bind receptors on the cell membrane and pass the signalling to an intracellular pathway that activates reorganisation of the actin cytoskeleton. Filopodia play a role in facilitating directionality of cell migration but the entire mechanism is still unclear. Lamellipodia are formed as flat sheets on the cell membrane located at the leading edge of migrating cells (Swaney et al., 2010, Iglesias and Devreotes, 2008). Analysis of the cytoskeletal reorganization at the scratch wound edge in HDMECs revealed that VEGF induced a number of cellular protrusions reminiscent of filopodia (Figure 3.12). This effect was blocked with siRNA mediated silencing of RCAN1 expression, as leading edge cells were devoid of any protrusions under both basal and VEGF-stimulated conditions, with an apparent cortical ring of polymerised actin at the leading edge. However, HGF was able to induce cytoskeletal reorganization even in HDMECS with depleted RCAN1 levels, revealing that RCAN1 knockdown did not block cytoskeletal reorganisation in response to all agonists (Figure 3.12).

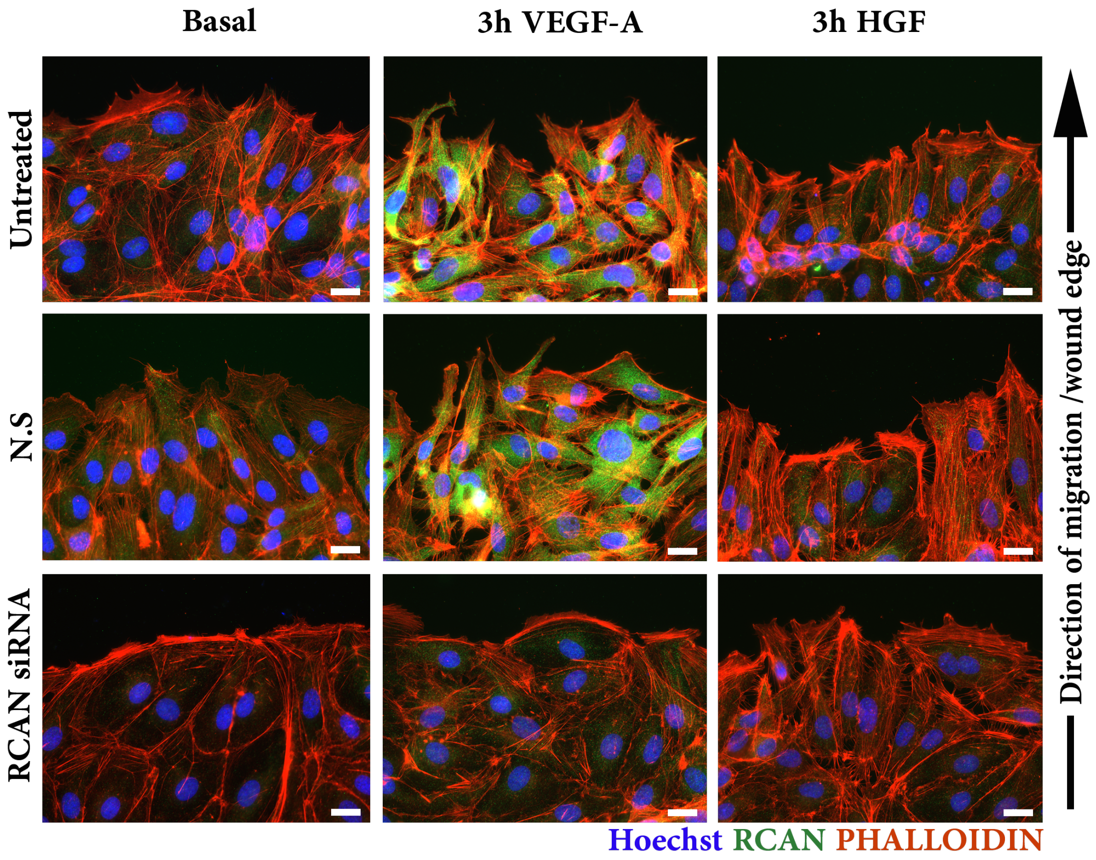

Figure 3.12: RCAN1 depletion and cytoskeleton reorganization

HDMECs were seeded at 7 × 10^4 cells/wells onto gelatin-coated glass coverslips for 24 hour using FGM. The following day cells were transfected with siRNA of RCAN1 and non-silencing (N.S) for 6 hours. Cells were serum starved in 1%FCS media overnight. A scratch was introduced to each well using a sterile 200µl Gilson pipette and stimulated with VEGF-A 50ng/ml or HGF for 3 hour. The cells were fixed with 2% PFA for 10 minutes. Cells were permeabilized with Triton X-100 for 10 minutes and blocked for 1 hour in 5%BSA then incubated for one hour for anti-RCAN1 (Sigma) following that secondary and phalloidin (Invitrogen) for one hour. Final staining with Hoechst for nuclei using Hoechst for 10 minutes. Images were taken pairwise with same exposure time for VEGF-A or HGF sample for each assay analyzed at 40x object using Zen software. Scale bar: 20µm**.** This data is representative of three experiments.

3.4.1 Disruption of RCAN1 lead to loss of cells polarity

Directed cell migration in response to agonists requires asymmetric activation of cell membrane receptors to induce polarised signals that result in the generation of protrusions at front of the cell (leading edge) and retraction at the back of the cell (trailing edge) (Iglesias and Devreotes, 2008, Swaney et al., 2010). In light of the known roles of RCAN1 in regulating HDMEC cell migration, analysis of the effect of RCAN1 depletion on cell polarity was performed. The scratch wound assay allows analysis of cell polarity as directed migration in this assay is accompanied by reorganisation of the centrosome and Golgi apparatus, relative to the nucleus, to face the direction of cell migration (Uetrecht and Bear, 2009, Chaki et al., 2013). To analyse the effect of RCAN1 on HDMEC cell polarity, the orientation of the Golgi apparatus was visualised using an antibody to GM130 and the centrosome using an antibody to pericentrin (Figure 3.13). Following VEGF stimulation of HDMECs cell polarity increased at the leading edge over a period of 6 hours from 28% to 75%. This increase in cell polarity was considerably reduced in RCAN1-depleted cells, achieving a maximum of only 50% (Figure3.14).

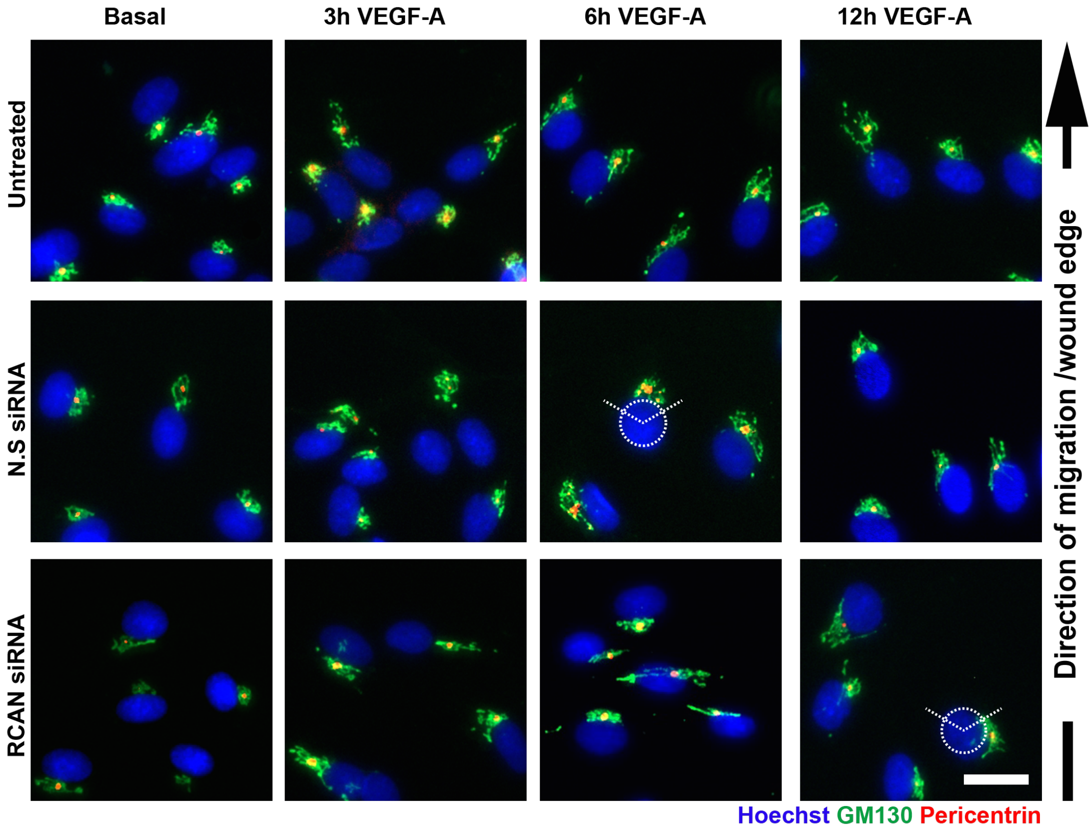

Figure 3.13: Analysis of Golgi and Centrosome polarization in RCAN1 knockdown

HDMECs treated with control, two duplexes RCAN1 siRNA for 48 hours were scratch wounded and then stimulated for 0, 3, 6 and 12 hours as showed. The cells were fixed and stained with antibodies to the centriolar marker pericentrin and to the Golgi marker GM130. Also DNA was stained with Hoechst. The scale bar is 20 µm. Cell polarization towards the wound was assessed by drawing a circle centred over the nucleus with a 120° segment facing the wound and counted. Ten images were taken per condition. This data is representative of three experiments.

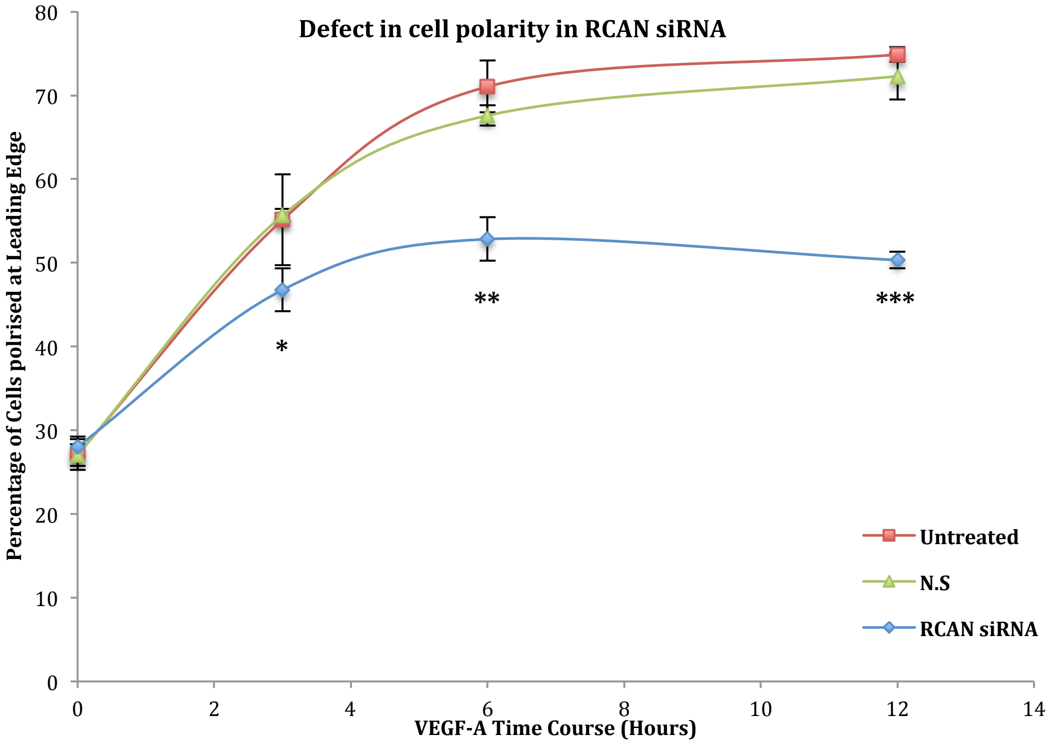

Figure 3.14: Analysis of Centrosome and Golgi polarization in RCAN1 Knockdown

Cell polarisation at 0, 3, 6 and 12 is plotted in the bar graph. Error bars indicate the standard error of the mean (n=3). *P<0.05, **<0.01,***<0.001, siRNA versus N.S unpaired student's t-test. The data is representative of three experiments.

3.5 *In vitro* 3D collagen study optimization

Angiogenesis requires coordinated cell migration. It has previously been reported that RCAN1 regulates efficient tubular morphogenesis in HDMEC cells in a 3D collagen gel assay (Holmes et al., 2010). This assay was chosen to allow visualisation of cells depleted of RCAN1 and control siRNA treated cells in the same sample to allow closer visualisation of the defect in tubular morphogenesis. Initial validation of Cell Tracker dyes was performed in order to optimise dye concentrations to minimise effects of cell labelling on tubular morphogenesis in HDMECs. Firstly Green CMFDA Dye (Life Technologies) and Red CMTPX Dye (Life Technologies) were selected to label HDMECs on collagen gel. Cells were plated on a plastic dish pre-coated with 1% gelatin and serum-starved overnight. The following day, cells were labelled with 1μM or 5μM of Green or Red Cell Tracker dye for 45 minutes and washed with serum-free media.

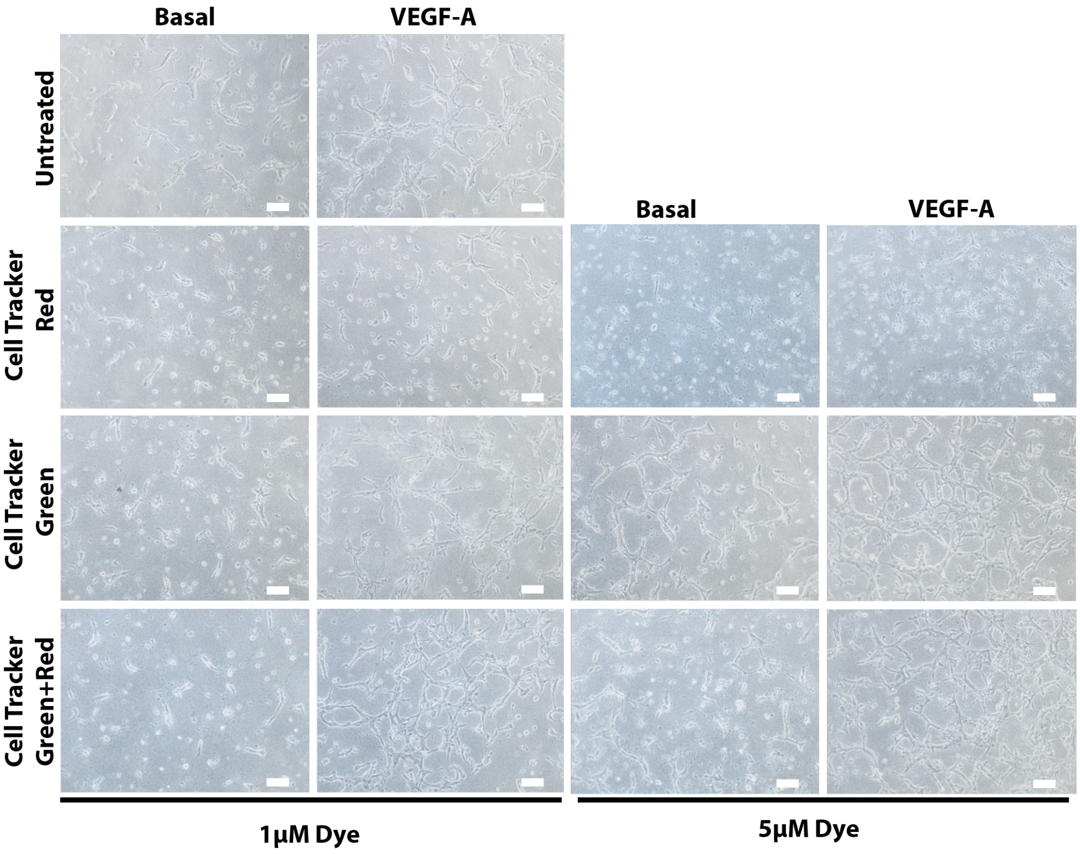

Figure 3.15: CellTracker Dye Red and Green validation

HDMECs were seeded at 7 × 10^4 cells/wells onto pre-coated gelatin for 24 hour using FGM. Cells were serum starved in 1%FCS media overnight followed by staining for 45 minutes with 1 or 5µM Cell Tracker dye Red and Green. Cells were lift in serum free media for one hour and seeded onto collagen matrix, and stimulated with VEGF-A_{165} 50ng/ml. for 18 hours. The cells were fixed with 2% PFA for 10 minutes. Images were taken using a Nikon imaging microscope at × 10 objective. Scale bar: 100µm. This experiment has been performed once.

Cells were incubated for one hour after staining before detachment with accutase and plating onto a collagen layer. After two hours a second layer of collagen was introduced on top of the cells. Cells were then stimulated with VEGF-A for 18 hours and then cells fixed with 4% PFA and stained with Hoechst. Cells were visualised in bright field using phase contrast microscopy (Figure 3.15) and immunofluorescence microscopy (Figure 3.16). With Red Cell Tracker dye at 1 or 5µM it appeared cells died on collagen gel in comparison to Green Cell Tracker dye, suggesting that the Red dye interfered with tubular morphogenesis via an unknown mechanism.

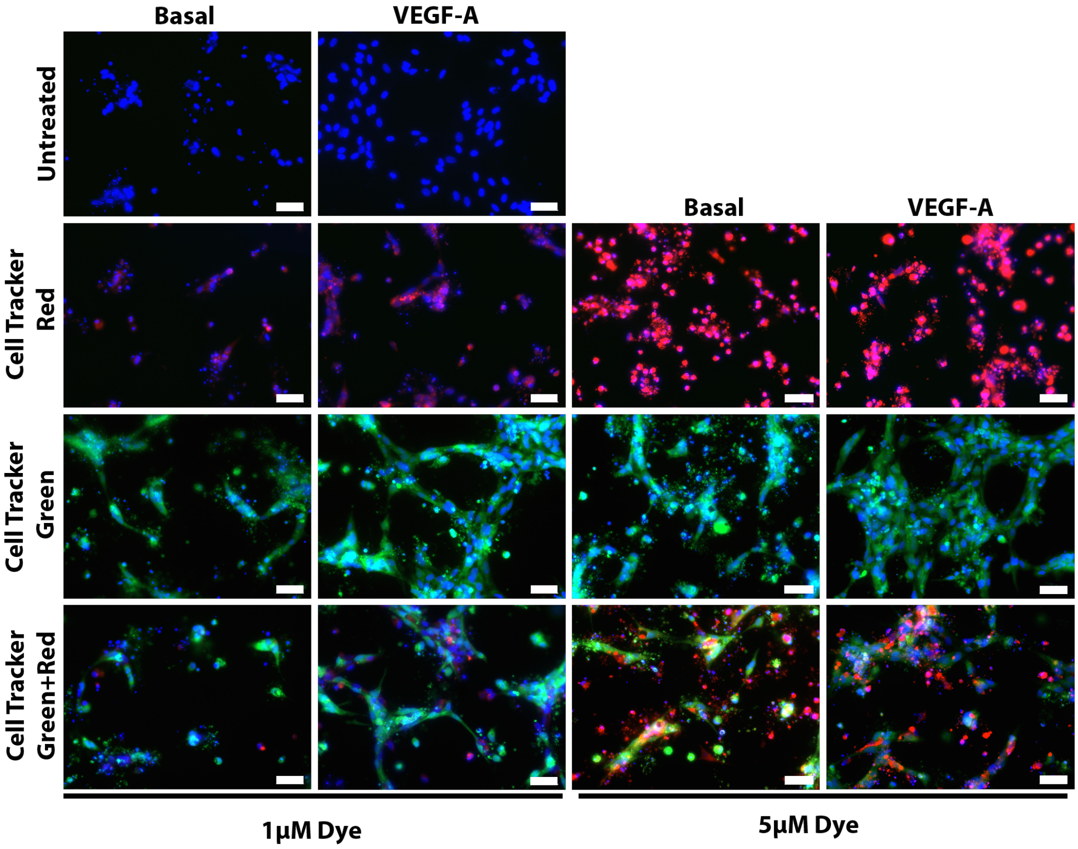

Figure 3.16: CellTracker Dye Red and Green IF

HDMECs were seeded at 7 × 104 cells/wells onto pre-coated gelatin for 24 hour using FGM. Cells were serum starved in 1%FCS media overnight followed by staining for 45 minutes with 1 or 5µM Cell Tracker dye Red and Green. Cells were left in serum free media for one hour and seeded onto collagen matrix, and stimulated with VEGF-A165 50ng/ml. for 18 hours. The cells were fixed with 2% PFA for 10 minutes. Final staining with Hoechst for nuclei using Hoechst for 10 minutes. Images were taken for each assay analyzed at 20x object using Zen software. Scale bar: 50µm. This experiment has been performed once.

Further optimisations of Cell Tracker dyes used Blue CMAC Dye (Life Technologies) or Orange CMTMR Dye (Life Technologies). Serial dilutions of the dyes used 1, 5, 10 and 20 µM for Blue dye (Figure 3.17 and Figure 3.18). Dilution of Blue dye below 10 µM gave a weak staining of HDMECs (data not shown). Concentrations of 10 and 20 µM gave cell staining although toxicity was evident. In contrast, cells labelled with Orange dye retained the ability to undergo efficient tubular morphogenesis (Figure 3.17 and Figure 3.18). In conclusion Green and Orange dye was chosen for further study in this project.

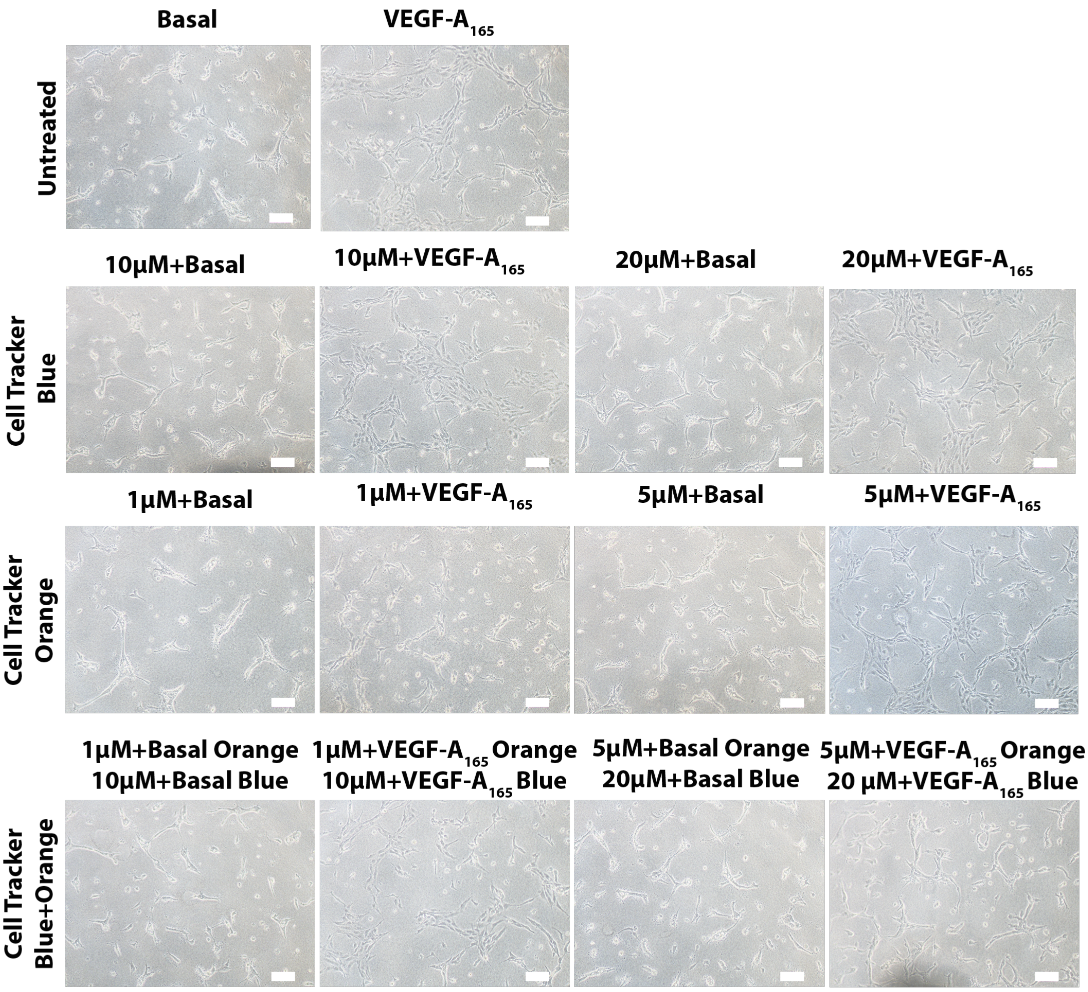

Figure 3.17: CellTracker Dye Blue and Orange validation

HDMECs were seeded at 7 × 10^4 cells/wells onto pre-coated gelatin for 24 hour using FGM. Cells were serum starved in 1%FCS media overnight followed by staining for 45 minutes with 1, 5, 10 or 20µM Cell Tracker dye Blue and Orange. Cells were left in serum free media for one hour and seeded onto collagen matrix, and stimulated with VEGF-A 50ng/ml. for 18 hours. The cells were fixed with 2% PFA for 10 minutes. Images were taken using a Nikon imaging microscope at × 10 objective. Scale bar: 100µm. This experiment has been performed once.

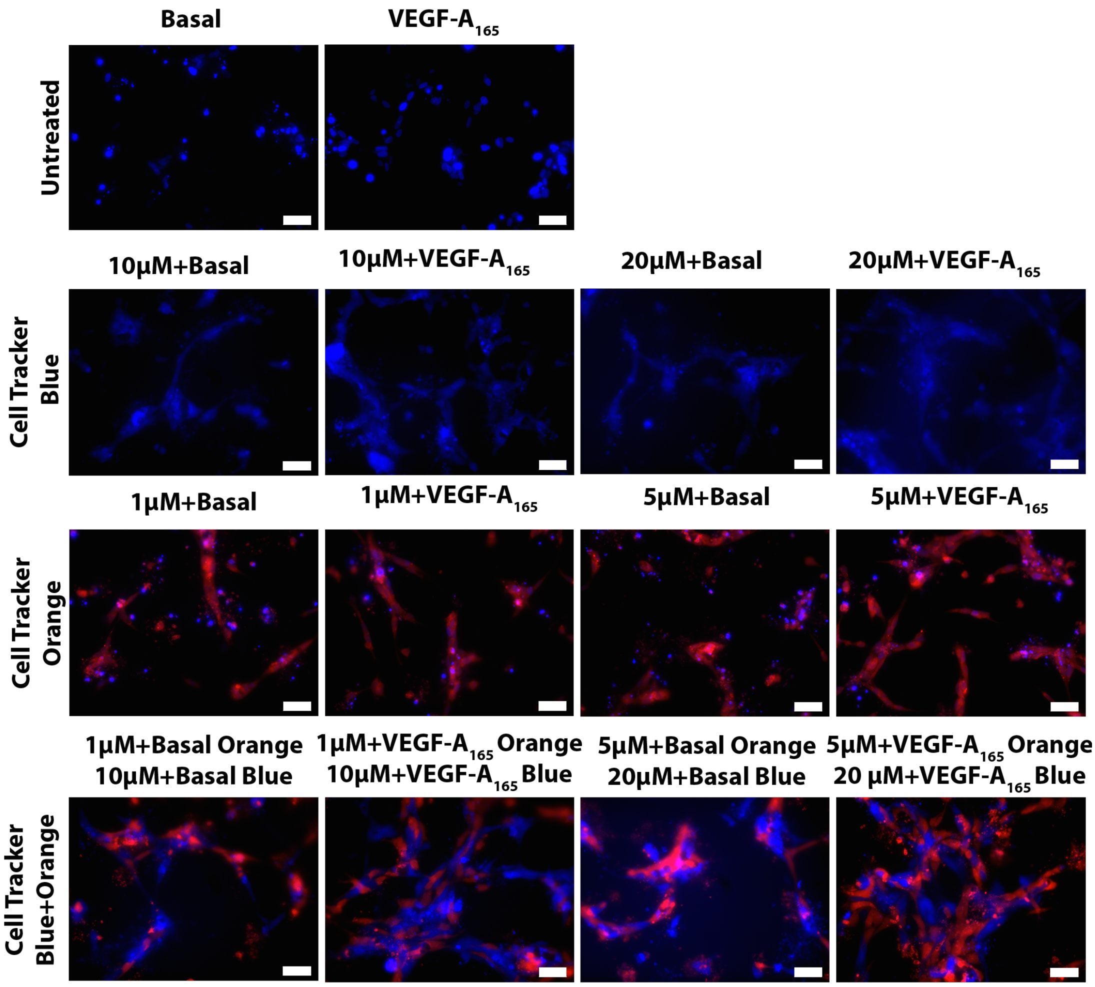

Figure 3.18: CellTracker Dye Blue and Orange validation

HDMECs were seeded at 7 × 10^4 cells/wells onto pre-coated gelatin for 24 hour using FGM. Cells were serum starved in 1%FCS media overnight followed by staining for 45 minutes with 1, 5, 20, 30 or 100µM Cell Tracker dye Blue and Orange. Cells were lift in serum free media for one hour and seeded onto collagen matrix, and stimulated with VEGF-A_{165} 50ng/ml. for 18 hours. The cells were fixed with 2% PFA for 10 minutes. Staining with Hoechst for nuclei using Hoechst for 10 minutes. Images were taken for each assay analyzed at 20x object using Zen software. Scale bar: 50µm**.** This experiment has been performed once.

3.5.1 *In vitro 3D* collagen study

To study HDMECs in a 3D model the cells needed to be labelled prior to plating onto a collagen matrix. A Cell Tracker dye was validated for this study. Cells were plated on plastic dishes pre-coated with 1% gelatin and siRNA transfection method was used to knockdown RCAN1. Cells were serum-starved overnight and the following day cells were labelled with 5µM of Green Cell Tracker dye for the non-silencing siRNA and 5µM of Orange Cell Tracker for RCAN1 siRNA for 45 minutes and washed with serum free media. Labelled HMDEC populations were detached by accutase and mixed equally before performing the 3D collagen gel assay. Cells were fixed and washed with PBS to be ready for imaging with a Zeiss microscope. Tube formation was quantified by measuring the connecting cells distance using a ruler in Zen software (µm).

HDMECs incubated in the absence of growth factor did not undergo any tube formation visualised by phase contrast and immunofluorescence (Figure 3.19). In contrast, stimulation with VEGF-A induced tubular morphogenesis of HDMECs, by formation of capillary structures that consists of many aligned endothelial cells. Furthermore, stimulation of HDMECs with HGF induced capillary sprouting in some HDMECs but these capillary sprouts did not efficiently form tubules compared to VEGF-A stimulation. It was evident from the immunofluorescence images, which allowed discrimination between cells with RCAN1 silencing (Red colour) and control non-silencing siRNA (Green colour), that cells with depleted RCAN1 levels were not able to align properly and form continuous tubes (Figure 3.19). This was confirmed by quantification, showing that VEGF-A stimulated of HDMECs with depleted RCAN1 levels failed to align.

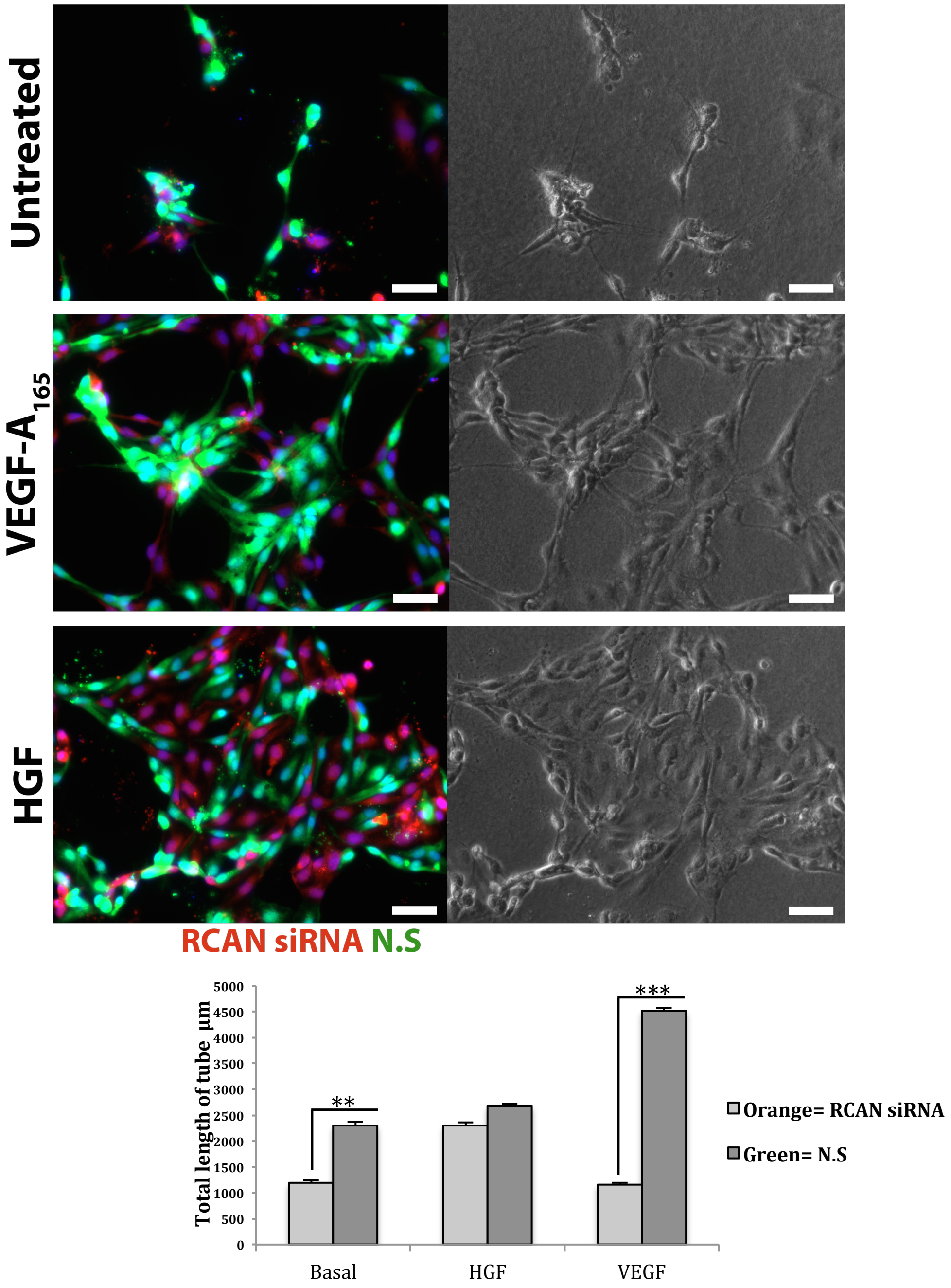

Figure 3.19: The role of RCAN1 in tubular morphogenesis

HDMECs were seeded at 7 × 10^4 cells/wells onto pre-coated gelatin for 24 hour using FGM. Following day cells were transfected with siRNA of RCAN1 and non-silencing (N.S). Cells were serum starved in 1%FCS media overnight followed by staining for 45 minutes with 5µM Cell Tracker dyes Green and Orange. Cells were left in serum free media for one hour and mixed then seeded onto collagen matrix, and stimulated with VEGF-A 50ng/ml. for 18 hours. The cells were fixed with 2% PFA for 10 minutes. Staining with Hoechst for nuclei using Hoechst for 10 minutes. Images were taken for each assay analyzed at 20x object using Zen software. Scale bar: 50µm. This figure illustrated the total length of tube quantified from 15 fields (x20 objective) per conditions per experiments using Zen software as described in method chapter. Data shows ± SD,(N=3), (**P<0.01,***P<0.001, siRNA versus N.S). The data is representative of three experiments.

3.5.2 *In vivo* 3D spheroid on collagen study

Sprouting angiogenesis requires endothelial tip cells to become polarised and extend filopodia with the coordinated regulation of stalk cells allowing the formation and stabilisation of the sprout and ultimately a lumen containing vessel (De Smet et al., 2009). It has previously been shown that RCAN1 is required for efficient tubular morphogenesis using a collagen gel assay (Holmes et al., 2010) pointing to a role for RCAN1 in allowing efficient tubular morphogenesis. Cells were plated on plastic dishes pre-coated with 1% gelatin and the siRNA transfection method was used to knockdown RCAN1. Cells were serum-starved over night and the following day cells were labelled for 45 mins with 5μM of Green Cell Tracker dye for the non-silencing condition and 5μM of Orange Cell Tracker for RCAN1 siRNA silencing. Labelled HMDEC populations were detached by accutase and mixed equally 1:1. The mixtures were plated in 96 non-adherent well plates with methylcellulose and grown overnight. The following day, 3D spheroids were embedded onto a collagen gel then growth factors were added for 18 hours to examine sprouting tubular morphogenesis in HDMECs with Cell Tracker dyes. Cells were fixed and washed with PBS ready for imaging with a Zeiss microscope. Tube formation quantification was carried out by measuring the length of cells from edge of the spheroids to end of sprouting using a ruler in Zen software and the measurement unit was μm.

RCAN1 depleted HDMECs showed a reduced ability to achieve a tip position resulting in reduced sprouting compared to control cells when stimulated with VEGF (Figure 3.20).

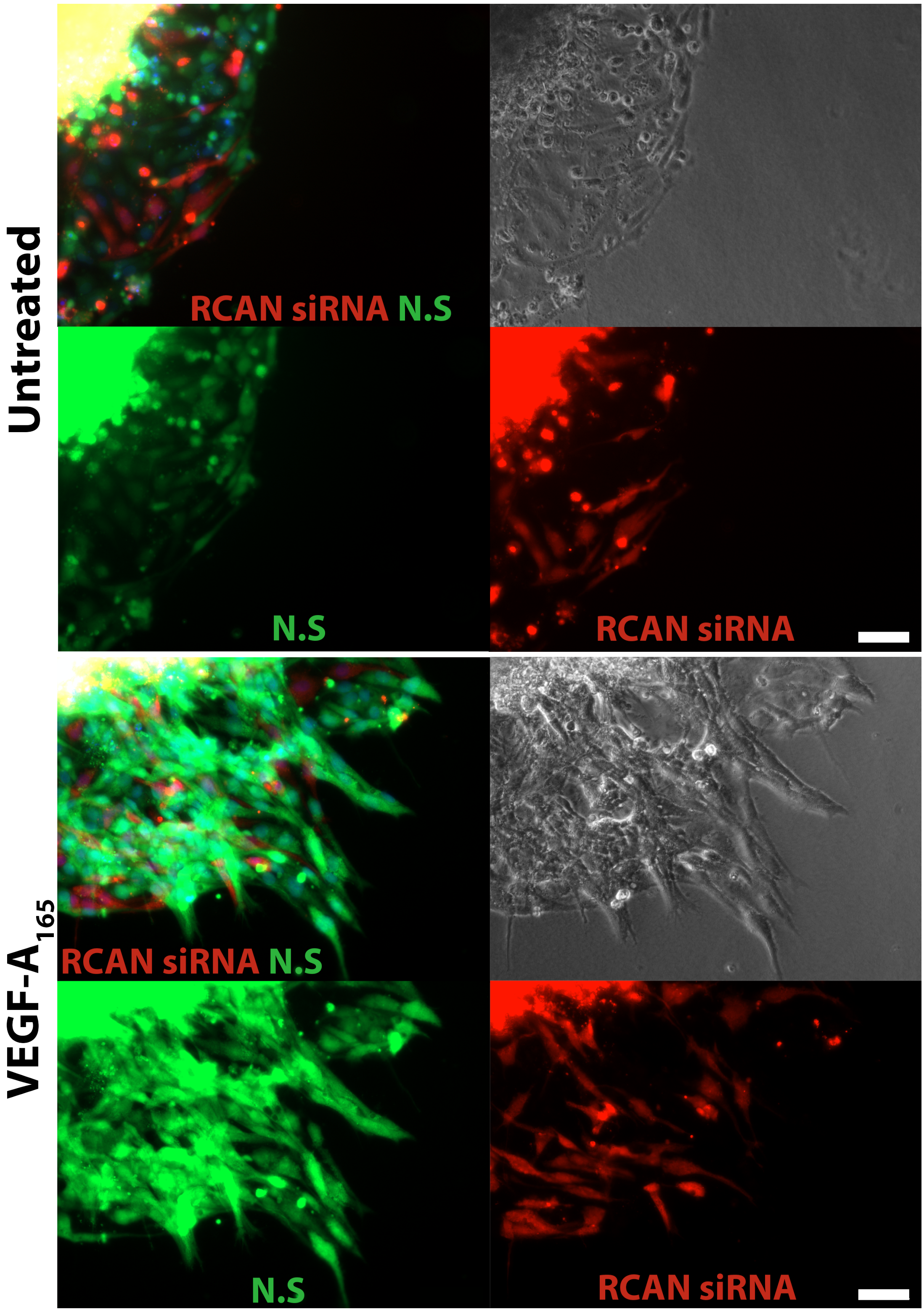
Untreated
RCAN siRNA N.S
N.S
RCAN siRNA
VEGF-A165
RCAN siRNA N.S
N.S
RCAN siRNA

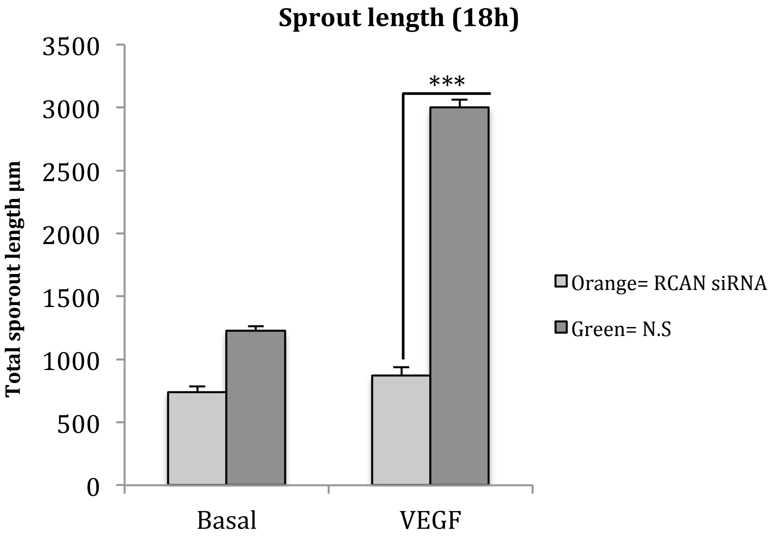

Figure 3.20: The role of RCAN1 in VEGF-A-mediated sprouting angiogenesis

HDMECs were seeded at 7 × 10^4 cells/wells onto pre-coated gelatin for 24 hour using FGM. Following day cells were transfected with RCAN1 siRNA and non-silencing siRNA (N.S). Cells were serum starved in 1%FCS media overnight followed by staining for 45 minutes with 5µM Cell Tracker dye Green and Orange. Cells were mixed with carboxymethylcellulose in non-adherent bottom 96-well plates for 18 hours before spheroids were embedded and seeded onto collagen matrix, and stimulated with VEGF-A FGF and HGF 50 ng/ml for 18 hours. The cells were fixed with 2% PFA for 10 minutes. Images were taken for each assay analyzed at 20x object using Zen software. Scale bar: 50µm. This figure illustrated the total sprouting length of tube was quantified from 10 fields (x20 objective) per condition per experiment using Zen software as described in method chapter. Data shows ± SD,(N=3), (***P<0.001, siRNA versus N.S Student's t-test). The data is representative of three experiments.

3.6 Discussion

It has previously been reported that in addition to its established role in inhibiting calcineurin function and subsequently VEGF-stimulated gene expression, RCAN1 is able to regulate VEGF-mediated tubular morphogenesis in endothelial cells (Holmes et al., 2010). The aim of this chapter was to determine the mechanism through which RCAN1 is able to regulate VEGFR-2 signalling and affect endothelial cell function.

Work in the group has previously shown that RCAN1.4 expression is stimulated by VEGF in HDMECs, unlike other growth factors such as FGF-2 and HGF (Holmes et al., 2010). The siRNA duplexes used in this study did not discriminate between the two RCAN1 isoforms and it was confirmed that both isoforms were silenced in HDMECs with these duplexes (3.1). The initial experiments confirmed that VEGF was able to induce expression of the RCAN1.4 isoform but not RCAN1.1 isoform as measured by mRNA and western blotting.

The ligand induced activation of RTKs and their subsequent internalisation and trafficking allows signalling from the plasma membrane and endosomal compartments as well as cessation of signalling via lysosomal degradation of receptors (Horowitz and Seerapu, 2012). The initial data defined a role for RCAN1 in regulating ligand activated VEGFR-2 internalisation (Figure 3.3) but not HGFR (Figure 3.4), suggesting a specific role for RCAN1 in VEGF signalling. Previous work has shown that VEGF is unique, compared with other growth factors such as FGF and HGF, in stimulating RCAN1.4 expression in HDMECs via a pathway requiring calcineurin and PKC-delta (Holmes et al., 2010). However, the effect on VEGFR-2 internalisation occurred prior to an increase in RCAN1.4 levels showing that basal RCAN1 levels were able to regulate VEGFR-2 internalisation. Furthermore, VEGF-mediated internalisation of VEGFR-2 was not sensitive to the calcineurin inhibitor cyclosporin A (CsA) (data not shown), which is known to prevent VEGF-mediated induction of RCAN1 mRNA and protein (Holmes et al., 2010). This data suggests a novel role for RCAN1, distinct from its previous assigned role in inhibiting calcineurin and playing a negative regulatory role in VEGF signalling (Hesser et al., 2004).

RTK internalisation follows the canonical clathrin-dependent endocytic route involving the small GTP binding protein Rab5 (Goh and Sorkin, 2013). Immunoprecipitation experiments to identify co-localisation of VEGFR-2 and RCAN1 were inconclusive, although the data suggested a transient association. However, use of a proximity ligation assay (PLA) showed a close association between VEGFR-2 and RCAN1 in response to VEGF, which was rapid and transient. The PLA assay has proved successful in identifying weak transient interactions between proteins in endothelial cells (Figure 3.11) (Mellberg et al., 2009). It was not possible to explore this interaction between RCAN1 and VEGFR-2 further during the course of these studies and this is something which would be interesting to explore further through the use of VEGFR-2 mutants lacking specific tyrosine residues and C-terminal truncations.

Analysis of the amino acid sequence of RCAN1 reveals no classical SH2 or SH3 domains required for association with RTKs suggesting that RCAN1 may interact with VEGFR-2 by a novel mechanism. The ability of RCAN1 silencing to affect VEGFR-2 internalisation relative to HGFR suggests that RCAN1 may either interact directly with the VEGFR-2 or ancilliary proteins specifically required for VEGFR-2 internalisation, such as neuropilin 1 (Nrp-1) (Soker et al., 1998), synectin (Lanahan et al., 2010) and recently ephrin–B2 (Sawamiphak et al., 2010).

It is also possible that RCAN1 can influence VEGFR-2 phosphorylation as RCAN1 depletion resulted in decreased VEGFR-2 degradation and increased transient phosphorylation on Y1175 (Figure 3.3). Dephosphorylation of VEGFR-2 is regulated by a number of recently identified phosphatases such as VE-PTP (Mellberg et al., 2009) and DEP1, which causes delayed VEGFR-2 internalisation (Lampugnani et al., 2003). Previous data has shown that VEGFR-2 internalisation is required for phosphorylation of Y1175 in VEGFR-2 in mouse endothelial cells (Sawamiphak et al., 2010). However, the data in HDMECs suggests that reducing RCAN1 expression delays VEGFR-2 internalisation and transiently increases Y1175 phosphorylation.

Studies on guided cell migration in *Drosophila* have revealed the physiological role of RTK endocytosis is to ensure localized intracellular response to guidance cues by stimulating spatial restriction of signalling allowing organised cell migration (Jékely et al., 2005). siRNA mediated silencing of RCAN1 had a profound effect on VEGFR-2 mediated cytoskeletal reorganisation in HDMECs (Figure 3.12). The lack of actin remodelling and filopodia was restricted to VEGF, as addition of HGF allowed agonist-dependent remodelling of the cytoskeleton. This important finding suggests that RCAN1 did not regulate cytoskeletal remodelling at the level of the small molecular weight GTP binding proteins such as Rho, important for actin stress fibre formation (Ridley et al., 1992) Rac, important for lamellipodia formation (Ridley et al., 1992) and Cdc42 important for filopodia (Nobes and Hall, 1995) as a block at the level of these GTP binding proteins would be expected to affect all agonist stimulated cytoskeletal reorganisation.

Migrating cells are known to undergo polarisation where the nucleus, the Golgi apparatus and microtubules act in concert with cytoskeletal reorganisation to facilitate migration (Omelchenko et al., 2002). siRNA mediated silencing of RCAN1 resulted in a profound reduction in HDMEC cell polarisation in response to VEGF, suggesting that cells were not able to efficiently generate polarity for directed migration. Cdc 42 plays a key role in establishing cell polarity (Etienne-Manneville, 2004). However, it is unlikely that RCAN1 transduces its effects through Cdc42 as HGFR signalling was not affected by RCAN1 silencing as discussed above. Effects on Cdc42 would be expected to affect all growth factor signalling and prevent cell polarity and cell migration.

Efficient migration of endothelial cells establishes a vascular sprout through establishment of tip cells and stalk cells (De Smet et al., 2009). siRNA mediated silencing of RCAN1 resulted in defective tubular morphogenesis (Figure 3.19) and in defective sprout formation (Figure 3.20). HDMECs in which RCAN1 gene expression was reduced were unable to efficiently compete to be tip cells. Research over the last decade has shown that tip cells induce the Notch receptors Dll4 which binds to the Notch receptor on adjacent stalk cells leading to intracellular cleavage of Notch generating the Notch intracellular domain (NICD) that acts as a transcriptional regulator to downregulate VEGFR-2 and upregulate VEGFR-1 which results in dampened VEGF-A signalling in these stalk cells (Gerhardt et al., 2003). Our data would suggest that RCAN1 is also working to allow efficient directed migration of tip cells in response to VEGF-A.

In conclusion, the results in this chapter describe a novel role for the RCAN1 protein in endothelial cell function, distinct from its previously established role in acting as a negative regulator of VEGF-mediated gene expression. RCAN1 regulates VEGF-mediated acute effects with respect to VEGFR-2 internalisation and cell polarity and cytoskeletal reorganisation, which ultimately allows the orchestration of directed cellular migration.

Chapter 4

The role of RCAN1.4 in regulating VEGF-mediated endothelial cell migration

4.1 RCAN1 regulates VEGF-mediated migration in endothelial cells

Cell migration is a fundamental process for multicellular organisms. It is a vital part of wound healing, embryonic development, tissue engineering, and immunity. Understanding the mechanisms behind cell migration may lead to the development of new therapeutic targets for aberrant cell migration during pathologies such as tumour metastasis. Cells respond to extracellular stimuli including chemical or physical signalling, to migrate (Girard and Springer, 1995, Lamalice et al., 2007, Takahashi and Shibuya, 2005).

Endothelial cells play a critical function in the angiogenic process. They form a thin lining between the capillary blood flow and the surrounding tissue. During angiogenesis, these endothelial cells must migrate in response to stimuli to form new vessels, which involves finely regulated migration and interactions with the surrounding extracellular matrix. This angiogenic process can even involve the careful coordination of other cell types such as smooth muscle and pericytes (Lamalice et al., 2007).

VEGF induces endothelial cell migration both *in vivo* and *in vitro* (Zachary, 2003). Utilising *in vitro* assays, cell migration can be studied to try to understand angiogenesis mechanisms, using extracellular stimuli that can be managed. Many factors could play a critical role in cell migration such as serum, cell number and extracellular matrix proteins. A classical assay used to study cell migration is the scratch wound assay in which a confluent lawn of cells is wounded leaving a gap across which cells can migrate (Liang et al., 2007). This method is a well-established tool to study cell migration, cell polarity and cell directionality. There are many advantages of the scratch wound assay as it mimics cell migration *in vivo* and is relatively easy to perform.

The role of RCAN1 in regulating growth factor-stimulated endothelial cell migration was assessed by an *in vitro* scratch wound assay. This protocol was used to mimic endothelial cell migration *in vivo* and allows for easy quantification of migration as well as fluorescent staining and further image analysis. Migration experiments in this study measure the relative degree of endothelial cell migration induced by a range of growth factors including VEGF-A_{165}, VEGF-A_{121}, EGF, FGF-2, and HGF.

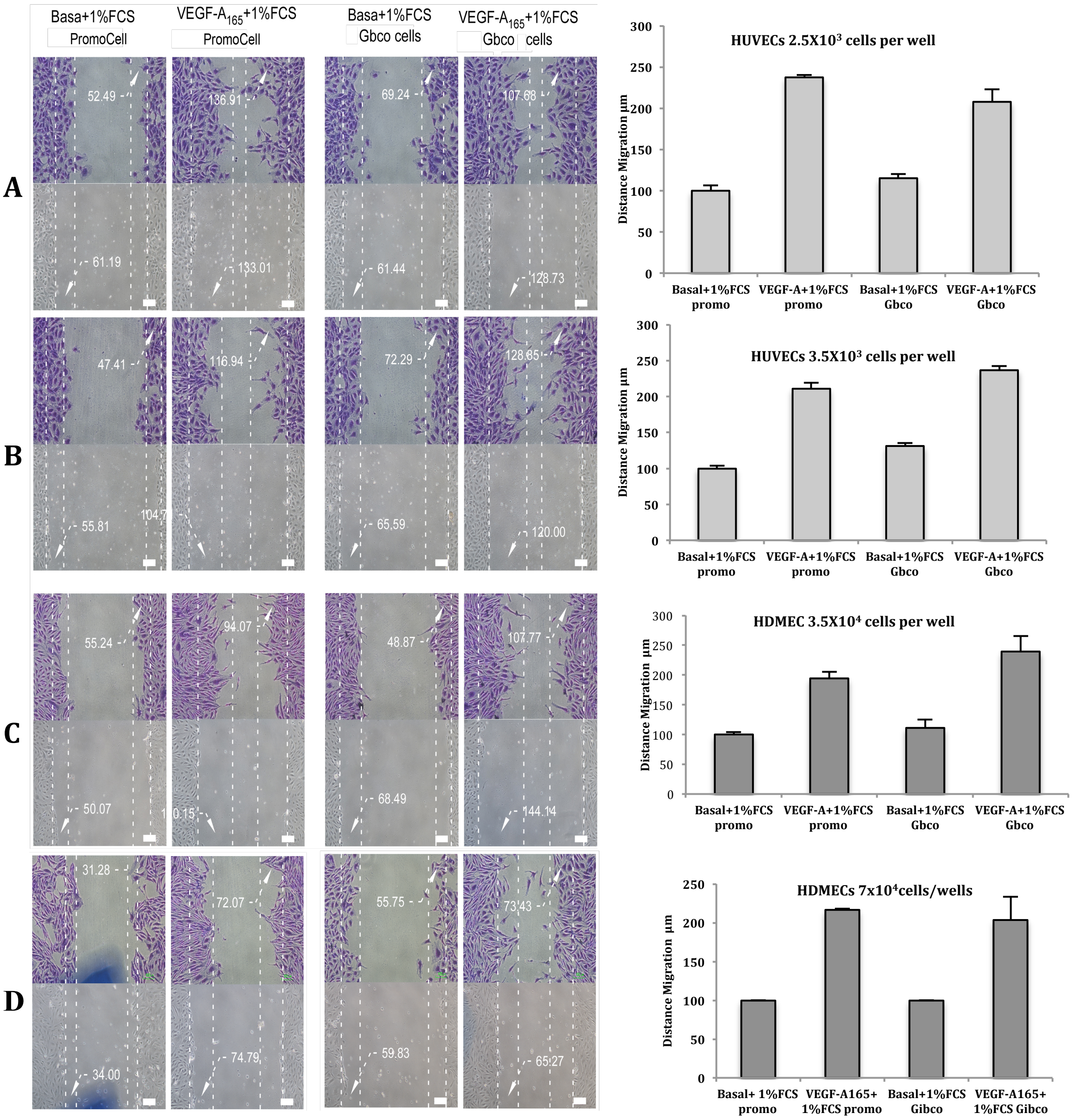

Figure 4.1: Cell migration at different cell densities and in the presence of different sera

In all conditions, the cells were seeded onto gelatine pre-coated 12-well plates for 24 hours in FGM. Cells were serum starved in media supplemented with either 1% PromoCell FCS or 1% Gibco FCS for 24 hours. A scratch was introduced using a sterile 200-µl Gilson pipette tip and stimulated with VEGF-A165 (50 ng/ml) for 18 hours. Cells were then washed with PBS, fixed with 2% PFA for 15 minutes and stained with Crystal Violet. Images were taken using a Nikon imaging microscope at ×10 objective. The lower phase contrast image represents the wound at time point zero and the upper Crystal Violet stained image represents the wound after 18 hours of migration. The migration distance was calculated from this (µm). **A.** HUVECs were seeded at 2.5 × 103 cells per well **B.** HUVECs were seeded at 3.5 × 103 cells per well **C.** HDMECs were plated at 3.5 × 103 cells per well and **D.** HDMECs were plated at 7 × 104 cells per well. Data shows mean ± SD. The data is representative of three experiments.

4.1.1 Optimisation and Validation of the Scratch Wound Assay

HUVECs or HDMECs were plated for 48 hours prior to serum starvation with 1% FCS for 16 hours before the introduction of a scratch wound in the monolayer. Cells were then stimulated with a range of agonists. Two sera from commercially available sources (PromoCell and Gibco) were compared. Previous work in the group has suggested that variation in the serum utilised for starvation can have a profound effect on endothelial cell migration (data not shown). HUVECs were seeded at either 2.5×10^3 cells per well (Figure 4.1A) or 3.5×10^3 cells per well (Figure 4.1B) in a 12-well plate and the migration response to VEGF-A_{165} in the presence of either 1% PromoCell FCS or 1% Gibco FCS was compared. VEGF-A_{165} consistently stimulated an increase in migration; however there appeared to be no significant difference between the sera or cell seeding densities. Similarly HDMECs were seeded at either 3.5×10^4 (Figure 4.1C) or 7×10^4 (Figure 4.1D) cells per well in 12 well plates and again migration was studied in response to VEGF-A_{165} in the presence of either 1% PromoCell FCS or 1% Gibco FCS. Again, VEGF-A_{165} consistently stimulated an increase in migration without any significant difference observed between the sera or seeding densities.

Therefore, all experiments were conducted using PromoCell serum as this was the same supplier that the cells were originally sourced from and the main full growth media was purchased through, thus providing consistency between the media in which the cells were grown and the media in which experiments were conducted.

4.1.2 RCAN1 Regulates VEGF-Mediated Endothelial Cell Migration

Previous work within the group has identified a role for RCAN1 in the regulation of VEGF-mediated migration of endothelial cells using a scratch wound assay (Holmes et al., 2010). It has further been shown that RCAN1 has a significant role in the regulation of endothelial cell migration both *in vitro* as well as *in vivo* (Iizuka et al., 2004). Work presented in the previous chapter has defined a role for RCAN1 in regulating VEGFR-2 and establishing cell polarity and cytoskeletal reorganisation in response to VEGF. This data was based on siRNA-mediated gene silencing. The aim of this chapter was to focus on the effect of RCAN1 on cell migration using both siRNA- and adenoviral-mediated overexpression of the RCAN1.4 isoform.

To investigate this the role of RCAN1 in the migration response of HDMEC cells was examined after stimulation with VEGF-A_{165}, and other known pro-angiogenic growth factors including VEGF-A_{121}, FGF-2 and HGF.
Once again a scratch wound assay was used to analyse cell migration, but only after the use of selective siRNA gene silencing targeted against human RCAN1.1 and RCAN1.4, to specifically knock down RCAN1 expression, or a scrambled non-silencing control. Two duplexes of RCAN1 siRNA were selected to ensure efficient knockdown and used as a pool. HDMECs were seeded for 24 hours before transfection with siRNA using 10v nM of each RCAN1 silencing duplex to give a final concentration of 20 nM RCAN1 siRNA pool, or 20 nM non-silencing siRNA (N.S). This transfection mix was incubated with the cells for 6 hours before returning them to full growth media. The following day cells were serum starved with media supplemented with 1% PromoCell FCS and incubated for a further 24 hours before introducing a scratch in the HDMEC monolayer. Cells were then stimulated with VEGF-A_{165}, VEGF-A_{121}, FGF-2 or HGF (50 ng/ml) for 18 hours and cells allowed to migrate.

This experiment was conducted after seeding the cells at either 3.7×10^4 cells per well in a 12-well plate (Figure 4.2) or 7×10^4 cells per well (Figure 4.3). When the cells were seeded at 3.7×10^4 cells per well, all basal samples of HDMECs, including untreated, non-silencing and RCAN1 siRNA showed no significant migration; whereas upon stimulation with growth factors in untreated and non-silencing samples, there was a greater than twofold increase in HDMEC migration. Upon siRNA knockdown of RCAN1, this migration response was notably diminished in VEGF-A_{165}, VEGF-A_{121} and FGF-2 conditions but did not reduce HGF-induced migration (Figure 4.2).

By comparison, with an increased number of cells seeded per well of 7×10^4 cells (Figure 4.3) it was found that there was a more consistent increase in cell migration between the different growth factors in the untreated and N.S siRNA conditions, with an approximate doubling in migration over basal conditions. This suggests that the more confluent monolayer is a more consistent model; so perhaps at the lower seeding density there was more variation in the surface area of cells exposed to the growth factor or there is more variation in the spacing between the cells, all of which might alter migration responses. At this cell density, knockdown of RCAN1 was discovered to prevent 80% of VEGF-A_{165}- and VEGF-A_{121}-induced migration whereas it had a much smaller effect on FGF-2 and HGF.

To conclude, RCAN1 silencing specifically inhibited migration in response to VEGF-A_{165} and VEGF-A_{121} but not in response to FGF-2 or HGF. Unlike VEGF-A_{165}, VEGF-A_{121} does not bind the VEGFR-2 co-receptor Nrp1. As RCAN1 knockdown reduced the migration stimulated by both isoforms of VEGF-A, it suggests that Nrp1 is potentially not required for RCAN1 to regulate VEGFR-2 mediated endothelial cell migration.

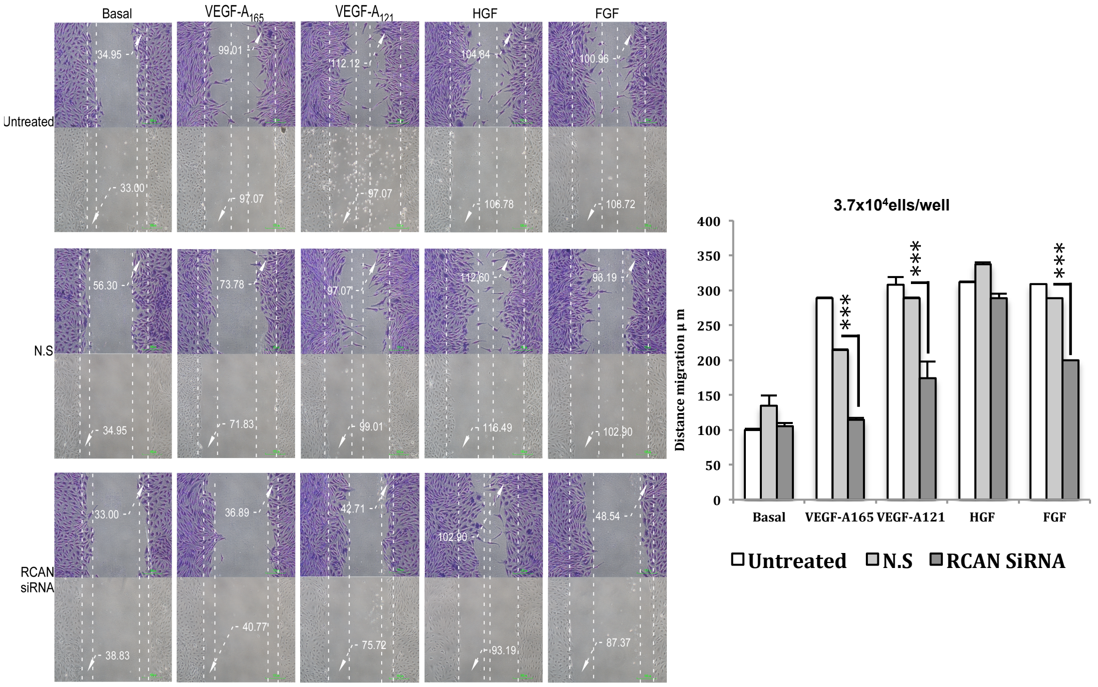

Figure 4.2: Effect of RCAN1 knockdown on HDMEC migration in response to different growth factors

HDMECs were seeded at 3.7 × 10^4 cells per well in a gelatine pre-coated 12-well plate for 24 hours in FGM before being transfected with siRNA targeting RCAN1.1 and 1.4 or a non-silencing sequence (N.S) for 48 hours. Cells were serum starved with media supplemented with 1% PromoCell FCS for 24 hours prior to introduction of a scratch in each well using a sterile 200-µl Gilson pipette tip and cells stimulated with VEGF-A_{165}, VEGF-A_{121}, FGF-2 or HGF (50 ng/ml) for 18 hours. Cells were washed with PBS, fixed with 2% PFA for 15 minutes and stained with Crystal Violet. Images were taken using a Nikon imaging microscope at ×10 objective. The lower phase contrast image represents the wound at time point zero and the upper Crystal Violet stained image represents the wound after 18 hours of migration. The migration distance was calculated from this (µm). Data shows ± SD, (N = 3), (***$P < 0.001$, siRNA versus N.S. Student's t-test). The data is representative of three experiments.

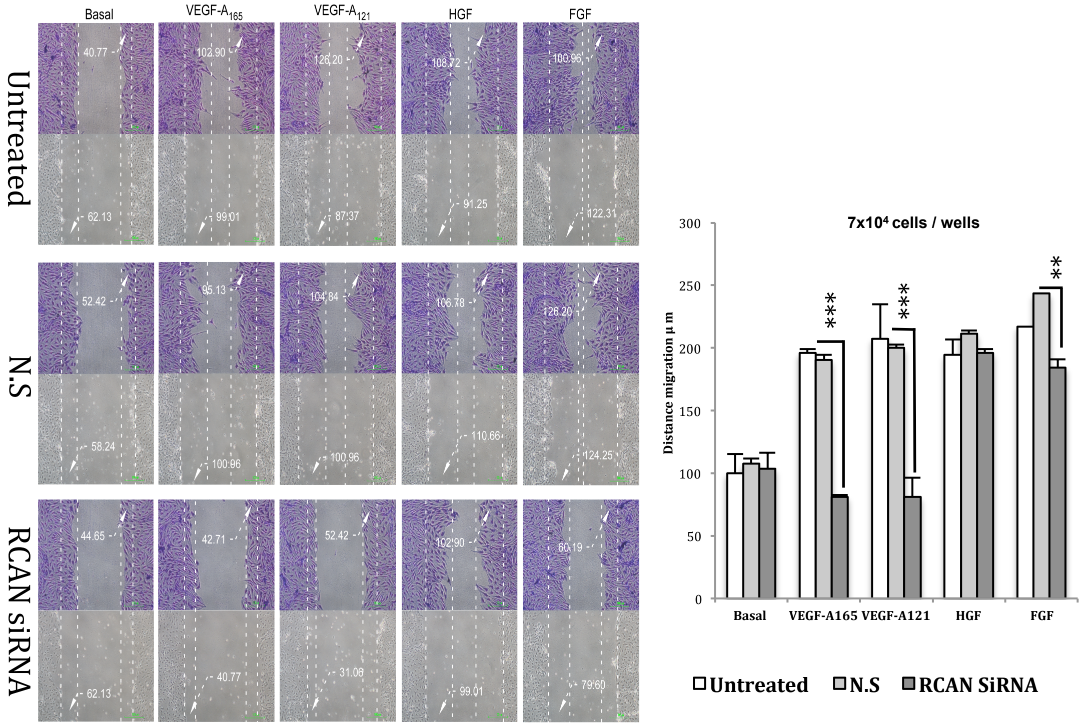

Figure 4.3: Effect of RCAN1 knockdown on HDMEC migration in response to different growth factors

HDMECs were seeded at 7 × 10^4 cells per well in a gelatine pre-coated 12-well plate for 24 hours in FGM before being transfected with siRNA targeting RCAN1.1 and 1.4 or a non-silencing scramble sequence (N.S) for 48 hours. Cells were serum starved with media supplemented with 1% PromoCell FCS for 24 hours prior to introduction of a scratch in each well using a sterile 200-µl Gilson pipette tip and cells stimulated with VEGF-A_{165}, VEGF-A_{121}, FGF-8 or HGF (50 ng/ml) for 18 hours. Cells were washed with PBS, fixed with 2% PFA for 15 minutes and stained with Crystal Violet. Images were taken using a Nikon imaging microscope at ×10 objective. The lower phase contrast image represents the wound at time point zero and the upper Crystal Violet stained image represents the wound after 18 hours of migration. The migration distance was calculated using this (µm) unit. Data shows ± SD, (N = 3), (**P < 0.01, ***P < 0.001, siRNA versus N.S. Student's t-test). The data is representative of three experiments.

4.1.3 RCAN1 is Required for Cell Directionality

The directionality of a cell is vital to co-ordinated and efficient cell migration. After demonstrating that RCAN1 depletion causes a defect in cell migration and the establishment of cell polarity, we wanted to examine if RCAN1 played a role in the directionality of migration. In order to do this, time-lapse DIC imaging of HDMECs was utilised during the scratch wound assay in response to agonist stimulation with VEGF-A or HGF. HDMECs were once again seeded at 7 × 10^4 cells per well in a gelatine pre-coated 12-well plate, before transfecting with siRNA targeted against RCAN1.1 and 1.4 or a non-silencing scrambled sequence. After 24 hours the cells were serum starved in 1% PromoCell FCS for 24 hours before a wound was introduced using a 200-µl Gilson pipette tip, and agonists were added. Live cell imaging was then started and images taken every three minutes for 24 hours (Figure 4.4).

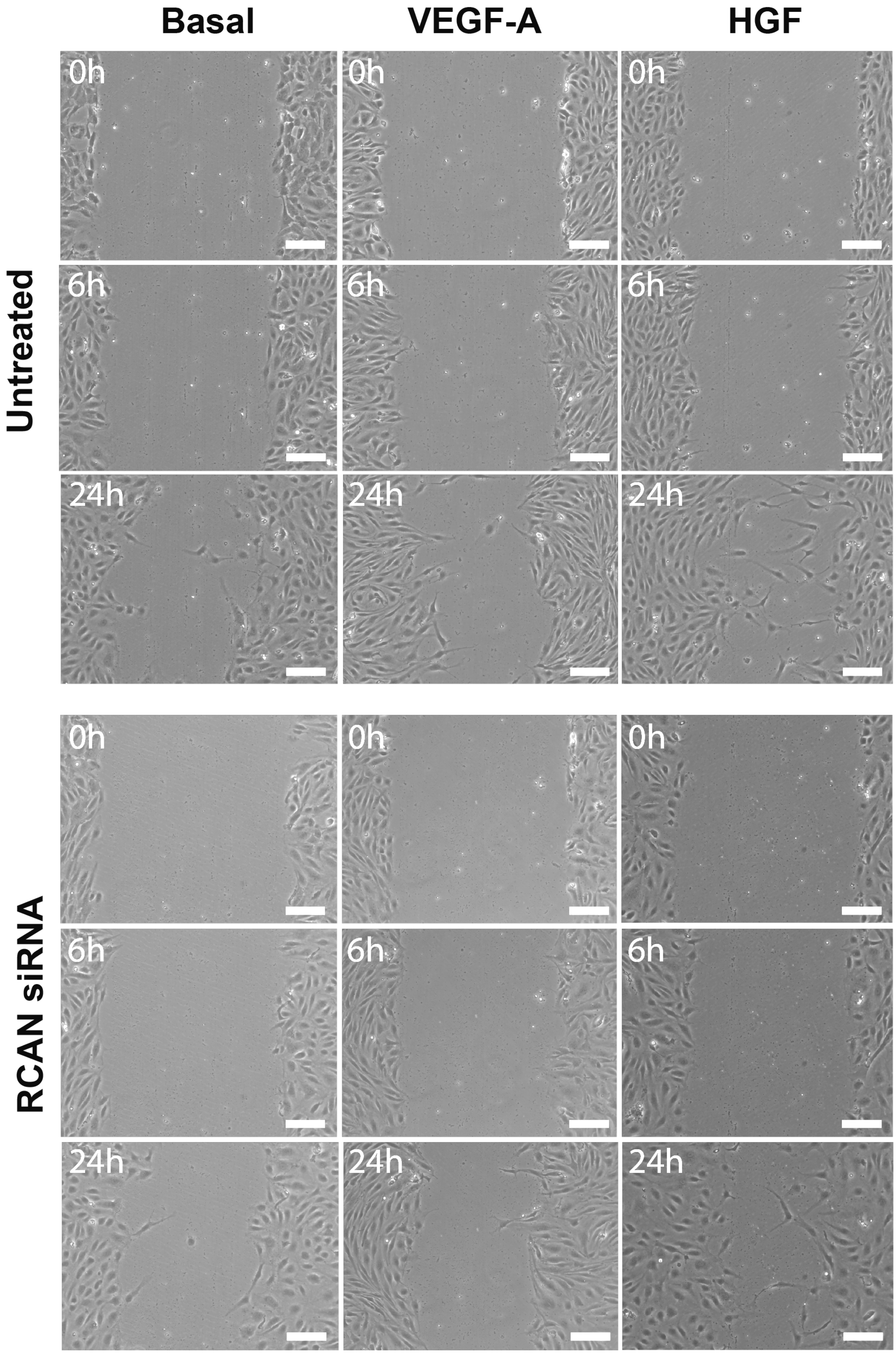

Figure 4.4: Frames from live cell imaging of RCAN1 knockdown experiment.

HDMECs were seeded at 7 × 10^4 cells per well in a gelatine pre-coated 12-well plate for 24 hours in FGM before being transfected with siRNA targeting RCAN1.1 and 1.4 or a non-silencing scramble sequence (N.S) for 48 hours. Cells were serum starved with media supplemented with 1% PromoCell FCS for 24 hours prior to introduction of a scratch in each well using a sterile 200-µl Gilson pipette tip and cells stimulated with VEGF-A, or HGF (50 ng/ml) for 24 hours. Scale bar: 50µm. Extended time course for this figure is shown in appendix 1, pages 154-155.

Migration trajectories were tracked for 20 individual cells over 24 hours using free software (Ibidi®) for visualisation to quantitate cell migration. This analysis is able to track movement of single cells toward the leading edge of wound healing over a period of 24 hours. It is clear that cells stimulated with VEGF-A_{165} or HGF demonstrate strong directionality compared to basal media alone. However, depletion of RCAN1 resulted in a reduced migration directionality compared to the control non-silencing siRNA in the VEGF-A_{165} treated condition specifically (Figure 4.5A and B).

This is quantified in Figure 4.5C, showing that RCAN1 depletion resulted in a slower and more convoluted migration in response to VEGF-A_{165} compared to untransfected and non-silencing conditions. In contrast, RCAN1 depletion did not affect HGF-stimulated cells, which showed normal migration distance and trajectory indicating that RCAN1 did not influence HGF-induced migration. A number of different parameters were measured: velocity (total path length [µm]/time [min]), straightness (displacement [µm]/total path length [µm]), and forward migration index which represents the efficiency of forward migration. All three parameters were reduced following RCAN1 depletion and stimulated with VEGF-A_{165}, compared with untreated and non-silencing VEGF-A_{165} stimulated cells, suggesting that both cell directionality and overall migration speed are dependent on RCAN1 and upon VEGF-A-induced migration.

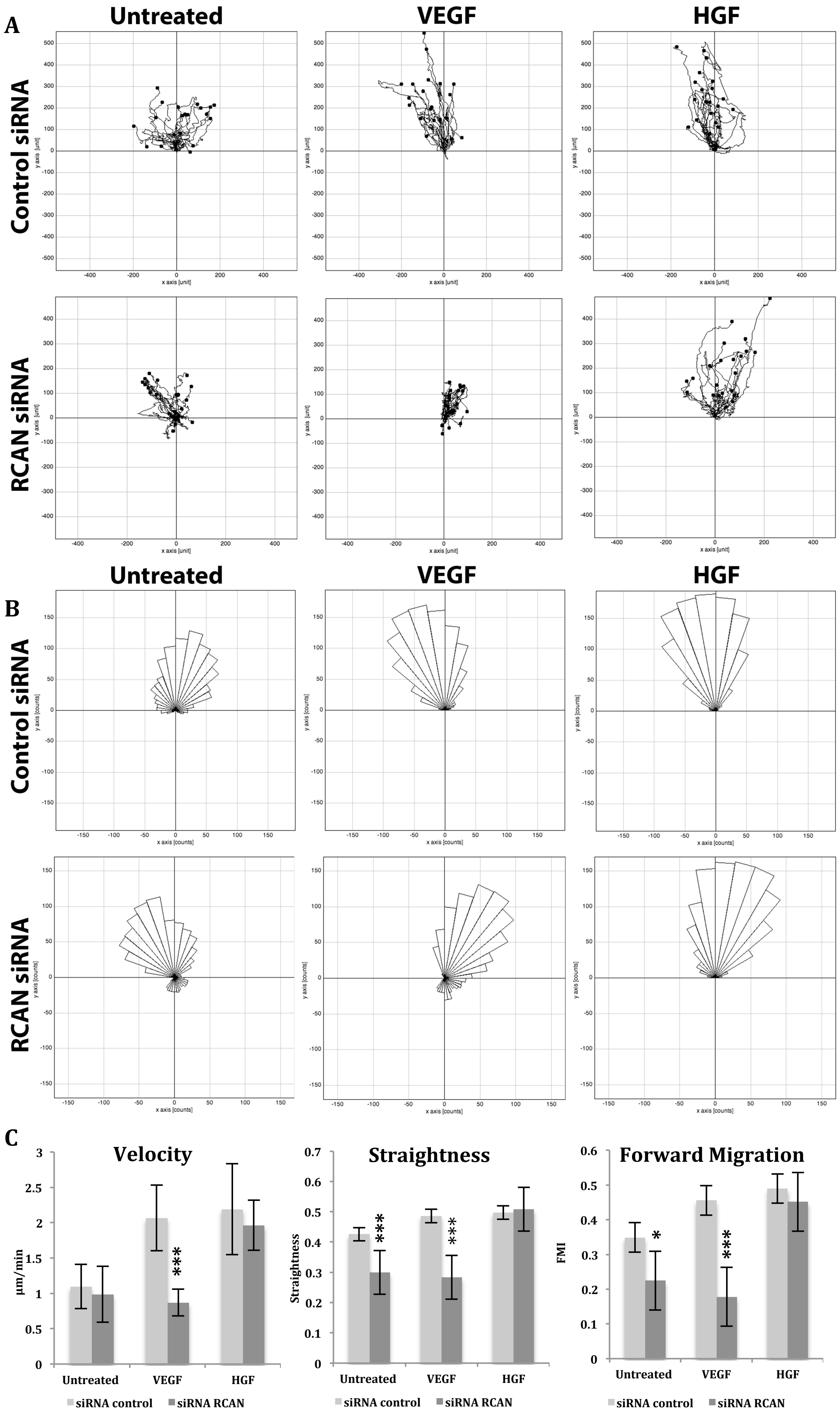
A
Untreated
VEGF
HGF
Control siRNA
RCAN siRNA
y axis [unit]
x axis [unit]
B
Untreated
VEGF
HGF
Control siRNA
RCAN siRNA
y axis [counts]
x axis [counts]
C
Velocity
μm/min
Straightness
Straightness
Forward Migration
FMI
Untreated
VEGF
HGF
siRNA control
siRNA RCAN
***
*

Figure 4.5: RCAN1 is required for cell directionality

HDMECs were seeded at 7 × 10^4 cells per well in a gelatine pre-coated 12-well plate for 24 hours in FGM before being transfected with siRNA targeting RCAN1.1 and 1.4 or a non-silencing scramble sequence (N.S) for 48 hours. Cells were serum starved with media supplemented with 1% PromoCell FCS for 24 hours prior to introduction of a scratch in each well using a sterile 200-µl Gilson pipette tip and cells stimulated with VEGF-A, or HGF (50 ng/ml) for 24 hours. **A.** Migration trajectories of representative cells (n = 20) from non-silencing siRNA control and RCAN1 siRNA knockdown. Each track presented from the start. **B.** Rose diagram illustrating the distribution of the trajectories and migration angles. **C.** Graphs representing the (total path length [µm]/time [min]), (displacement [µm]/total path length [µm]), and forward migration index (FMI). Data shows ± SD, (N = 3), (*P < 0.05, ***P < 0.001, siRNA versus N.S. Student's t-test). This data is representative of three repeats from single experiments.

To investigate the defect in cell polarity and migration further in RCAN1 depleted cells the migration of HDMEC cells treated with non-silencing siRNA and RCAN1 siRNA were simultaneously analysed using specific Cell Tracker dyes. Two populations of HDMEC were treated with either non-silencing siRNA or RCAN1 specific siRNA before each population was labelled with either Cell Tracker Green or Cell Tracker Orange fluorescent dye, mixed together and seeded as usual for the scratch wound assay. Cells were then stimulated with VEGF-A for 0, 3, 6, and 12 hours and the average number of cells from each population that was at the leading edge was quantified. It was therefore possible to analyse the effect of RCAN1 knockdown on cell migration in this mixed cell population (Figure 4.6).

Cells with depleted RCAN1 were defective in orientating themselves at the leading edge of the wound following stimulation with VEGF-$A_{165,}$ as fewer RCAN1 knockdown cells reached the leading edge of the wound. As a further control, the labelling dye for each condition was switched and the same result was observed.

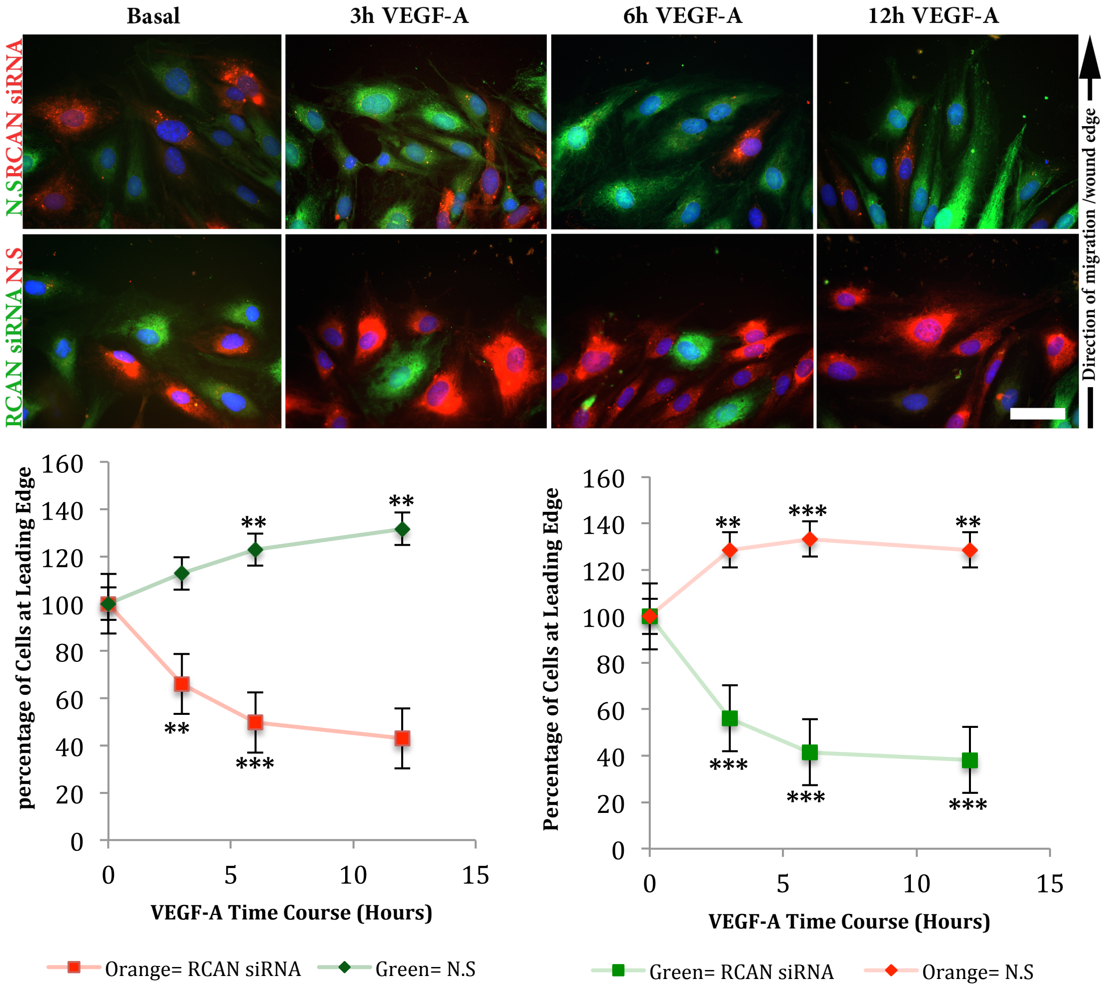

Figure 4.6: Tracking the effect of RCAN1 knockdown in a mixed cell population

After siRNA knockdown HDMECs were grown on a pre-coated gelatine dish for 24 hours in FGM. Cells were serum starved in 1% PromoCell FCS media overnight followed by staining for 45 minutes with either 5 µM Cell Tracker dye red or green. Cells were then left in serum-free media for 1 hour and seeded onto glass cover slips pre-coated with gelatine for 24 hours in FGM. Cells were serum starved with 1% PromoCell FCS media for 24 hours. A scratch was introduced to each well using a sterile 200-µl Gilson pipette tip and cells were stimulated with VEGF-A_{165} (50 ng/ml) for 3, 6 and 12 hours. Scale bar: 20 µm. Average number of cells at leading edge was collected and plotted in scatter chart. Data shows ± SD, (N = 3), (**$P < 0.01$, ***$P < 0.001$, siRNA or N.S versus basal. Student's t-test).

4.1.4 RCAN1.4 Requires VEGFR2 Activation to Drive Migration

To confirm that the RCAN1.4 isoform was able to regulate VEGFR2 mediated migration in HDMECs adenovirus-mediated gene transduction has already been used to specifically overexpress the RCAN1.4 isoform in HDMECs. Infection with this virus resulted in an increase in HDMEC migration to a level similar to that seen with agonist stimulation and therefore, it was important to determine if this effect was independent of VEGFR2. To do this, three selective inhibitors were utilised. Firstly, the cell permeable small molecule receptor tyrosine kinase inhibitor ZM323881 (Toullec et al., 1991) which specifically blocks VEGFR2. Secondly, SGX-523, which is an ATP-competitive inhibitor with a high affinity for the HGFR (Buchanan et al., 2009). And finally, cyclosporin A, which is a potent inhibitor of the calcineurin pathway (Fruman et al., 1992) that blocks VEGFR2-mediated RCAN1.4 induction (Holmes et al., 2010).

In order to confirm the specific effects of these inhibitors. western blot analysis was performed, and the specificity of these inhibitors against their intended target was confirmed (Figure 4.7A), with ZM323881 specifically inhibiting activated VEGFR-2 and SGX-523 specifically inhibiting activated HGFR. Then using the classical scratch wound assay their effects on migration were assessed (Figure 4.7B and C). VEGF-A_{165} and HGF showed a strong induction of migration in untreated and DMSO vehicle control conditions (Figure 4.7). However, blocking VEGFR2 with ZM323881 was found to prevent VEGF-induced migration and not HGF induced migration. Conversely, the addition of SGX-523 which blocks the HGFR receptor was found to prevent HGF-induced migration and not VEGF-A induced migration. Interestingly, treatment with cyclosporin A was also found to specifically inhibit VEGF-induced migration but not HGF. This agent is known to block VEGF-induced RCAN1.4 induction (Holmes et al., 2010), confirming the importance of RCAN1.4 in regulating VEGF-A_{165} induced migration.

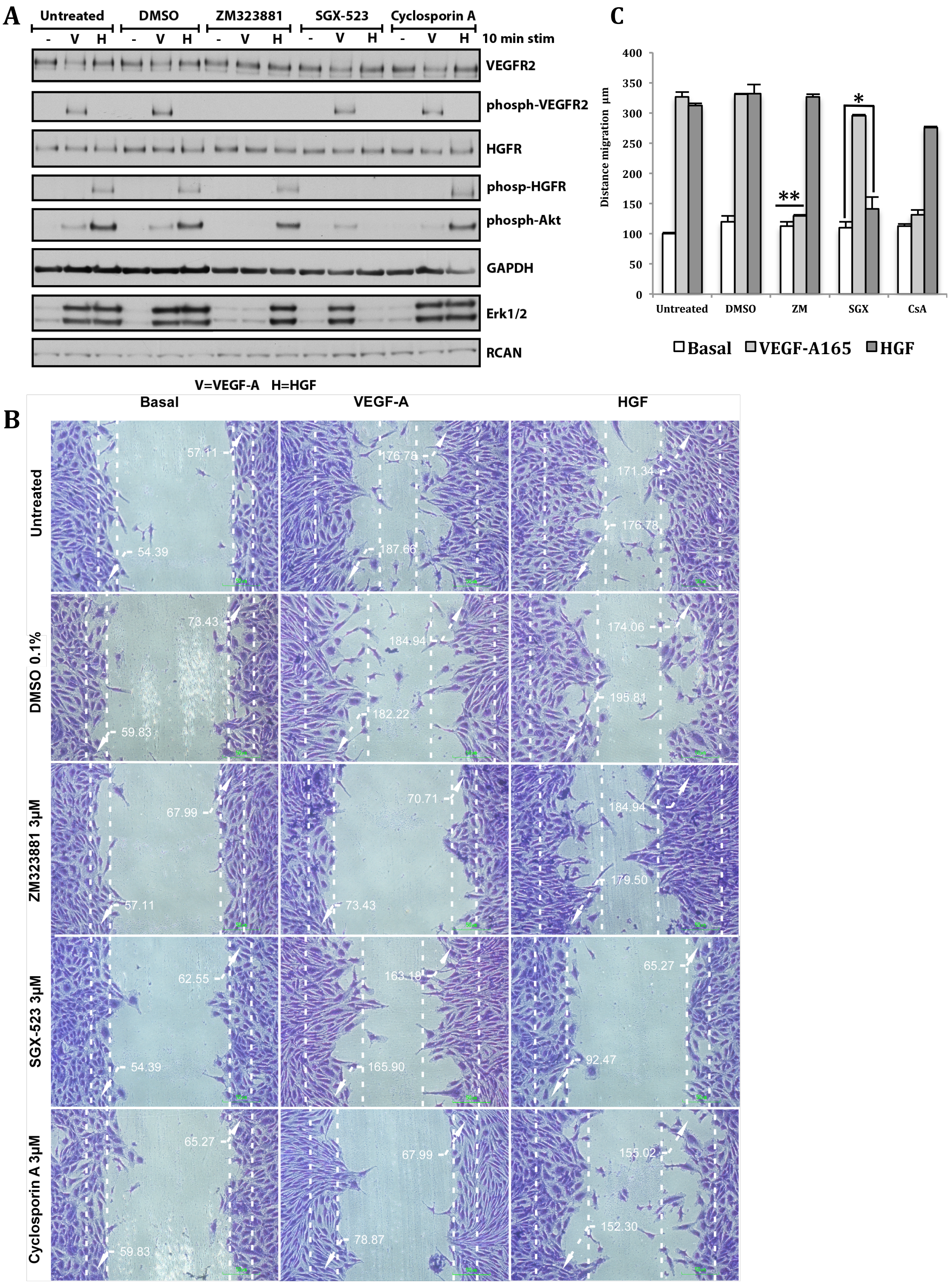

Figure 4.7: The Effects of Specific Inhibitors on Migration

A. Western blotting analysis of HDMECs seeded at 5 × 10^4 cells per well in a gelatine pre-coated 12-well plate for 24 hours in FGM. Cells were then serum starved with 1% PromoCell FCS media for 24 hours before being treated with DMSO vehicle control, 3 µM ZM323881, 3 µM SGX-523 and 3 nM Cyclosporin A for 30 minutes prior to stimulation with VEGF-A_{165} or HGF (50 ng/ml) for 10 minutes. Cells were washed with PBS and lysed with 1xLDS then analyzed by western blotting with specific antibodies to total VEGFR2, phospho-VEGFR2, total HGFR, phospho-HGFR, phospho-AKT, phospho-Erk1/2, and RCAN1. GAPDH was used as a loading control. **B.** HDMECs were seeded at 7 × 10^4 cells per well in a gelatine pre-coated 12-well plate for 24 hours in FGM. Cells were serum starved with 1% PromoCell FCS media for 24 hours. A scratch was introduced to each well using a sterile 200-µl Gilson pipette tip. Cells were then treated with vehicle control, 3 µM ZM323881, 3 µM SGX-523 and 3 nM Cyclosporin A and stimulated with VEGF-A_{165} or HGF (50 ng/ml) for 18 hours. Cells were washed with PBS, fixed with 2% PFA for 15 minutes and stained with Crystal Violet. Images taken using a Nikon imaging microscope at ×10 objective. **C.** Quantification of migration (µm) after stimulation with VEGF-A_{165} or HGF and inhibitors. Data shows mean ±SD, (N = 3), (*P < 0.05, **P < 0.01, VEGF-A, HGF versus untreated).

The siRNA complex used to knockdown RCAN1 in Figure 3.1B was not specific for RCAN1.4 but knocked down both RCAN1.1 and RCAN1.4 isoforms. Therefore, to confirm the specific role of RCAN1.4 in regulating VEGFR-2 mediated cell migration, an adenovirus that specifically expressed RCAN1.4 was used. In this overexpression study HDMECs were transduced either with this adenovirus or a control adenovirus encoding GFP and 24 hours later were plated out for use in the same scratch wound assay method (Figure 4.8). It was found that untreated, n.s. siRNA and adenovirus-control HDMECs underwent minimal migration in the basal condition, but on stimulation, VEGF-A_{165} and HGF induced strong migration. However, once again siRNA knockdown of RCAN1 was found to prevent VEGF-A_{165} induced migration but had no effect on HGF induced migration. Interestingly, overexpression of RCAN1.4 using adenoviral mediated gene delivery resulted in an increased migration of HDMECs, to the same degree as agonist stimulation with VEGF. This RCAN1.4 specific increase in migration suggests that the RCAN1.4 isoform plays an important role in VEGF-mediated cell migration.

Examining the cell morphology, it appears that lamellipodia and filopodia formation could be one possible mechanism for this RCAN1 regulation, as cell protrusions only appear in the VEGF-A_{165} and HGF stimulated conditions whereas they appear to be absent in the RCAN1-depleted conditions. These protrusions were also increased on RCAN1.4 overexpression, further suggesting a role for RCAN1.4 in cell migration.

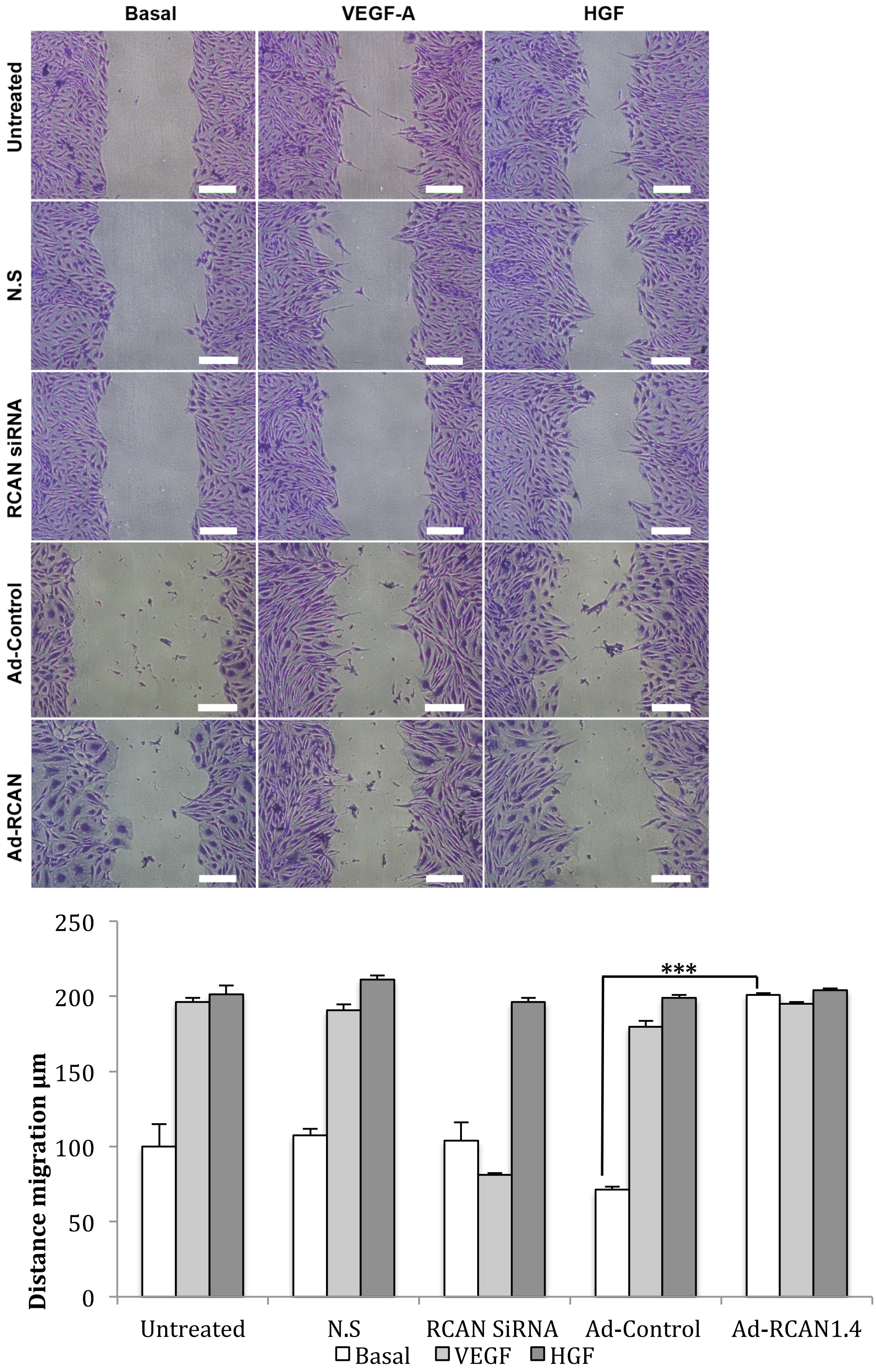

Figure 4.8: RCAN1.4 regulates VEGF-mediated migration of HDMECs

HDMEC were transfected with siRNA or adenovirus as indicated. 48 hours post-transfection cells were serum starved with media supplemented with 1% PromoCell FCS for 24 hours prior to introduction of a scratch in each well using a sterile 200-µl Gilson pipette tip and cells stimulated with VEGF-A_{165}, VEGF-A_{121}, FGF-2 or HGF (50 ng/ml) for 18 hours. Cells were washed with PBS, fixed with 2% PFA for 15 minutes and stained with Crystal Violet. Images were taken using a Nikon imaging microscope at ×10 objective. The graph shows quantification of the distance migrated (µm). Data shows mean ±SD, (N = 3), ***P < 0.001, Adeno-RCAN1.4 versus Adeno-Control, Student's t-test).

To study the requirement of VEGFR2 in RCAN1.4 mediated migration, RCAN1.4 was over-expressed in HDMECs using adenoviral-mediated gene transduction. The increased levels of RCAN1.4 were then subsequently verified by SDS-PAGE and western blot analysis (Figure 4.9A), where a clear increase in RCAN1.4 (29kDa) can be seen in the adenovirus RCAN1.4 transfected cells compared to those transfected with control adenoviruses. Furthermore, this analysis confirmed overexpression of RCAN1.4 did not cause any defect in the expression of VEGFR2 or HGFR.

Using the scratch wound assay, the effects of this overexpression, in combination with the selective inhibitors validated above, was then examined (Figure 4.9B). Cells transfected with the adenovirus encoding RCAN1.4 showed an increase in migration even in basal or DMSO conditions, unlike the adenovirus control. This migration was approximately double that of the cells treated with the VEGFR2 selective inhibitor, ZM323881. Although previous studies within the lab have demonstrated that RCAN1.4 plays a role in cell migration, this is the first time it has been shown that RCAN1.4 overexpression increases migration via a pathway requiring VEGFR-2 kinase activity.

Interestingly, samples treated with the HGFR inhibitor SGX-523 or cyclosporin A did not show this same inhibitory effect, with the RCAN1.4 overexpression still resulting in increased migration. This important result suggests RCAN1.4 overexpression is able to act independently of the CsA target calcineurin, defining a novel role for this protein in endothelial cell function.

To conclude this result, analysis of cell migration revealed that RCAN1.4-mediated cell migration was inhibited by the VEGFR2 kinase inhibitor ZM323881 but not the HGFR kinase inhibitor SGX-523 or the calcineurin pathway inhibitor cyclosporin A. Taken together, this data shows RCAN1.4 can drive cell migration in HDMECs via a mechanism requiring VEGFR2 kinase activity but is independent of calcineurin activity, the known target for RCAN1.4.

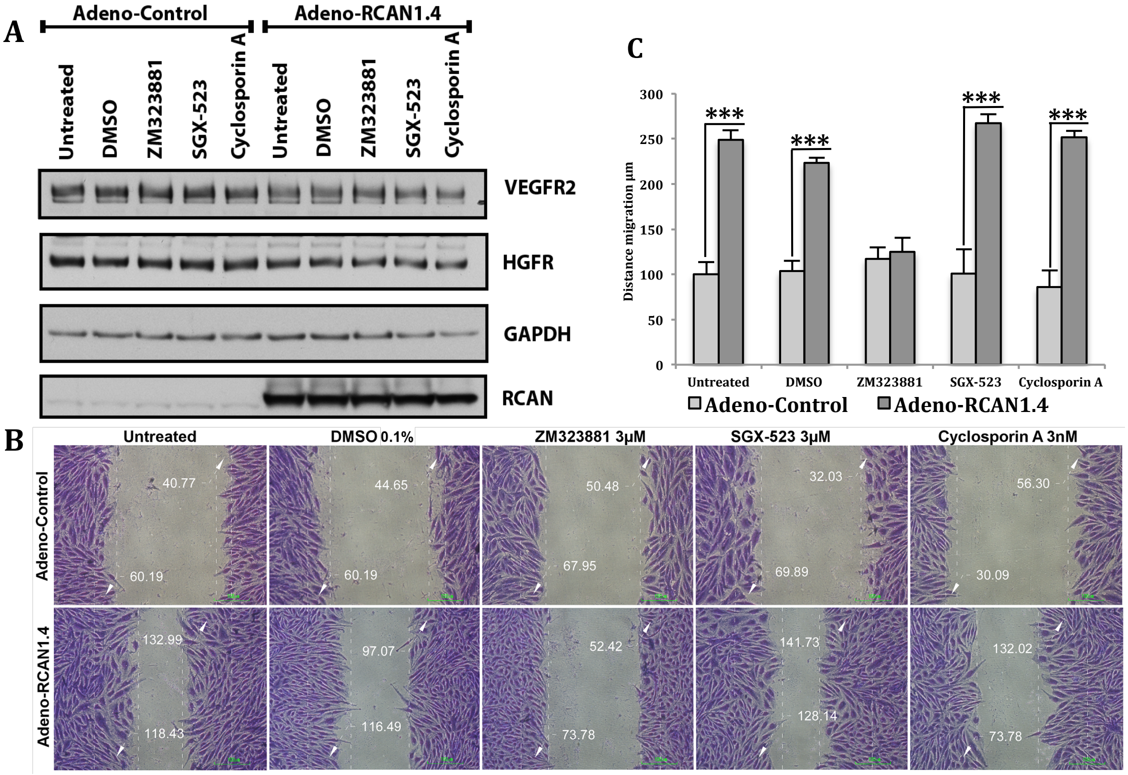

Figure 4.9: Adenoviral mediated overexpression of RCAN1.4

A. Western blotting analysis confirmed the overexpression of RCAN1.4 in HDMECs compared with adeno-control. HDMECs were seeded at 7 × 10^4 cells per well on gelatine pre-coated 12-well plates for 24 hours in FGM. Cells were serum starved with 1% PromoCell FCS media for 24 hours. They were then treated with vehicle control, 3 µM ZM323881, 3 µM SGX-523 and 3nM Cyclosporin A for 30 minutes before being washed with PBS and lysed with 1xLDS and subjected to western blotting analysis probing for Total VEGFR2, Total HGFR and RCAN1. GAPDH was used as a loading control. **B.** Scratch wound assay in which the HDMECs were seeded at 7 × 10^4 cells per well on gelatine pre-coated 12-well plates for 24 hours in FGM. Cells were transfected with adenovirus RCAN1.4 or adeno-control for 24 hours followed by serum starving with 1% PromoCell FCS media for 24 hours. A scratch was introduced to each well using a sterile 200-µl Gilson pipette tip. Cells were treated with vehicle control, 3 µM ZM323881, 3 µM SGX-523 and 3 nM Cyclosporin A. After 18 hours migration, cells were washed with PBS, fixed with 2% PFA for 15 minutes and stained with Crystal Violet. Images taken using a Nikon imaging microscope at ×10 objective. **C.** A graph quantifying migration distance (µm) after inhibitor treatment. Data shows mean ±SD, (N = 3), ***P < 0.001, Adeno-RCAN1.4 versus Adeno-Control, Student's t-test).

4.2 Discussion

The migration of endothelial cells is a critical component of angiogenesis as endothelial cells migrate towards a VEGF gradient and form a vascular sprout, which eventually differentiates into a lumen-containing vessel. This process is critical for normal physiological angiogenesis and pathological tumour angiogenesis.

Previous results in the group have revealed a role for RCAN1.1 in regulating VEGFR-2 mediated migration of HDMECs (Holmes et al., 2010). However, whilst this previous data showed that RCAN1.4 regulation was specifically induced by VEGF/VEGFR-2 it did not determine if RCAN1 regulation of endothelial cell migration was specific to VEGF. Analysis of VEGF-A, FGF and HGF-stimulated migration revealed that RCAN1 specifically regulated VEGF-A migration (Figure 4.2 and 4.3). This important result suggests that RCAN1 does not regulate cell migration at the level of small GTP binding proteins such as Rac and Cdc42, which are critical for cell migration in response to agonists (Ridley, 2012). Instead the data suggests that the regulation of migration in response to VEGF-A is specific to the VEGFR-2. It is possible that RCAN1 binds directly to VEGFR-2, although attempts to co-immunoprecipitate VEGFR-2 and RCAN1 presented in the previous chapter were not conclusive. A transient association was suggested by the proximity ligation assay (PLA) data presented in the previous chapter. The amino acid structure of RCAN1 does not reveal any obvious motifs known to bind to RTKs such as SH2 domain. However, a proline-rich domain is present in RCAN1 (Fuentes et al., 1995), which could potentially allow binding to SH3 domain containing proteins, which are then able to bind to VEGFR-2, meaning that RCAN1 indirectly links to VEGFR-2.

It is possible that RCAN1 links to VEGFR-2 via ancilliary molecules such as neuropilin, which is known to act as a co-receptor for VEGFR-2 (Soker et al., 1998). However, the ability of RCAN1 to regulate migration in response to both VEGF-A_{165} and the VEGF-A_{121} isoform would suggest that the co-receptor neuropilin is not involved in providing specificity to the VEGFR-2 response as in contrast to VEGF-A_{165}, VEGF-A_{121} does not bind to neuropilin-1 (Holmes et al., 2007).

Using time-lapse imaging it was possible to obtain more detail about the defect in migration following RCAN1 silencing. Analysis of the movie (supplementarty material and figure 4.4) showed that RCAN1 depleted cells were not able to send out protrusions to sense the leading edge. Quantification of cell movement using available software (Ibidi®) revealed that cells treated with non-silencing siRNA or untreated cells migrated faster, over longer distances and straighter than cells that had been depleted of RCAN1 (Figure 4.5). This data agrees with data from the previous chapter describing a role for RCAN1 in achieving cell polarity and cytoskeletal reorganisation. Indeed, analysis of cell alignment using a mixed population of cells with either non-silencing knockdown or RCAN1 knockdown confirmed a role for RCAN1 in cell alignment (Figure 4.6). The cell time-lapse imaging also revealed specificity in the VEGF response as HGF-stimulated migration did not appear to be affected by RCAN1 silencing. This appears to confirm previous findings in that RCAN1 appears to specifically regulate VEGFR-2 effects on migration.

Previous work utilising siRNA-mediated gene silencing has not been able to assign specific effects to either the RCAN1.1 or RCAN1.4 isoform as both are silenced by the commercial siRNA RCAN1 duplexes used. Whilst it has been shown in Chapter 3 that VEGF only induces expression of the RCAN1.4 isoform, suggesting that this isoform is more important for regulating VEGF effects, proof of the role of RCAN1.4 came from over-expression of this specific isoform in the endothelial cells. A number of methods were used for overexpression ranging from liposomal based methods (Lipofectamine 2000) and nucleofection (Amaxa). However, adenoviral mediated transduction offered the highest transfection efficiency with sustained expression in HDMECs. Using adenovirus encoding human RCAN1.4 it was evident that RCAN1.4 overexpression could induce HDMEC migration in the absence of ligand (Figure 4.9). Agonist stimulation did not increase this migration suggesting that RCAN1.4 overexpression achieved maximal stimulation. Use of cell permeable inhibitors targeting VEGFR-2 and HGFR revealed that RCAN1.4 overexpression required VEGFR-2 kinase activity to stimulate cell migration, but not HGFR kinase activity (Figure 4.9). Addition of cyclosporine-A, a potent inhibitor of calcineurin, revealed that VEGF-A mediated migration was dependent on calcineurin activity (Figure 4.7C). This probably reflects the ability of calcineurin to inhibit VEGF-A mediated RCAN1.4 expression (data not shown; Holmes et al., 2010). In contrast, addition of cyclosporin-A did not block the ability of adenoviral mediated expression of RCAN1.4 to stimulate HDMEC migration (Figure 4.9C) suggesting that RCAN1.4, once expressed, acts independently of calcineurin to regulate

HDMEC migration. From the data presented, it appears that RCAN1.4 overexpression is able to effectively substitute for VEGF-A activation of VEGFR-2 in stimulating cell migration. It would be interesting to also over-express the RCAN1.1 isoform to determine if this protein is also able to regulate cell migration. It was not possible to confirm RCAN1.4 mediated activation of VEGFR-2 kinase activity following overexpression of RCAN1.4 and a more detailed time-course experiment followed by western blotting for phospho-VEGFR-2 would be important in confirming this. However, it is possible that RCAN1 requires a basal VEGFR-2 kinase activity to keep the receptor in a conformation that is amenable to regulation and trafficking by RCAN1.4. It would be interesting to determine the effect of RCAN1.4 over-expression on VEGFR-2 trafficking and in this respect a GFP-tagged RCAN1.4 would be very useful for analysing intracellular localisation of this protein.

In conclusion, results in this chapter have confirmed a role for RCAN1 in regulating VEGF-A mediated migration and shown that this effect appears to be restricted to VEGFR-2 relative to other RTKs. Importantly, it has been possible to show that the RCAN1.4 isoform is able to stimulate migration in HDMECs via a pathway independent of calcineurin but requiring VEGFR-2 kinase activity suggesting a novel role for RCAN1.4 in directly regulating VEGFR-2 function.

Chapter 5

Role of PLD regulation in endothelial cells

5.1 Introduction

The role of phospholipase D in tumour angiogenesis and cancer has been demonstrated over the last ten years. Phospholipase D is a regulator of several cellular processes, including vesicle transport, endocytosis, exocytosis, cell migration and mitosis (Foster and Xu, 2003). Dysregulation of these processes occurs in carcinogenesis, and abnormalities in PLD expression have been implicated in the progression of several types of cancer (Exton, 2002, Peng and Frohman, 2012). Furthermore, a mutation conferring elevated PLD2 activity has been observed in several malignant breast cancers (Peng and Frohman, 2012). Elevated PLD expression has also been correlated with tumour size in colorectal carcinoma, gastric carcinoma and renal cancer (Saito et al., 2007). However, the molecular pathways through which PLD drives cancer progression remain unclear. One potential hypothesis identifies a critical role for phospholipase D in the activation of mTOR, a suppressor of cancer cell apoptosis (Rodrik et al., 2005). The ability of PLD to suppress apoptosis in cells with elevated tyrosine kinase activity makes it a candidate oncogene in cancers where such expression is typical (Rodrik et al., 2005, Saito et al., 2007). In addition, VEGF is known to activate PLD activity in endothelial cells (Seymour et al., 1996). VEGF is known to activate VEGFR2 in endothelial cells resulting in migration, tube formation, differentiation and proliferation (Holmes et al., 2007). In contrast to other phospholipases such as phospholipase C and phospholipase A2, the role of PLD in endothelial cell function has not been studied in detail.

PLD has been reported to become highly active in response to VEGF in HUVECs via a mechanism requiring PKC (Seymour et al., 1996, Cho et al., 2004). In this chapter, the physiological role of PLD activation will be addressed using a number of approaches, ranging from small molecule inhibitors of PLD1 and PLD2, siRNA-mediated gene knockdown of PLD and finally overexpression of PLD.

5.1.1 Cellular expression of PLD isoforms

PLD is known to be a ubiquitously expressed enzyme (Kam and Exton, 2001). PCR primers were designed for human PLD1 and PLD2 mRNA, and their expression was analysed in a range of human cell types and organ tissues. Expression of PLD1 was the most abundant and highest in the foetal heart and in HDMECs compared to PLD2 which was most highly expressed in HDMECs (Figure 5.1).

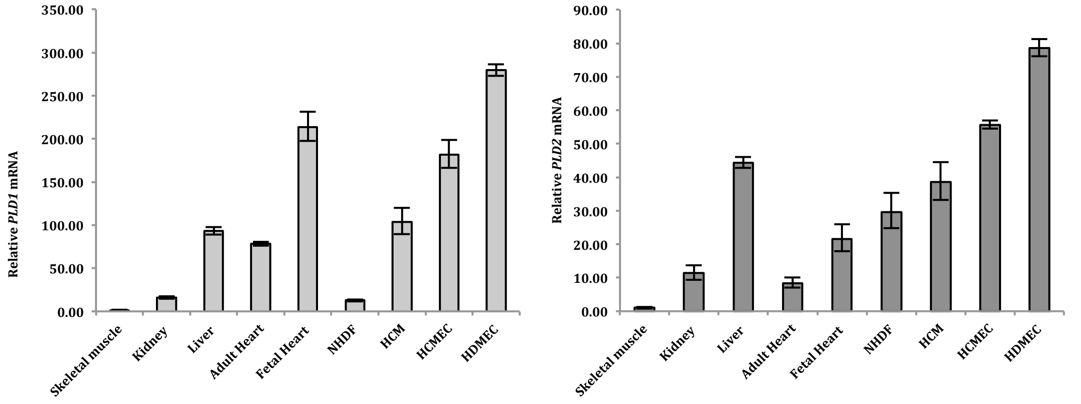

Figure 5.1: qRT-PCR analysis of PLD1or PLD2 mRNA splicing in various tissues and primary cells.

RNA and cDNA were extracted from cells and tissues and prepared. Data were analysed by the ΔΔCt value method and expression was normalized to β-actin expression and illustrated as fold change. HDMEC= human dermal microvascular endothelial cells, HCMEC= human cardiac microvascular endothelial cells, HCM= human cardiac myocytes and NHDF= normal human dermal fibroblasts. Data shows mean ± SD. The data is representative of three experiments.

5.1.2 Knockdown of PLD1 and PLD2 expression: siRNA validation and optimisation

Selective commercial siRNA duplexes targeting the human *PLD1* or *PLD2* gene used for this study (see Table 2.7) were purchased from Dharmacon. Furthermore, for controls in all experiments in this study, cells were transfected with non-silencing siRNA as a negative control (NS). Transfection was performed using the transfection reagent Lipofectamine RNAi MAX. The transfection efficiency for PLD1 was determined at the protein level and mRNA level by qRT-PCR, whereas PLD2 was only validated by qRT-PCR due to lack of a suitable antibody. To confirm that the PLD-specific siRNA duplexes were able to knock down PLD1&2 expression in HDMECs, cells, were lysed 48 hours after transfection and analysed using western blotting and anti-PLD1 antibody (Figure 5.2A). Duplexes appear to show significant knockdown of PLD1 at the protein level (Figure 5.2A) and mRNA level (Figure 5.2B). From this data, the PLD1 duplexes 1 and 2 were chosen for further study. For PLD2 validation, the lack of a good commercial antibody meant that it was not possible to perform western blotting. Validation of siRNA mediated gene silencing was performed by qRT-PCR, and PLD duplexes 2 and 6 were chosen for further study (Figure 5.2B).

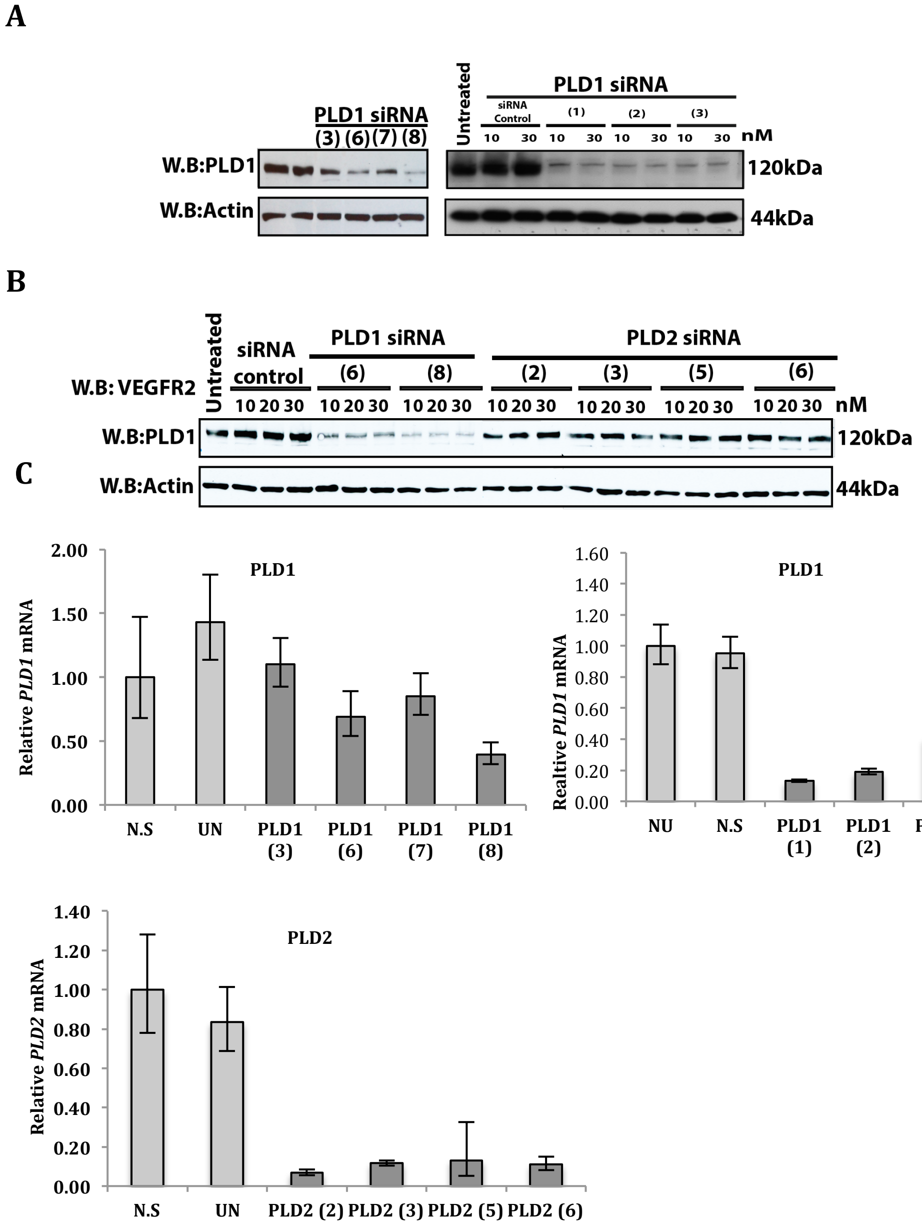

Figure 5.2: Analysis of PLD1&2 silencing in HDMECs.

A. and B. HDMECs were seeded at 7 × 10^4 cells/wells on to pre-coated gelatine for 24 hours using F.G.M. Many separate siRNA duplexes targeting PLD were used. HDMECs were transfected with siRNA to PLD1, PLD2 and NS siRNA as indicated. Actin was used as a loading control. **C.** qRT-PCR analysis for PLD1&2 mRNA level: RNA and cDNA were extracted from HDMECs and prepared. Data were analysed by the ΔΔCt value method and expression was normalized to β-actin expression and illustrated as fold increase. Data shows mean ± SD. The data is representative of three experiments.

5.1.3 Analysis of PLD expression in HDMECs

The expression of both PLD1 and PLD2 was induced in cells in response to growth factors and cytokines (Kang et al., 2013). To determine the profile of PLD1 expression in response to stimulation with growth factors, screening was conducted. Cells were treated with growth factors (VEGF-A, FGF-2, HGF) and the phorbol ester PMA, followed by cell lysis and analysis of RCAN1 and PLD activation using western blotting with selective antibodies (see Figure 5.3). It was found that VEGF is a potent activator of RCAN1 in HDMECs, whereas other growth factors did not induce RCAN1 up-regulation. However, PLD expression was not induced at the protein level with a range of growth factors.

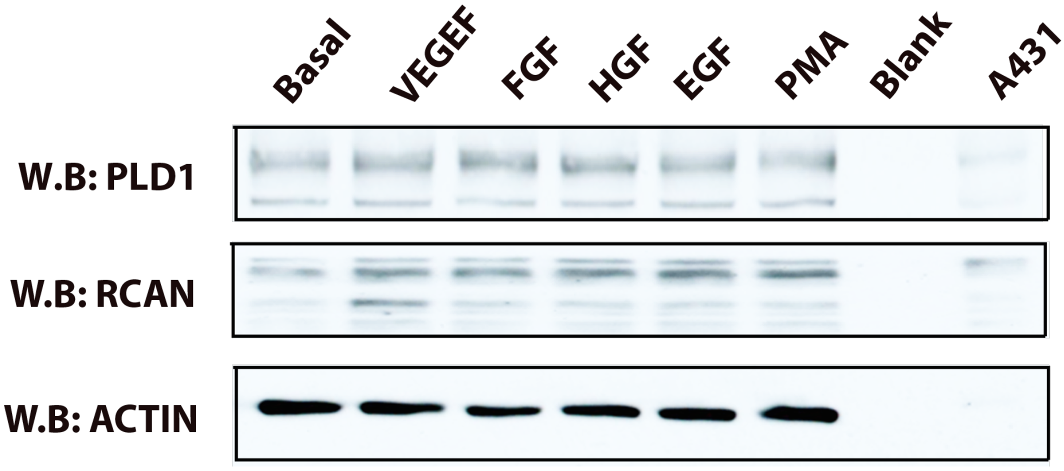

Figure 5.3: Growth factor screening.

HDMECs were seeded at 7 × 10^4 cells/wells onto gelatine-coated 12-well plates for 24 hours using growth media, incubated overnight and then serum-starved in 1% FCS media for 18 hours prior to stimulation. Cells were stimulated with Basal, 50 ng/ml VEGF; 50 ng/ml FGF-2; 50 ng/ml HGF or 100 nM PMA for 10 minutes each and A431= epidermal carcinoma expressed high levels of EGFR. Cell lysates were then separated on 4-12 Nu Page gel and probed with antibodies against PLD1, RCAN1 and actin as loading controls asindicated above in the figure. This experiment has been performed once.

5.1.4 Effect of PLD knockdown on VEGFR-2 signalling in HDMECs

In order to investigate the effect of PLD activity on VEGFR-2 signalling, the validated siRNA duplexes were utilised to silence both PLD1 and PLD2 in HDMECs and the activation of key downstream signalling molecules such as PLC-gamma and AKT were analysed. Cells were stimulated with VEGF for 10 minutes and 60 minutes to allow analysis of signalling pathways at two separate time points. siRNA-mediated silencing of PLD1 and PLD2 appeared to have a slight effect on activation of Akt at 10 mins, although there was variation between both duplexes. Analysis at the 1-hour stimulation time point revealed no significant effect of silencing PLD1 and PLD2 on VEGFR-2 mediated intracellular signalling (Figure 5.4).

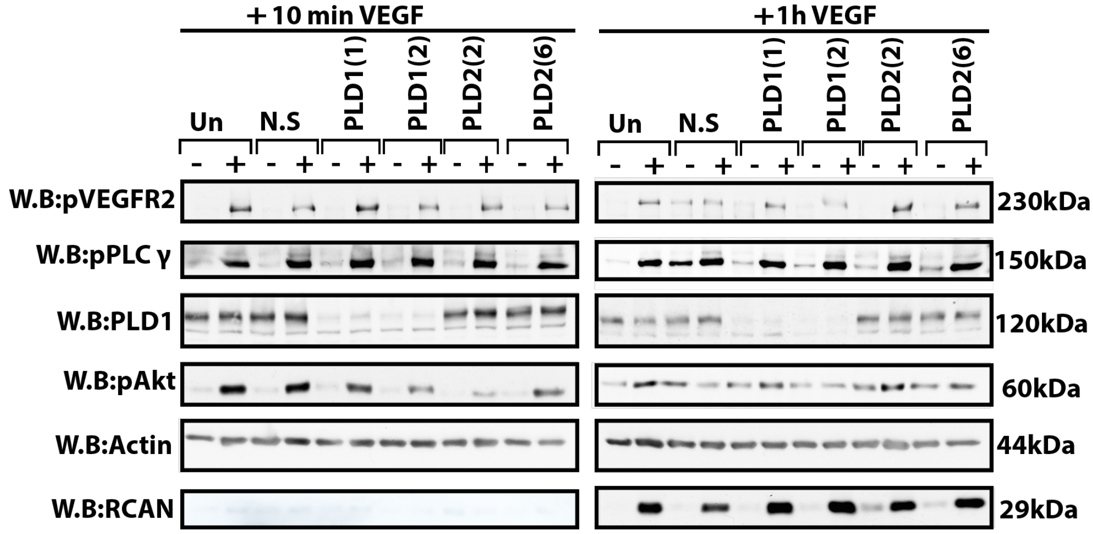

Figure 5.4: The role of PLD in VEGFR-2 signalling

HDMECs were seeded at 7 × 10^4 cells/wells onto pre-coated gelatine for 24 hours using F.G.M. Two separate siRNA duplexes were used targeting PLD1&2. HDMECs were transfected with siRNA to PLD1, PLD2 and NS siRNA control as indicated. HDMECs were stimulated with VEGF as illustrated in the diagram for 10 minutes and 1 hour. Actin was used as a loading control. The data is representative of three experiments.

5.1.5 Optimisation of PLD on collagen and gelatine

In response to stimulation with certain growth factors, endothelial cells undergo tubular morphogenesis and form capillary-like structures in 3D models (Holmes et al., 2010). To determine if PLD plays a role in angiogenesis, HDMECs were plated in parallel within a collagen gel and also onto gelatin-coated dishes. After growth factor stimulation overnight, cells were lysed to facilitate extraction of RNA and protein. According to the mRNA and protein levels from both collagen and gelatine, RCAN1 was highly up-regulated following stimulation with VEGF-A. In HDMECs, PLD1&2 did not show any induction in mRNA or protein level in response to VEGF-A (see Figure 5.5A,B,C,D).

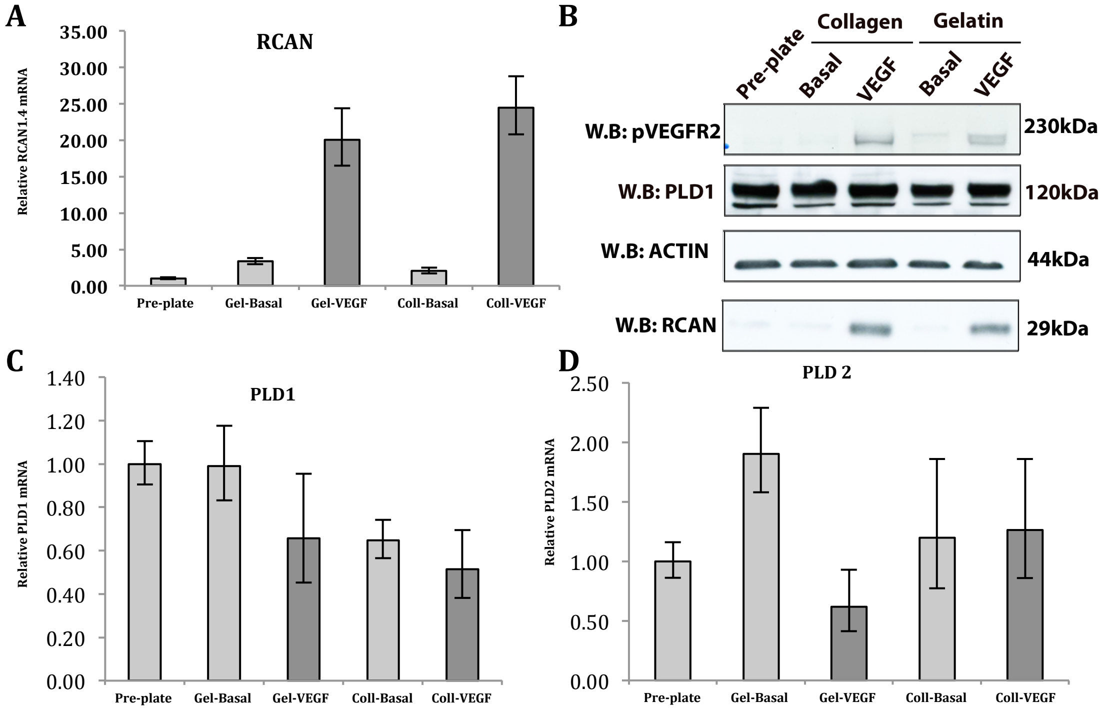

Figure 5.5: Analysis of PLD expression on collagen & gelatin

A. C. D. qRT-PCR analysis for RCAN and PLD1&2 mRNA level: RNA and cDNA were extracted from HDMECs and prepared. Data were analysed by the ΔΔCt value method, and expression was normalized to β-actin expression and illustrated as fold increase. Data shows mean ± SD. The data is representative of three experiments. **B.** HDMECs were seeded at 7 × 10^4 cells/wells on to pre-coated gelatine or for 24 hours using F.G.M. Used two separate siRNA duplexes targeting PLD1&2. HDMECs were transfected with siRNA to PLD1, PLD2 and NS siRNA control as indicated. HDMECs were stimulated with VEGF as illustrated in the diagram for 18 hours. Actin was used as a loading control.

5.2 PLD and the regulation of cellular migration

Cell migration is a critical component of the angiogenic cascade as endothelial cells migrate at the leading edge to form a capillary sprout. The scratch wound healing assay allows the study of the effects of growth factors upon cell migration in endothelial cells. To examine VEGF-A, EGF and HGF, HDMECs were plated on 12-well gelatine-coated dishes for 24 hours. The following day, cells were transfected with siRNA duplexes and the next day serum-starved with 1% FCS media. Cells were scratched with 200-μl yellow micropipette tips and washed with PBS to remove debris. Cells were stimulated with growth factors for 18 hours. Images were taken for time zero and additional images were taken after 18 hours. Every experimental sample was stimulated with VEGF-A or with HGF 50 ng/ml in

1% FCS media. From the five images, the width of each wound was assessed and averages of these measurements were plotted in a bar chart.

In this diagram (Figure 5.6.A), images were taken for HDMECs at time zero where images were stained with Crystal Violet taken after 18 hours of the experiment. It is clear that the edge of the monolayer in basal conditions did not migrate, whereas in the present VEGF-A and HGF in untreated and siRNA controls, the edge moved forward to close the wound. VEGF-A and HGF enhanced endothelial migration toward the leading edge. In contrast with PLD1&2 depletion, the figure illustrates a clear defect in cell migration as a result of VEGF-A, whereas in contrast HGF migration was not affected by PLD silencing.

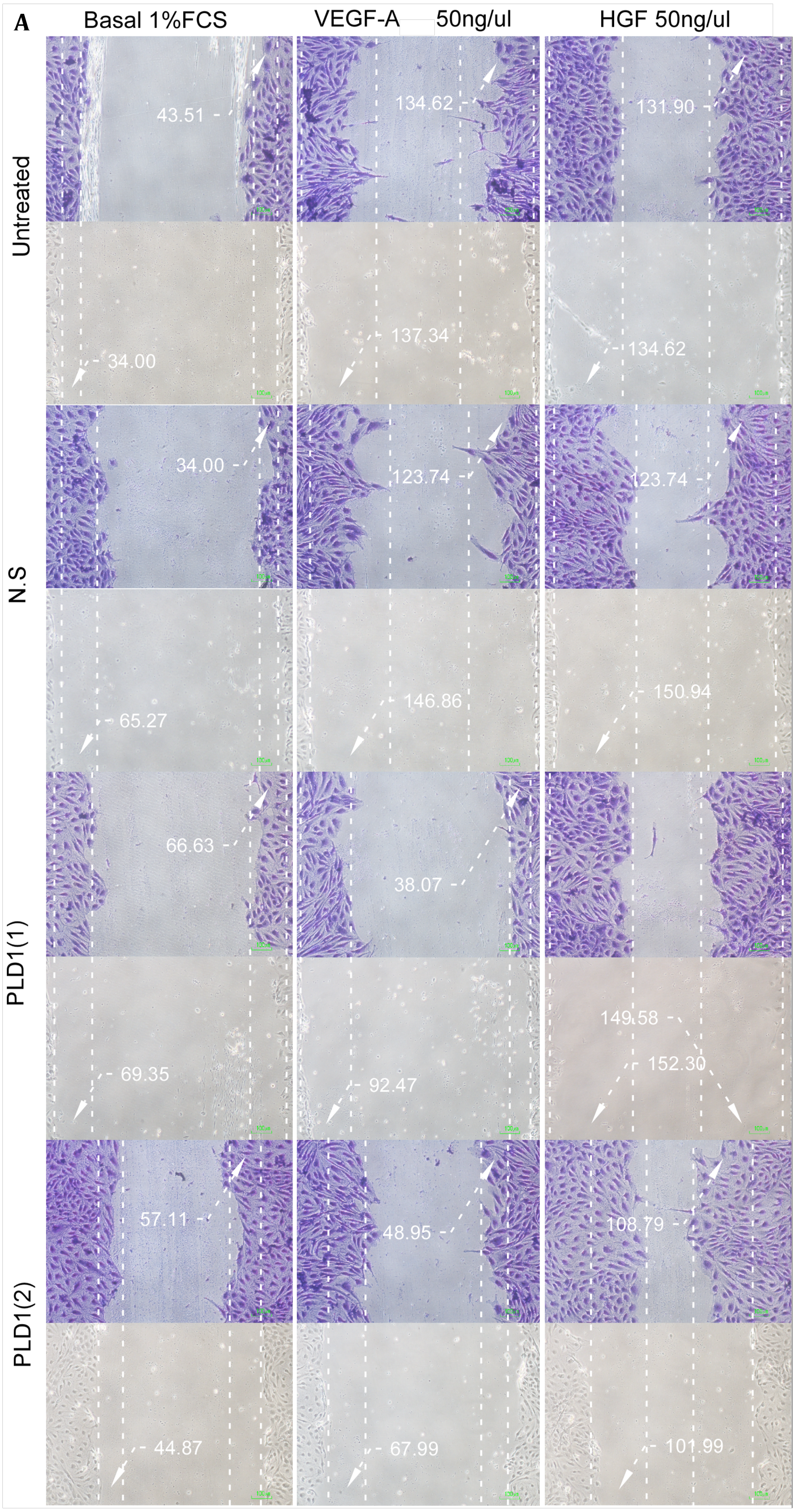
A
Basal 1%FCS
VEGF-A 50ng/ul
HGF 50ng/ul
Untreated
N.S
PLD1(1)
PLD1(2)
43.51
134.62
131.90
34.00
137.34
134.62
34.00
123.74
123.74
65.27
146.86
150.94
66.63
38.07
69.35
92.47
149.58
152.30
57.11
48.95
108.79
44.87
67.99
101.99

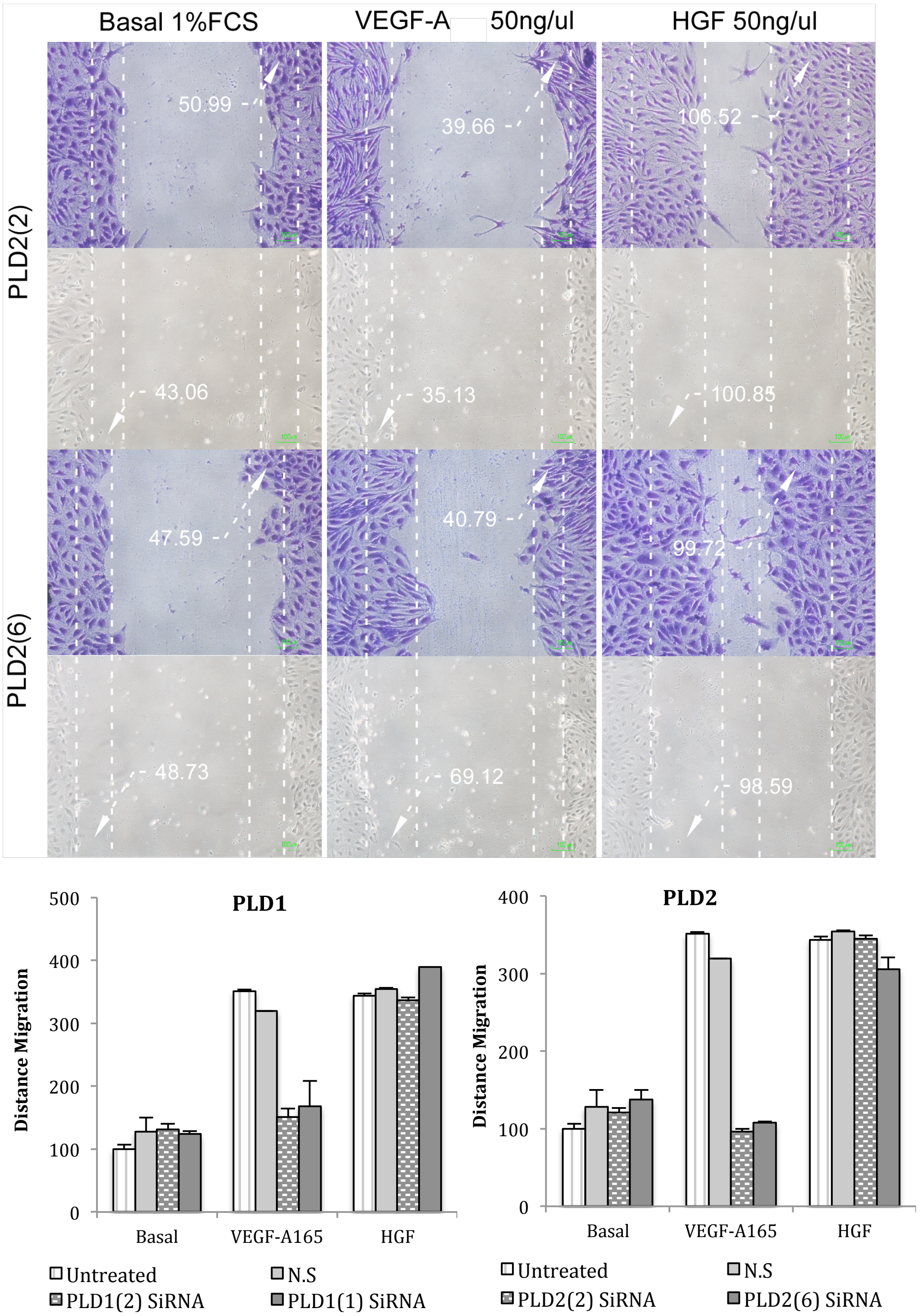

Figure 5.6: Effect of PLD on HDMEC migration.

Migration assay shows siRNA of PLD and non-silencing (NS) for 6 hours. Cells were serum-starved with (1% FCS PromoCells) media for 24 hours. A scratch was introduced to each well using a sterile 200-µl Gibson pipette tip and stimulated with VEGF-A_{165} and HGF 50ng/ml for 18 hours. Cells were washed with PBS, fixed with 2% PFA for 15 minutes and stained with Crystal Violet. Images were taken using a Nikon imaging microscope with a × 10 objective. This figure explains scratch distance (µm) after siRNA transfection followed by VEGF-A and HGF stimulation using 1% FCS Promo for 18 hours. Data shows mean ± SD. The data is representative of three experiments.

5.3 PLD and tubular morphogenesis

VEGF-A stimulates endothelial cells to form tube-like structures in 3D collagen gels. However, PLD activation and regulation on a collagen gel had not been reported. To examine the formation of PLD1&2 in *in vitro* vascular structures, tube formation analysis was undertaken to confirm physiological function. HDMECs were plated out onto a pre-coated dish with gelatin for 24 hours. HDMECs were transfected with siRNA for both PLD and PLD2 isoforms. Cells were serum-starved overnight and, on the following day, cells were detached by accutase and plated onto 3D collagen gel with VEGF-A for 18 hours. Subsequently, cell sprouts were imaged and the number of junctions or mesh areas were counted using ImageJ software.

Endothelial cell sprouting was seen after stimulation with VEGF-A for 18 hours on to HDMECs on collagen gel in untreated or siRNA control samples. Clearly, this figure illustrates strong sprouting in response to VEGF-A with respect to cellular junction formation (Figure 5.7A). SiRNA-mediated silencing of either PLD1 or PLD2 resulted in severely reduced tubular morphogenesis (Figure 5.7).

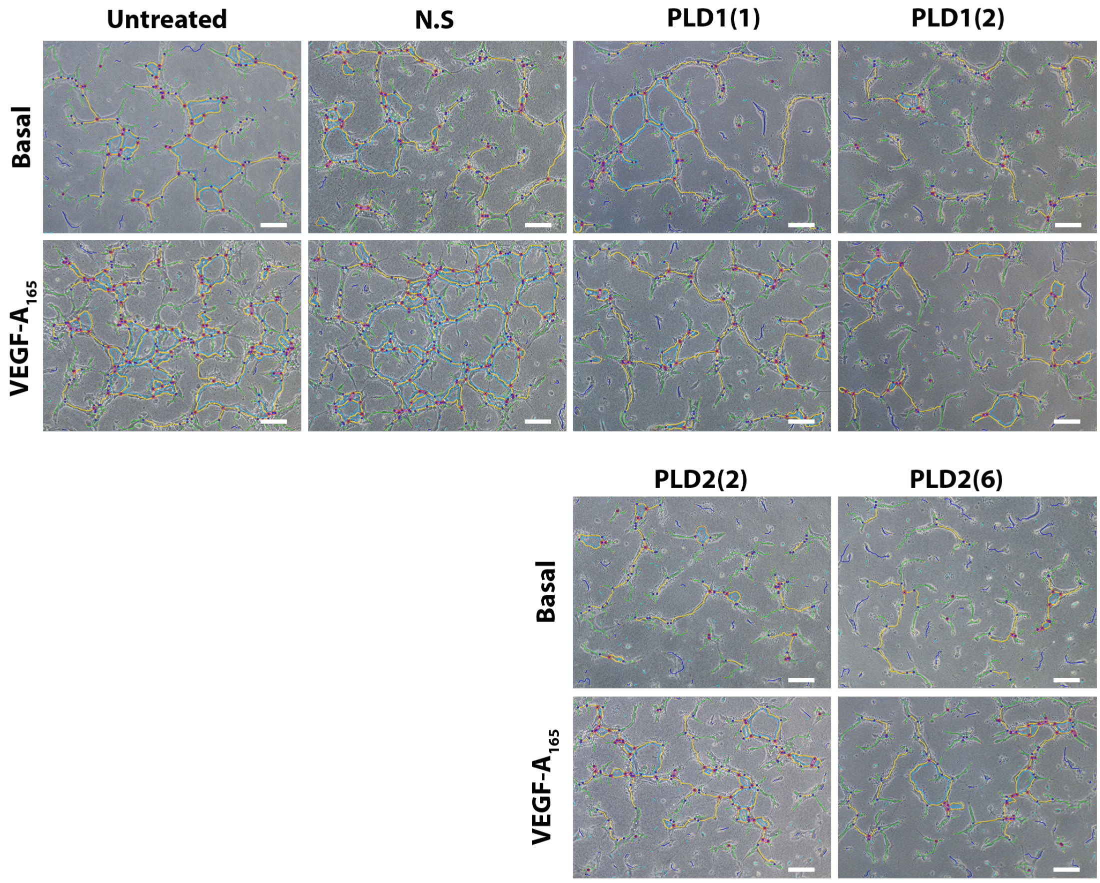

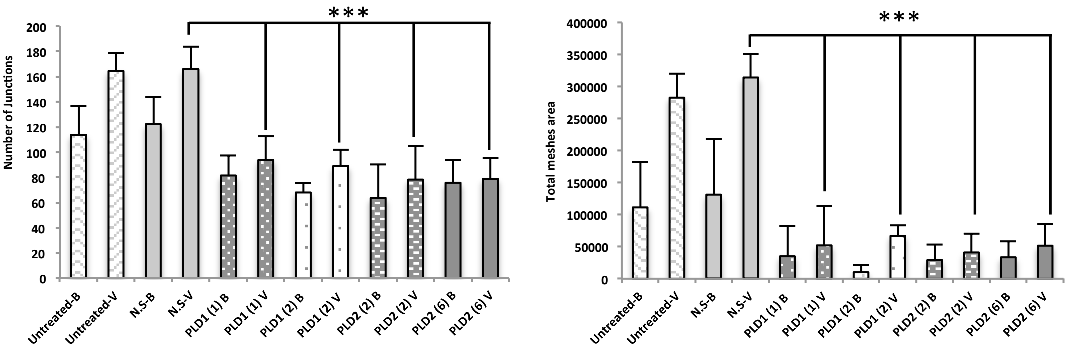

Figure 5.7: Phospholipase D1&2 are required for tubular morphogenesis in HDMECs

Cells were transfected with two individual siRNAs to PLD1, PLD2 and NS. Cells were plated on collagen matrix and stimulated with VEGF-A (50ng/ml). 3D collagen gels were fixed at 18 hours to determine visualization of tubules. Bar = 100µm. The figure illustrates quantification of tubular morphogenesis using ImageJ software plugins to quantify the number of cellular junctions and total meshes in an area. Data shows ± SD (N=4), (p***<0.001, siRNA versus NS. Students t-test). The data is representative of three experiments. B=Basal, V=VEGF-A.

5.4 Effects of PLD on the proliferation of HDMECs

PLD could play a role in cell physiology and could act as a proliferative factor in mammalian cells. The aim of these experiments was to examine the role of PLD in cell proliferation in response to VEGF-A, FGF-2 and HGF in human endothelial cells. HDMEC cells were plated at 7 × 10^4 cells per well in growth media for 24 hours, and siRNA was introduced on the following day. Cells were grown for 48 hours in low serum before stimulation with growth factors for 48 hours.

VEGF precipitated a twofold increase in cell viability as measured by ATP levels. siRNA-mediated silencing of PLD1 or PLD2 resulted in the inhibition of VEGF-mediated cell proliferation with no apparent effect on HGF-mediated proliferation (Figure 5.8).

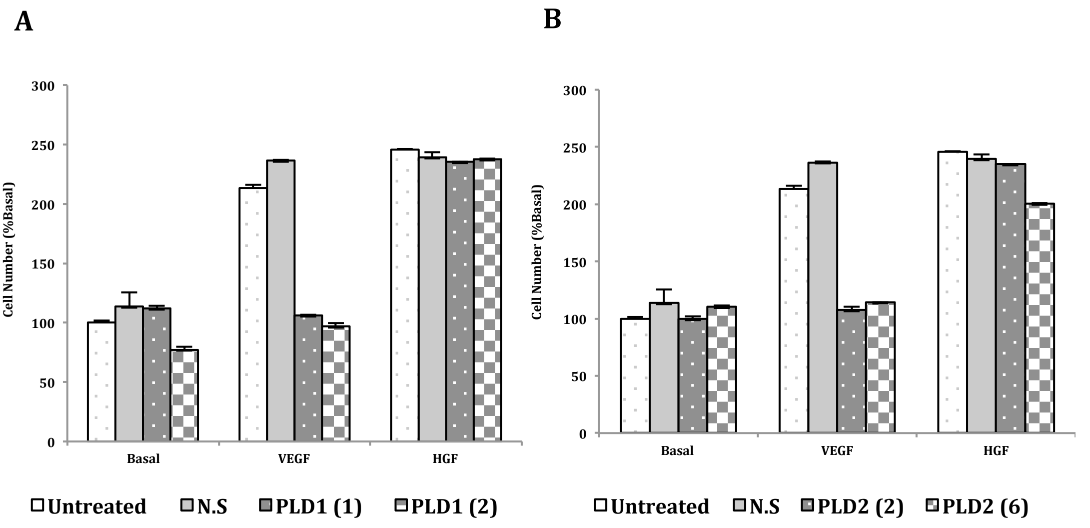

Figure 5.8: Phospholipase D1&2 are required for proliferation of HDMECs.

Cells were transfected with two individual siRNAs to phospholipase D1 and D2 or non-silencing (NS) and stimulated with VEGF-A and HGF (50ng/ml) for 72 hours. Cell proliferation was determined by measuring viable cells using Cell Titer Glow or Crystal Violet staining. Data shows mean ± SD. The data is representative of three experiments.

5.5 Characterization of PLD function by overexpression

HDMECs utilized in the following experiments were transfected with PLD1-GFP and PLD2-GFP in order to study the role of PLD1&2 in endothelial cells and to determine transfection efficiency so as to identify the most effective strategies for transfection. Three different methods of transfection were assessed for this study. The first transfection attempt was performed using the transfection reagent called Tans Pass NEB, but it did not work (data not shown). Then, another method to transfect these plasmids to HDMECs was tried using Lipofectamine 2000, but the transfection efficiency was too low. The most effective transfection of PLD-GFP was achieved with the Amaxa Nucleofector Technology kit (Lonza). HDMECs were electroporated using Amaxa solution at 4 × 10^5 cells per condition and plated on to dishes. Transfection efficiency was assessed by western blot and fluorescence microscopy.

Optimisation of transfection efficiency was run on western blots by plating HDMECs cells and transfected with PLD1&2 plasmids or pcDNA3.1 vector to determine if the overexpression of PLD1&2 was able to increase cell migration, proliferation and tube formation. As controls for this experiment, empty vector plasmids were transfected into HDMECs and compared with PLD1&2 plasmids (Figure 5.9). Transfection with untreated and empty vector did not show any significant expression with PLD1 and GFP antibody. In contrast, transfection with PLD1-GFP was highly successful due to availability of specific antibody and, in addition, transfection efficiency was very high.

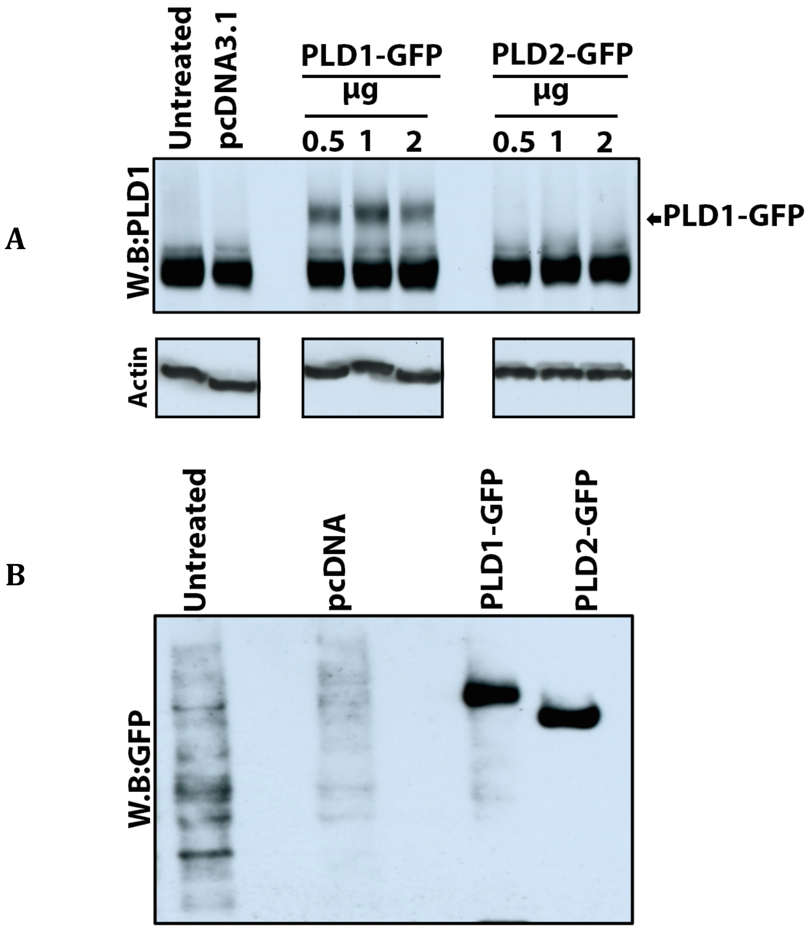

Figure 5.9: HDMECs transfected with PLD-GFP or pcDNA expression plasmid

HDMECs were seeded at 7 × 10^4 cells/wells on to pre-coated gelatine for 24 hours using F.G.M. Cells were transfected with plasmids using Amaxa according to the standard protocols included in the Amaxa Nucleofector Technology kit (Lonza). After transfection, the cells were plated into appropriate plates. After 24 hours, the cells were lysed with 1x LDS. PLD1 and GFP levels were determined by western blot. This experiment has been performed once.

5.5.1 Validation of PLD-GFP

HDMECS cells were transfected with the PLD1&2 plasmid to evaluate the effect when stimulated with growth factor. The first investigation was undertaken to assess the expression of PLD1-GFP with specific commercial antibody and PLD2-GFP. HDMECs were grown on plastic dishes and transfected with PLD1-GFP and PLD2-GFP using the Amaxa kit. The cells were then fixed and stained according to the immunofluorescence protocol. Figure 5.10 clearly shows the transfection of PLD1-GFP in immunofluorescence (bottom-left figure). In addition, PLD1 expression in comparison to PLD2 (bottom-right figure) only reveals PLD2-GFP due to lack of specific antibody for PLD2.

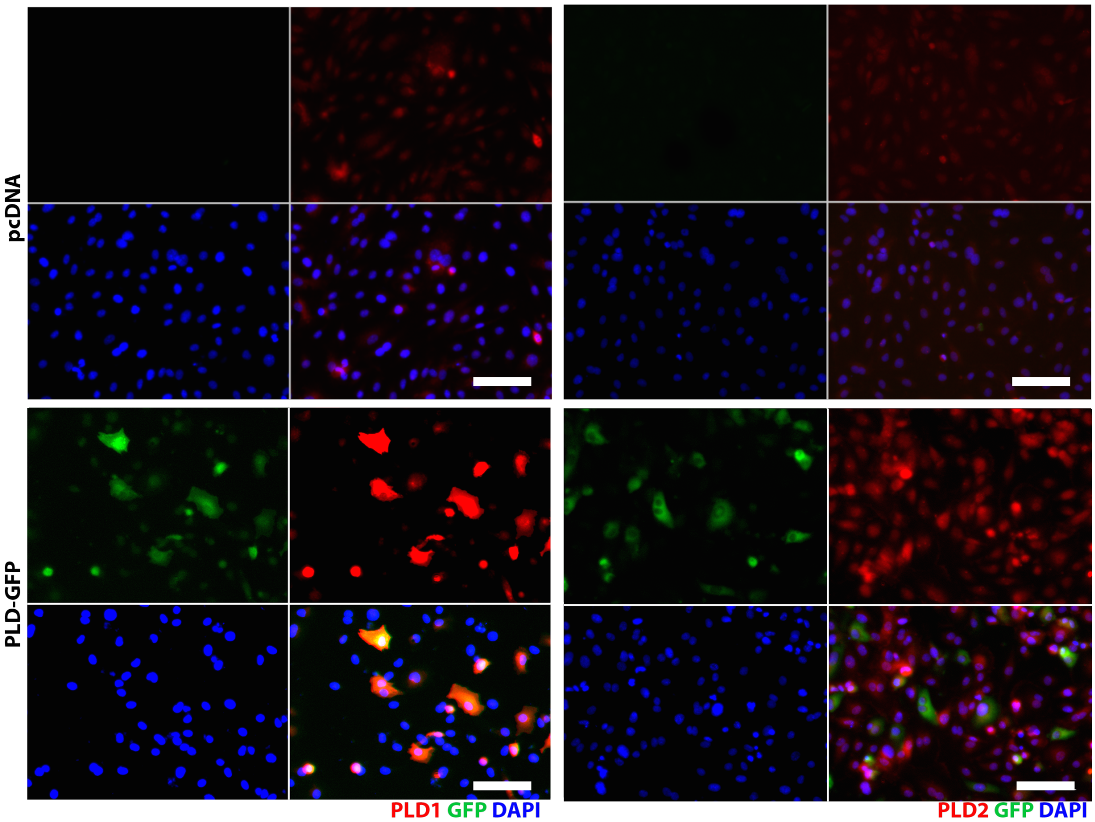

Figure 5.10: HDMECs transfected with PLD-GFP or pcDNA

HDMECs were seeded at 7 × 10^4 cells/wells on to pre-coated gelatine for 24 hours using F.G.M. Cells were transfected with plasmids using the standard protocols included in the Amaxa Nucleofector Technology kit (Lonza). After transfection, the cells were plated on to appropriate plates. After 24 hours, the cells were fixed in 2% formaldehyde followed by immuno-staining with PLD1 or PLD2 antibody. This experiment has been performed once. Scale bar: 100µm.

5.6 Discussion

PLD1 and *PLD2* mRNA was found to be highly expressed in endothelial cells compared to other types of cells and tissues. The physiological role of phospholipase D is thought to be endocytosis and membrane trafficking (Jones et al., 1999). The role of PLD in endothelial cells has not received widespread attention. Early work utilising porcine aortic endothelial (PAE) cells defined a novel role for PLD in LPA-mediated stress fibre formation (Cross et al., 1996). Further work with PAE cells showed that FGF-mediated PLD activation was downstream of FGFR-1 mediated autophosphorylation of Y766 and subsequent activation of PLC-gamma (Cross et al., 2000). VEGFR-2 mediated activation of PLD was first reported by Seymour (Seymour et al., 1996) but this has not been followed up with subsequent studies to define the physiological role for this enzyme in endothelial cell biology.

The data presented in this chapter shows that both PLD1 and PLD2 are required for VEGF-mediated migration, tubular morphogenesis and proliferation in endothelial cells. Despite these profound effects on cell physiology, an effect on acute VEGF intracellular signalling in endothelial cells was not observed following siRNA mediated silencing of both PLD1 and PLD2. This would suggest that PLD plays a novel role in VEGFR-2 mediated effects. Data from the previous chapter would potentially highlight an effect on VEGFR-2 internalisation, which is known to affect migration and tubular morphogenesis and could be investigated further. An effect on VEGFR-2 receptor internalisation may explain why HGFR (c-Met) effects were not blocked by si-RNA mediated silencing of PLD1 and PLD2

The work presented in this chapter was hampered by the lack of a reliable and specific antibody to PLD2. Whilst the mRNA analysis suggested efficient gene silencing it would have been good to confirm this by western blotting. Also, it was not possible to determine the contribution of each PLD isoform to the overall enzymatic generation of phosphatidic acid (PA) in response to VEGF and other agonists to determine the flux through each PLD isoform. ^{3}H myristate labelled endothelial cells would need to be utilised to allow radioactive incorporation into the phosphatdiylcholine pool. The transphosphatidylation reaction in the presence of butan-1-ol would then be utilised to generate ^{3}H phosphatidylbutanol, which can be isolated by thin layer chromatography (TLC). SiRNA mediated silencing of PLD1 or PLD2 would have allowed analysis of PLD activity using this method. Recently, this radioactive method has been superceded by lipidomics as each PA species analysed by mass spec (Wakelam et al., 2007). This has allowed analysis of the individual fatty acid species of the PA molecule, determining if it was originally generated by PLD or by interconversion of DAG generated by PLC mediated hydrolysis of phosphatidylinositol (4,5)bisphosphate by the enzyme DAG kinase (Hodgkin et al., 1998).

In summary, this study suggests a role for phospholipase D (PLD) in VEGFR-2 signalling in endothelial cells with the subsequent regulation of cell proliferation, migration and tubular morphogenesis.

Chapter 6

General Discussion

6.1 RCAN1 and the regulation of VEGFR-2 signalling

The regulators of calcineurin family (RCAN1; formerly known as DSCR) are known to regulate cellular function through inhibition of calcineurin (Serrano-Candelas et al., 2014). The original discovery of RCAN1.4 as a VEGF-regulated gene outlined its role as an endogenous inhibitor of VEGFR-2 mediated gene transcription (Hesser et al., 2004). In this context, RCAN1.4 induction via transcription and translation is expected to act as a negative feedback to effectively reduce flux through the calcineurin/NFAT pathway leading to transcription of genes such as *Cox-2* and *E-selectin,* which are implicated in inflammatory responses. Hence it was originally thought that RCAN1.4 operates to regulate inflammatory responses in the vasculature, similar to its role in other cell types. Previous work in the group has discovered a novel pathway regulating the expression of RCAN1.4 that involves the classical calcineurin/NFAT pathways and a calcineurin independent pathway requiring protein kinase C-delta (Holmes et al., 2010). Both pathways converge to allow maximal induction of RCAN1.4, which plays a role in regulating endothelial cell migration and tubular morphogenesis (Holmes et al., 2010). The work presented in this thesis builds on the previous data in the group to define a novel role for RCAN1.4 in regulating VEGFR-2 function at the level of receptor internalisation in addition to its previously assigned function in regulating VEGFR-2 mediated gene expression via inhibition of calcineurin.

6.2 RCAN1 and regulation of VEGFR-2 internalisation and endothelial migration.

The data presented in chapter 3 outlined a role for RCAN1 in regulating VEGFR-2 internalisation. The use of siRNA targeting both RCAN1.1 and RCAN1.4 meant it was not possible to definitively define a role for each RCAN1 isoform in regulating this acute response. Furthermore, the effect on internalisation was evident on 10 minutes, which is a time point before induction of the RCAN1.4 isoform is seen in response to VEGF. Previous work in the group also showed that VEGFR-2 internalisation was not sensitive to the calcineurin inhibitor cyclosporin A (K. Holmes, unpublished results), suggesting that basal rather than induced RCAN1 levels were responsible for acute VEGFR-2 effects. It is therefore possible that the basal level of both isoforms is able to regulate VEGFR-2 internalisation. The major question regarding this effect is how RCAN1 actually physically regulates VEGFR-2 internalisation. The lack of effect on the HGFR internalisation suggests that this effect could be specific to VEGFR-2, suggesting that the canonical clathrin-dependent endocytic pathway for RTKs, which include the small GTP binding protein Rab5 (Horowitz and Seerapu, 2012, Goh and Sorkin, 2013) is not the route through which RCAN1 regulates VEGFR-2 internalisation. It is possible that RCAN1 interacts with proteins specifically implicated in VEGFR-2 internalisation such as neuropilin 1 (Soker et al., 1998), ephrin-B2 (Sawamiphak et al., 2010) and synectin (Lanahan et al., 2010). However, the lack of a differential effect between VEGF-A165 and VEGF-A121 also suggests that neuropilin is not required for the RCAN1 mediated effect on internalisation. The proximity ligation (PLA) data suggested a rapid transient interaction between RCAN1 and VEGFR-2 at the leading edge of cells. This would suggest a potential mechanism whereby RCAN1 is able to sense VEGFR-2 activation at the leading edge and allow internalisation of VEGFR-2 at this site allowing the establishment of cell polarity and cytoskeletal reorganisation aimed at facilitating efficient directed migration of the endothelial cell. In *Drosophila*, studies on cell migration directionality have revealed the role of receptor tyrosine kinase endocytosis in stimulating spatial restriction of signalling allowing organised cell migration (Jékely et al., 2005). The results presented show that RCAN1 facilitates the coupling of VEGFR-2 internalisation to the establishment of cell polarity at the leading edge and ultimately angiogenic sprout formation.

The mechanism of RCAN1 interaction with VEGFR-2 remains obscure and could be investigated further using immunoprecipitation experiments with cells over-expressing VEGFR-2 and receptor mutants in which parts of the receptor have been mutated or truncated. It is technically possible to IP RCAN1 and to western blot for VEGFR-2 which would allow one to determine if there is a physical interaction between RCAN1 and VEGFR-2. Similarly, it would also be feasible to utilise RCAN1.1 and RCAN1.4 receptor mutants to define the region of RCAN1 that potentially interacts with the VEGFR-2.

In defining a role for RCAN1 in regulating cellular migration, overexpression of RCAN1.4 confirmed that this isoform was capable of regulating VEGFR-2 mediated migration. This backed up the siRNA mediated silencing of RCAN1, which showed that RCAN1 was required for endothelial cells to polarise, undergo cytoskeletal reorganisation and orientate themselves at the leading edge to undergo directed migration. Importantly, the RCAN1.4 overexpression showed that this effect on migration was independent of calcineurin activity, as the effect was not blocked by cyclosporin A. However, VEGF-stimulated migration of HDMECs was blocked by cyclosporin A, which is known to block induction of RCAN1.4 (Holmes et al., 2010). This would suggest that sustained induced RCAN1.4 expression is required for VEGF-stimulated migration but not VEGFR-2 internalisation and that once expression has been induced, RCAN1.4 acts independently of calcineurin to regulate cellular migration. The ability of the VEGFR-2 kinase inhibitor ZM323881 to block RCAN1.4-mediated HDMEC migration suggests that an association between phosphorylated VEGFR-2 and RCAN1.4 is required for sustained cell migration. This allows us to generate an overall hypothesis based on the data presented in chapter 3 and 4 to explain the role of RCAN1 in regulating VEGFR-2 mediated effects (Figure 6.1). VEGF stimulation induces VEGFR-2 activation on the cell surface and internalisation in an RCAN1.1 and RCAN1.4 driven process over time periods of 10-30 mins. Following stimulation for 60-180mins, VEGFR-2 induces expression of RCAN1.4 via a classical pathway requiring the $Ca^{2+/}$calcineurin/NFAT signalling axis and also PKC-delta (Holmes et al., 2010). This sustained level of RCAN1.4 facilitates cytoskeletal reorganisation and cell polarisation, ultimately allowing cell migration to occur over 3-12 hours. The RCAN1.4 protein is subject to proteosomal degradation with a half-life of approximately 15 mins (Beverley Rothermel, personal communication). This would suggest that constant VEGF stimulation is required to maintain sustained RCAN1.4 levels and ultimately stimulate cell migration. Phosphorylation of RCAN1 is another posttranslational modification that has been shown to affect protein half-life (Genescà et al., 2003). Recent data has shown the protein kinase CK2 can phosphorylate RCAN1 on serine residues in the CIC motif resulting in increased affinity for calcineurin and inhibition of NFAT function (Martínez-Høyer et al., 2013). It is a distinct possibility that activation of VEGFR-2 leads to phosphorylation of RCAN1.1 and RCAN1.4, which could be investigated by analysing retardation of phosphorylated species in a Phos-Tag acrylamide gel (Kinoshita et al., 2006). Quantitative phospho-proteomic analysis could also be performed using mass spectrometry to identify actual phosphorylation sites in the RCAN1 proteins.

6.3 The physiological role of RCAN1

The data presented in this thesis suggests that RCAN1 plays a profound role in endothelial cell function. The role of RCAN1 *in vivo* has been studied in RCAN$^{-/-}$ mice where gene ablation of RCAN1.1 and RCAN1.4 resulted in mice with no anatomical differences (Hoeffer et al., 2007). The fact that a more profound phenotype was not observed in the knockout mice may be due to a potentially different role of RCAN1 in mice and the fact that RCAN1 represents a gene family with RCAN1, RCAN2 and RCAN 3 (Serrano-Candelas et al., 2014) offering the potential for redundancy. Whilst members of this gene family can inhibit calcineurin, so far only RCAN1.4 has been shown to be induced by VEGF. A more recent study with RCAN$^{-/-}$ mice focussing on tumour angiogenesis reported hyperactivation of the calcineurin/NFAT pathway resulting in endothelial cell apoptosis. This led to decreased tumour angiogenesis in a human tumour xenograft study (Ryeom et al., 2008). The data presented in this thesis would suggest decreased levels of RCAN1 will also lead an inhibition of endothelial cell migration, which would be interesting to examine in endothelial cells from the DSCR-1$^{-/-}$ mice. Analysis of RCAN1 ortholog knockdown in zebrafish (*Danio rerio*) using morpholino anti-sense methodology would be interesting in determining the role of RCAN1.1 and RCAN1.4 in vascular function using Fli-GFP transgenic zebrafish embryos.

People with Down Syndrome possess an extra copy of chromosome 21 leading to elevated levels of a number of genes including DYRK1A and RCAN1. These patients exhibit abnormal brain function and often cardiovascular defects (Wiseman et al., 2009). Over-expression of RCAN1 in mice causes Down syndrome-like hippocampal deficits that alter learning and memory (Martin et al., 2012). The data presented in this thesis would suggest that elevated levels of RCAN1 could potentially lead to increased endothelial migration and potentially aberrant angiogenesis in patients.

Therapeutically, inhibiting RCAN1 function could prevent endothelial cell migration and inhibit angiogenesis. However, other researchers have shown that silencing of RCAN1 in cancer cells leads to increased cell migration (Wiseman et al., 2009), suggesting that this strategy, if possible, may have a number of pleiotropic effects. The long-term therapeutic use of the immunosuppressive drug cyclosporin A has been associated with a number of adverse effects that include nephrotoxicity, renal vascular damage and hypertension (Morris et al., 2000). The data presented in this thesis would suggest that cyclosporin can prevent VEGF-induced RCAN1.4 expression and VEGF-mediated endothelial cell migration, which may contribute to some of the adverse effects seen in patients taking cyclosporin A.

In order to take the research on RCAN1 forward it will be interesting to determine the expression level of both RCAN1.1 and RCAN1.4 in endothelial cells from different vascular beds in humans under both normal and disease conditions known to affect vascular function/angiogenesis such as cancer and diabetes. Aberrant expression of RCAN1 may affect vascular homeostasis and offer a potential biomarker of vascular disease and aberrant angiogenesis.

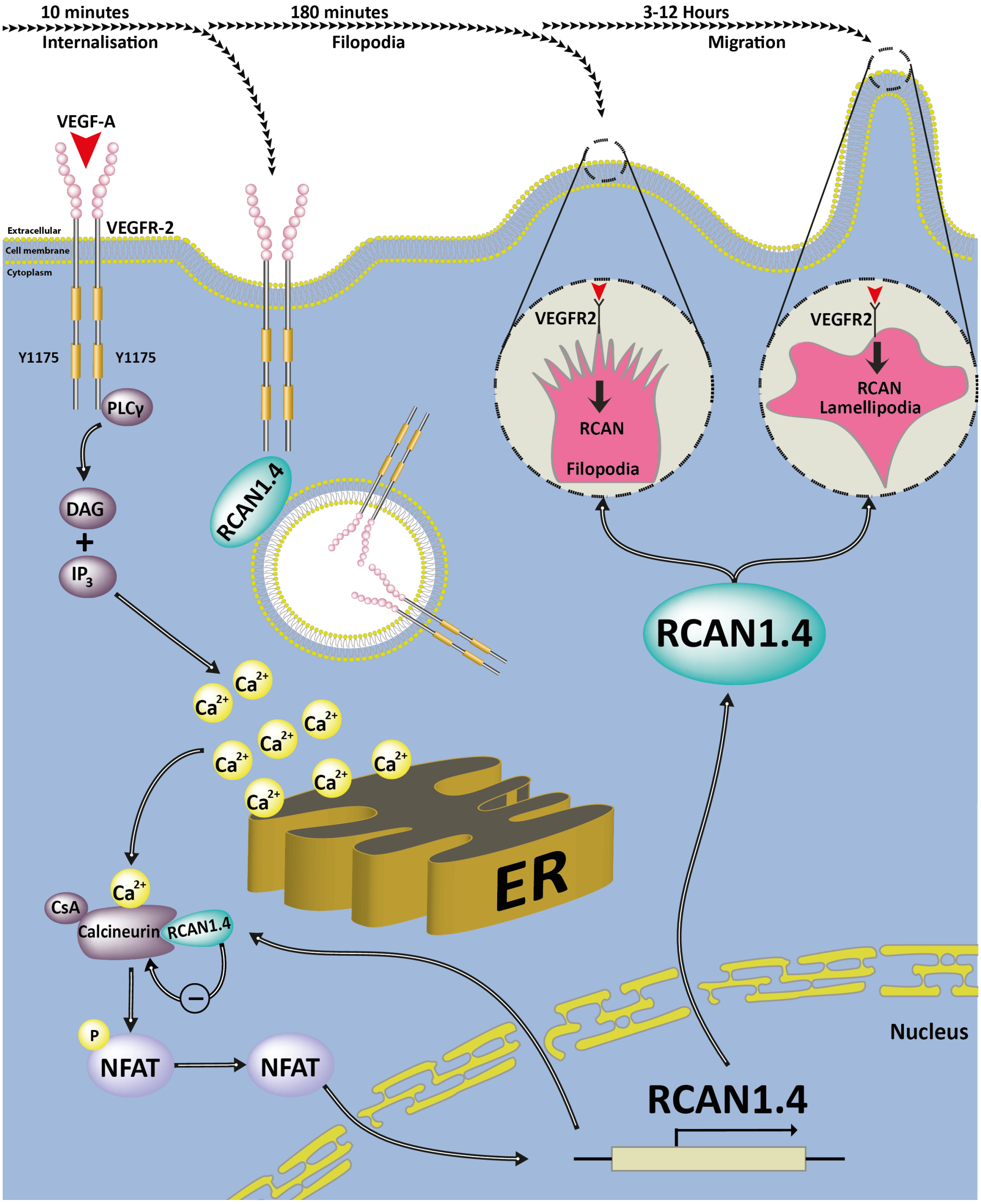

Figure 6.1: RCAN1 regulates VEGFR-2 function via a novel mechanism in endothelial cells

VEGFR-2 activation leads to PLC-γ activation and increase in intracellular Ca^{2+} that causes activation of calcineurin and dephosphorylation of NFAT. This allows the nuclear translocation of NFAT and the transcriptional regulation of RCAN1.4 via NFAT binding sites in the promoter region. Basal levels of RCAN1.1 and RCAN1.4 can regulate VEGFR-2 internalisation via a transient association with the VEGFR-2 at the leading edge of migrating cells. Following transcription and translational increases in the level of RCAN1.4 protein, this newly synthesised protein acts as both an endogenous inhibitor of calcineurin and as a regulator of cytoskeletal reorganisation in response to VEGF. Hence RCAN1 acts to regulate spatiotemporal VEGFR-2 activation and downstream effects leading to cell migration.

6.4 PLD1&2 are involved in regulating endothelial cell physiology

The role of PLD in cell physiology is only recently being addressed as tools such as antibodies, small molecule inhibitors and siRNA duplexes become available to researchers. Mice lacking Pld1 have a defect in thrombus formation (Elvers et al., 2010) whilst mice lacking Pld2 appear normal (Norton et al., 2011). The role of PLD1 and PLD2 in endothelial cell function has not been addressed. The data presented in this thesis shows that endothelial cells express relatively high levels of PLD1 and PLD2 mRNA. siRNA mediated silencing of each PLD isoform showed that both PLD1 and PLD2 were required for VEGF mediated endothelial cell proliferation, migration and tubular morphogenesis suggesting that these enzymes play a critical function in VEGF-mediated signalling. Recent experiments have defined a role for Pld1 in inter-segmental blood vessel development in zebrafish (Zeng et al., 2009), suggesting that this isoform is critical for vascular development. The lack of effect of PLD silencing on HGF-stimulated migration and proliferation would suggest a degree of specificity in regulating the VEGF response. It is possible that PLD is activated downstream of PLC, as is the case for FGF-stimulated PLD activity in porcine aortic endothelial cells (Cross et al., 2000), as VEGF but not HGF is known to activate PLC-gamma in HDMECs (Holmes et al., 2010). It was not possible to measure PLD activity directly to determine the amount of phosphatidic acid (PA) generation attributable to each isoform of PLD on VEGF stimulation in HDMECs. One possibility is to utilise lipidomics based on mass spectrometry to measure the actual molecular species of PA and DAG as this allows discrimination of PA derived directly from PLD mediated hydrolysis of PtdCho and that derived from phosphorylation of DAG derived from PLC mediated hydrolysis of PtdIns(4,5)P2 (Hodgkin et al., 1998, Wakelam et al., 2007). The precise mechanism through which PLD has a profound effect on VEGF-mediated endothelial cell physiology remains obscure. It is possible that PLD derived PA is required for MAP Kinase activation as one of the early functions assigned to PLD was regulation of Raf-1 (Rizzo et al., 1999). PLD is also known to play a critical role in cytoskeletal reorganisation (Cross et al., 1996). Recent data has shown a role for PLD2 in regulating endothelial cell permeability via cytoskeletal reorganisation (Zeiller et al., 2009), thus it is possible that PLD-regulated cytoskeletal reorganisation is a critical component for a number of physiological responses in endothelial cells.

Appendix 1

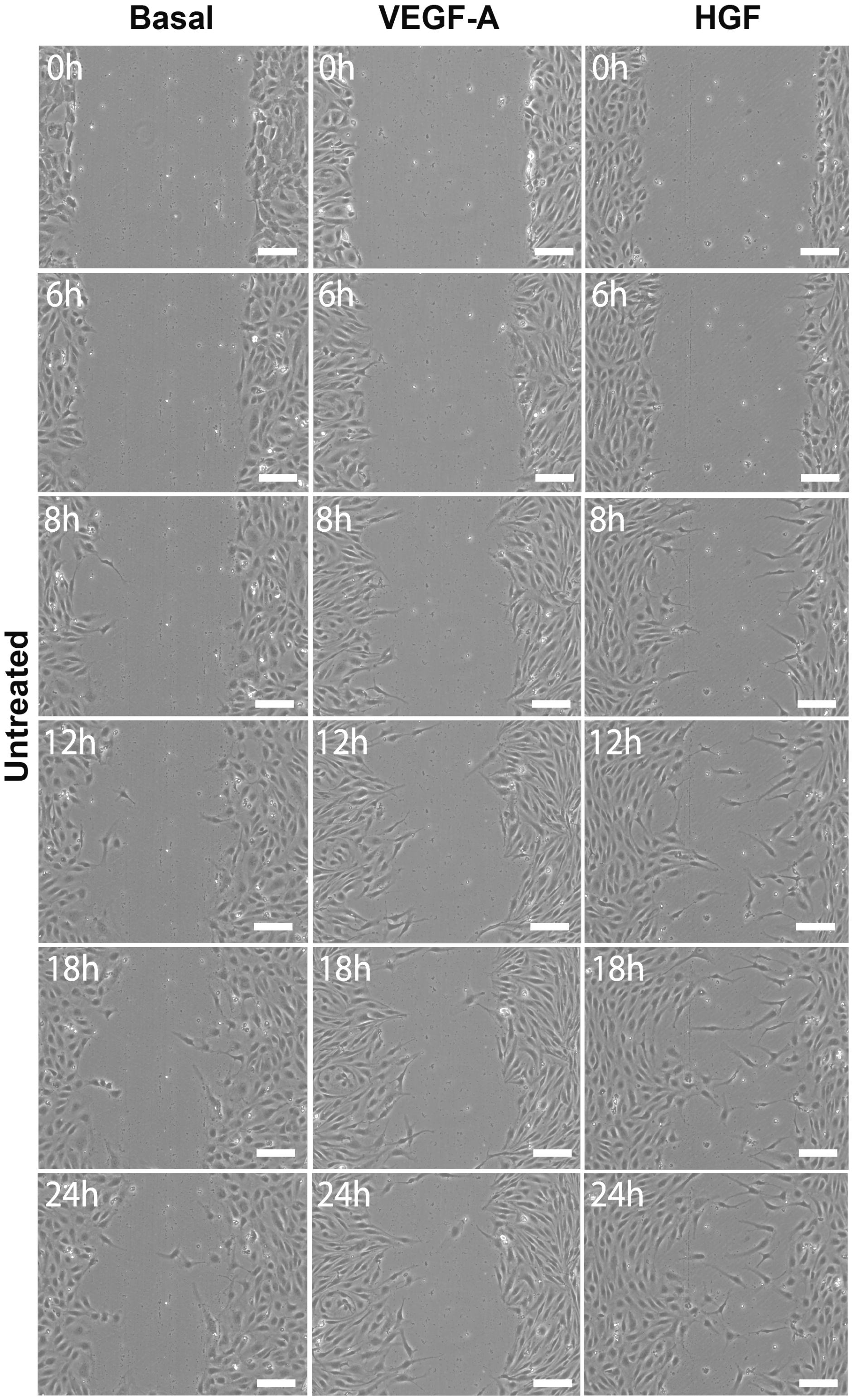

Extended time course for figure 4.4 (page 115). RCAN1. siRNA knockdown control experiment. For conditions refer to figure 4.4.

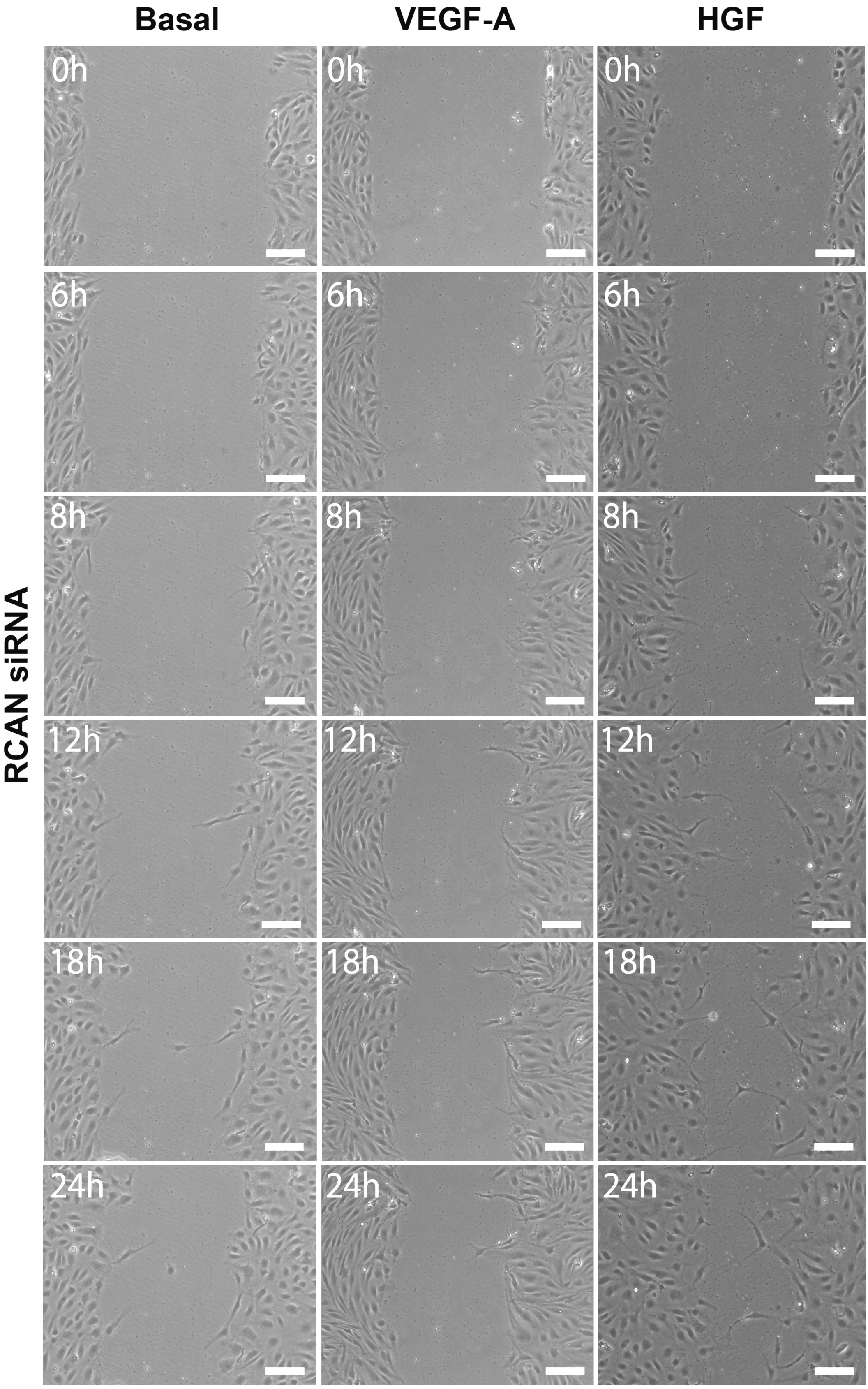

Extended time course for figure 4.4 (page 115). RCAN1 siRNA knockdown experiment. For conditions refer to figure 4.4.

Bibliography

Affolter, M., Zeller, R. & Caussinus, E. 2009. Tissue remodelling through branching morphogenesis. *Nature Reviews Molecular Cell Biology,* 10**,** 831-842.

Aird, W. C. 2007. Phenotypic heterogeneity of the endothelium II. Representative vascular beds. *Circulation research,* 100**,** 174-190.

Augustin, H. G., Koh, G. Y., Thurston, G. & Alitalo, K. 2009. Control of vascular morphogenesis and homeostasis through the angiopoietin–Tie system. *Nature reviews Molecular cell biology,* 10**,** 165-177.

Baird, P. A. & Sadovnick, A. D. 1987. Life expectancy in Down syndrome. *The Journal of pediatrics,* 110**,** 849-854.

Balboa, M. A. & Insel, P. A. 1995. Nuclear Phospholipase D in madin-darby canine kidney cells guanosine 5′ -O-(Thiotriphosphate)-stimulated activation is mediated by RhoA and is dwonstrem of protein kinase C. *Journal of Biological Chemistry,* 270**,** 29843-29847.

Ballmer-Hofer, K., Andersson, A. E., Ratcliffe, L. E. & Berger, P. 2011. Neuropilin-1 promotes VEGFR-2 trafficking through Rab11 vesicles thereby specifying signal output. *Blood,* 118**,** 816-826.

Bates, D. O., Cui, T.-G., Doughty, J. M., Winkler, M., Sugiono, M., Shields, J. D., Peat, D., Gillatt, D. & Harper, S. J. 2002. VEGF165b, an inhibitory splice variant of vascular endothelial growth factor, is down-regulated in renal cell carcinoma. *Cancer Research,* 62**,** 4123-4131.

Berse, B., Brown, L. F., Van De Water, L., Dvorak, H. F. & Senger, D. R. 1992. Vascular permeability factor (vascular endothelial growth factor) gene is expressed differentially in normal tissues, macrophages, and tumors. *Molecular Biology of the Cell,* 3**,** 211.

Bocckino, S. B., Wilson, P. B. & Exton, J. H. 1991. Phosphatidate-dependent protein phosphorylation. *Proceedings of the National Academy of Sciences,* 88**,** 6210-6213.

Boghozian, R., Azizi, G. & Mirshafiey, A. 2013. Molecular Pattern of Angiogenesis Phenomenon and Inflammatory Cytokines in Rheumatoid Arthritis. *angiogenesis,* 16**,** 17.

Bonnet, C. & Walsh, D. 2005. Osteoarthritis, angiogenesis and inflammation. *Rheumatology,* 44**,** 7-16.

Brait, V. H., Martin, K. R., Corlett, A., Broughton, B. R., Kim, H. A., Thundyil, J., Drummond, G. R., Arumugam, T. V., Pritchard, M. A. & Sobey, C. G. 2012. Over-expression of DSCR1 protects against post-ischemic neuronal injury. *PloS one,* 7**,** e47841.

Brown, F. D., Thompson, N., Saqib, K. M., Clark, J. M., Powner, D., Thompson, N. T., Solari, R. & Wakelam, M. J. 1998. Phospholipase D1 localises to secretory granules and lysosomes and is plasma-membrane translocated on cellular stimulation. *Current biology,* 8**,** 835-838.

Brown, H. A., Gutowski, S., Kahn, R. A. & Sternweis, P. C. 1995. Partial purification and characterization of Arf-sensitive phospholipase D from porcine brain. *Journal of Biological Chemistry,* 270**,** 14935-14943.

Brown, H. A., Gutowski, S., Moomaw, C. R., Slaughter, C. & Sternwels, P. C. 1993. ADP-ribosylation factor, a small GTP-dependent regulatory protein, stimulates phospholipase D activity. *Cell,* 75**,** 1137-1144.

Brunet, A., Roux, D., Lenormand, P., Dowd, S., Keyse, S. & Pouysségur, J. 1999. Nuclear translocation of p42/p44 mitogen - activated protein kinase is required for growth factor - induced gene expression and cell cycle entry. *The EMBO journal,* 18**,** 664-674.

Buchanan, S. G., Hendle, J., Lee, P. S., Smith, C. R., Bounaud, P.-Y., Jessen, K. A., Tang, C. M., Huser, N. H., Felce, J. D. & Froning, K. J. 2009. SGX523 is an exquisitely selective, ATP-competitive inhibitor of the MET receptor tyrosine kinase with antitumor activity in vivo. *Molecular cancer therapeutics,* 8**,** 3181-3190.

Cantley, L. C. 2002. The phosphoinositide 3-kinase pathway. *Science,* 296**,** 1655-1657.

Cardone, M. H., Roy, N., Stennicke, H. R., Salvesen, G. S., Franke, T. F., Stanbridge, E., Frisch, S. & Reed, J. C. 1998. Regulation of cell death protease caspase-9 by phosphorylation. *Science,* 282**,** 1318-1321.

Carmeliet, P., Ferreira, V., Breier, G., Pollefeyt, S., Kieckens, L., Gertsenstein, M., Fahrig, M., Vandenhoeck, A., Harpal, K. & Eberhardt, C. 1996. Abnormal blood vessel development and lethality in embryos lacking a single VEGF allele. *Nature,* 380**,** 435-439.

Castagna, M., Takai, Y., Kaibuchi, K., Sano, K., Kikkawa, U. & Nishizuka, Y. 1982. Direct activation of calcium-activated, phospholipid-dependent protein kinase by tumor-promoting phorbol esters. *Journal of Biological Chemistry,* 257**,** 7847-7851.

Chaki, S. P., Barhoumi, R., Berginski, M. E., Sreenivasappa, H., Trache, A., Gomez, S. M. & Rivera, G. M. 2013. Nck enables directional cell migration through the coordination of polarized membrane protrusion with adhesion dynamics. *Journal of cell science,* 126**,** 1637-1649.

Chan, B., Greenan, G., Mckeon, F. & Ellenberger, T. 2005. Identification of a peptide fragment of DSCR1 that competitively inhibits calcineurin activity in vitro and in vivo. *Proceedings of the National Academy of Sciences of the United States of America,* 102**,** 13075-13080.

Cho, C.-H., Lee, C. S., Chang, M., Jang, I.-H., Kim, S. J., Hwang, I., Ryu, S. H., Lee, C. O. & Koh, G. Y. 2004. Localization of VEGFR-2 and PLD2 in endothelial caveolae is involved in VEGF-induced phosphorylation of MEK and ERK. *American Journal of Physiology-Heart and Circulatory Physiology,* 286**,** H1881-H1888.

Clauss, M. & Breier, G. 2005. *Mechanisms of angiogenesis*, Springer.

Colley, W., Altshuller, Y., Sue-Ling, C., Copeland, N., Gilbert, D., Jenkins, N., Branch, K., Tsirka, S., Bollag, R. & Bollag, W. 1997. Cloning and expression analysis of murine phospholipase D1. *Biochem. J,* 326**,** 745-753.

Crawford, D. R., Leahy, K. P., Abramova, N., Lan, L., Wang, Y. & Davies, K. J. 1997. Hamster< i> adapt78</i> mRNA Is a Down Syndrome Critical Region Homologue That Is Inducible by Oxidative Stress. *Archives of biochemistry and biophysics,* 342**,** 6-12.

Cross, M. J., Hodgkin, M. N., Roberts, S., Landgren, E., Wakelam, M. & Claesson-Welsh, L. 2000. Tyrosine 766 in the fibroblast growth factor receptor-1 is required for FGF-stimulation of phospholipase C, phospholipase D, phospholipase A (2), phosphoinositide 3-kinase and cytoskeletal reorganisation in porcine aortic endothelial cells. *Journal of cell science,* 113**,** 643-651.

Cross, M. J., Roberts, S., Ridley, A. J., Hodgkin, M. N., Stewart, A., Welsh, L. C. & Wakelam, M. J. 1996. Stimulation of actin stress fibre formation mediated by activation of phospholipase D. *Current Biology,* 6**,** 588-597.

Cunningham, S. A., Arrate, M. P., Brock, T. A. & Waxham, M. N. 1997. Interactions of FLT-1 and KDR with phospholipase C γ: identification of the phosphotyrosine binding sites. *Biochemical and biophysical research communications,* 240**,** 635-639.

Dall'armi, C., Hurtado-Lorenzo, A., Tian, H., Morel, E., Nezu, A., Chan, R. B., Yu, W. H., Robinson, K. S., Yeku, O. & Small, S. A. 2010. The phospholipase D1 pathway modulates macroautophagy. *Nature communications,* 1**,** 142.

Dance, M., Montagner, A., Yart, A., Masri, B., Audigier, Y., Perret, B., Salles, J.-P. & Raynal, P. 2006. The adaptor protein Gab1 couples the stimulation of vascular endothelial growth factor receptor-2 to the activation of phosphoinositide 3-kinase. *Journal of Biological Chemistry,* 281**,** 23285-23295.

Davies, K. J., Ermak, G., Rothermel, B. A., Pritchard, M., Heitman, J., Ahnn, J., Henrique-Silva, F., Crawford, D., Canaider, S. & Strippoli, P. 2007. Renaming the DSCR1/Adapt78 gene family as RCAN: regulators of calcineurin. *The FASEB Journal,* 21**,** 3023-3028.

De Smet, F., Segura, I., De Bock, K., Hohensinner, P. J. & Carmeliet, P. 2009. Mechanisms of vessel branching filopodia on endothelial tip cells lead the way. *Arteriosclerosis, thrombosis, and vascular biology,* 29**,** 639-649.

De Souza, L. B., Da Silva, L. L. P., Jamur, M. C. & Oliver, C. 2014. Phospholipase D Is Involved in the Formation of Golgi Associated Clathrin Coated Vesicles in Human Parotid Duct Cells. *PloS one,* 9**,** e91868.

Disse, J., Vitale, N., Bader, M.-F. & Gerke, V. 2009. Phospholipase D1 is specifically required for regulated secretion of von Willebrand factor from endothelial cells. *Blood,* 113**,** 973-980.

Divecha, N., Roefs, M., Halstead, J. R., D'andrea, S., Fernandez‐Borga, M., Oomen, L., Saqib, K. M., Wakelam, M. J. & D'santos, C. 2000. Interaction of the Type Iα PIPkinase with phospholipase D: a role for the local generation of phosphatidylinositol 4, 5‐bisphosphate in the regulation of PLD2 activity. *The EMBO journal,* 19**,** 5440-5449.

Doughervermazen, M., Hulmes, J. D., Bohlen, P. & Terman, B. I. 1994. Biological activity and phosphorylation sites of the bacterially expressed cytosolic domain of the KDR VEGF-receptor. *Biochemical and biophysical research communications,* 205**,** 728-738.

Douglas, N. C., Nakhuda, G. S., Sauer, M. V. & Zimmermann, R. C. 2005. Angiogenesis and ovarian function. *Journal für Fertilität und Reproduktion,* 14**,** 7-15.

Du, G., Altshuller, Y. M., Vitale, N., Huang, P., Chasserot-Golaz, S., Morris, A. J., Bader, M.-F. & Frohman, M. A. 2003. Regulation of phospholipase D1 subcellular cycling through coordination of multiple membrane association motifs. *The Journal of cell biology,* 162**,** 305-315.

Du, G., Huang, P., Liang, B. T. & Frohman, M. A. 2004. Phospholipase D2 localizes to the plasma membrane and regulates angiotensin II receptor endocytosis. *Molecular biology of the cell,* 15**,** 1024-1030.

Dubyak, G. R., Schomisch, S. J., Kusner, D. J. & Xie, M. 1993. Phospholipase D activity in phagocytic leucocytes is synergistically regulated by G-protein- and tyrosine kinase-based mechanisms. *Biochem. J,* 292**,** 121-128.

Dulak, J. 2005. Nutraceuticals as anti-angiogenic agents: hopes and reality. *Journal of Physiology and Pharmacology. Supplement,* 56**,** 51-69.

Elvers, M., Stegner, D., Hagedorn, I., Kleinschnitz, C., Braun, A., Kuijpers, M. E., Boesl, M., Chen, Q., Heemskerk, J. W. & Stoll, G. 2010. Impaired {alpha} IIb {beta} 3 integrin activation and shear-dependent thrombus formation in mice lacking phospholipase D1. *Science Signaling,* 3**,** ra1.

Eriksson, K., Magnusson, P., Dixelius, J., Claesson-Welsh, L. & Cross, M. J. 2003. Angiostatin and endostatin inhibit endothelial cell migration in response to FGF and VEGF without interfering with specific intracellular signal transduction pathways. *FEBS letters,* 536**,** 19-24.

Ermak, G., Morgan, T. E. & Davies, K. J. 2001. Chronic overexpression of the calcineurin inhibitory gene DSCR1 (Adapt78) is associated with Alzheimer's disease. *Journal of Biological Chemistry,* 276**,** 38787-38794.

Etienne-Manneville, S. 2004. Cdc42-the centre of polarity. *Journal of cell science,* 117**,** 1291-1300.

Exton, J. H. 1997. New developments in phospholipase D. *Journal of Biological Chemistry,* 272**,** 15579-15582.

Exton, J. H. 2002. Phospholipase D—structure, regulation and function. *Reviews of physiology, biochemistry and pharmacology.* Springer.

Fang, Y., Park, I.-H., Wu, A.-L., Du, G., Huang, P., Frohman, M. A., Walker, S. J., Brown, H. A. & Chen, J. 2003. PLD1 regulates mTOR signaling and mediates Cdc42 activation of S6K1. *Current biology,* 13**,** 2037-2044.

Felmeden, D., Blann, A. & Lip, G. 2003. Angiogenesis: basic pathophysiology and implications for disease. *European heart journal,* 24**,** 586-603.

Ferrara, N., Carver Moore, K., Chen, H., Dowd, M., Lu, L., O'shea, K. S., Powell Braxton, L., Hillan, K. J. & Moore, M. W. 1996. Heterozygous embryonic lethality induced by targeted inactivation of the VEGF gene.

Fiedler, U. & Augustin, H. G. 2006. Angiopoietins: a link between angiogenesis and inflammation. *Trends in immunology,* 27**,** 552-558.

Fiedler, U., Reiss, Y., Scharpfenecker, M., Grunow, V., Koidl, S., Thurston, G., Gale, N. W., Witzenrath, M., Rosseau, S. & Suttorp, N. 2006. Angiopoietin-2 sensitizes endothelial cells to TNF-α and has a crucial role in the induction of inflammation. *Nature medicine,* 12**,** 235-239.

Florey, L. 1966. The endothelial cell. *Br Med J,* 2**,** 487-90.

Flower, R. J. & Blackwell, G. J. 1979. Anti-inflammatory steroids induce biosynthesis of a phospholipase A2 inhibitor which prevents prostaglandin generation. *Nature,* 278**,** 456-459.

Förstermann, U., Closs, E. I., Pollock, J. S., Nakane, M., Schwarz, P., Gath, I. & Kleinert, H. 1994. Nitric oxide synthase isozymes. Characterization, purification, molecular cloning, and functions. *Hypertension,* 23**,** 1121-1131.

Förstermann, U. & Münzel, T. 2006. Endothelial nitric oxide synthase in vascular disease from marvel to menace. *Circulation,* 113**,** 1708-1714.

Foster, D. A. & Xu, L. 2003. Phospholipase D in Cell Proliferation and Cancer11National Cancer Institute, and the institutional support from the Research Centers in Minority Institutions (RCMI) program of the NIH. *Molecular Cancer Research,* 1**,** 789-800.

Fraisl, P., Mazzone, M., Schmidt, T. & Carmeliet, P. 2009. Regulation of angiogenesis by oxygen and metabolism. *Developmental cell,* 16**,** 167-179.

Frohman, M. A. & Morris, A. J. 1999. Phospholipase D structure and regulation. *Chemistry and physics of lipids,* 98**,** 127-140.

Fruman, D. A., Klee, C. B., Bierer, B. E. & Burakoff, S. J. 1992. Calcineurin phosphatase activity in T lymphocytes is inhibited by FK 506 and cyclosporin A. *Proceedings of the National Academy of Sciences,* 89**,** 3686-3690.

Fuentes, J., Pritchard, M. & Estivill, X. 1997. Genomic Organization, Alternative Splicing, and Expression Patterns of the< i> DSCR1</i>(Down Syndrome Candidate Region 1) Gene. *Genomics,* 44**,** 358-361.

Fuentes, J.-J., Pritchard, M. A., Planas, A. M., Bosch, A., Ferrer, I. & Estivill, X. 1995. A new human gene from the Down syndrome critical region encodes a proline-rich protein highly expressed in fetal brain and heart. *Human molecular genetics,* 4**,** 1935-1944.

Fuentes, J. J., Genescà, L., Kingsbury, T. J., Cunningham, K. W., Pérez-Riba, M., Estivill, X. & De La Luna, S. 2000. DSCR1, overexpressed in Down syndrome, is an inhibitor of calcineurin-mediated signaling pathways. *Human Molecular Genetics,* 9, 1681-1690.

Genescà, L., Aubareda, A., Fuentes, J., Estivill, X., Delaluna, S. & Pérez-Riba, M. 2003. Phosphorylation of calcipressin 1 increases its ability to inhibit calcineurin and decreases calcipressin half-life. *Biochem. J,* 374, 567-575.

Gerber, H.-P., Dixit, V. & Ferrara, N. 1998a. Vascular endothelial growth factor induces expression of the antiapoptotic proteins Bcl-2 and A1 in vascular endothelial cells. *Journal of Biological Chemistry,* 273, 13313-13316.

Gerber, H.-P., Mcmurtrey, A., Kowalski, J., Yan, M., Keyt, B. A., Dixit, V. & Ferrara, N. 1998b. Vascular endothelial growth factor regulates endothelial cell survival through the phosphatidylinositol 3′ -Kinase/Akt signal transduction pathwasy requirment for Flk-1/KDR activation. *Journal of Biological Chemistry,* 273, 30336-30343.

Gerhardt, H., Golding, M., Fruttiger, M., Ruhrberg, C., Lundkvist, A., Abramsson, A., Jeltsch, M., Mitchell, C., Alitalo, K. & Shima, D. 2003. VEGF guides angiogenic sprouting utilizing endothelial tip cell filopodia. *The Journal of cell biology,* 161, 1163-1177.

Girard, J.-P. & Springer, T. A. 1995. High endothelial venules (HEVs): specialized endothelium for lymphocyte migration. *Immunology today,* 16, 449-457.

Goh, L. K. & Sorkin, A. 2013. Endocytosis of receptor tyrosine kinases. *Cold Spring Harbor perspectives in biology,* 5, a017459.

Good, D. J., Polverini, P. J., Rastinejad, F., Le Beau, M. M., Lemons, R. S., Frazier, W. A. & Bouck, N. P. 1990. A tumor suppressor-dependent inhibitor of angiogenesis is immunologically and functionally indistinguishable from a fragment of thrombospondin. *Proceedings of the National Academy of Sciences,* 87, 6624-6628.

Gorshkova, I., He, D., Berdyshev, E., Usatuyk, P., Burns, M., Kalari, S., Zhao, Y., Pendyala, S., Garcia, J. G. & Pyne, N. J. 2008. Protein kinase C-ϵ regulates sphingosine 1-phosphate-mediated migration of human lung endothelial cells through activation of phospholipase D2, protein kinase C-ζ, and Rac1. *Journal of Biological Chemistry,* 283**,** 11794-11806.

Hagberg, C. E., Falkevall, A., Wang, X., Larsson, E., Huusko, J., Nilsson, I., Van Meeteren, L. A., Samen, E., Lu, L. & Vanwildemeersch, M. 2010. Vascular endothelial growth factor B controls endothelial fatty acid uptake. *Nature,* 464**,** 917-921.

Hagele, T. J., Mazerik, J. N., Gregory, A., Kaufman, B., Magalang, U., Kuppusamy, M. L., Marsh, C. B., Kuppusamy, P. & Parinandi, N. L. 2007. Mercury activates vascular endothelial cell phospholipase D through thiols and oxidative stress. *International journal of toxicology,* 26**,** 57-69.

Hall, A. 1998. Rho GTPases and the actin cytoskeleton. *Science,* 279**,** 509-514.

Hammond, S. M., Jenco, J. M., Nakashima, S., Cadwallader, K., Gu, Q.-M., Cook, S., Nozawa, Y., Prestwich, G. D., Frohman, M. A. & Morris, A. J. 1997. Characterization of two alternately spliced forms of Phospholipase D1 activation of the purified enzymes by phosphatidylinositol 4, 5-bisphosphate, ADP-ribosylation factor, and Rho family monomeric GTP-binding proteins and protein kinase C-α. *Journal of Biological Chemistry,* 272**,** 3860-3868.

Han, L., Stope, M. B., De Jesús, M. L., Oude Weernink, P. A., Urban, M., Wieland, T., Rosskopf, D., Mizuno, K., Jakobs, K. H. & Schmidt, M. 2007. Direct stimulation of receptor‐controlled phospholipase D1 by phospho‐cofilin. *The EMBO journal,* 26**,** 4189-4202.

Hanahan, D. J. & Chaikoff, I. 1947. The phosphorus-containing lipides of the carrot. *Journal of Biological Chemistry,* 168**,** 233-240.

Hanahan, D. J. & Chaikoff, I. 1948. On the nature of the phosphorus-containing lipides of cabbage leaves and their relation to a phospholipide-splitting enzyme contained in these leaves. *Journal of Biological Chemistry,* 172**,** 191-198.

Harper, S. J. & Bates, D. O. 2008. VEGF-A splicing: the key to anti-angiogenic therapeutics? *Nature Reviews Cancer,* 8**,** 880-887.

Hayden, M. S. & Ghosh, S. 2004. Signaling to NF-kappaB. *Genes Dev,* 18**,** 2195-224.

Henkels, K., Boivin, G., Dudley, E., Berberich, S. & Gomez-Cambronero, J. 2013. Phospholipase D (PLD) drives cell invasion, tumor growth and metastasis in a human breast cancer xenograph model. *Oncogene,* 32**,** 5551-5562.

Hesser, B. A., Liang, X. H., Camenisch, G., Yang, S., Lewin, D. A., Scheller, R., Ferrara, N. & Gerber, H.-P. 2004. Down syndrome critical region protein 1 (DSCR1), a novel VEGF target gene that regulates expression of inflammatory markers on activated endothelial cells. *Blood,* 104**,** 149-158.

Hodgkin, M. N., Masson, M. R., Powner, D., Saqib, K. M., Ponting, C. P. & Wakelam, M. J. 2000. Phospholipase D regulation and localisation is dependent upon a phosphatidylinositol 4, 5-bisphosphate-specific PH domain. *Current Biology,* 10**,** 43-46.

Hodgkin, M. N., Pettitt, T. R., Martin, A., Michell, R. H., Pemberton, A. J. & Wakelam, M. J. 1998. Diacylglycerols and phosphatidates: which molecular species are intracellular messengers? *Trends in biochemical sciences,* 23**,** 200-204.

Hoeben, A., Landuyt, B., Highley, M. S., Wildiers, H., Van Oosterom, A. T. & De Bruijn, E. A. 2004. Vascular endothelial growth factor and angiogenesis. *Pharmacological reviews,* 56**,** 549-580.

Hoeffer, C. A., Dey, A., Sachan, N., Wong, H., Patterson, R. J., Shelton, J. M., Richardson, J. A., Klann, E. & Rothermel, B. A. 2007. The Down syndrome critical region protein RCAN1 regulates long-term potentiation and memory via inhibition of phosphatase signaling. *The Journal of Neuroscience,* 27**,** 13161-13172.

Holmes, K., Chapman, E., See, V. & Cross, M. J. 2010. VEGF Stimulates RCAN1. 4 Expression in Endothelial Cells via a Pathway Requiring Ca2+/Calcineurin and Protein Kinase C-δ. *PloS one,* 5**,** e11435.

Holmes, K., Roberts, O. L., Thomas, A. M. & Cross, M. J. 2007. Vascular endothelial growth factor receptor-2: structure, function, intracellular signalling and therapeutic inhibition. *Cellular signalling,* 19**,** 2003-2012.

Holmqvist, K., Cross, M. J., Rolny, C., Hägerkvist, R., Rahimi, N., Matsumoto, T., Claesson-Welsh, L. & Welsh, M. 2004. The adaptor protein shb binds to tyrosine 1175 in vascular endothelial growth factor (VEGF) receptor-2 and regulates VEGF-dependent cellular migration. *Journal of Biological Chemistry,* 279**,** 22267-22275.

Horowitz, A. & Seerapu, H. R. 2012. Regulation of VEGF signaling by membrane traffic. *Cellular signalling,* 24**,** 1810-1820.

Hsu, Y.-L., Hung, J.-Y., Ko, Y.-C., Hung, C.-H., Huang, M.-S. & Kuo, P.-L. 2010. Phospholipase D signaling pathway is involved in lung cancer-derived IL-8 increased osteoclastogenesis. *Carcinogenesis,* 31**,** 587-596.

Iglesias, P. A. & Devreotes, P. N. 2008. Navigating through models of chemotaxis. *Current opinion in cell biology,* 20**,** 35-40.

Iizuka, M., Abe, M., Shiiba, K., Sasaki, I. & Sato, Y. 2004. Down syndrome candidate region 1,a downstream target of VEGF, participates in endothelial cell migration and angiogenesis. *J Vasc Res,* 41**,** 334-44.

Jékely, G., Sung, H.-H., Luque, C. M. & Rørth, P. 2005. Regulators of endocytosis maintain localized receptor tyrosine kinase signaling in guided migration. *Developmental cell,* 9**,** 197-207.

Jones, D., Morgan, C. & Cockcroft, S. 1999. Phospholipase D and membrane traffic: potential roles in regulated exocytosis, membrane delivery and vesicle budding. *Biochimica et Biophysica Acta (BBA)-Molecular and Cell Biology of Lipids,* 1439**,** 229-244.

Joukov, V., Pajusola, K., Kaipainen, A., Chilov, D., Lahtinen, I., Kukk, E., Saksela, O., Kalkkinen, N. & Alitalo, K. 1996. A novel vascular endothelial growth factor, VEGF-C, is a ligand for the Flt4 (VEGFR-3) and KDR (VEGFR-2) receptor tyrosine kinases. *The EMBO journal,* 15**,** 290.

Kam, Y. & Exton, J. H. 2001. Phospholipase D activity is required for actin stress fiber formation in fibroblasts. *Molecular and cellular biology,* 21**,** 4055-4066.

Kang, D. W., Park, M.-K., Oh, H.-J., Lee, D.-G., Park, S.-H., Choi, K.-Y. & Cho, M.-L. 2013. Phospholipase D1 Has a Pivotal Role in Interleukin-1β-Driven Chronic Autoimmune Arthritis through Regulation of NF-κB, Hypoxia-Inducible Factor 1α, and FoxO3a. *Molecular and cellular biology,* 33**,** 2760-2772.

Kaur, S., Leszczynska, K., Abraham, S., Scarcia, M., Hiltbrunner, S., Marshall, C. J., Mavria, G., Bicknell, R. & Heath, V. L. 2011. RhoJ/TCL regulates endothelial motility and tube formation and modulates actomyosin contractility and focal adhesion numbers. *Arteriosclerosis, thrombosis, and vascular biology,* 31**,** 657-664.

Kawamura, H., Li, X., Harper, S. J., Bates, D. O. & Claesson-Welsh, L. 2008. Vascular endothelial growth factor (VEGF)-A165b is a weak in vitro agonist for VEGF receptor-2 due to lack of coreceptor binding and deficient regulation of kinase activity. *Cancer Research,* 68**,** 4683-4692.

Kelly, J., Moore, T., Babal, P., Diwan, A., Stevens, T. & Thompson, W. 1998. Pulmonary microvascular and macrovascular endothelial cells: differential regulation of Ca2+ and permeability. *American Journal of Physiology-Lung Cellular and Molecular Physiology,* 274**,** L810-L819.

Kheradmand, F., Werner, E., Tremble, P., Symons, M. & Werb, Z. 1998. Role of Rac1 and oxygen radicals in collagenase-1 expression induced by cell shape change. *Science,* 280**,** 898-902.

Kim, E.-G. & Exton, J. H. 1998. Involvement of tyrosine phosphorylation and protein kinase C in the activation of phospholipase D by H2O2 in Swiss 3T3 fibroblasts. *Journal of Biological Chemistry,* 273**,** 29986-29994.

Kinoshita, E., Kinoshita-Kikuta, E., Takiyama, K. & Koike, T. 2006. Phosphate-binding tag, a new tool to visualize phosphorylated proteins. *Molecular & Cellular Proteomics,* 5**,** 749-757.

Komarova, Y. & Malik, A. B. 2010. Regulation of endothelial permeability via paracellular and transcellular transport pathways. *Annual review of physiology,* 72**,** 463-493.

Kozma, R., Ahmed, S., Best, A. & Lim, L. 1995. The Ras-related protein Cdc42Hs and bradykinin promote formation of peripheral actin microspikes and filopodia in Swiss 3T3 fibroblasts. *Molecular and cellular biology,* 15**,** 1942-1952.

Ktistakis, N. T., Brown, H. A., Sternweis, P. C. & Roth, M. G. 1995. Phospholipase D is present on Golgi-enriched membranes and its activation by ADP ribosylation factor is sensitive to brefeldin A. *Proceedings of the National Academy of Sciences,* 92**,** 4952-4956.

Lamalice, L., Houle, F., Jourdan, G. & Huot, J. 2004. Phosphorylation of tyrosine 1214 on VEGFR2 is required for VEGF-induced activation of Cdc42 upstream of SAPK2/p38. *Oncogene,* 23**,** 434-445.

Lamalice, L., Le Boeuf, F. & Huot, J. 2007. Endothelial cell migration during angiogenesis. *Circulation research,* 100**,** 782-794.

Lampugnani, M. G., Orsenigo, F., Gagliani, M. C., Tacchetti, C. & Dejana, E. 2006. Vascular endothelial cadherin controls VEGFR-2 internalization and signaling from intracellular compartments. *The Journal of cell biology,* 174**,** 593-604.

Lampugnani, M. G., Zanetti, A., Corada, M., Takahashi, T., Balconi, G., Breviario, F., Orsenigo, F., Cattelino, A., Kemler, R. & Daniel, T. O. 2003. Contact inhibition of VEGF-induced proliferation requires vascular endothelial cadherin, β-catenin, and the phosphatase DEP-1/CD148. *The Journal of cell biology,* 161**,** 793-804.

Lanahan, A. A., Hermans, K., Claes, F., Kerley-Hamilton, J. S., Zhuang, Z. W., Giordano, F. J., Carmeliet, P. & Simons, M. 2010. VEGF receptor 2 endocytic trafficking regulates arterial morphogenesis. *Developmental cell,* 18**,** 713-724.

Lauber, K., Bohn, E., Kröber, S. M., Xiao, Y.-J., Blumenthal, S. G., Lindemann, R. K., Marini, P., Wiedig, C., Zobywalski, A. & Baksh, S. 2003. Apoptotic cells induce migration of phagocytes via caspase-3-mediated release of a lipid attraction signal. *Cell,* 113**,** 717-730.

Lauffenburger, D. A. & Horwitz, A. F. 1996. Cell migration: a physically integrated molecular process. *Cell,* 84**,** 359-369.

Laughner, E., Taghavi, P., Chiles, K., Mahon, P. C. & Semenza, G. L. 2001. HER2 (neu) signaling increases the rate of hypoxia-inducible factor 1α (HIF-1α) synthesis: novel mechanism for HIF-1-mediated vascular endothelial growth factor expression. *Molecular and cellular biology,* 21**,** 3995-4004.

Lawler, P. R. & Lawler, J. 2012. Molecular basis for the regulation of angiogenesis by thrombospondin-1 and-2. *Cold Spring Harbor perspectives in medicine,* 2**,** a006627.

Lawlor, M. A. & Alessi, D. R. 2001. PKB/Akt a key mediator of cell proliferation, survival and insulin responses? *Journal of cell science,* 114**,** 2903-2910.

Lee, S., Jilani, S. M., Nikolova, G. V., Carpizo, D. & Iruela-Arispe, M. L. 2005. Processing of VEGF-A by matrix metalloproteinases regulates bioavailability and vascular patterning in tumors. *The Journal of cell biology,* 169**,** 681-691.

Leon, A. S., Franklin, B. A., Costa, F., Balady, G. J., Berra, K. A., Stewart, K. J., Thompson, P. D., Williams, M. A. & Lauer, M. S. 2005. Cardiac rehabilitation and secondary prevention of coronary heart disease an american heart association scientific statement from the council on clinical cardiology (subcommittee on exercise, cardiac rehabilitation, and prevention) and the council on nutrition, physical activity, and metabolism (subcommittee on physical activity), in collaboration with the american association of cardiovascular and pulmonary rehabilitation. *Circulation,* 111**,** 369-376.

Liang, C.-C., Park, A. Y. & Guan, J.-L. 2007. In vitro scratch assay: a convenient and inexpensive method for analysis of cell migration in vitro. *Nature protocols,* 2**,** 329-333.

Linford, A., Yoshimura, S.-I., Bastos, R. N., Langemeyer, L., Gerondopoulos, A., Rigden, D. J. & Barr, F. A. 2012. Rab14 and its exchange factor FAM116 link endocytic recycling and adherens junction stability in migrating cells. *Developmental cell,* 22**,** 952-966.

Lohela, M., Bry, M., Tammela, T. & Alitalo, K. 2009. VEGFs and receptors involved in angiogenesis versus lymphangiogenesis. *Current opinion in cell biology,* 21**,** 154-165.

Lok, C. N. & Ponka, P. 1999. Identification of a hypoxia response element in the transferrin receptor gene. *Journal of Biological Chemistry,* 274**,** 24147-24152.

Lucocq, J., Manifava, M., Bi, K., Roth, M. G. & Ktistakis, N. T. 2001. Immunolocalisation of phospholipase D1 on tubular vesicular membranes of endocytic and secretory origin. *European journal of cell biology,* 80**,** 508-520.

Maisonpierre, P. C., Suri, C., Jones, P. F., Bartunkova, S., Wiegand, S. J., Radziejewski, C., Compton, D., Mcclain, J., Aldrich, T. H. & Papadopoulos, N. 1997. Angiopoietin-2, a natural antagonist for Tie2 that disrupts in vivo angiogenesis. *Science,* 277**,** 55-60.

Mäkinen, T., Veikkola, T., Mustjoki, S., Karpanen, T., Catimel, B., Nice, E. C., Wise, L., Mercer, A., Kowalski, H. & Kerjaschki, D. 2001. Isolated lymphatic endothelial cells transduce growth, survival and migratory signals via the VEGF‐C/D receptor VEGFR‐3. *The EMBO journal,* 20**,** 4762-4773.

Manetti, M., Guiducci, S., Romano, E., Ceccarelli, C., Bellando-Randone, S., Conforti, M. L., Ibba-Manneschi, L. & Matucci-Cerinic, M. 2011. Overexpression of VEGF165b, an inhibitory splice variant of vascular endothelial growth factor, leads to insufficient angiogenesis in patients with systemic sclerosis. *Circulation Research,* 109**,** e14-e26.

Martin, K. R., Corlett, A., Dubach, D., Mustafa, T., Coleman, H. A., Parkington, H. C., Merson, T. D., Bourne, J. A., Porta, S. & Arbonés, M. L. 2012. Over-expression of RCAN1 causes Down syndrome-like hippocampal deficits that alter learning and memory. *Human molecular genetics***,** dds134.

Martin, T. W. & Michaelis, K. 1989. P2-purinergic agonists stimulate phosphodiesteratic cleavage of phosphatidylcholine in endothelial cells. Evidence for activation of phospholipase D. *Journal of Biological Chemistry,* 264**,** 8847-8856.

Martínez-Høyer, S., Aranguren-Ibáñez, Á., García-García, J., Serrano-Candelas, E., Vilardell, J., Nunes, V., Aguado, F., Oliva, B., Itarte, E. & Pérez-Riba, M. 2013. Protein kinase CK2-dependent phosphorylation of the human Regulators of Calcineurin reveals a novel mechanism regulating the calcineurin–NFATc signaling pathway. *Biochimica et Biophysica Acta (BBA)-Molecular Cell Research,* 1833**,** 2311-2321.

Masson, N., Willam, C., Maxwell, P. H., Pugh, C. W. & Ratcliffe, P. J. 2001. Independent function of two destruction domains in hypoxia‐inducible factor‐α chains activated by prolyl hydroxylation. *The EMBO journal,* 20**,** 5197-5206.

Matsumoto, T., Bohman, S., Dixelius, J., Berge, T., Dimberg, A., Magnusson, P., Wang, L., Wikner, C., Qi, J. H. & Wernstedt, C. 2005. VEGF receptor-2 Y951 signaling and a role for the adapter molecule TSAd in tumor angiogenesis. *The EMBO journal,* 24**,** 2342-2353.

Mcdermott, M., Wakelam, M. J. & Morris, A. J. 2004. Phospholipase d. *Biochemistry and cell biology,* 82**,** 225-253.

Meadows, K. N., Bryant, P. & Pumiglia, K. 2001. Vascular endothelial growth factor induction of the angiogenic phenotype requires Ras activation. *Journal of Biological Chemistry,* 276**,** 49289-49298.

Meier, K. E., Gibbs, T. C., Knoepp, S. M. & Ella, K. M. 1999. Expression of phospholipase D isoforms in mammalian cells. *Biochimica et Biophysica Acta (BBA)-Molecular and Cell Biology of Lipids,* 1439**,** 199-213.

Mellberg, S., Dimberg, A., Bahram, F., Hayashi, M., Rennel, E., Ameur, A., Westholm, J. O., Larsson, E., Lindahl, P. & Cross, M. J. 2009. Transcriptional profiling reveals a critical role for tyrosine phosphatase VE-PTP in regulation of VEGFR2 activity and endothelial cell morphogenesis. *The FASEB journal,* 23**,** 1490-1502.

Meyer, M., Clauss, M., Lepple‐Wienhues, A., Waltenberger, J., Augustin, H. G., Ziche, M., Lanz, C., Büttner, M., Rziha, H. J. & Dehio, C. 1999. A novel vascular endothelial growth factor encoded by Orf virus, VEGF‐E, mediates angiogenesis via signalling through VEGFR‐2 (KDR) but not VEGFR‐1 (Flt‐1) receptor tyrosine kinases. *The EMBO journal,* 18**,** 363-374.

Minami, T., Horiuchi, K., Miura, M., Abid, M. R., Takabe, W., Noguchi, N., Kohro, T., Ge, X., Aburatani, H. & Hamakubo, T. 2004. Vascular endothelial growth factor-and thrombin-induced termination factor, Down syndrome critical region-1, attenuates endothelial cell proliferation and angiogenesis. *Journal of Biological Chemistry,* 279**,** 50537-50554.

Minchenko, A., Salceda, S., Bauer, T. & Caro, J. 1993. Hypoxia regulatory elements of the human vascular endothelial growth factor gene. *Cellular & molecular biology research,* 40**,** 35-39.

Miyasaka, M. & Tanaka, T. 2004. Lymphocyte trafficking across high endothelial venules: dogmas and enigmas. *Nature Reviews Immunology,* 4**,** 360-370.

Monovich, L., Mugrage, B., Quadros, E., Toscano, K., Tommasi, R., Lavoie, S., Liu, E., Du, Z., Lasala, D. & Boyar, W. 2007. Optimization of halopemide for phospholipase D2 inhibition. *Bioorganic & medicinal chemistry letters,* 17**,** 2310-2311.

Morris, S. T., Mcmurray, J. J., Rodger, R. S. C., Farmer, R. & Jardine, A. G. 2000. Endothelial dysfunction in renal transplant recipients maintained on cyclosporine. *Kidney international,* 57**,** 1100-1106.

Murphy, G. & Gavrilovic, J. 1999. Proteolysis and cell migration: creating a path? *Current opinion in cell biology,* 11**,** 614-621.

Murphy, J. E., Padilla, B. E., Hasdemir, B., Cottrell, G. S. & Bunnett, N. W. 2009. Endosomes: a legitimate platform for the signaling train. *Proceedings of the National Academy of Sciences,* 106**,** 17615-17622.

Nishida, T., Shimokawa, H., Oi, K., Tatewaki, H., Uwatoku, T., Abe, K., Matsumoto, Y., Kajihara, N., Eto, M. & Matsuda, T. 2004. Extracorporeal cardiac shock wave therapy markedly ameliorates ischemia-induced myocardial dysfunction in pigs in vivo. *Circulation,* 110**,** 3055-3061.

Nobes, C. D. & Hall, A. 1995. Rho, rac, and cdc42 GTPases regulate the assembly of multimolecular focal complexes associated with actin stress fibers, lamellipodia, and filopodia. *Cell,* 81**,** 53-62.

Norton, L. J., Zhang, Q., Saqib, K. M., Schrewe, H., Macura, K., Anderson, K. E., Lindsley, C. W., Brown, H. A., Rudge, S. A. & Wakelam, M. J. 2011. PLD1 rather than PLD2 regulates phorbol-ester-, adhesion-dependent and Fcγ-receptor-stimulated ROS production in neutrophils. *Journal of cell science,* 124**,** 1973-1983.

O'luanaigh, N., Pardo, R., Fensome, A., Allen-Baume, V., Jones, D., Holt, M. R. & Cockcroft, S. 2002. Continual production of phosphatidic acid by phospholipase D is essential for antigen-stimulated membrane ruffling in cultured mast cells. *Molecular biology of the cell,* 13**,** 3730-3746.

O'reilly, M. S., Boehm, T., Shing, Y., Fukai, N., Vasios, G., Lane, W. S., Flynn, E., Birkhead, J. R., Olsen, B. R. & Folkman, J. 1997. Endostatin: an endogenous inhibitor of angiogenesis and tumor growth. *cell,* 88**,** 277-285.

O'reilly, M. S., Holmgren, L., Shing, Y., Chen, C., Rosenthal, R. A., Moses, M., Lane, W. S., Cao, Y., Sage, E. H. & Folkman, J. 1994. Angiostatin: a novel angiogenesis inhibitor that mediates the suppression of metastases by a Lewis lung carcinoma. *cell,* 79**,** 315-328.

Oh, M., Dey, A., Gerard, R. D., Hill, J. A. & Rothermel, B. A. 2010. The CCAAT/enhancer binding protein β (C/EBPβ) cooperates with NFAT to control expression of the calcineurin regulatory protein RCAN1–4. *Journal of Biological Chemistry,* 285**,** 16623-16631.

Oliveira, T. G., Chan, R. B., Tian, H., Laredo, M., Shui, G., Staniszewski, A., Zhang, H., Wang, L., Kim, T.-W. & Duff, K. E. 2010. Phospholipase d2 ablation ameliorates Alzheimer's disease-linked synaptic dysfunction and cognitive deficits. *The Journal of Neuroscience,* 30**,** 16419-16428.

Olofsson, B., Korpelainen, E., Pepper, M. S., Mandriota, S. J., Aase, K., Kumar, V., Gunji, Y., Jeltsch, M. M., Shibuya, M. & Alitalo, K. 1998. Vascular endothelial growth factor B (VEGF-B) binds to VEGF receptor-1 and regulates plasminogen activator activity in endothelial cells. *Proceedings of the National Academy of Sciences,* 95**,** 11709-11714.

Olsson, A.-K., Dimberg, A., Kreuger, J. & Claesson-Welsh, L. 2006. VEGF receptor signalling? In control of vascular function. *Nature Reviews Molecular Cell Biology,* 7**,** 359-371.

Omelchenko, T., Vasiliev, J., Gelfand, I., Feder, H. & Bonder, E. 2002. Mechanisms of polarization of the shape of fibroblasts and epitheliocytes: separation of the roles of microtubules and Rho-dependent actin–myosin contractility. *Proceedings of the National Academy of Sciences,* 99**,** 10452-10457.

Palecek, S. P., Huttenlocher, A., Horwitz, A. F. & Lauffenburger, D. A. 1998. Physical and biochemical regulation of integrin release during rear detachment of migrating cells. *Journal of Cell Science,* 111**,** 929-940.

Park, J. E., Keller, G.-A. & Ferrara, N. 1993. The vascular endothelial growth factor (VEGF) isoforms: differential deposition into the subepithelial extracellular matrix and bioactivity of extracellular matrix-bound VEGF. *Molecular Biology of the Cell,* 4**,** 1317.

Park, S., Chun, Y., Ryu, S., Suh, P. & Kim, H. 1998a. Assignment1 of human PLD1 to human chromosome band 3q26 by fluorescence in situ hybridization. *Cytogenetic and Genome Research,* 82**,** 224-224.

Park, S., Ryu, S., Suh, P. & Kim, H. 1998b. Assignment1 of human PLD2 to chromosome band 17p13. 1 by fluorescence in situ hybridization. *Cytogenetic and Genome Research,* 82**,** 225-225.

Peiris, H., Raghupathi, R., Jessup, C. F., Zanin, M. P., Mohanasundaram, D., Mackenzie, K. D., Chataway, T., Clarke, J. N., Brealey, J. & Coates, P. T. 2012. Increased expression of the glucose-responsive gene, RCAN1, causes hypoinsulinemia, β-cell dysfunction, and diabetes. *Endocrinology,* 153**,** 5212-5221.

Peng, X. & Frohman, M. A. 2012. Mammalian phospholipase D physiological and pathological roles. *Acta physiologica,* 204**,** 219-226.

Perrin, R., Konopatskaya, O., Qiu, Y., Harper, S., Bates, D. & Churchill, A. 2005. Diabetic retinopathy is associated with a switch in splicing from anti-to pro-angiogenic isoforms of vascular endothelial growth factor. *Diabetologia,* 48**,** 2422-2427.

Porta, S., Serra, S. A., Huch, M., Valverde, M. A., Llorens, F., Estivill, X., Arbonés, M. L. & Martí, E. 2007. RCAN1 (DSCR1) increases neuronal susceptibility to oxidative stress: a potential pathogenic process in neurodegeneration. *Human Molecular Genetics,* 16**,** 1039-1050.

Powner, D. J., Pettitt, T. R., Anderson, R., Nash, G. B. & Wakelam, M. J. 2007. Stable adhesion and migration of human neutrophils requires phospholipase D-mediated activation of the integrin CD11b/CD18. *Molecular immunology,* 44**,** 3211-3221.

Pritchard, M. A. & Martin, K. R. 2013. RCAN1 and Its Potential Contribution to the Down Syndrome Phenotype. *InTech*.

Provost, J., Fudge, J., Israelit, S., Siddiqi, A. & Exton, J. 1996. Tissue-specific distribution and subcellular distribution of phospholipase D in rat: evidence for distinct RhoA-and ADP-ribosylation factor (ARF)-regulated isoenzymes. *Biochem. J,* 319**,** 285-291.

Pugh, C. W. & Ratcliffe, P. J. 2003. Regulation of angiogenesis by hypoxia: role of the HIF system. *Nature medicine,* 9**,** 677-684.

Ridley, A. J. 2012. Historical overview of Rho GTPases. *Rho GTPases.* Springer.

Ridley, A. J. & Hall, A. 1992. The small GTP-binding protein rho regulates the assembly of focal adhesions and actin stress fibers in response to growth factors. *Cell,* 70**,** 389-399.

Ridley, A. J., Paterson, H. F., Johnston, C. L., Diekmann, D. & Hall, A. 1992. The small GTP-binding protein rac regulates growth factor-induced membrane ruffling. *Cell,* 70**,** 401-410.

Rizzo, M. A., Shome, K., Vasudevan, C., Stolz, D. B., Sung, T.-C., Frohman, M. A., Watkins, S. C. & Romero, G. 1999. Phospholipase D and its product, phosphatidic acid, mediate agonist-dependent raf-1 translocation to the plasma membrane and the activation of the mitogen-activated protein kinase pathway. *Journal of Biological Chemistry,* 274**,** 1131-1139.

Roberts, O. L., Holmes, K., Müller, J., Cross, D. A. & Cross, M. J. 2010. ERK5 is required for VEGF-mediated survival and tubular morphogenesis of primary human microvascular endothelial cells. *Journal of cell science,* 123**,** 3189-3200.

Robinson, C. J. & Stringer, S. E. 2001. The splice variants of vascular endothelial growth factor (VEGF) and their receptors. *Journal of cell science,* 114**,** 853-865.

Rodrik, V., Zheng, Y., Harrow, F., Chen, Y. & Foster, D. A. 2005. Survival signals generated by estrogen and phospholipase D in MCF-7 breast cancer cells are dependent on Myc. *Molecular and cellular biology,* 25**,** 7917-7925.

Rothermel, B., Vega, R. B., Yang, J., Wu, H., Bassel-Duby, R. & Williams, R. S. 2000. A protein encoded within the Down syndrome critical region is enriched in striated muscles and inhibits calcineurin signaling. *Journal of Biological Chemistry,* 275**,** 8719-8725.

Rudge, S. A. & Wakelam, M. J. 2009. Inter-regulatory dynamics of phospholipase D and the actin cytoskeleton. *Biochimica et Biophysica Acta (BBA)-Molecular and Cell Biology of Lipids,* 1791**,** 856-861.

Rusnak, F. & Mertz, P. 2000. Calcineurin: form and function. *Physiological reviews,* 80**,** 1483-1521.

Rydzewska, G. & Morisset, J. 1995. Activation of pancreatic acinar cell phospholipase D by epidermal, insulin-like, and basic fibroblast growth factors involves tyrosine kinase. *Pancreas,* 10**,** 59-65.

Ryeom, S., Baek, K.-H., Rioth, M. J., Lynch, R. C., Zaslavsky, A., Birsner, A., Yoon, S. S. & Mckeon, F. 2008. Targeted deletion of the calcineurin inhibitor DSCR1 suppresses tumor growth. *Cancer cell,* 13**,** 420-431.

Saharinen, P., Eklund, L., Miettinen, J., Wirkkala, R., Anisimov, A., Winderlich, M., Nottebaum, A., Vestweber, D., Deutsch, U. & Koh, G. Y. 2008. Angiopoietins assemble distinct Tie2 signalling complexes in endothelial cell–cell and cell–matrix contacts. *Nature cell biology,* 10**,** 527-537.

Sait, S., Dougher-Vermazen, M., Shows, T. & Terman, B. 1995. The kinase insert domain receptor gene (KDR) has been relocated to chromosome 4q11→ q12. *Cytogenetic and Genome Research,* 70**,** 145-146.

Saito, M., Iwadate, M., Higashimoto, M., Ono, K., Takebayashi, Y. & Takenoshita, S. 2007. Expression of phospholipase D2 in human colorectal carcinoma. *Oncology reports,* 18**,** 1329-1334.

Salceda, S. & Caro, J. 1997. Hypoxia-inducible factor 1α (HIF-1α) protein is rapidly degraded by the ubiquitin-proteasome system under normoxic conditions its stabilization by hypoxia depends on redox-inducde changes. *Journal of Biological Chemistry,* 272**,** 22642-22647.

Sawamiphak, S., Seidel, S., Essmann, C. L., Wilkinson, G. A., Pitulescu, M. E., Acker, T. & Acker-Palmer, A. 2010. Ephrin-B2 regulates VEGFR2 function in developmental and tumour angiogenesis. *Nature,* 465**,** 487-491.

Sciorra, V. A., Rudge, S. A., Wang, J., Mclaughlin, S., Engebrecht, J. & Morris, A. J. 2002. Dual role for phosphoinositides in regulation of yeast and mammalian phospholipase D enzymes. *The Journal of cell biology,* 159**,** 1039-1049.

Scott, S. A., Selvy, P. E., Buck, J. R., Cho, H. P., Criswell, T. L., Thomas, A. L., Armstrong, M. D., Arteaga, C. L., Lindsley, C. W. & Brown, H. A. 2009. Design of isoform-selective phospholipase D inhibitors that modulate cancer cell invasiveness. *Nature chemical biology,* 5**,** 108-117.

Seegar, T., Eller, B., Tzvetkova-Robev, D., Kolev, M. V., Henderson, S. C., Nikolov, D. B. & Barton, W. A. 2010. Tie1-Tie2 interactions mediate functional differences between angiopoietin ligands. *Molecular cell,* 37**,** 643-655.

Senger, D. R., Claffey, K. P., Benes, J. E., Perruzzi, C. A., Sergiou, A. P. & Detmar, M. 1997. Angiogenesis promoted by vascular endothelial growth factor: regulation through α1β1 and α2β1 integrins. *Proceedings of the National Academy of Sciences,* 94**,** 13612-13617.

Seppä, H., Grotendorst, G., Seppä, S., Schiffmann, E. & Martin, G. R. 1982. Platelet-derived growth factor in chemotactic for fibroblasts. *The Journal of cell biology,* 92**,** 584-588.

Serrano-Candelas, E., Farré, D., Aranguren-Ibáñez, Á., Martínez-Høyer, S. & Pérez-Riba, M. 2014. The Vertebrate RCAN Gene Family: Novel Insights into Evolution, Structure and Regulation. *PloS one,* 9**,** e85539.

Seymour, L. W., Shoaibi, M. A., Martin, A., Ahmed, A., Elvin, P., Kerr, D. J. & Wakelam, M. 1996. Vascular endothelial growth factor stimulates protein kinase C-dependent phospholipase D activity in endothelial cells. *Laboratory investigation; a journal of technical methods and pathology,* 75**,** 427-437.

Shalaby, F., Rossant, J., Yamaguchi, T. P., Gertsenstein, M., Wu, X.-F., Breitman, M. L. & Schuh, A. C. 1995. Failure of blood-island formation and vasculogenesis in Flk-1-deficient mice. *Nature,* 376**,** 62-66.

Sherwani, S. I., Pabon, S., Patel, R. B., Sayyid, M. M., Hagele, T., Kotha, S. R., Magalang, U. J., Maddipati, K. R. & Parinandi, N. L. 2013. Eicosanoid signaling and vascular dysfunction: methylmercury-induced phospholipase D activation in vascular endothelial cells. *Cell biochemistry and biophysics,* 67**,** 317-329.

Shibuya, M. 2002. Vascular endothelial growth factor receptor family genes: when did the three genes phylogenetically segregate? *Biological chemistry,* 383**,** 1573-1579.

Shu, X., Wu, W., Mosteller, R. D. & Broek, D. 2002. Sphingosine kinase mediates vascular endothelial growth factor-induced activation of ras and mitogen-activated protein kinases. *Molecular and cellular biology,* 22**,** 7758-7768.

Shweiki, D., Itin, A., Soffer, D. & Keshet, E. 1992. Vascular endothelial growth factor induced by hypoxia may mediate hypoxia-initiated angiogenesis. *Nature,* 359**,** 843-845.

Simionescu, N. & Simionescu, M. 1992. *Endothelial cell dysfunctions*, Springer.

Simons, M. 2012. An inside view: VEGF receptor trafficking and signaling. *Physiology,* 27**,** 213-222.

Slaaby, R., Jensen, T., Hansen, H. S., Frohman, M. A. & Seedorf, K. 1998. PLD2 complexes with the EGF receptor and undergoes tyrosine phosphorylation at a single site upon agonist stimulation. *Journal of Biological Chemistry,* 273**,** 33722-33727.

Snyder, S. H., Sabatini, D. M., Lai, M. M., Steiner, J. P., Hamilton, G. S. & Suzdak, P. D. 1998. Neural actions of immunophilin ligands. *Trends in pharmacological sciences,* 19**,** 21-26.

Söderberg, O., Gullberg, M., Jarvius, M., Ridderstråle, K., Leuchowius, K.-J., Jarvius, J., Wester, K., Hydbring, P., Bahram, F. & Larsson, L.-G. 2006. Direct observation of individual endogenous protein complexes in situ by proximity ligation. *Nature methods,* 3**,** 995-1000.

Soker, S., Miao, H. Q., Nomi, M., Takashima, S. & Klagsbrun, M. 2002. VEGF165 mediates formation of complexes containing VEGFR‐2 and neuropilin‐1 that enhance VEGF165‐receptor binding. *Journal of cellular biochemistry,* 85**,** 357-368.

Soker, S., Takashima, S., Miao, H. Q., Neufeld, G. & Klagsbrun, M. 1998. Neuropilin-1 is expressed by endothelial and tumor cells as an isoform-specific receptor for vascular endothelial growth factor. *Cell,* 92**,** 735-745.

Soldi, R., Mitola, S., Strasly, M., Defilippi, P., Tarone, G. & Bussolino, F. 1999. Role of αvβ3 integrin in the activation of vascular endothelial growth factor receptor-2. *The EMBO journal,* 18**,** 882-892.

Song, G., Ouyang, G. & Bao, S. 2005. The activation of Akt/PKB signaling pathway and cell survival. *Journal of cellular and molecular medicine,* 9**,** 59-71.

Stenmark, H. 2009. Rab GTPases as coordinators of vesicle traffic. *Nature reviews Molecular cell biology,* 10**,** 513-525.

Su, W., Chen, Q. & Frohman, M. A. 2009. Targeting phospholipase D with small-molecule inhibitors as a potential therapeutic approach for cancer metastasis. *Future Oncology,* 5**,** 1477-1486.

Sung, T. C., Roper, R. L., Zhang, Y., Rudge, S. A., Temel, R., Hammond, S. M., Morris, A. J., Moss, B., Engebrecht, J. & Frohman, M. A. 1997. Mutagenesis of phospholipase D defines a superfamily including a trans‐Golgi viral protein required for poxvirus pathogenicity. *The EMBO journal,* 16**,** 4519-4530.

Suto, K., Yamazaki, Y., Morita, T. & Mizuno, H. 2005. Crystal structures of novel vascular endothelial growth factors (VEGF) from snake venoms insight into selective VEGF binding to kinase insert domain-containing receptor but not to fms-like tyrosine kinase-1. *Journal of Biological Chemistry,* 280**,** 2126-2131.

Swaney, K. F., Huang, C.-H. & Devreotes, P. N. 2010. Eukaryotic chemotaxis: a network of signaling pathways controls motility, directional sensing, and polarity. *Annual review of biophysics,* 39**,** 265-289.

Tabruyn, S. P. & Griffioen, A. W. 2007. Molecular pathways of angiogenesis inhibition. *Biochemical and biophysical research communications,* 355**,** 1-5.

Takahashi, H. & Shibuya, M. 2005. The vascular endothelial growth factor (VEGF)/VEGF receptor system and its role under physiological and pathological conditions. *Clinical Science,* 109**,** 227-241.

Takahashi, T. & Shibuya, M. 1997. The 230 kDa mature form of KDR/Flk-1 (VEGF receptor-2) activates the PLC-gamma pathway and partially induces mitotic signals in NIH3T3 fibroblasts. *Oncogene,* 14**,** 2079-2089.

Takahashi, T., Ueno, H. & Shibuya, M. 1999. VEGF activates protein kinase C-dependent, but Ras-independent Raf-MEK-MAP kinase pathway for DNA synthesis in primary endothelial cells. *Oncogene,* 18**,** 2221-2230.

Takahashi, T., Yamaguchi, S., Chida, K. & Shibuya, M. 2001. A single autophosphorylation site on KDR/Flk-1 is essential for VEGF-A-dependent activation of PLC-γ and DNA synthesis in vascular endothelial cells. *The EMBO journal,* 20**,** 2768-2778.

Terman, B. I., Carrion, M., Kovacs, E., Rasmussen, B., Eddy, R. & Shows, T. 1991. Identification of a new endothelial cell growth factor receptor tyrosine kinase. *Oncogene,* 6**,** 1677-1683.

Toda, K., Nogami, M., Murakami, K., Kanaho, Y. & Nakayama, K. 1999. Colocalization of phospholipase D1 and GTP-binding-defective mutant of ADP-ribosylation factor 6 to endosomes and lysosomes. *FEBS letters,* 442**,** 221-225.

Toker, A. & Marmiroli, S. 2014. Signaling specificity in the Akt pathway in biology and disease. *Advances in biological regulation*.

Topper, J. N., Cai, J., Falb, D. & Gimbrone, M. A. 1996. Identification of vascular endothelial genes differentially responsive to fluid mechanical stimuli: cyclooxygenase-2, manganese superoxide dismutase, and endothelial cell nitric oxide synthase are selectively up-regulated by steady laminar shear stress. *Proceedings of the National Academy of Sciences,* 93**,** 10417-10422.

Toullec, D., Pianetti, P., Coste, H., Bellevergue, P., Grand-Perret, T., Ajakane, M., Baudet, V., Boissin, P., Boursier, E. & Loriolle, F. 1991. The bisindolylmaleimide GF 109203X is a potent and selective inhibitor of protein kinase C. *Journal of Biological Chemistry,* 266**,** 15771-15781.

Tung, J. J., Tattersall, I. W. & Kitajewski, J. 2012. Tips, stalks, tubes: Notch-mediated cell fate determination and mechanisms of tubulogenesis during angiogenesis. *Cold Spring Harbor perspectives in medicine,* 2**,** a006601.

Uetrecht, A. C. & Bear, J. E. 2009. Golgi polarity does not correlate with speed or persistence of freely migrating fibroblasts. *European journal of cell biology,* 88**,** 711-717.

Van Hinsbergh, V. W. Endothelium—role in regulation of coagulation and inflammation. Seminars in immunopathology, 2012. Springer, 93-106.

Vasudevan, D. M., Sreekumari, S. & Vaidyanathan, K. 2010. *Textbook of Biochemistry for medical students*, JAYPEE BROTHERS PUBLISHERS.

Vega, R. B., Yang, J., Rothermel, B. A., Bassel-Duby, R. & Williams, R. S. 2002. Multiple domains of MCIP1 contribute to inhibition of calcineurin activity. *Journal of Biological Chemistry,* 277**,** 30401-30407.

Vicente-Manzanares, M., Koach, M. A., Whitmore, L., Lamers, M. L. & Horwitz, A. F. 2008. Segregation and activation of myosin IIB creates a rear in migrating cells. *The Journal of cell biology,* 183**,** 543-554.

Vincenti, V., Cassano, C., Rocchi, M. & Persico, M. G. 1996. Assignment of the vascular endothelial growth factor gene to human chromosome 6p21. 3. *Circulation,* 93**,** 1493-1495.

Wakelam, M. J., Pettitt, T. R. & Postle, A. D. 2007. Lipidomic analysis of signaling pathways. *Methods in enzymology,* 432**,** 233-246.

Wang, G. L. & Semenza, G. L. 1995. Purification and characterization of hypoxia-inducible factor 1. *Journal of Biological Chemistry,* 270**,** 1230-1237.

Weiser, D. C. & Shenolikar, S. 2003. Use of protein phosphatase inhibitors. *Current Protocols in Protein Science***,** 13.10. 1-13.10. 13.

Weksler, B. B., Marcus, A. J. & Jaffe, E. A. 1977. Synthesis of prostaglandin I2 (prostacyclin) by cultured human and bovine endothelial cells. *Proceedings of the National Academy of Sciences,* 74**,** 3922-3926.

Wellner, M., Maasch, C., Kupprion, C., Lindschau, C., Luft, F. C. & Haller, H. 1999. The proliferative effect of vascular endothelial growth factor requires protein kinase C-α and protein kinase C-ζ. *Arteriosclerosis, thrombosis, and vascular biology,* 19**,** 178-185.

Whitaker, G. B., Limberg, B. J. & Rosenbaum, J. S. 2001. Vascular endothelial growth factor receptor-2 and neuropilin-1 form a receptor complex that is responsible for the differential signaling potency of VEGF165 and VEGF121. *Journal of Biological Chemistry,* 276**,** 25520-25531.

Wilkins, B. J., Dai, Y.-S., Bueno, O. F., Parsons, S. A., Xu, J., Plank, D. M., Jones, F., Kimball, T. R. & Molkentin, J. D. 2004. Calcineurin/NFAT coupling participates in pathological, but not physiological, cardiac hypertrophy. *Circulation research,* 94**,** 110-118.

Wilson, E., Leszczynska, K., Poulter, N. S., Edelmann, F., Salisbury, V. A., Noy, P. J., Bacon, A., Rappoport, J. Z., Heath, J. K. & Bicknell, R. 2014. RhoJ interacts with the GIT–PIX complex and regulates focal adhesion disassembly. *Journal of cell science,* 127**,** 3039-3051.

Winder, D. G. & Sweatt, J. D. 2001. Roles of serine/threonine phosphatases in hippocampel synaptic plasticity. *Nature Reviews Neuroscience,* 2**,** 461-474.

Wiseman, F. K., Alford, K. A., Tybulewicz, V. L. & Fisher, E. M. 2009. Down syndrome—recent progress and future prospects. *Human Molecular Genetics,* 18**,** R75-R83.

Wojciak-Stothard, B. & Ridley, A. J. 2002. Rho GTPases and the regulation of endothelial permeability. *Vascular pharmacology,* 39**,** 187-199.

Wu, L.-W., Mayo, L. D., Dunbar, J. D., Kessler, K. M., Ozes, O. N., Warren, R. S. & Donner, D. B. 2000. VRAP is an adaptor protein that binds KDR, a receptor for vascular endothelial cell growth factor. *Journal of Biological Chemistry,* 275**,** 6059-6062.

Xia, P., Aiello, L. P., Ishii, H., Jiang, Z. Y., Park, D. J., Robinson, G. S., Takagi, H., Newsome, W. P., Jirousek, M. R. & King, G. L. 1996. Characterization of vascular endothelial growth factor's effect on the activation of protein kinase C, its isoforms, and endothelial cell growth. *Journal of Clinical Investigation,* 98**,** 2018.

Xie, Z., Ho, W.-T. & Exton, J. H. 1998. Association of N-and C-terminal domains of phospholipase D is required for catalytic activity. *Journal of Biological Chemistry,* 273**,** 34679-34682.

Xu, Y., Seet, L., Hanson, B. & Hong, W. 2001. The Phox homology (PX) domain, a new player in phosphoinositide signalling. *Biochem. J,* 360, 513-530.

Yamaguchi, T. P., Dumont, D. J., Conlon, R. A., Breitman, M. L. & Rossant, J. 1993. flk-1, an flt-related receptor tyrosine kinase is an early marker for endothelial cell precursors. *Development,* 118, 489-498.

Yang, J., Rothermel, B., Vega, R. B., Frey, N., Mckinsey, T. A., Olson, E. N., Bassel-Duby, R. & Williams, R. S. 2000. Independent signals control expression of the calcineurin inhibitory proteins MCIP1 and MCIP2 in striated muscles. *Circulation research,* 87, e61-e68.

Zacharoulis, D., Hatzitheofilou, C., Athanasiou, E. & Zacharoulis, S. 2005. Antiangiogenic strategies in hepatocellular carcinoma: current status.

Zachary, I. 2003. VEGF signalling: integration and multi-tasking in endothelial cell biology. *Biochemical Society Transactions,* 31, 1171-1177.

Zeiller, C., Mebarek, S., Jaafar, R., Pirola, L., Lagarde, M., Prigent, A.-F. & Némoz, G. 2009. Phospholipase D2 regulates endothelial permeability through cytoskeleton reorganization and occludin downregulation. *Biochimica et Biophysica Acta (BBA)-Molecular Cell Research,* 1793, 1236-1249.

Zeng, H., Chattarji, S., Barbarosie, M., Rondi-Reig, L., Philpot, B. D., Miyakawa, T., Bear, M. F. & Tonegawa, S. 2001. Forebrain-specific calcineurin knockout selectively impairs bidirectional synaptic plasticity and working/episodic-like memory. *Cell,* 107, 617-629.

Zeng, H., Zhao, D. & Mukhopadhyay, D. 2002. KDR stimulates endothelial cell migration through heterotrimeric G protein Gq/11-mediated activation of a small GTPase RhoA. *Journal of Biological Chemistry,* 277, 46791-46798.

Zeng, X.-X. I., Zheng, X., Xiang, Y., Cho, H. P., Jessen, J. R., Zhong, T. P., Solnica-Krezel, L. & Brown, H. A. 2009. Phospholipase D1 is required for angiogenesis of intersegmental blood vessels in zebrafish. *Developmental biology,* 328**,** 363-376.

Zhai, J., Lin, H., Nie, Z., Wu, J., Cañete-Soler, R., Schlaepfer, W. W. & Schlaepfer, D. D. 2003. Direct interaction of focal adhesion kinase with p190RhoGEF. *Journal of Biological Chemistry,* 278**,** 24865-24873.

Zhao, P., Xiao, X., Kim, A. S., Leite, M. F., Xu, J., Zhu, X., Ren, J. & Li, J. 2008. c-Jun inhibits thapsigargin-induced ER stress through up-regulation of DSCR1/Adapt78. *Experimental Biology and Medicine,* 233**,** 1289-1300.

Zhuge, Y. & Xu, J. 2001. Rac1 mediates type I collagen-dependent MMP-2 activation role in cell invasion across collagen barrier. *Journal of Biological Chemistry,* 276**,** 16248-16256.